

Tracking spatiotemporal localisation and interactions of the innate immune sensor STING

Présentée le 10 février 2023

Faculté des sciences de la vie
Unité de la Prof. Ablasser
Programme doctoral en biotechnologie et génie biologique

pour l'obtention du grade de Docteur ès Sciences

par

Sophie Marie Elisabeth RIVARA

Acceptée sur proposition du jury

Prof. D. M. Suter, président du jury
Prof. A. Ablasser, directrice de thèse
Prof. P. Broz, rapporteur
Dr C. de Oliveira Mann, rapporteuse
Prof. G. D'Angelo, rapporteur

Table of content

SUMMARY	4
RÉSUMÉ	5
LIST OF ABBREVIATIONS	6
CHAPTER 1 – INTRODUCTION	10
1.1 – Innate immunity: a crucial first line of defence	10
1.2 – Nucleic acids as target for PRRs	12
1.3 – The cGAS-STING axis	13
1.3.1 – cGAS: a highly conserved ubiquitous innate immune receptor	14
1.3.2 – Downstream of cGAMP: the adaptor protein STING	16
1.3.3 – STING-independent regulation of the cGAS-STING pathway	18
1.4 – STING-specific regulation	20
1.4.1 – STING-mediated IFN I signalling	20
1.4.2 – Besides IFN: NF-κB-dependent STING signalling	24
1.5 – STING trafficking in details: a journey through the cell	26
1.5.1 – ER-ERGIC-Golgi and back	27
1.5.2 – The end of the journey: Golgi to lysosomes	28
1.5.3 – The side road: autophagy	29
1.6 – Rationale and aim of the thesis	30
CHAPTER 2 – STING ER-TO-GOLGI TRAFFICKING	32
2.1 – GFP-based tracking of mSting in HEK293T cells underlines the importance of the second transmembrane cytosolic loop in trafficking	32
2.2 – Small chemical compounds screen to identify STING-specific ER-to-Golgi trafficking inhibitors	33
2.3 – MS/MS-based screen identifies ELMOD2 as potentially regulating STING ER-to-Golgi trafficking	39
2.4 – ELMOD2 depletion impacts STING signalling at various levels and yields conflicting phenotypes	41
2.5 – STING C-terminal cytosolic head systematic mutagenesis helps mapping regions of STING important for trafficking regulation.	45
2.6 – Discussion	47

2.7 – Material and methods	50
2.8 – Contributions	59
CHAPTER 3 – CLATHRIN-ASSOCIATED AP-1 CONTROLS TERMINATION OF STING SIGNALLING	61
3.1 – Introductory remarks	61
3.2 – Main	62
3.2.1 – Abstract	62
3.2.2 – Introduction	62
3.2.3 – Activated STING traffics from the Golgi to lysosomes via CCVs	63
3.2.4 – AP-1 sorts STING into CCVs	69
3.2.5 – AP-1 restricts STING signalling	72
3.2.6 – Direct engagement of STING by AP-1	76
3.2.7 – Phospho-regulation of STING binding AP-1	78
3.2.8 – Structure of the p-STING-AP-1-Arf1 complex	81
3.2.9 – Discussion	86
3.2.10 – Methods	87
3.2.11 – Additional paper sections	100
CHAPTER 4 – GLOBAL DISCUSSION AND PERSPECTIVES	101
4.1 – Summary and significance of findings	101
4.2 – Perspectives	102
4.2.1 – Implications of STING regulation by conformation and localisation changes	102
4.2.2 – What evolution tells us about STING	104
4.2.3 – STING dysregulation as a powerful tool to understand homeostatic regulation	106
4.2.4 – The advantages and limits of microscopy-based approaches in studying STING	107
4.2.5 – Open questions and how to address them	109
4.2.6 – Concluding remarks	110
ACKNOWLEDGEMENTS	112
REFERENCES	120
APPENDIX	130

Summary

Innate immunity, the very first line of defence of our cells, relies on the detection of universal pathogen- or danger-associated signals to launch an inflammatory response. A crucial part of our innate immune system is based on the recognition of out-of-context DNA as an indicator of pathogenic attack, loss of cellular integrity, or homeostatic disruption. The main pathway involved in this detection is the cGAS-STING pathway, that is activated by foreign or out-of-context intracellular DNA and triggers downstream activation of the pro-inflammatory transcription factors IRF3 and NF- κ B—leading to production of type I interferons and pro-inflammatory cytokines, respectively—and the induction of autophagy. The cGAS-STING axis is central during infection, a key player in anti-tumoral immunity and linked with several autoinflammatory syndromes. The present thesis focuses on unresolved aspects of STING regulation related to its cellular trafficking, both upon initial activation and at signal termination.

Two screenings, a microscopy-based one for chemical inhibitors of STING endoplasmic reticulum to Golgi trafficking and a mass spectrometry-based one for interactors implied in this re-localisation, led us to the conclusion that STING relied extensively on essential proteins during this step. Indeed, hits that attenuated STING trafficking also significantly impacted the global cellular state or viability. Furthermore, we pinpointed a potential modulator of STING signalling, ELMOD2, an Arl/Arf-family GTPase activating protein, whose depletion also triggered downstream STING-independent effects, leading to some conflicting results. We therefore moved on to a mutagenesis-based approach which, when combined with high throughput microscopy, could map regions of STING with potentially critical residues involved in trafficking regulation.

In parallel, we investigated the mechanisms underlying STING terminal trafficking and its degradation, allowing us to observe colocalization of active phospho-STING molecules with clathrins, as well as with adaptor protein (AP)-1 subunits. We followed STING post-Golgi trafficking with super-high-resolution microscopy and confirmed the presence of STING in clathrin-coated vesicles as well as implication of AP-1 in signalling termination. We were also able to capture STING C-terminal tail in complex with AP-1 and show that AP-1 has greater affinity for phosphorylated STING. Together, our results show that STING phosphorylation at the Golgi, while allowing for downstream IRF3 recruitment and signalling, simultaneously triggers the recruitment of AP-1 and initiates pathway termination. We hence unravelled an elegant feedback mechanism in which STING activation and degradation are directly interconnected, as the residues responsible for IRF3 and AP-1 recruitment partially overlap, indicating a probable concomitant evolution.

The data presented in this thesis contribute to extending the knowledge of mechanisms of STING regulation and also shed light on the impact of its cellular localisation on signalling. Furthermore, they give some insights on the importance of the co-evolution of activating and inhibitory mechanisms and embedded feedback loops in innate immune proteins.

Key words: innate immunity; STING; ER-to-Golgi trafficking; adaptor protein-1 (AP-1); clathrin-coated vesicles (CCVs); microscopy-based cellular localisation.

Résumé

L'immunité innée constitue la première ligne de défense de nos cellules et repose sur la détection de signaux universels associés à des pathogènes ou des dangers pour déclencher une réponse inflammatoire. Un élément essentiel de notre système immunitaire inné est la reconnaissance de l'ADN hors-contexte, un indicateur d'attaque pathogénique, de perte de l'intégrité cellulaire ou de perturbation homéostatique. La principale voie de signalisation impliquée dans cette détection est cGAS-STING, qui permet l'activation en aval des facteurs de transcription IRF3 et NF- κ B—engendrant la production d'interférons de type I et de cytokines pro-inflammatoires—ainsi que l'induction de l'autophagie. L'axe cGAS-STING, central lors d'infections ou pour l'immunité antitumorale, est aussi associé à plusieurs syndromes auto-inflammatoires. Cette thèse se penche sur des aspects non résolus de la régulation de STING et de son trafic cellulaire, tant lors de son activation initiale qu'au moment de la terminaison du signal.

Deux criblages, reposant sur la microscopie pour identifier des inhibiteurs chimiques du trafic de STING entre le réticulum endoplasmique et l'appareil de Golgi, et sur la spectroscopie de masse pour identifier des interacteurs impliqués dans cette relocalisation, ont montré que STING dépendait largement de protéines essentielles lors de cette étape. En effet, les hits qui atténuent le trafic de STING ont aussi un impact considérable sur l'état global des cellules et leur viabilité. De plus, un potentiel modulateur de STING repéré dans notre criblage, ELMOD2, est une protéine activant les Arl/Arf-GTPases, et sa déplétion a déclenché en aval des effets indépendants de STING, conduisant à des résultats contradictoires. Nous nous sommes alors dirigés vers une approche basée sur de la mutagenèse combinée avec de la microscopie à haut débit pour identifier des régions de STING aux résidus potentiellement critiques pour la régulation du trafic.

En parallèle, nous avons étudié les mécanismes sous-jacents au trafic terminal de STING et à sa dégradation, montrant que la forme active phosphorylée de STING colocalisait avec des clathrines et des sous-unités de la protéine adaptatrice AP-1. En suivant le trafic post-Golgi de STING grâce à des techniques de microscopie à très haute résolution, la présence de STING dans des vésicules mantelées de clathrines et l'implication de AP-1 dans la terminaison du signal a été établie. Nous avons aussi capturé la queue C-terminale de STING en complexe avec AP-1 et montré une plus grande affinité de AP-1 pour STING phosphorylé. L'ensemble de nos résultats démontre que la phosphorylation de STING au Golgi permet de recruter à la fois IRF3, pour transmettre le signal en aval, mais également AP-1, pour initier la terminaison de la voie de signalisation. Ainsi, nous avons dévoilé un élégant mécanisme de rétroaction lors duquel l'activation et la dégradation de STING apparaissent directement interconnectés, puisque les résidus responsables du recrutement d'IRF3 et de AP-1 se recoupent en partie, indiquant au passage une probable évolution concomitante.

Les données présentées dans cette thèse contribuent à la connaissance des mécanismes de régulation de STING et mettent en exergue l'impact de sa localisation cellulaire sur la signalisation. En outre, elles révèlent l'importance de la coévolution de mécanismes activateurs et inhibiteurs avec des rétrocontrôles pour les protéines de l'immunité innée.

Mots clés : immunité innée ; STING ; trafic du réticulum endoplasmique au Golgi ; protéine adaptatrice 1 (AP-1) ; vésicules mantelées de clathrines (CCVs) ; localisation cellulaire basée sur la microscopie

List of abbreviations

aa	Amino acid
ADP	Adenosine diphosphate
AIM2	Absent in melanoma 2
Ala-scan	Alanine-scanning
ALR	AIM2-like receptor
AP-1-5	Adaptor protein 1-5
ARF	ADP ribosylation factor 1
Atg / ATG	Autophagy-related gene
ATP	Adenosine triphosphate
BAF	Barrier-to-autointegration factor
BFA	Brefeldin A
BioEM	Biological Electron Microscopy Facility
BIOP	Bioimaging and Optics Platform
BSF	Biomolecular Screening Facility
CARD	Caspase recruitment domain
Cas9	CRISPR-associated protein 9
CCV	Clathrin-coated vesicle
CDN	Cyclic di-nucleotide
cGAMP	cyclic GMP-AMP
cGAS	cyclic GMP-AMP synthase
CHC	Clathrin heavy chain
CLC	Clathrin light chain
CLEM	Correlated light and electron microscopy
CLR	C-type lectin-like receptor
CMA	10-carboxymethyl-9-acridanone
COPI/II	Coat protein I/II
CRISPR	Clustered regularly interspaced short palindromic repeats
Cryo-EM	Cryogenic electron microscopy
CTT	C-terminal tail
DAI	DNA-dependent activator of IRF
DAMP	Danger-associated molecular pattern
diABZI	Diamidobenzimidazole
DMEM	Dulbecco's Modified Eagle Medium

DMSO	Dimethyl sulfoxide
DMXAA	5,6-dimethylxanthenone-4-acetic acid
DNA	Deoxyribonucleic acid
ds	Double stranded
EEA1	Early endosome antigen 1
EGFP	Enhanced green fluorescent protein
EIF3S5	Eukaryotic translation initiation factor 3, subunit 5
ELMO	Engulfment and cell motility
ELMOD2	ELMO domain containing protein 2
EM	Electron microscopy
EMDB	Electron microscopy Data Bank
ER	Endoplasmic reticulum
ERGIC	ER-Golgi intermediate compartment
ERIS	Endoplasmic reticulum interferon stimulator
FACS	Fluorescence-activated cell sorting
FBS	Fetal bovine serum
FDA	Food and drug administration (United States of America)
Fig.	Figure
GAP	GTPase-activating protein
GEF	Guanine exchange factor
GFP	Green fluorescent protein
GM130	130 kDa cis-Golgi matrix protein
GTP	Guanosine triphosphate
HRP	Horseradish peroxidase
hSTING	Human STING
HSV-1	Herpes simplex virus-1
IFI16	Interferon gamma-inducible protein 16
IFN	Interferon
IFN I	Type I interferon
IL	Interleukin
IP	Immunoprecipitation/immunoprecipitated
IpaJ	Invasion plasmid antigen J
IRF	Interferon regulatory factor
iRhom2	Inactive rhomboid protein 2
ISG	Interferon stimulated genes

JAK	Janus tyrosine kinase
KD	Knockdown
KO	Knock-out
LAMP1	Lysosome-associated membrane protein 1
LBD	Ligand binding domain
LRR	Leucine-rich repeats
MAVS	Mitochondrial antiviral signalling protein
MDA5	Melanoma differentiation-associated protein 5
MEDNIK	Mental retardation, enteropathy, deafness, peripheral neuropathy, ichthyosis, and keratoderma)
MEF	Mouse embryonic fibroblast
MOI	Multiplicity of infection
MS	Mass spectrometry
MS/MS	Tandem mass spectrometry
mSting	Mouse STING
MyD88	Myeloid differentiation factor 88
NC	Non-targeting control
Nef	Negative factor
NF- κ B	Nuclear factor- κ B
NLR	NOD-like receptor
NOD	Nucleotide oligomerisation domain
NPC1	Niemann-Pick type C1
p-	phospho-
PAMP	Pathogen-associated molecular pattern
PBS	Phosphate-buffered saline
PCR	Polymerase chain reaction
PDB	Protein Data Bank
PI	Phosphatidylinositol
PI3P	Phosphatidylinositol 3-phosphate
PMSF	Phenylmethanesulfonyl fluoride
PRR	Pattern recognition receptor
PTM	Post-translational modification
PYD	Pyrin domain
RIG-I	Retinoic acid-inducible gene-I
RLR	RIG-I-like receptor

RNA	Ribonucleic acid
RT-qPCR	Quantitative real-time PCR
RUSH	Retention Using Selective Hooks
Sar1	Secretion associated ras-superfamily gene1
SAVI	STING-Associated Vasculopathy with onset in Infancy
s.d.	Standard deviation
SDS	Sodium dodecyl sulfate
s.e.m.	Standard error of the mean
sgRNA	Single guide RNA
siRNA	Small interfering RNA
SMOC	Supramolecular organising centre
SQSTM1	Sequestosome-1
STAT1	Signal transducer and activator of transcription 1
STED	Stimulated emission depletion
STEEP	STING ER exit protein
STIM1	Stromal interaction molecule 1
STING	Stimulator of interferon genes
SURF4	Surfeit locus protein 4
TANK	TRAF family member-associated NF- κ B activator
TBK1	TANK binding kinase 1
TBS-T	Tris-buffered saline-Tween
TGN	trans-Golgi network
TIR	Toll/interleukin-1 receptor
TLR	Toll-like receptors
TMEM173	Transmembrane protein 173
TNF	Tumour necrosis factor
TRAF	Tumour necrosis factor receptor-associated factor
TRAM	TRIF-related adapter molecule
TRAP	Translocon-associated protein complex
TREX1	Three prime repair exonuclease 1
TRIF	TIR domain-containing adaptor protein inducing interferon β
ULK1	UNC-51-like kinase
WCL	Whole cell lysate
WIPI2	WD40 repeat protein interacting with phosphoinositides 2
WT	Wild-type

Chapter 1 – Introduction

1.1 – Innate immunity: a crucial first line of defence

Our bodies continuously face a wide variety of dangers, both from the external environment and from within, necessitating a robust defence strategy to protect our cells. This strategy revolves around the immune system, a complex defence system generally broken down into two major arms by the scientific community: innate and adaptive immunity. While adaptive immunity's primary aim is to generate specific antibodies or receptors to recognise and fight dangers in a highly targeted fashion, this type of response takes time to launch and can be mounted only after an actual threat has been identified. Innate immunity, on the other hand, takes care of this initial detection, launching adaptive immunity if and when needed, and restraining the danger until adaptive immunity can kick in, typically not earlier than after one or two weeks for a newly encountered pathogen¹. Hence, innate immunity constitutes the first line of defence of our cells. Its central principle is based on the recognition of pathogen- or danger-associated molecular patterns (PAMPs or DAMPs, respectively). This means that our innate immune system can recognise a broad array of potential threats through few converging factors. This detection strategy is resource- and time-efficient and ensures proper initial defence and controlled launching of the subsequent adaptive immune response.

PAMPs are typically molecules found abundantly and mostly on pathogens (such as lipopolysaccharide from bacteria's envelopes), while DAMPs can be anything related to a danger-associated disruption of classical homeostasis, triggered by the presence of a tumour or dying cell, for example. Those signals are recognised by pattern recognition receptors (PRRs), innate immune proteins that are specialised in detecting PAMPs and DAMPs. PRRs come in all flavours, however both common traits and subdivisions emerged. The first well characterised PRRs were Toll-like receptors (TLRs), a family of proteins that trigger an antimicrobial response. While originally identified in *Drosophila*², they were subsequently found to be a crucial innate immune sensor family in humans, across the vertebrate phylum and in some invertebrates³. TLRs are extracellular or endosomal transmembrane proteins and encompass a family of 10 members (in humans), allowing for detection of a broad range of extracytosolic PAMPs or DAMPs, from bacterial cell wall components and flagellin to endosomal nucleic acids. They are constituted of a leucine-rich repeats (LRR) region responsible for ligand detection and a cytosolic Toll/interleukin (IL)-1 receptor (TIR) domain that allows for downstream signalling via the recruitment of the adaptor MyD88 (or sometimes TRIF/TRAM)^{4,5}. Alongside TLRs, another class of extracellular transmembrane PRRs are C-type lectin-like receptors (CLRs). CLRs comprise at least one carbohydrate detection domain

and are specialized in recognition of sugar-PAMPs⁶. Both TLRs and CLRs signalling pathways ultimately converge towards the activation of proinflammatory nuclear transcription factors such as activator protein 1, interferon (IFN)-regulatory factor (IRF) family members or nuclear factor (NF)- κ B, resulting in the production of IFNs and various proinflammatory cytokines that contribute to the antimicrobial defences and can launch the adaptive immune response^{4,6}. In addition to those two families, which detect danger outside of the cell, there is also a need for cytosolic (and nuclear) danger detection. This falls under the responsibility of nucleotide oligomerisation domain (NOD)-like receptors (NLRs), retinoic acid-inducible gene-I (RIG-I)-like receptors (RLRs), DNA sensors or the adaptor and cyclic di-nucleotides (CDNs) sensor stimulator of interferon genes (STING), which will be the main focus of this thesis. NLRs are a broad family of cytoplasmic soluble receptors that generally share three common characteristics: a C-terminal LRR region, that constitutes the ligand detecting domain of the protein, an N-terminal responsible for protein-protein interaction, most often via a caspase recruitment domain (CARD) or pyrin domain (PYD), and an intermediate nucleotide-binding NOD participating into self-oligomerisation of the NLRs⁷. NLRs, similarly to TLRs, detect a wide range of PAMPs or DAMPs and their signalling culminates into two types of responses: production of various pro-inflammatory cytokines via activation of NF- κ B or activator protein 1 transcription factors, or activation of the inflammasomes, cellular platforms that mediate caspase-1 activation by cleaving pro-caspase-1, resulting in cell death by pyroptosis and production of IL-1 β and IL-18 pro-inflammatory cytokines⁷⁻⁹. Another well-established family of cytosolic PRRs is the RLRs family, comprised of three members: RIG-I, MDA5 (melanoma differentiation-associated protein 5) and LGP2, which detect cytosolic RNA. While LGP2 acts by directly modulating RIG-I and MDA5 signalling, the latter two receptors exhibit a CARD domain that allows them to interact with the downstream adaptor mitochondrial antiviral signalling protein (MAVS) and thereby signal via TANK binding kinase 1 (TBK1) to activate IRF and NF- κ B transcription factors. They specifically bind to double stranded (ds)RNA, their activating ligand, via their C-terminal and central helicase domains, which also confer them the ability to self-oligomerise to increase signalling efficiency¹⁰. Finally, some cytosolic DNA sensors that don't fit in the above families have been described, most notably the inflammasome-forming proteins absent in melanoma 2 (AIM2) and related AIM2-like receptors (ALRs)^{11,12}, as well as interferon gamma-inducible protein 16 (IFI16)¹³ and cyclic GMP-AMP (cGAMP) synthase (cGAS), that will be discussed in more details below. The broad range of locations and ligands covered by PRRs implies that often, multiple PRRs become stimulated over the course of an infection, transformation or other. By integrating the received signals

through intermingled downstream signalling pathways, our innate immune cells can respond to each threat in a tailored manner.

One common layer of control between PRR signalling pathways is the use of supramolecular organising centres (SMOCs). This concept was coined to describe complexes triggered upon PRRs activation that, by increasing local signalling component concentrations, contribute to an increased response and can explain some all-or-nothing responses. SMOCs originally encompassed NLRs- or ALRs-triggered inflammasomes, TLRs-triggered myddosomes and filamentous MAVS triggered by RLR signalling complexes¹⁴. Interestingly, while it was initially proposed that the DNA sensor cGAS could bypass the need for SMOCs thanks to its more canonical use of a second messenger (cGAMP) and the downstream adaptor STING, later research showed that dsDNA-bound cGAS complexes could undergo liquid-liquid phase separation, creating membrane-less signalling hubs with enhanced enzymatic activity¹⁵. Also considering the propensity for STING to oligomerise upon activation¹⁶, it appears that SMOCs formation is a ubiquitous concept in PRRs regulation.

1.2 – Nucleic acids as target for PRRs

Nucleic acids are one prominent family of molecules that are at the crossroads of PAMPs and DAMPs. Due to their universal presence in living organisms, they allow for detection of a very large spectrum of pathogens upon infection. In addition, out-of-context host DNA is also a very efficient signal of danger-related cell homeostasis' rupture, as it can be released from the mitochondria or the nucleus into the cytosol or even extracellular space upon cellular damage or stress. It is hence not surprising that our cells are equipped with a broad variety of nucleic acid sensors. While various TLRs (TLR3, 7, 8, 9 and 13) allow cells to detect diverse forms of endolysosomal RNA or DNA, once nucleic acids reach the cytosol, they are out of range for the TLRs. There, RLRs react to dsRNA, while dsDNA can be detected by various cytosolic sensors, the two main ones being AIM2, that forms an inflammasome upon dsDNA binding, and cGAS, that then signals via the cGAS-STING pathway¹⁷, which we will focus on in the scope of this thesis.

The ubiquitous presence of nucleic acids and their receptors also implies that RNA- and DNA-sensing innate immune pathways have to be very tightly regulated at multiple levels to avoid aberrant inflammation and autoinflammatory disorders. Interferonopathies are a good example of pathologies arising when these pathways activate independent of exogenous nucleic acid, resulting in aberrant IFN I production¹⁸. Among the regulation strategies are self-versus non-self-recognition, compartmentalisation of endogenous nucleic acids in the nucleus

and mitochondria, or expression of endonucleases in the cytoplasm¹⁰, that we will cover in a bit more details below. Finally, nucleic acid sensing pathways are directly regulated at the level of their players by protein-protein interactions and SMOCs formation, feedback loops, intracellular trafficking, protein level regulation, post-translational modifications (PTMs) or conformational changes. These systems are often intermingled and constitute very complex regulatory networks.

1.3 – The cGAS-STING axis

We will focus here in more detail on the main DNA-sensing pathway at the core of this thesis, the cGAS-STING pathway (**Fig. 1.1**). A particularity of cGAS as a PRR is that it functions upstream of an adaptor protein, STING (sometimes named ERIS, MITA or TMEM173), which can also directly act as a PRR itself. Indeed, the cGAS-STING pathway works on at least two levels: upon DNA-recognition by cGAS (independently of its origin or sequence), the production of a secondary messenger, cGAMP, is catalysed^{19–21}. This CDN can then be recognised by the adaptor protein STING, an endoplasmic reticulum (ER)-based membrane protein also able to directly bind CDNs from bacterial origin^{22–24}. Upon activation, STING translocates to the ER-Golgi intermediate compartment (ERGIC) and then the Golgi, where it initiates a TBK1-dependent downstream phosphorylation cascade culminating with phospho-IRF3 dimers translocating to the nucleus to launch the type I interferon (IFN I)-related antiviral response. Additionally, STING activation also leads to downstream autophagy and NF-κB activation^{25,26}. One of the strengths of the cGAS-STING pathway, which also makes it complex to study, is that this multi-level architecture allows numerous regulatory mechanisms to fine-tune the immune response and adapt it to a range of triggers.

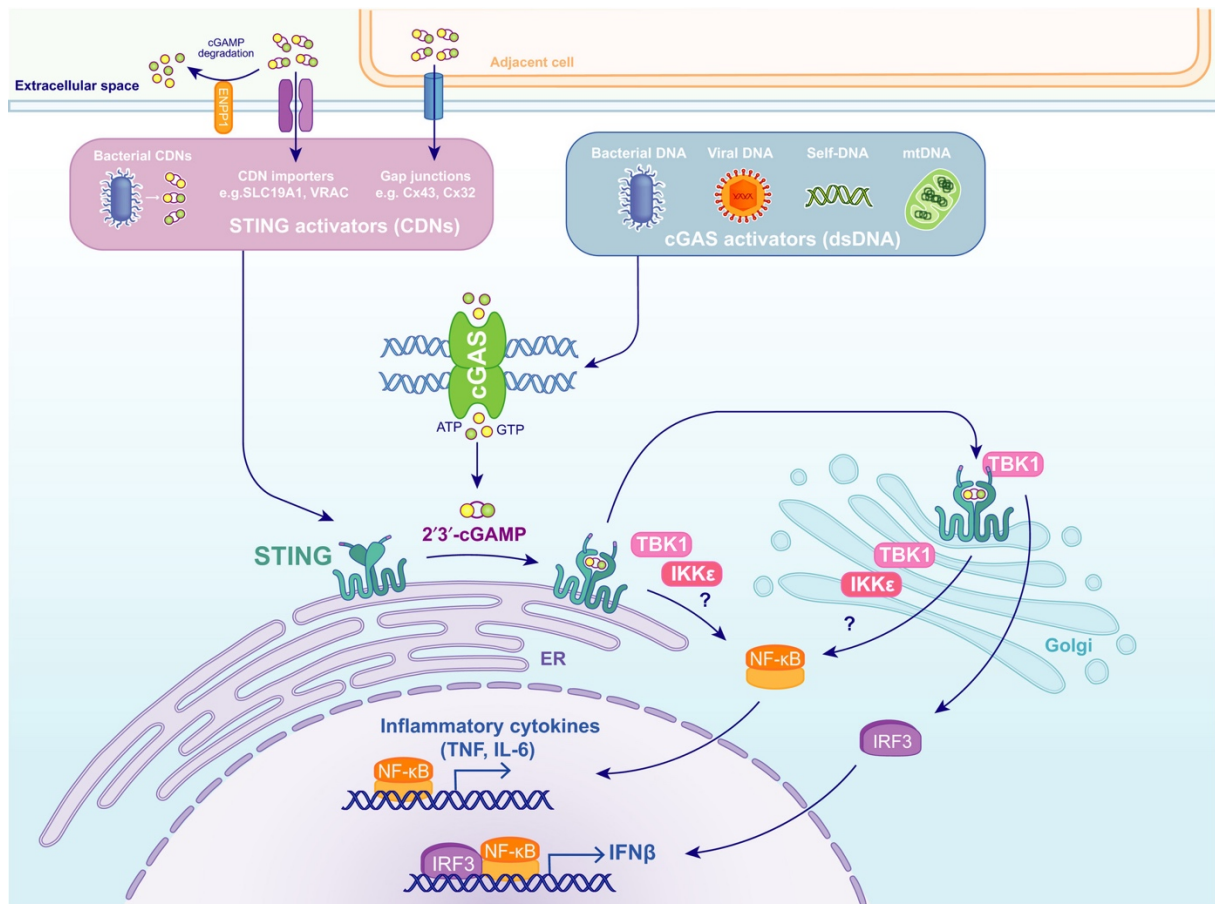


Figure 1.1 | The cGAS-STING pathway. As cGAS detects dsDNA independently of its origin, there are multiple sources of cytosolic DNA that can activate cGAS activity. In particular, pathogens can be sensed via cGAS recognition of bacterial or viral DNA, while if exposed in the cytosol self genomic DNA or mtDNA can also act as a trigger for cGAS activation. Once bound by dsDNA, cGAS catalyses formation of 2'3'-cGAMP, the endogenous second messenger that activates STING. STING can also be activated by bacterial CDNs (e.g. c-di-AMP, c-di-GMP). Gap junctions and CDN transporters can amplify cGAS response by spreading CDNs between cells. In addition, 2'3'-cGAMP can be degraded in the extracellular space via the membrane-bound enzyme ENPP1. Once activated by CDN binding, STING traffics to the Golgi and activates the TBK1-IRF3 axis leading to type I IFN production. STING also activates NF-κB activity via TBK1 and IKKε to promote expression of proinflammatory cytokines. © Figure and legend reproduced from Balka and De Nardo, 2021 (ref²⁷).

1.3.1 – cGAS: a highly conserved ubiquitous innate immune receptor

After the identification of the adaptor STING (see details below) in 2008^{22,28}, the nucleic acid-related immunity field was actively seeking the missing piece linking DNA detection with STING and downstream IFN I activation. While intracellular DNA-sensing by AIM2 was found to trigger downstream inflammasome activation, leading to proinflammatory IL-1β or IL-18 production and cell death^{11,29}, a major upstream IFN I activator was still missing. Some rather context-specific sensors such as DAI, IFI16, or DDX41, had been identified^{13,30,31}, but they appeared redundant and non-essential for cytosolic DNA detection¹⁷, and a more central

player was still to be discovered. Starting in 2013, several groups identified cGAS as the master receptor upstream of STING and that binds dsDNA via its sugar-phosphate backbone, independently of its origin or sequence^{32,33}. DNA-binding activates cGAS, producing the secondary messenger 2'3'-cGAMP, which binds to STING and triggers downstream signalling.

Structural insights in cGAS explain these characteristics. The enzymatically active site of the 60 kDa protein is a highly conserved nucleotidyl transferase domain. It is formed by two lobes surrounding a cleft. Around this domain, the preceding N-terminal consists of a series of 150 poorly conserved unstructured residues, while the rest of cGAS C-terminal contains three DNA-binding sites allowing for interaction with the sugar-phosphate backbone of dsDNA^{33–35}. Upon binding of DNA by cGAS, the catalytic pocket gets rearranged, leading to activation of the nucleotidyl transferase domain and 2'3'-cGAMP synthesis. Furthermore, DNA binding leads to dimerization of cGAS around two DNA strains, forming a 2:2 minimal complex unit in which one DNA strain interacts with DNA-binding site 1 of the first cGAS and DNA-binding site 2 of the second cGAS, while the second DNA strain occupies site 2 of first cGAS and site 1 of second cGAS^{36,37} (**Fig. 1.2**). Clustering is further enhanced through multivalent interactions with DNA via both the positively charged N-terminal domain of cGAS and the third DNA-binding site on each cGAS protein. These interactions lead to a liquid-liquid phase-separation that optimises enzymatic activity and increases cGAMP production^{15,35}, efficiently amplifying the signal even before reaching the adaptor protein STING.

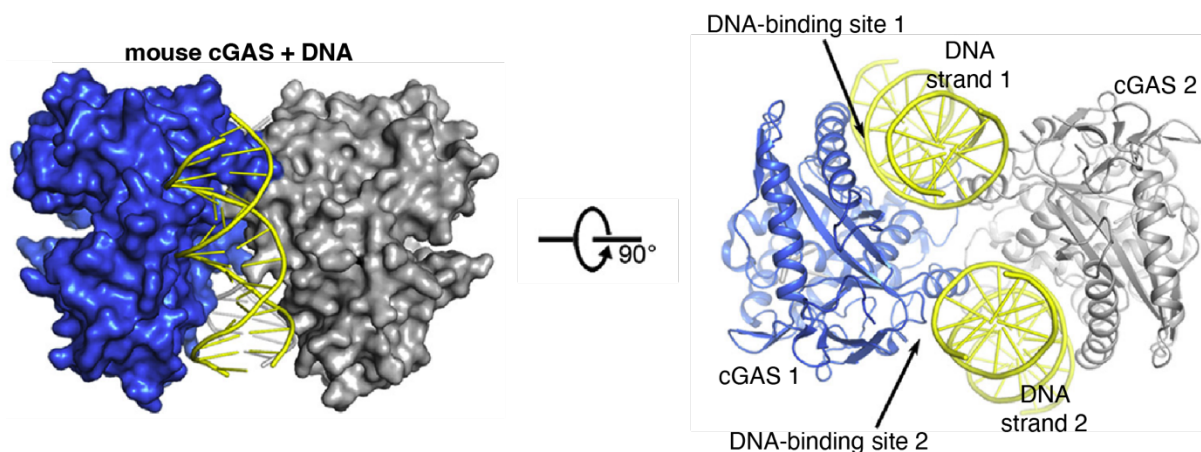


Figure 1.2 | cGAS forms a 2:2 complex with DNA. Crystal structure of mouse cGAS in complex with a 16 bp dsDNA. Each asymmetric unit contains one 2:2 complex, composed of two protein molecules and two DNA molecules. Two perpendicular views are shown. © Figure and legend reproduced and adapted from Zhang et al., 2014 (ref³⁶).

Remarkably, the Human Protein Atlas shows that, in contrast to AIM2, cGAS is expressed in a broad array of cell types, not just immune specific cells³⁸, adding to its “sentinel” DNA-detector role. Furthermore, cGAS is highly evolutionarily conserved. In fact, cGAS homologues can be found in a broad range of animal species, from insects and anemones to mammals^{39–41}, and cGAS-like archaic immune nucleotidyl transferase proteins can even be found back in bacteria^{42,43}. Of note, these more distant cGAS homologues don’t directly bind DNA, although they seem to be involved in resistance to viruses or bacteriophages. Indeed, direct DNA-binding by cGAS only appeared in vertebrates, and co-evolved with STING C-terminal tail (CTT) and the development of anti-viral IFN I signalling^{41,44,45}. Nonetheless, taken together, these discoveries confirm the view of cGAS as a ubiquitous primary innate immune viral sensor.

1.3.2 – Downstream of cGAMP: the adaptor protein STING

Immediately downstream of cGAS and cGAMP lays STING, a transmembrane ER-residing protein shown to be a major activator of the antiviral IFN I pathway. STING has a particularly high affinity for 2’3’-cGAMP in addition to detecting CDNs of bacterial origin^{22,28}. Furthermore, multiple chemical compounds have now been identified to act as STING agonists, sometimes in a species-specific fashion^{46–50}. Interestingly, STING, similarly to cGAS, has been found to be ubiquitously expressed³⁸ and highly conserved, with homologues in drosophila, sea anemone, choanoflagellate and even bacteria, although the downstream pathway activation, described below, varies throughout evolution^{41,44,51,52}.

STING possesses a short cytosolic N-terminal tail followed by four transmembrane helixes and a bigger C-terminal domain, including a dimerization interface, the ligand-binding domain and a CTT. In their resting state, STING molecules form dimers at the ER and their C-terminal cytosolic heads are “interleaved”. Upon ligand-binding, the heads go through a 180° rotation which, through a not fully resolved mechanism, enables STING to traffic towards the Golgi^{16,53–55} (**Fig. 1.3**). Despite intensive research about the events at work during this step, there is still no clear consensus as to the exact sequence and causality of downstream activation. Identified mechanisms and regulators will be discussed in more details below.

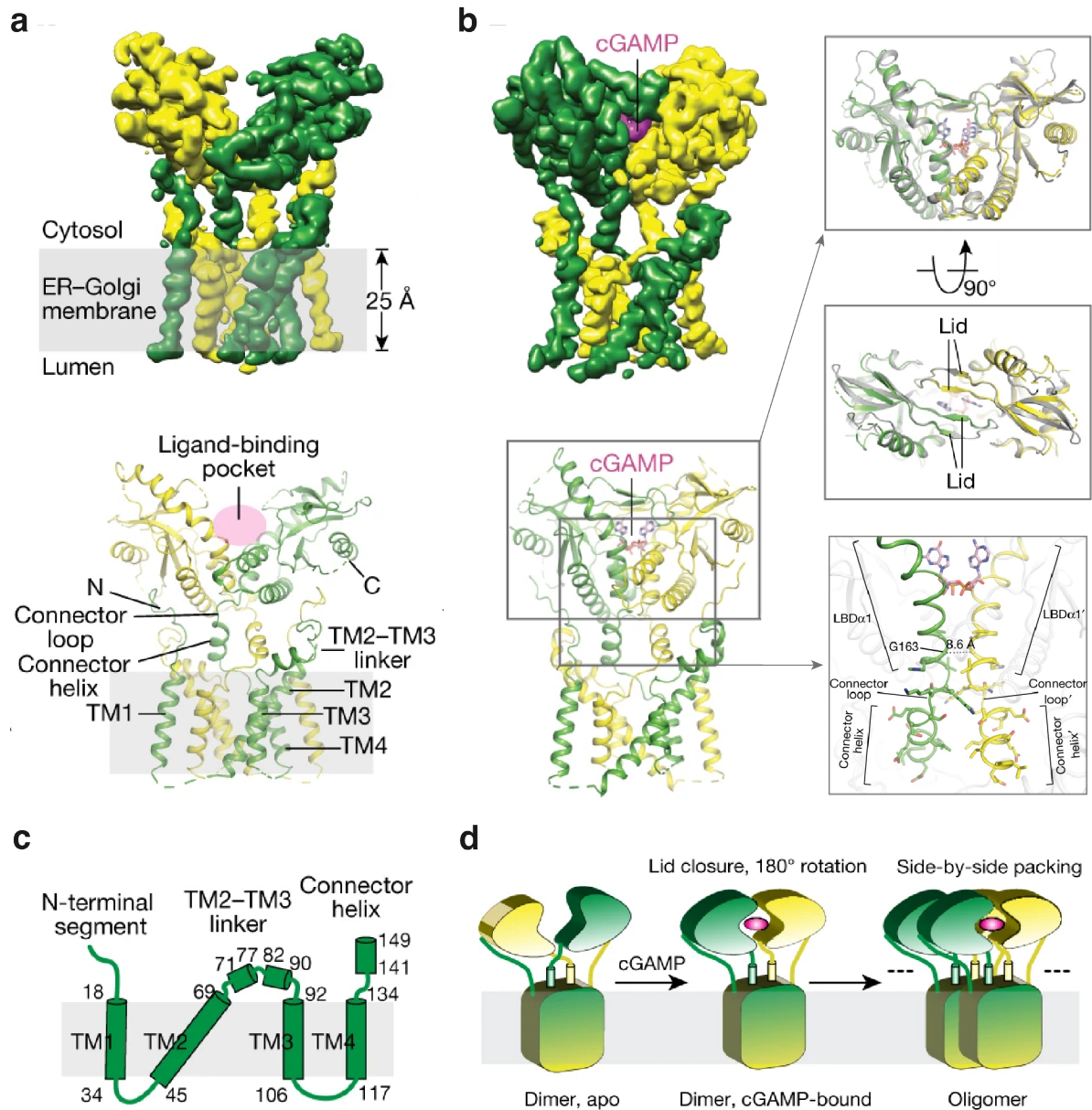


Figure 1.3 | Structure of STING at rest (human STING) and upon ligand-binding (chicken STING). **a**, Structure of full-length human STING in the apo state: side view of the cryo-EM 3D reconstruction (top) and its cartoon representation (bottom). The two subunits in the dimer are coloured in yellow and green. TM — transmembrane helix. **b**, Structure of full-length chicken STING bound to cGAMP: side view of the cryo-EM 3D reconstruction (top left) and cartoon representation of the structure (bottom left). The squared excerpts show (top) comparison of the cGAMP-bound ligand binding domain (LBD) in full-length STING with that of STING that lacks the transmembrane domain (PDB code 4KSY, shown in grey), in two different orientations, and (bottom) the 180° rotation of the LBD relative to the transmembrane when converting from the inactive to the active state of STING. The connector and LBDα1, which are at the centre of the rotation, are highlighted. **c**, Topological diagram of the transmembrane domain of human STING. **d**, Cartoon model of cGAMP-induced conformational changes and oligomerisation of STING. © Figures and legends reproduced and adapted from Shang et al., 2019 (ref⁵).

Upon reaching the trans-Golgi network, STING oligomers, whose heads form a binding platform, recruit TBK1. Several TBK1 molecules then cross-phosphorylate each other, leading to their activation. Active TBK1 can then phosphorylate STING, including at serine 366⁵⁶. As phospho (p)-S366 is part of the recognition motif of the transcription factor IRF3, this in turn allows the recruitment and phosphorylation of IRF3 by TBK1. This cascade leads to the dimerization of p-IRF3 that subsequently translocates into the nucleus to activate downstream IFN I signalling⁵⁷. In parallel, STING activation also leads to NF- κ B activation and downstream TNF α and IL-6 production, as well as autophagy^{58–61}. While the steps leading to STING activation are better and better understood, pathway shutdown is less well defined, with some evidence suggesting involvement from lysosomes⁶². The details of this end-signalling and shuttle towards lysosomal degradation is one of the major focuses of the present thesis (see **Chapter 3**).

1.3.3 – STING-independent regulation of the cGAS-STING pathway

Distinct mechanisms contribute to the regulation of the cGAS-STING pathway at nearly all levels. Upstream of the pathway itself are regulatory mechanisms governed by nucleases: cells possess several of those, the main ones being TREX1 (three prime repair exonuclease 1) and DNase II, constantly degrading cytosolic or lysosomal dsDNA, respectively. Those enzymes prevent accumulation of out-of-context DNA, digesting it at a rate that allows to counteract homeostatic dsDNA release into the cytosol or lysosomes. Imbalance in this system is either a sign of cellular damage, pathogenic DNA entry, or caused by nucleases' defects, which lead to interferonopathies by constantly stimulating the IFN I pathway^{63–67}. Downstream of DNA level modulation, each player of the pathway has its own additional regulatory mechanisms.

1.3.3.1 – cGAS-specific regulation

It was long considered that the first and most obvious cGAS activation control mechanism was compartmentalisation. Indeed, cGAS cannot distinguish self- from non-self-DNA, unlike other nucleic acid sensors—for example, TLR9 recognises unmethylated CpG-rich DNA, a motif prevalent only in bacterial DNA⁶⁸. However, cGAS had been described as a cytosolic DNA sensor, and under normal conditions, DNA is constrained inside the nucleus and mitochondria. Hence, it was thought that cGAS would only react to cytosolic DNA, which should either be a sign of cellular stress (nuclear or mitochondrial leakage) or be of pathogenic origin^{33,36,44,69}. After cGAS was shown to be highly localised in the nucleus as well⁷⁰, the mystery of its control grew thicker. How cGAS could remain inactive when present in the nucleus or during mitosis

remained understood. Two distinct nuclear-specific inhibition mechanisms of cGAS were finally discovered: cGAS is inhibited upon interaction with nucleosomes^{71–76}, and in addition, a nuclear chromatin architectural protein, barrier-to-autointegration factor (BAF), can compete for cGAS binding on DNA⁷⁷. Combined, these two mechanisms can explain both the absence of cGAS signalling during mitosis as well as a compartment-specific inhibition of basal cGAS signalling inside the nucleus.

Additional mechanisms are at play in regulating cGAS activity, such as various PTMs, including ubiquitination, phosphorylation, SUMOylation and glutamylation, that can impact cGAS stability, activity or DNA-recognition ability^{78–85}. Furthermore, cGAS can be cleaved by caspases activated downstream of inflammasome signalling⁸⁶, giving an example of the numerous possible interplays between the several arms of our innate immunity.

1.3.3.2 – cGAMP-specific regulation

As mentioned above, the role of cGAS in the cGAS-STING axis is the production of 2'3'-cGAMP. This CDN differs from canonical bacterial CDNs, that possess two 3'5'-phosphoester bonds, in that it is asymmetric and possesses one 2'5'-phosphoester bound. Due to this specific non-canonical linkage, 2'3'-cGAMP can bind STING with an increased affinity compared to bacterial CDNs and is hence able to potently trigger downstream IFN I signalling and NF- κ B pathway activation^{20,21}. Additionally, the secondary messenger 2'3'-cGAMP can be transmitted from activated cells to their neighbours via GAP-junctions⁸⁷ and virions^{88,89}, or by uptake of extracellular cGAMP^{90,91}, rendering this detection system particularly efficient to prevent or slow viral infection spread.

While cGAMP spread amongst threatened cells is important for innate immune defence, tight control is needed to be able to shut down signalling to prevent overactivation. Surprisingly, to date, no intracellular protein able to degrade 2'3'-cGAMP has been identified. The only 2'3'-cGAMP-degrading enzyme identified so far in mammalian cells is ENPP1, an extracellular membrane-anchored phosphodiesterase⁹². Similarly, while cGAMP secretion has been described in some cancer cell lines⁹², no unique exporter has been identified to date¹⁰. However, several reports mention LRRC8 as a channel through which cGAMP could navigate between the intra- and extracellular spaces^{93–96}. Whether those are the main players regulating cGAMP level or whether another protein able to sequester or degrade cGAMP intracellularly will one day be identified remains an open question.

Of note, such enzymes have recently been identified in viruses: poxins have been shown to be able to efficiently degrade 2'3'-cGAMP⁹⁷. This is relevant in immune escape, as viruses can use those poxins to attenuate IFN I response upon infection. Furthermore, poxin

homologues have been identified in the genomes of butterflies and moths, as well as in the insect-specific baculoviruses, but not in mammalian genome, indicating that they might originate from cGAS-STING escape mechanisms having evolved outside of the mammalian world. In any event, the conservation of poxins across viruses targeting different hosts strongly suggests that the cGAS-cGAMP-STING axis evolved as a primordial antiviral defence mechanism^{97,98}.

1.4 – STING-specific regulation

1.4.1 – STING-mediated IFN I signalling

STING has been observed to rapidly relocate inside the cell upon activation, and it appears that its spatiotemporal localisation is key to its signalling. One of the main pieces of evidence that STING regulation heavily relies on trafficking is given by two subsets of interferonopathies: STING-Associated Vasculopathy with onset in Infancy (SAVI) and COPA syndrome. Both autoinflammatory diseases have been associated with aberrant STING-dependent IFN I activation.

Phenotypically, SAVI is a highly severe autoinflammatory disease leading to skin rashes, finger tips necrosis, pulmonary fibrosis and ultimately death in young patients. Genetically, it is caused by a set of single point mutations in STING that lead to constitutive trafficking towards the Golgi, which bypasses the need for CDNs for activation. The SAVI-causing mutations identified to date are: V147M/L, N154S, V155M, G166E, C206Y, G207E, R281Q/W, R284G/S, and the combined mutations S102P-F279L^{26,99–105}. Interestingly, most of these mutations are grouped in key structural motifs associated with STING oligomerisation. Some are grouped in the connector helix (amino acid (aa) 141-149) and connector loop (aa 150-156), a region that links the fourth transmembrane domain with the first helix of STING's ligand-binding domain (starting at aa 157). These connector regions are responsible for the 180° twist of STING ligand binding-domain heads (**Fig. 1.3**) that enables STING to further oligomerise and traffic. This rotation, which is ligand binding-dependent in STING wild-type (WT), is thought to become constitutive in these STING mutants. Most of the other described mutations (from aa 206 to aa 284) are shown in STING structure to be near the 273-280 loop, which is a crucial part of STING tetramer interface, important for higher order multimerization of STING dimers. This loop is normally structurally impacted by STING's heads untwisting upon ligand-binding, in a way that permits tetramerization. Mutations here could bypass this checkpoint and allow for tetramerization independently of the ligand-binding domain rotation, removing the need for upstream activation⁵⁵. In parallel, another group also observed STING

oligomerisation upon activation and described the formation of stacks of STING dimers necessary and sufficient for efficient trafficking and activation. They showed that the oligomeric STING fibres are consolidated by di-sulfide bridges between their cysteine 148 (ref¹⁶), a cysteine that lays in the structural key connector helix of STING⁵⁵. They also documented sequestration of STING unstructured CTT by the multimerization interface and showed that this interaction was lost with STING R284S. This suggests that the SAVI mutations identified between aa 206 and aa 284 could be preventing self-CTT sequestration, rendering constitutively available the multimerization interface and priming STING for self-aggregation¹⁶. Together, these results strongly suggest that SAVI mutants all induce conformational modifications that enable STING to oligomerise and traffic downstream in absence of ligand.

In COPA syndrome, a mutation in α -COP, a constitutive player of the coat protein (COP)I machinery usually responsible for shuttling proteins back from the Golgi to the ER, prevents STING retrograde trafficking and creates an imbalance in STING levels at the Golgi. Patients suffering from this syndrome generally fare slightly better than SAVI patients, probably owing to various degree of basal cGAS activation, and hence variable levels of STING sent to the Golgi¹⁰⁶. The discovery of this syndrome provided insight to the cGAS-STING community that there is low-level basal cGAS/cGAMP activation, yielding some degree of cycling of STING from the ER to the Golgi and back. While under normal conditions, STING is shuttled back without having time to signal downstream, α -COP mutation blocks STING in the Golgi, where it remains free to signal. Thus, similarly to what is observed in SAVI, the accumulation of STING in the Golgi is triggering interferonopathy^{107–110}.

Together, insights from SAVI and COPA patients emphasise how trafficking towards the Golgi is sufficient to activate STING downstream signalling¹⁰⁶. Combined with the structural insights on STING, the SAVI mutations tend to indicate that STING oligomerisation is key to this Golgi trafficking and potentially sufficient to trigger downstream IFN I activation^{16,26,55}.

It is also interesting to note that not all ligands induce the exact same conformational changes, as the angle in STING dimer's heads can vary. These different angles prevent proper stacking of STING molecules with one another, a mechanism by which several STING agonists can inhibit each other. Indeed, if the secondary agonist blocks STING dimers with a distinct head-head angle compared to the primary activator, then this dimer conformation is not compatible with the extending STING stack generated by the primary activator. This is exemplified with cyclic di-GMP, a STING agonist that acts as an inhibitor in presence of cGAMP¹⁶. Interestingly, some synthetic STING agonists, like DMXAA or non-CDN cGAMP-analogue SR-717, induce a "closed" STING activated conformation (similar to that induced by 2'3'-cGAMP)¹¹¹, while others, such as diABZI, activate STING in an "open" dimer conformation

(similar the one induced by cyclic di-GMP)^{48,112}. The exact impact of these differences is not understood yet, but both conformations, as long as they are not mixed together, can trigger high-degree of STING activation and downstream signalling.

Considering how critical STING ER-to-Golgi trafficking is in activation, it is not surprising that several STING regulators modulate this process (**Fig. 1.4**). The detailed impact on trafficking of all these partners will be described below (see **1.5 – STING trafficking in details: a journey through the cell**), but we will briefly recapitulate the main players here. While STING ER-to-Golgi trafficking is mediated by the canonical COPII transport system, including the Sar1 GTPase¹¹³, STING recruitment to the translocon-associated protein complex (TRAP) β complex, necessary for signalling, has been shown to depend on inactive rhomboid protein 2 (iRhom2)¹¹⁴. Furthermore, a STING-specific ER-anchor, stromal interaction molecule 1 (STIM1), that can only interact with ligand-free STING, has been proposed to prevent unwanted trafficking¹¹⁵. A STING ER exit protein (STEEP) has also been identified, that recruits a phosphatidylinositol (PI) 3 kinase, VPS34. Upon STING activation, VPS34 leads to the accumulation of PI 3-phosphate (PI3P) moieties in the ER membrane, increasing its curvature and thus favouring downstream trafficking¹¹⁶. Concomitant with arrival at the Golgi, STING can interact with the adaptor SURF4 to be directed back to the ER via COPI-mediated retrograde trafficking, a system that is defective in COPA syndrome patient due to a defective α subunit of the COPI complex^{108,109}. Once successfully in the Golgi, STING oligomers travel towards the trans-Golgi network (TGN), where they interact sequentially with TBK1 and IRF3 as described above to launch downstream IFN I response^{56,57,117,118}. Partners and mechanisms at play in further trafficking towards the lysosomes for degradation have been uncovered during the scope of research of this thesis and are the main focus of **Chapter 3**.

Like for most proteins, STING's stability or activity are prone to PTMs-mediated modulation. Early work on STING led to the identification of a number of ubiquitination sites, with K27-linked ubiquitination on lysines 137, 150, 224 and 236, and K63-linked ubiquitination on lysines 20, 150, 224 and 236, being associated with increased TBK1 recruitment and downstream signalling^{119,120}. In contrast, K48-linked ubiquitination on lysines 150 or 275 reportedly target STING for degradation, dampening its signalling^{114,121,122}. PTMs modulating STING activity are also linked with localisation, as they only happen in specific locations within the cell. A key modification is the phosphorylation of serine 366, which is the hallmark of STING activation upon TBK1 recruitment and necessary to recruit IRF3 for downstream IFN I activation⁵⁷. This phosphorylation event was shown to only occur in STING molecules forming oligomeric dimers stacks at the TGN^{56,123}. In addition to oligomerisation and TGN localisation,

palmitoylations on cysteine residues 88 and 91 are essential for STING activation¹²³. This was confirmed by the mode of action of the first identified specific chemical inhibitors of STING, nitrofuran derivatives, which specifically target cysteine 91, covalently modifying it and preventing palmitoylation. In cells treated with these inhibitors, trafficking could be observed, but downstream signalling was blocked¹²⁴. However, uncertainty remains as to the exact causative events between palmitoylation, oligomerisation and trafficking of STING. Indeed, while palmitoylation happens in the Golgi and was initially thought to allow clustering of STING¹²³, later studies showed that STING oligomers could be found in the ER upon trafficking inhibition by Brefeldin A (BFA) and that STING multimerization was essential to enable its trafficking towards the Golgi^{27,55,124}. Taguchi et al. proposed that these discrepancies could be explained by qualitative differences in ER and Golgi specific STING oligomers; palmitoylation would be a requirement only for the Golgi-located STING oligomers and efficient downstream recruitment of TBK1¹²⁵, but no experimental evidences currently supports this. Nevertheless, the current consensus remains that oligomerisation, palmitoylation and TGN localisation of STING are all essential for downstream IFN I signalling.

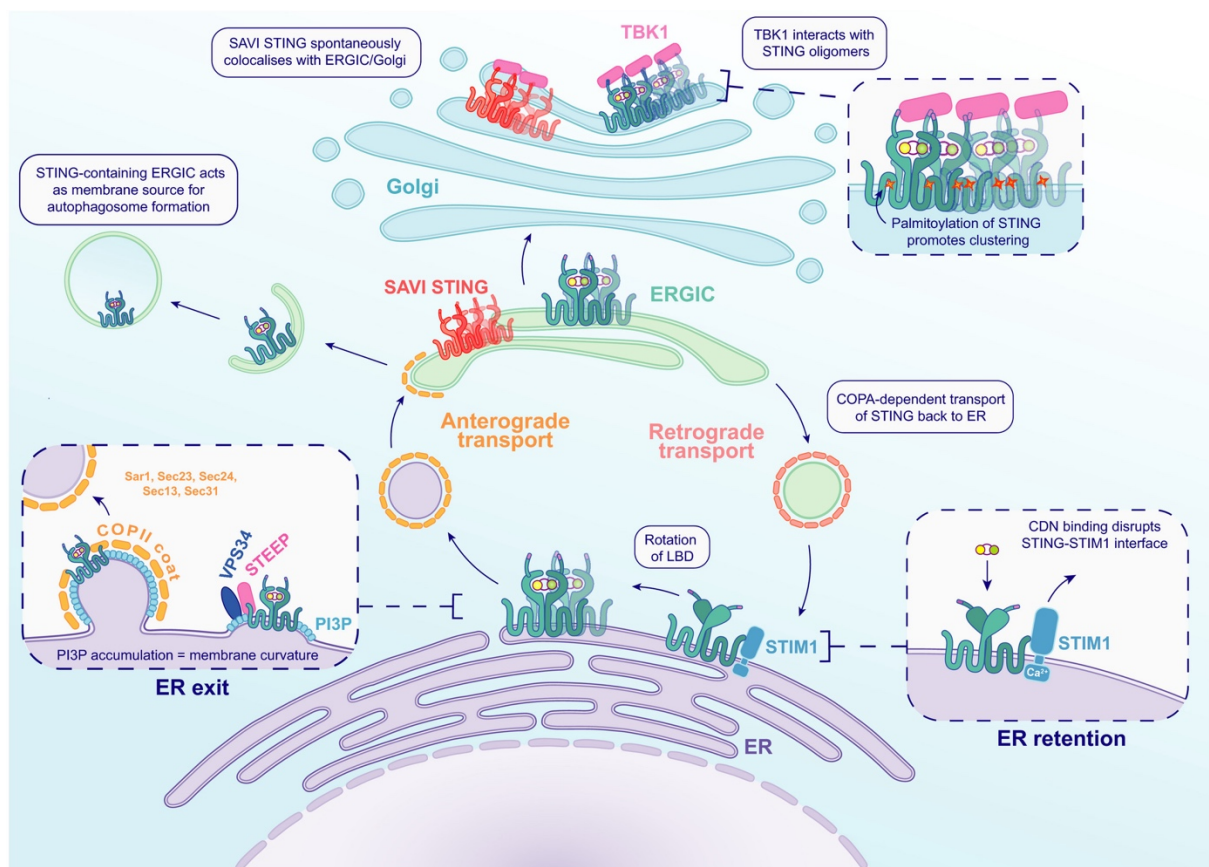


Figure 1.4 | STING undergoes trafficking from the ER to the Golgi following its activation. STING is localised to the ER membrane in resting conditions, where it is held via interactions with STIM1. Ligand binding induces conformational changes including a 180-degree rotation of the ligand-binding domain which interrupts interactions

with STIM1 promoting ER exit. STEEP facilitates the formation of PI3P species at the membrane via the kinase VPS34. This induces membrane curvature and promotes the formation of STING-containing COPII-coated vesicles which transport STING to the ERGIC/Golgi. Following STING activation, ERGIC membranes can provide a lipid source for formation of autophagosomes and the autophagy pathway. STING forms clusters at the Golgi promoted by the palmitoylation of STING, which allows TBK1 to interact for downstream signalling and activation of IRF3/IFN β . STING possessing autoactivating SAV1 patient mutations constitutively localises the ERGIC/Golgi. COPA-mediated retrograde transport of STING to the ER can also modulate the STING response. © Figure and legend reproduced from Balka and De Nardo, 2021 (ref²⁷).

Finally, STING is also regulated via strict control over its cellular level. However, this area is not yet fully understood. It has been shown that, depending on the activation pathway it follows, STING can either be directed to lysosomes directly from the TGN (see **1.5.2 – The end of the journey: Golgi to lysosomes** and **Chapter 3**) or via autophagosomes (see **1.5.3 – The side road: autophagy**). In addition to these primary mechanisms, proteasome-mediated STING degradation has also been documented as exerting control over its abundance. Indeed, iRhom2, one of the first identified regulators of STING, has been observed to recruit the deubiquitinase EIF3S5 to remove proteasome-targeting K48-linked ubiquitin moieties from STING, preventing its degradation. Silencing of iRhom2 increased K48-linked ubiquitination and decreased cellular level of STING, and both effects were rescued by treatment with the proteasome inhibitor MG132 (ref¹⁴).

1.4.2 – Besides IFN: NF- κ B-dependent STING signalling

Although the cGAS-STING pathway was identified as the missing link between cytosolic DNA and IFN I response, both sensors have been shown to elicit IFN-independent responses. Downstream of STING, the main secondary signalling module is linked with NF- κ B. In fact, evolutionarily, STING's ability to activate IFN I is a quite recent—vertebrate—invention, concomitant with cGAS direct DNA sensing as well as with the apparition of STING CTT^{45,126}. STING-dependent NF- κ B activation, on the other hand, appears much more ancient, being conserved in drosophila and probably sea anemone^{41,52,127}. While IFN I-based anti-viral immunity is now considered the main outcome of cGAS-STING activation, even in mammals, the NF- κ B-dependent responses still play a crucial role in the innate immune response¹¹². An emblematic example of this importance is found in mice models where STING carries an S365A mutation (equivalent to human S366A) selectively preventing binding and activation of IRF3 and hence specifically inhibiting the IFN I response, but allowing NF- κ B signalling. These mice exhibit intact resistance to herpes simplex virus 1 (HSV-1) virus infection, indicating that viral control in this particular case does not rely on IFN I response^{128,129}. Interestingly, multiple mouse tumour models were shown to co-opt STING activation, leading to IFN I-independent,

but STING-dependent, intratumoral T cell death and immune evasion¹²⁹. In a similar fashion, previous work had also revealed that STING activation can trigger NF- κ B-dependent, IFN-independent, block of T lymphocytes proliferation¹³⁰. There are also reports of tumour models where chromosomal instability-induced cytosolic DNA triggers cGAS-STING-dependent non-canonical NF- κ B (RELB-p52) activation, promoting tumorigenesis, tumour progression, metastasis and radioresistance^{131,132}. Indeed, the inhibition of canonical (RELA-p50 or IFN- β) by non-canonical (RELB-p52) NF- κ B signalling is a good example of the complexity of the signalling triggered downstream of STING, and underlines the potential impact of cell type specificities in balancing the immune outcome of a given stimulus¹¹². How this balancing is achieved remains a critical question within the field.

Another controversial point in IFN I-independent STING signalling revolves around the requirement, or not, for TBK1. TBK1 was primarily reported to be necessary for NF- κ B induction in a direct STING-TRAF6-TBK1 axis. In this model, STING recruits TBK1 at the Golgi via its CTT-located recruitment motif—similarly to recruitment of TBK1 upstream of IRF3 activation—, and TBK1 can subsequently interact with TRAF6 to activate NF- κ B¹³³. However, a later study showed that NF- κ B, in contrast to IRF3, could be activated by STING in a TBK1-independent fashion via the protein kinase IKK ϵ in myeloid cells¹³⁴. In fact, NF- κ B signalling downstream of STING was reported to sometimes partially, but not fully, rely on TBK1 (ref^{130,135}), while another study demonstrated a complete dependence on the STING CTT-located TBK1 binding motif¹³⁶. These contradictions might either be caused by cell-type specificities, or indicate a function for other proteins than TBK1 that would rely on the same amino acid in STING CTT. While one can only speculate on cell-cell distinctions (conferred for example by variations in the level of expression of interacting partners), inter-species variability is certainly linked at least partially with STING CTT. Indeed, this region of STING first evolved in vertebrates and appears to be a modular stretch comprised of multiple recruiting motifs. These have a huge impact on determining whether the outcome of signalling downstream of STING will be skewed towards activation of NF- κ B or of IRF3¹³⁵. Human STING is no exception to this rule and its CTT concentrates several recruitment motifs, namely the TBK1 and IRF3 recruitment motifs^{56,117,118}, and the newly identified AP-1 motif¹³⁷, covered in detail in **Chapter 3**. Some vertebrates, such as the zebrafish and related ray-finned fishes, have evolved a supplementary portion of the CTT that carries the motif PxExxD, which accounts for a substantial increase in NF- κ B signalling in a TRAF6-dependent, TBK-1 and IRF-3 independent, manner. Intriguingly, while adding the zebrafish signalling module (DPVETTDY) on human STING could enhance NF- κ B to similar levels, doing so while conserving the human IRF3-binding motif also increased downstream IFN I signalling¹³⁵. This

indicates that STING CTT is highly modular, and acquisition of small new motifs can reshape the innate immune response drastically. Furthermore, it underlines how specific single amino acid substitutions in the CTT have the potential to fine-tune the level of activation in downstream signalling^{135,136}. Indeed, in zebrafish STING, a mutation in the IRF3 recruitment motif (compared to the mammalian one) almost completely abolishes IRF3-mediated response, an evolution that could compensate for increased STING-induced inflammation caused by the NF- κ B enhancing cassette. Additionally, in bat STING, loss of S358 attenuates the IFN response, allowing the bats to coexist with a high number of viruses without overreaction of their innate immune systems, and likely contributing to their long life-span and propensity to constitute large viral reservoirs¹³⁸. Together, this area of research stresses the impressive versatility and modularity of the immune response downstream of STING and how small cell-cell or species-species differences can drastically impact and fine tune the activated modules and their signalling levels.

1.5 – STING trafficking in details: a journey through the cell

As discussed, STING activation is intimately linked with its trafficking from the ER to the Golgi^{26,107,123,125} upon activation and later to autophagosomes^{59,139} or to the lysosomes⁶² for degradation. Along these routes, some major canonical and non-canonical pathways are involved in helping STING properly traffic.

In many instances, trafficking events between endomembrane-based organelles in our cells are mediated by dedicated “coat proteins”. Those protein complexes fall in three main categories: coatomer complexes (COPI and COPII), adaptor protein (AP)-based coats (AP-1 to AP-5) and the retromer complex¹⁴⁰, named after the dense electron coat that the vesicles they form display in electron microscopy¹⁴¹. They all share basic characteristics: they are composed of membrane-proximal adaptors that recognise the specific cargo to be transported and outer scaffolding proteins building up the coat itself. These layers are recruited to the membrane thanks to specific lipids, notably phosphoinositides, and docking factors such as GTPases, all of which are further regulated by phosphoinositide kinases or phosphatases as well as by guanine exchange factors (GEFs) and GTPase-activating proteins (GAPs). Coats recognise their respective cargos via canonical, often linear, short sorting motifs. Upon recognition, cargos are bound and concentrated by the coat proteins, a phenomenon that triggers membrane curvature and initiates the budding process of the vesicle-to-be membrane region¹⁴⁰.

1.5.1 – ER-ERGIC-Golgi and back

1.5.1.1 – COPII brings STING to the Golgi

When STING was discovered, it was classified as an ER-resident member of the TRAP complex, as it happened to be found associated with ER translocon elements TRAP β - and Sec61b²⁸. Later on, it was shown that STING trafficking and downstream activation could be inhibited by *Shigella* protein IpaJ, a selective inhibitor of the human ADP ribosylation factor (ARF)-GTPase family²⁶. Moreover, knock-down (KD) of the small GTPase Sar1 was shown to abolish STING trafficking and IFN signalling¹¹³. Together, those results would fit with a model in which STING ER-to-Golgi trafficking is mediated via COPII. Indeed, COPII, the canonical ER-to-Golgi coatomer, is composed of the following minimal elements: Sec23/24 complex as cargo adaptor, Sec13/31 as scaffolds and the ARF/Sar1-family GTPase Sar1 as docking factor^{142,143}. The importance of COPII in STING trafficking was confirmed by groups showing that upon activation, STING interacts with Sar1, Sec24, Sec23B, Sec31A and Sec13^{59,144}. Furthermore, the Yip family protein YIPF5 appears essential to help recruiting STING to nascent COPII vesicles, as its depletion dampens STING trafficking while its overexpression results in stronger interactions between STING and Sec23B or Sec31A¹⁴⁴. Finally, STING-Sec24C interaction is strengthened upon cGAMP binding-induced conformational changes in STING dimers⁵⁹. This last discovery validates the model and offers an insight into how ligand-binding-triggered conformational change can be mechanistically linked with trafficking induction.

Despite the clear identification of COPII as the machinery transporting STING towards the Golgi, there is no single non-equivocal mechanism identified to this day that explains exactly what the most proximal trigger of STING ER-to-Golgi trafficking is. However, as various elements are piling up, it is tempting to propose a model in which ligand- or mutation-induced STING oligomerisation¹⁶ allows to liberate STING from STIM1-anchoring¹¹⁵ while favouring its interaction with STEEP and the associated local increase in membrane PI groups, promoting a budding-favourable membrane curvature¹¹⁶. The now freed STING dimers' stacks could interact with COPII adaptor heterodimer Sec23/24 and be concentrated, allowing for a cooperative and clustering-enhanced quick build-up of COPII vesicles, prompting STING oligomers' trafficking towards the ERGIC and the Golgi (**Fig. 1.4**).

1.5.1.2 – COPI retrieves STING back to the ER

As discussed above, important insights in STING localisation have been gained by the study of the interferonopathy triggered by the COPA syndrome. The main associated discoveries were the understanding of the detailed COPI-mediated retrograde trafficking of STING from

the Golgi back to the ER, as well as the notion that under homeostatic conditions, there seems to be some basal cycling of STING between the ER and Golgi and back without reaching a level at which this triggers IFN signalling^{106–110,145}. COPI, the coatome responsible for retrograde trafficking from the ERGIC and cis-Golgi back to the ER, is composed by the seven subunits α , β' , ϵ (the F-subcomplex, or “scaffold”-forming ones), and β , γ , δ and ζ (the B-subcomplex forming ones, that are closer inside the formed vesicle)¹⁴⁶. Its assembly is triggered by ARF1 GTPases¹⁴⁷. Of note, in COPI, in contrast to COPII vesicles and despite general structural homology, the inner (adaptor, here B-subcomplex) and outer (scaffold, here F-subcomplex) layers are not recruited sequentially, but rather all together, and all subunits are in close contact with the membrane and potential cargos¹⁴⁰. As such, although α -COP is technically part of the scaffold of the COPI vesicle, it is also responsible for direct interaction with potential cargos¹⁴⁸. This later point explains why mutations in this α subunit can impact cargo-recognition. Additionally, STING retrograde trafficking necessitates a Golgi-based intermediate, SURF4, that bridges the COPI subunit α -COP with STING, which lacks the canonical signal to be directly recognised by COPI. As SURF4 possess a dilysine motif that α -COP can recognise and is also able to interact with STING, it can act as an adaptor between STING and COPI to allow its retrieval towards the ER. Mutations in the WD40 domain of α -COP prevent recognition of SURF4 and hence block STING retrograde trafficking, causing its accumulation in the Golgi and the activation of downstream signalling responsible for the symptoms of the COPA syndrome^{27,108,109}.

1.5.2 – The end of the journey: Golgi to lysosomes

Once it sits at the Golgi, how exactly STING reaches the TGN remains unclear. Similarly, the mechanisms at play in post-Golgi trafficking have been poorly characterised, and the route towards degradation taken by STING to reach Rab7+ endosomes and finally lysosomes⁶² was unknown. However, the present thesis contains a paper where we describe how activated p-STING is recognised by AP-1 to be loaded into clathrin-coated vesicles (CCVs) and thereby directed for endolysosomal trafficking and consecutive lysosomal degradation¹³⁷ (see **Chapter 3**).

The canonical vesicular system bridging the TGN, plasma membrane and endolysosomal network relies on AP coat complexes 1 to 5. Similar to COPII, AP coat complexes are formed of membrane proximal adaptors conferring cargo and destination specificities to the transport vesicle¹⁴⁹—one of the heterotetrameric AP-1 to 5 proteins, each comprising a small, a medium and two big subunits—, and distal scaffolds ensuring its structural strength. Their recruitment is mediated by phosphoinositide species and the

GTPase ARF1 as docking factors¹⁴⁰. Out of these five coat complexes, AP-1 complex is responsible for the bidirectional Golgi-to-endosomes trafficking. It consists of AP-1 proteins—composed of the large subunits β 1-adaptin and γ -adaptin and of the medium one μ 1(A/B) and small one σ 1(A/B/C)—and clathrin triskelia¹⁴⁰—a triskelion is a building block constituted of three heavy and three light chains of clathrin, CHC and CLC, respectively^{150,151}—assembled under the impulsion of phosphatidylinositol 4-phosphate and ARF1 as docking factors^{152,153}. Cargo binding is mediated through recognition of the sorting signals Yxx \emptyset (where x is any amino acid and \emptyset any amino acid with a bulky hydrophobic side chain) by the C-terminal of AP-1 μ 1 subunit^{154,155} or recognition of the sorting signal [D/E]xxxL[L/I] by AP-1 σ 1 and γ -adaptin subunits^{156,157}. Details on how these players contribute to the journey of STING from the Golgi towards the lysosomes have been explored in **Chapter 3** of the present thesis¹³⁷.

1.5.3 – The side road: autophagy

In addition to Golgi departure towards the lysosomes, an alternative route, branching from the Golgi or even the ERGIC, has STING targeted for autophagy. In contrast to IRF3- and NF- κ B-mediated transcriptional response, this is a crucial and immediate cellular response triggered upon STING activation, that can have direct antiviral impact such as resistance to infection by HSV-1^{59,60}. Furthermore, tumour-associated replicative stress-induced cell death has been linked with DNA-cGAS-STING-triggered autophagy, and escape from STING-mediated autophagy is proposed to be necessary for tumours to prevent cell death and initiate growth¹⁵⁸. In addition, autophagy might have been one of the primordial function of STING, as distant STING homologues, such as the one found in sea anemone, do not trigger an IFN I response, but have been shown to trigger autophagy^{59,159}. It is also noteworthy that autophagy can be both an outcome or a regulatory mechanism for STING signalling. Despite this central role for STING-related autophagy, the exact molecular mechanisms at play remain an open area of research, and it seems to be yet another aspect of the pathway that can exhibit strong cell-type- or species-associated variations.

STING was first reported to be degraded by autophagy in LC3 positive compartments in an autophagy-related gene (Atg) 9a-dependent mechanism, independent of Atg7. Abrogation of this pathway by Atg9a deletion could enhance signalling downstream of the STING-TBK1 axis²⁵. Later reports found STING to also be negatively regulated by UNC-51-like kinase (ULK1/ATG1)-mediated autophagy. Of note, ULK1 activity was itself upregulated by cGAMP in a mechanism where cGAMP triggers both STING activation and its programmed degradation, forming an elegant negative feedback loop⁵⁸ similar to other regulatory networks that continue to be identified along the cGAS-STING axis. On the other hand, STING has also

been reported to directly interact with LC3 in a way that allows direct autophagy downstream of HSV-1- or cGAMP-triggered STING activation, and is solely dependent on ATG5, bypassing the requirement for other canonical autophagy-related proteins such as Atg9a, ULK, Beclin 1 or p62⁶⁰. Similarly, ULK- and VPS34-beclin-independent autophagy was shown to be initiated at the ERGIC by direct recruitment of activated STING to LC3 positive vesicles via WIPI2 and ATG5⁵⁹. Conversely, autophagy-mediated degradation of active STING has been reported to depend on p62/SQSTM1 to target ubiquitinated STING to autophagosomes, here again with an embedded feedback mechanism, as STING-activated TBK1 is the kinase responsible for p62 activation¹³⁹. Lastly, Fischer et al. demonstrated that STING was able to directly activate LC3B lipidation to trigger autophagy, using the WD40 domain of ATG16L, other canonical autophagy proteins being dispensable. However, surprisingly, they also found that the constituted autophagosomes had a single membrane and that the LC3B lipidation depended on V-ATPase, indicating that this autophagy mechanism was distinct from the ones triggering classically described double-membrane autophagosomes¹⁵⁹.

All these various paths followed by STING to get degraded by autophagy—cumulated with other degradation processes discussed in the present thesis—greatly emphasise how tightly STING activity is controlled and the numerous feedback and regulation mechanisms at play to ensure fine-tuning of the triggered innate immune response.

1.6 – Rationale and aim of the thesis

As nucleic acid-triggered innate immune activation has been proven to be crucial in many instances, most notably to resist viral infections and detect aberrant tumour-triggered cell growth¹⁰, the focus on the cGAS-STING pathway has been on the rise in the past decade. Potential therapeutic approaches centred around cGAS-STING pathway modulation flourish concomitantly with new fundamental discoveries about its regulatory mechanisms. The fields that can benefit from increased knowledge about detailed cGAS-STING molecular processes span a vast range of human health-related topics, from infection biology and vaccine development¹⁶⁰ to autoimmune and autoinflammatory diseases^{18,26,161}, but also cancer biology^{48,132} and aging-related pathologies^{162,163}. Indeed, in addition to better informing researchers on fundamental infection biology and cellular signalling in general, advances in the cGAS-STING field from the past years have led to numerous promising concrete applications. Among them are the use of CDNs, cGAMP mimetics or other STING agonists alone or combined with anti-tumour therapies to promote cancer regression^{48,111,164–167} or as vaccine adjuvant¹⁶⁰. On the other hand, inhibiting cGAS-STING-mediated signalling also

proved useful to reduce detrimental autoinflammation in various pathological settings such as SAVI, COPA, or other disease-related sterile over-inflammations^{161,168}.

In the present thesis, the focus is put on STING spatiotemporal localisation and the partners potentially involved in its regulation. Indeed, despite strong evidence connecting STING localisation to its activation status, the mechanisms of trafficking regulation were mostly unknown at the beginning of my doctoral studies. The work described here aims to decipher some of these molecular mechanisms and their impact on STING signalling. The main questions we address can be separated into two major axes: on one hand, we aim to better characterise the regulation mechanisms revolving around initial STING ER-to-Golgi trafficking upon activation. On the other hand, we also focus on STING late post-activation trafficking to elucidate which route can explain STING removal from the Golgi and signalling termination.

By extensively investigating the shuttling routes of STING inside the cell, we aim to contribute to the detailed understanding of cGAS-STING pathway regulation on a fundamental level. This knowledge is key to predict our innate immune response upon confrontation with some infectious agents, as well as to anticipate the development of tumours and their response to anti-cancer therapies. It can also prove central in comprehending the symptoms and evolution of autoinflammatory diseases. Altogether, by contributing to the fundamental research on STING, we also pave the way for the future development of clinically relevant treatments and therapeutic approaches, in particular for cancer patients or individuals suffering from autoimmunity-related disorders or complications.

Chapter 2 – STING ER-to-Golgi trafficking

2.1 – GFP-based tracking of mSting in HEK293T cells underlines the importance of the second transmembrane cytosolic loop in trafficking

In our quest to understand the spatiotemporal localisation of STING upon activation, we first focused on its trafficking from the ER to the Golgi. For this, we transduced HEK293T cells to constitutively overexpress EGFP-tagged mouse STING (mSting) WT (HEK293T^{GFP-mSting WT}). Indeed, HEK293T cells do not express endogenous cGAS or STING³², removing the possibility of interference from endogenous protein. In addition, a murine specific small-molecule chemical agonist of STING, 10-carboxymethyl-9-acridanone (CMA)⁴⁶, allowing for timed activation without the need for transfection of cGAMP or cGAS and DNA in the system, was readily available when the study was initiated, while no such compound existed for efficient activation of human STING at the time. We validated the phenotype of the newly developed cell line by observing the expected GFP-STING distribution in the ER at rest (diffuse cytosolic distribution with lower resolution microscopy) and the formation of a bright GFP-STING speck in the nuclear periphery upon activation, compatible with trafficking towards the Golgi^{22,123} (**Fig. 2.1a, b**). These cells thus constitute a suitable model to track STING by fluorescent microscopy upon pathway activation.

In parallel, we generated similar HEK293T cell lines with mutant constructs of STING. Indeed, we wanted to assess the impact of single mutations in STING transmembrane domain's second cytosolic loop (aa 70-91⁵⁵, at this point thought to encompass aa 68-87¹²³), as this region contains several highly evolutionarily conserved amino acids. We found that, in contrast to mSting^{WT}, mutants of highly conserved amino acids (mSting^{E69A} or mSting^{R76A}) were not at all (R76A) or less (E69A) able to be activated by CMA, as assessed by absence or reduction of trafficking to the Golgi upon activation. Furthermore, mutation at V73 (mSting^{V73A}), a non-conserved amino acid of the same loop, yielded an intermediary phenotype of observable but reduced trafficking (**Fig. 2.1a, b**). Together, these observations confirm that STING's second transmembrane cytosolic loop plays an important role in the regulation of trafficking.

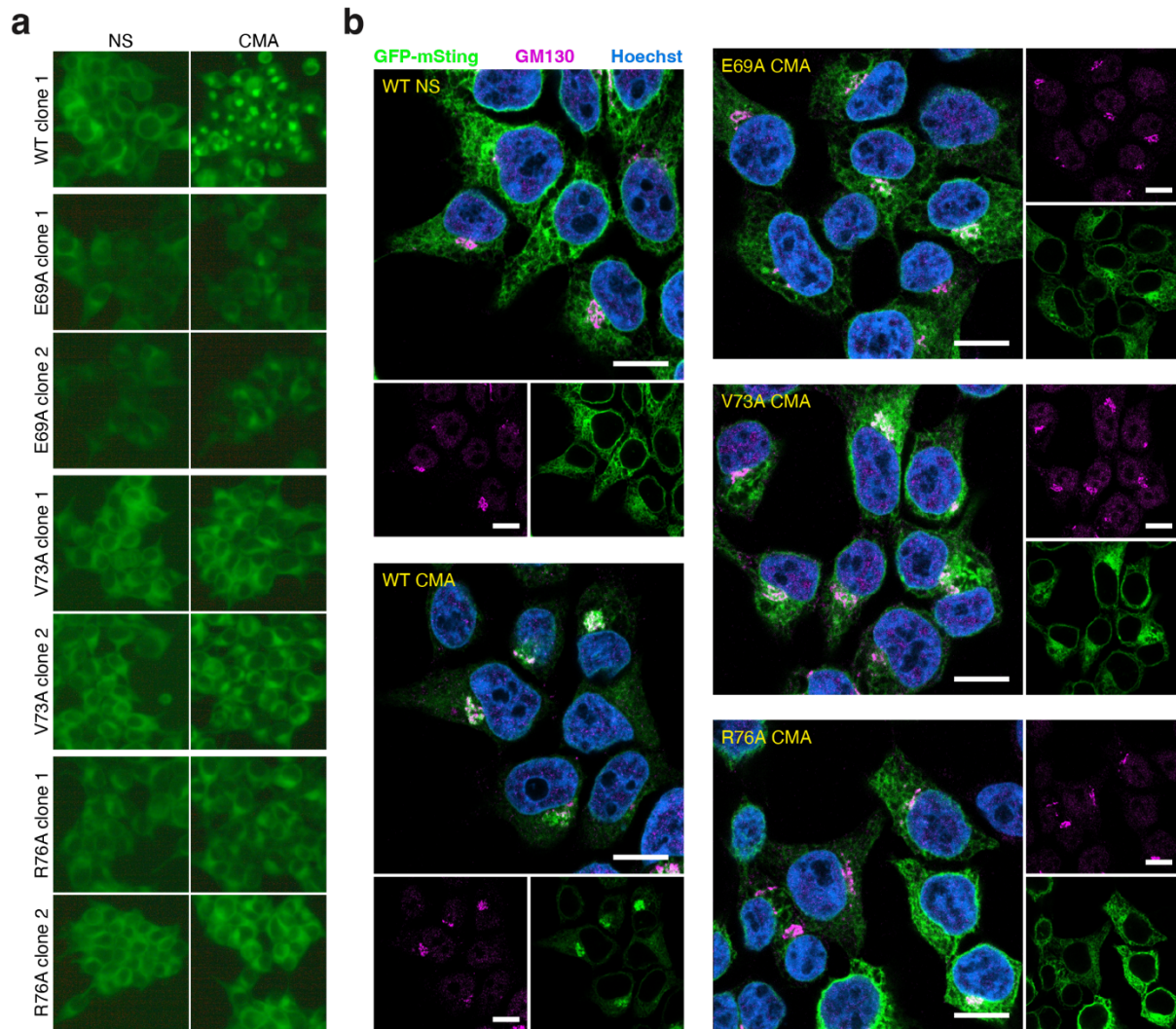


Figure 2.1 | HEK293T^{GFP-mSting} cells allow for visualisation of STING ER-to-Golgi trafficking and characterisation of non-trafficking STING mutants. **a**, HEK293T cells were stably transduced with GFP-mSting WT, R76A, E69A or V73A and clonally selected. Indicated clones were then stimulated for 5 hours with CMA at 312.5 $\mu\text{g}/\text{mL}$ or not. Live cells were then imaged with a fluorescent light microscope (40x objective). Representative images of technical triplicates from $n = 2$ independent experiments. Green – GFP-Sting. **b**, HEK293T^{GFP-mSting} stable lines expressing WT or mutant STING (WT and V73A clonal populations, E69A and R76A global pooled populations right after transduction and selection) were incubated for 2 hours with 250 $\mu\text{g}/\text{mL}$ CMA and then fixed and stained for GM130 (cis-Golgi marker) and with Hoechst (nuclear dye). Some GFP-STING WT cells were kept untreated as control. Scale bars 10 μm .

2.2 – Small chemical compounds screen to identify STING-specific ER-to-Golgi trafficking inhibitors

We then used HEK293T^{GFP-mSting} WT cells in a screen aimed at discovering small-molecule chemical inhibitors of STING trafficking and the downstream pathway. To achieve this, we worked with the Prestwick library¹⁶⁹, a small chemical compounds library containing, at the

time, 1280 FDA-approved small molecules with mostly well described modes of action (the catalogue of the exact library composition as used for this screen is in the **Appendix**). By using a known documented compound library, we hoped to both contribute to the basic understanding of the trafficking process (owing to known modes of action of potential inhibitory compounds) as well as to potentially repurpose readily available therapeutics for STING-related autoinflammatory diseases. For this high-throughput microscopy-based assay, HEK293T^{GFP-mSting^{WT}} cells were treated with the compounds, stimulated with CMA, imaged and assessed for trafficking by machine-learning. We used DMSO as negative control (normal trafficking) and BFA, a known STING trafficking inhibitor acting by inhibiting Arf-family GEFs and hence blocking all ER-Golgi trafficking in both directions¹⁷⁰, as a positive control (**Fig. 2.2a**). Machine learning-based automated analysis of the screen yielded 48 hits, from which 23 were confirmed by individual inspection. We classified them according to their known target (**Fig. 2.2b**) and excluded four out of five tubulin inhibitors, as they were likely to all exhibit similar effects and block general, not STING-specific, trafficking. We also kept only one hit per family of chemically extremely related compounds, further excluding protriptyline hydrochloride, digitoxigenin and digoxigenin. Finally, we chose to start by investigating only one of the two histone deacetylase inhibitors and to exclude the two ion channels inhibitors, yielding a final short-list of 13 hits (**Fig. 2.2b**).

These hits were first tested to assess their effect on general trafficking with the Retention Using Selective Hooks (RUSH) system¹⁷¹. Briefly, the system functions by co-expression of one “hook” protein—an ER-anchored streptavidin moiety—together with a “reporter” protein—an EGFP- and streptavidin-binding protein-tagged Golgi resident protein. Upon addition of biotin to the system, the reporter-hook interaction is disrupted by the biotin’s higher affinity towards streptavidin and the reporter protein is freed, hence launching trafficking towards the Golgi. We generated RUSH reporting cell lines by transducing HEK293T cells with the RUSH system plasmids (using truncated sialyltransferase and truncated mannosidase II as Golgi anchored proteins). We then treated these cells with the hits identified above before adding biotin to trigger trafficking (**Fig. 2.2c**). This revealed that, in addition to our positive control, BFA, only nocodazole and auranofin blocked the trafficking of both reporter proteins, while haloprogin blocked sialyltransferase trafficking only. The remaining compounds did not prevent trafficking to the Golgi. These results further reduced the number of STING-trafficking specific hits (as opposed to general ER-to-Golgi trafficking inhibitors) to 10 (**Fig. 2.2b, c**).

Of note, the phenotype triggered by nocodazole-mediated inhibition of STING trafficking was different from that observed with BFA or other compounds, with the formation

of multiple diffuse punctae instead of an unchanged homogenous diffuse distribution in activated versus stimulated cells. This was the case for both CMA- (data not shown) or DMXAA-triggered STING activation (**Fig. 2.2d**).

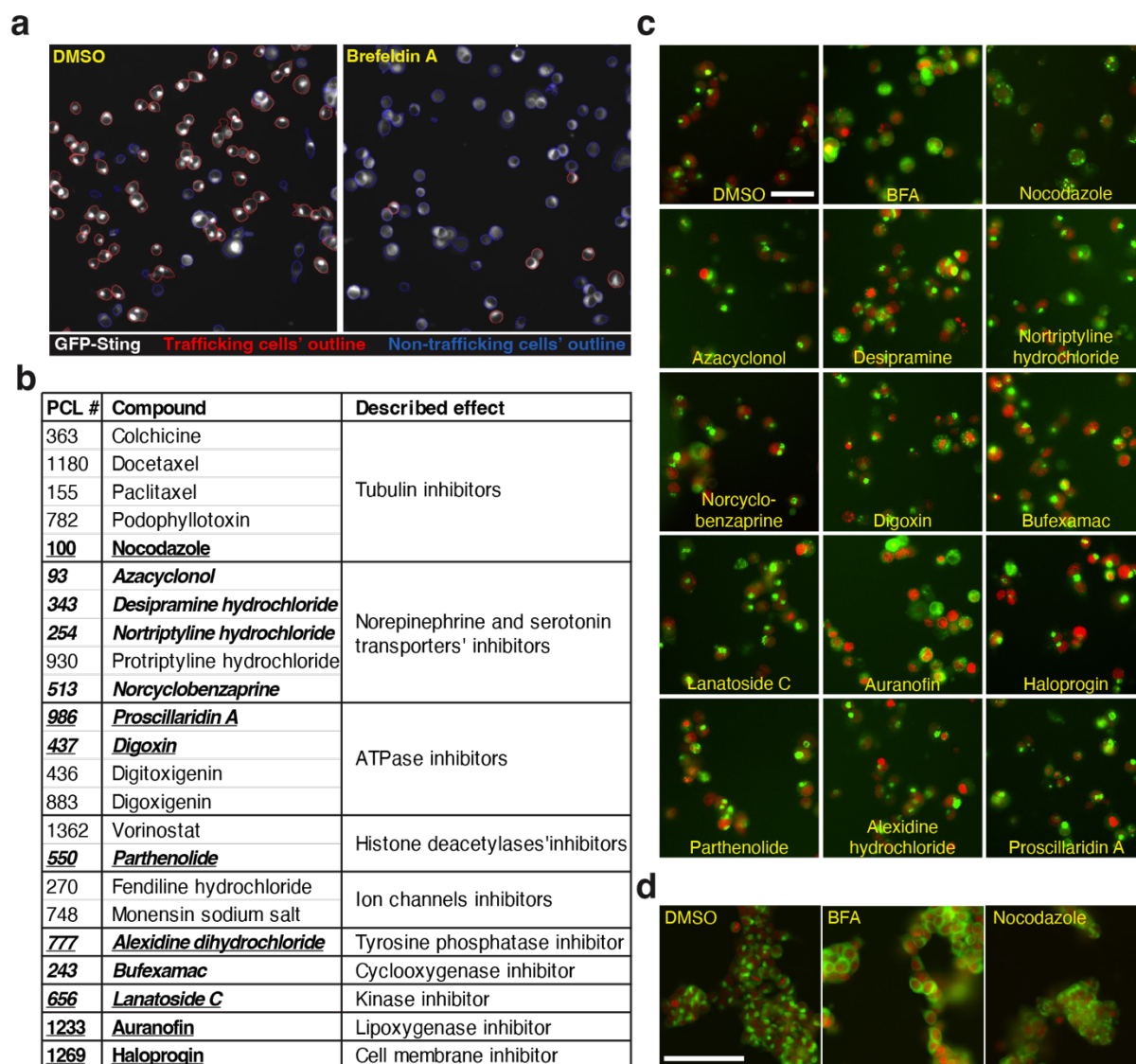


Figure 2.2 | Small chemical compounds microscopy screen used to identify STING trafficking specific inhibitors. **a**, HEK293T^{GFP-mSting} WT cells were used for a microscopy-based chemical compounds screening aimed at detecting molecules blocking STING trafficking. Briefly, cells were treated with compounds, stimulated with CMA and imaged on an IN Cell Analyzer 2200 microscope at 20x, segmented and finally classified as trafficking or not depending on the distribution of their GFP-Sting signal by machine-learning based algorithm. Representative images of a negative control (DMSO-treated cells trafficking normally) and a positive control (BFA-treated cells, trafficking blocked) analysis outputs from CellCognition 2-class classification are shown here. The screen was performed in duplicates for each of the 1280 tested chemical compounds and $n = 256$ wells of both controls distributed over the plates (8 per plate on 32 plates total). **b**, Table showing the positive hits (blocking trafficking) validated after visual verification of each candidate hit. The table contains the Prestwick identifier (used later in Fig.

2.3), compound's name and documented mode of action of all hits. Bold compounds were investigated further. Italicized ones proved to be specifically inhibiting STING trafficking, as assessed by RUSH. Underlined ones could also inhibit cGAS-dependent trafficking. **c**, Stable RUSH cell lines generated by transduction of HEK293T cells with GFP-tagged truncated mannosidase II were treated with the indicated STING trafficking-inhibitor potential hits and imaged 3 hours post biotin addition (IN Cell Analyzer 2200, 20x). Representative images of 1 out of $n = 3$ independent experiments. Red is the signal from the nuclear dye Draq5, green from the GFP constructs. Scale bar 40 μm . **d**, HEK293T^{GFP-mSting} WT cells were pre-treated for 2 hours with DMSO, BFA or nocodazole at 10 μM and then stimulated with DMXAA at 237 $\mu\text{g}/\text{mL}$ for 5 hours and imaged (IN Cell Analyzer 2200, 20x). Pictures are representative of $n = 3$ independent experiments. Red is the signal from the nuclear dye Draq5, green from GFP-Sting. Scale bar 100 μm .

In parallel, we assessed the capacity of these compounds to inhibit trafficking of STING after cGAS/DNA transfection. We first confirmed that in our assay conditions, control DMSO-treated HEK293T^{GFP-mSting} WT cells exhibited STING trafficking after cGAS transfection. This was the case, however, we observed “patches” of trafficking cells rather than homogenous activation throughout the well, probably caused by local variations of transfection efficiency associated with the capacity of activated cells to stimulate their neighbours. We then repeated this cGAS-dependent trafficking assay on compound-treated HEK293T^{GFP-mSting} WT cells and quantified trafficking. Quantification was done manually for this assay, because analysis with the previously-developed machine-learning algorithms—optimised on homogeneously chemically activated cells during the screen—failed at representing the observed “activation patches” phenotype. Interestingly, from the 13 original tested hits, 4 norepinephrine or serotonin transporters inhibitors and 1 cyclooxygenase inhibitor (**Fig. 2.2b**) failed to prevent cGAS-triggered GFP-STING foci formation, suggesting that they specifically block CMA-induced trafficking (**Fig. 2.3a, b**). We hypothesised that a stimulus-specific inhibition triggered by direct competition with CMA could explain this phenotype. Correspondingly, the chemical structures of the four norepinephrine or serotonin transporters inhibitors appear to share some features (2 aromatic rings) with xanthone, the central chemical compound from which both CMA and another STING agonist, DMXAA, are derived (**Fig. 2.3c**).

Next, we titrated the CMA dose used to stimulate the cells. In control DMSO-treated cells, higher CMA concentrations (500 or 1000 $\mu\text{g}/\text{mL}$) could slightly increase trafficking—from ~60% of the cells with our standard 250 $\mu\text{g}/\text{mL}$ stimulatory dose to ~75%—, while lower CMA concentrations yielded only mild or no trafficking (**Fig. 2.3d**). In compounds-treated cells, this dose dependent effect allowed us to classify the 10 STING-trafficking specific inhibitors in three distinct categories: i) digoxin, lanatoside C and proscillaridin A triggered low basal trafficking in the absence of CMA, but this level remained stably low upon CMA dose increase; ii) bufexamac, parthenolide and alexidine hydrochloride continued inhibiting trafficking at

increased CMA doses, but only partially (40-50% cells trafficking at 1000 $\mu\text{g}/\text{mL}$ CMA, versus 74% for DMSO-treated cells and 6% for BFA-treated ones); and iii) azacyclonol, desipramine hydrochloride, nortriptyline hydrochloride and norcyclobenzaprine showed no more inhibitory effect at increased doses of CMA stimulation (**Fig. 2.3d**), an observation corroborating the hypothesis of those inhibitors functioning as direct competitors for CMA.

Simultaneously, we also investigated the potential of a subset of hit compounds to influence STING signalling by evaluating their ability to inhibit TBK1 phosphorylation in HEK293T^{GFP-mSting} WT (**Fig. 2.3e**), raw cells (murine macrophages) and HeLa WT (using cGAMP transfection instead of CMA, as those cells have human STING, which is not activated by CMA) (**Fig. 2.3f**). In addition, while performing time-course stimulation experiments and visualising the cells at early post-stimulatory time points, we observed that hits from group i)—the ATPase and kinase inhibitors—had in fact no inhibitory effect on early trafficking, but rather exhibited some degree of toxicity. The triggered cell death phenotype was originally misinterpreted as trafficking inhibition at the time of image collection.

After these characterisation experiments, two non-toxic and specific hits inhibiting STING trafficking in a CMA-independent fashion remained: the tyrosine phosphatase inhibitor, alexidine dihydrochloride, and the histone deacetylase inhibitor, parthenolide. Unfortunately, these two remaining compounds failed to block downstream phosphorylation of TBK1, precluding any compound from the screen from being used as a functional downstream inhibitor of STING. While not exhaustive, these findings indicated that a functional specific STING inhibitor was unlikely to be found in pre-existing drugs, concluding that a novel compound was likely needed for such investigations. We therefore moved away from investigative strategies that would require small compounds, instead opting for alternative approaches.

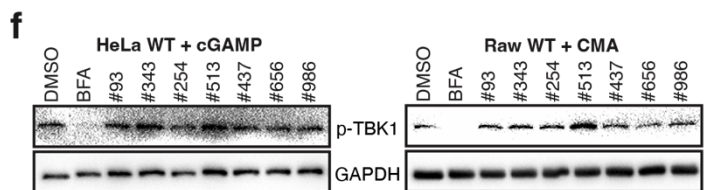
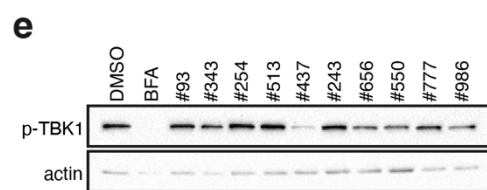
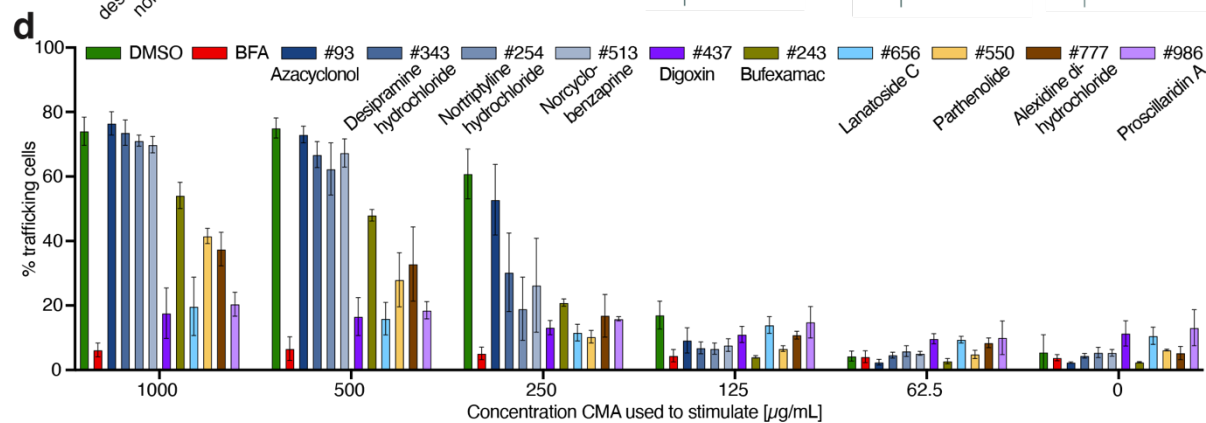
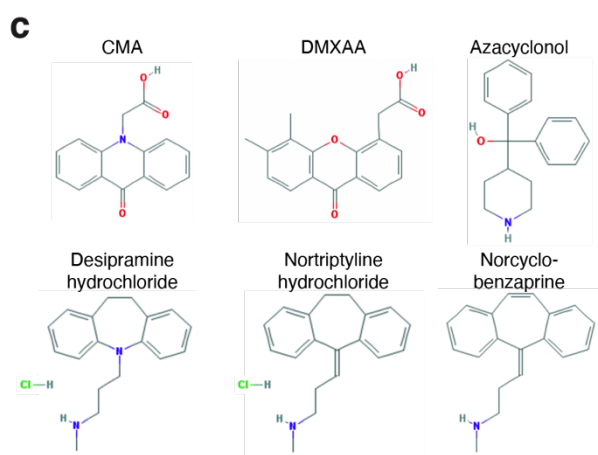
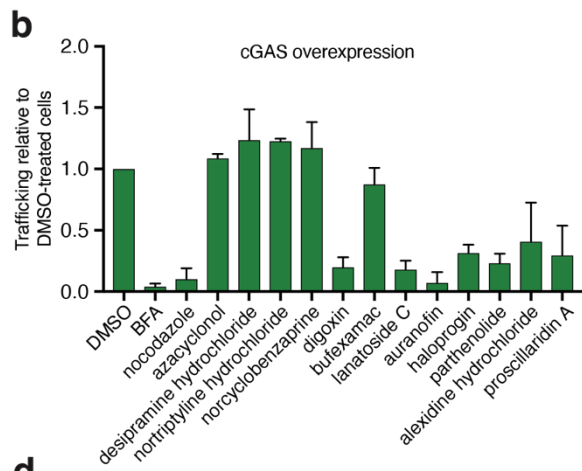
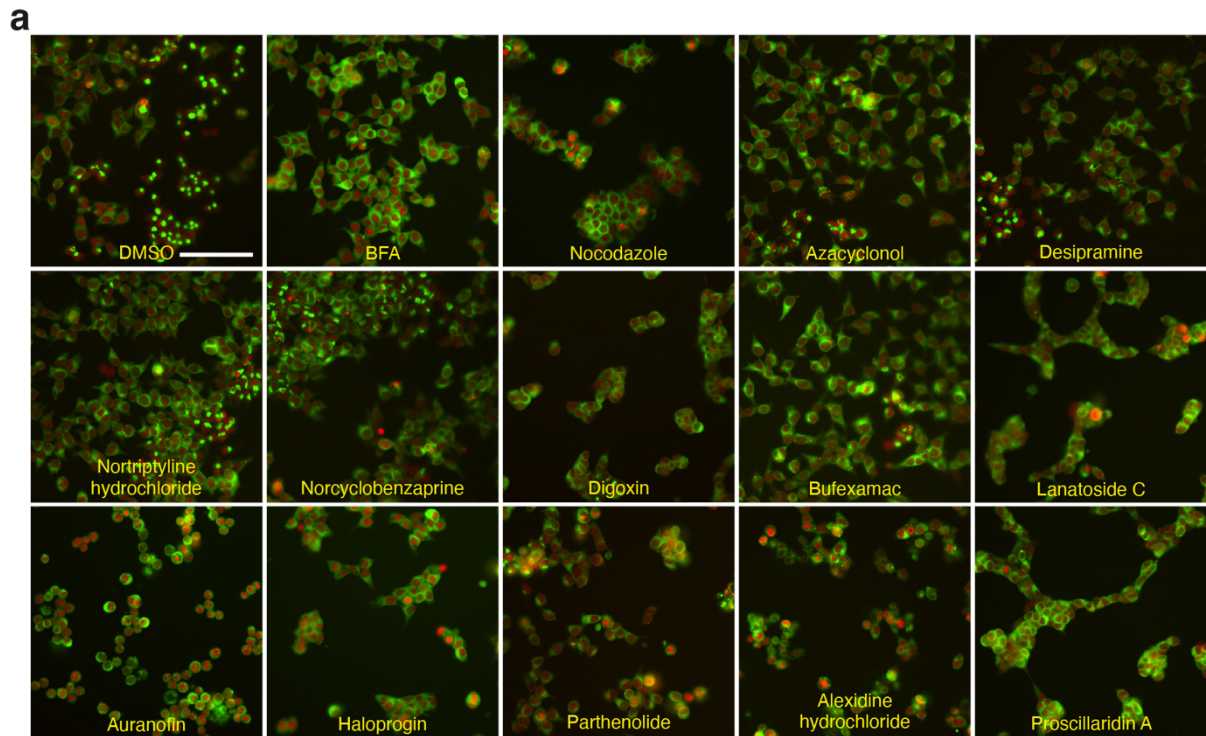


Figure 2.3 | In-depth characterisation of potential STING inhibitor compounds. a, b, HEK293T^{GFP-mSting} WT cells were transfected to overexpress cGAS. They were treated with the indicated compounds at 10 μ M 2 hours post-transfection and imaged 10 hours post-transfection (IN Cell Analyzer 2200, 20x). **a,** Images are representative of the observed patches of activated cells in 1 out of $n = 3$ independent experiments. Red is the nuclear dye Draq5, green GFP-mSting. Scale bar 100 μ m. **b,** Corresponding quantification of STING trafficking degree relative to DMSO-treated cells. Mean \pm standard deviation (s.d.) of $n = 3$ independent experiments where 9 fields of view per well and 1 well per condition were observed. Quantification was performed manually (as the transfection-triggered “activation patches” phenotype altered the performance of our automated CellProfiler trafficking quantification pipeline), blinded, and with an arbitrary trafficking assessing scoring system going from 0 to 3. **c,** Structures of the murine STING agonists CMA and DMXAA and of the four hits sharing a xanthone central moiety. **d,** HEK293T^{GFP-mSting} WT cells were pre-treated for 2 hours with the indicated compounds at 10 μ M and then treated with the indicated dose of CMA for 4.5 hours before imaging and subsequent quantification. Mean \pm s.d. of $n = 3$ independent experiments where 9 fields of view per well and 1 well per condition were observed. Quantification was performed using a CellProfiler pipeline evaluating the % of trafficking cells. **e,** HEK293T^{GFP-mSting} WT cells were pre-treated for 3 hours with the indicated compounds at 10 μ M and then treated with CMA at 250 μ g/mL for 3 hours before collection, lysis and immunoblotting against p-TBK1 and actin (used as loading control). Representative of $n = 3$ independent experiments exhibiting some degree of variability (global tendency of increase in p-TBK1 in #93, #343, #254, #513 and #777, reduction in #986, #437 and #656, unclear phenotypes for #550 and #243, some degree of toxicity observed for #243 and #656). The names of the corresponding compounds are listed next to their Prestwick # either in panel d, or in Fig. 2.2b. **f,** HeLa cells or murine Raw macrophages were pre-treated for 1 hour with the indicated compounds at 10 μ M (5 μ M for BFA) before activation by cGAMP transfection (HeLa; 1 μ g cGAMP per well on a 24-well plate) or CMA (Raw cells; 250 μ g/mL), respectively. After 2 hours, cells were lysed and immunoblotted against p-TBK1 and GAPDH (used as loading control). Reproduced only once.

2.3 – MS/MS-based screen identifies ELMOD2 as potentially regulating STING ER-to-Golgi trafficking

To complement the small compound inhibitor approach in our effort to better decipher the exact regulation of STING trafficking, we also focused on STING’s potential binding partners. To do so, we initiated a collaboration with the group of the Prof. Felix Meissner, from the Max Planck institute in Munich, with whom we performed a tandem mass spectrometry (MS/MS) STING interactome screen. We stimulated HEK293T^{GFP-mSting} WT cells with CMA and performed time course immunoprecipitation using their GFP moiety and then analysed these samples by MS/MS. This allowed us to identify several STING-binding partners that potentially play a role in STING trafficking. We decided to focus on proteins with the greatest variation in abundance post-stimulation compared to pre-stimulation. The rationale behind this choice was to detect either ER-anchors preventing STING departure from the ER that might be displaced upon activation, or co-trafficking factors that might appear upon stimulation only. This approach yielded a list of 30 potential interesting interaction partners (**Fig. 2.4a**). We further

investigated some of those hits to assess their implication in STING trafficking by individually silencing them in our CMA-activated HEK293T^{GFP-mSting} WT model and monitoring the cells for trafficking (Fig. 2.4b, c). This led to the identification of engulfment and cell motility (ELMO) domain containing protein 2 (ELMOD2) as a protein of interest. We found ELMOD2 to be associated with STING at the ER but to disappear upon activation, and its depletion seemed to reduce STING ER-to-Golgi trafficking upon activation (Fig. 2.4a, c).

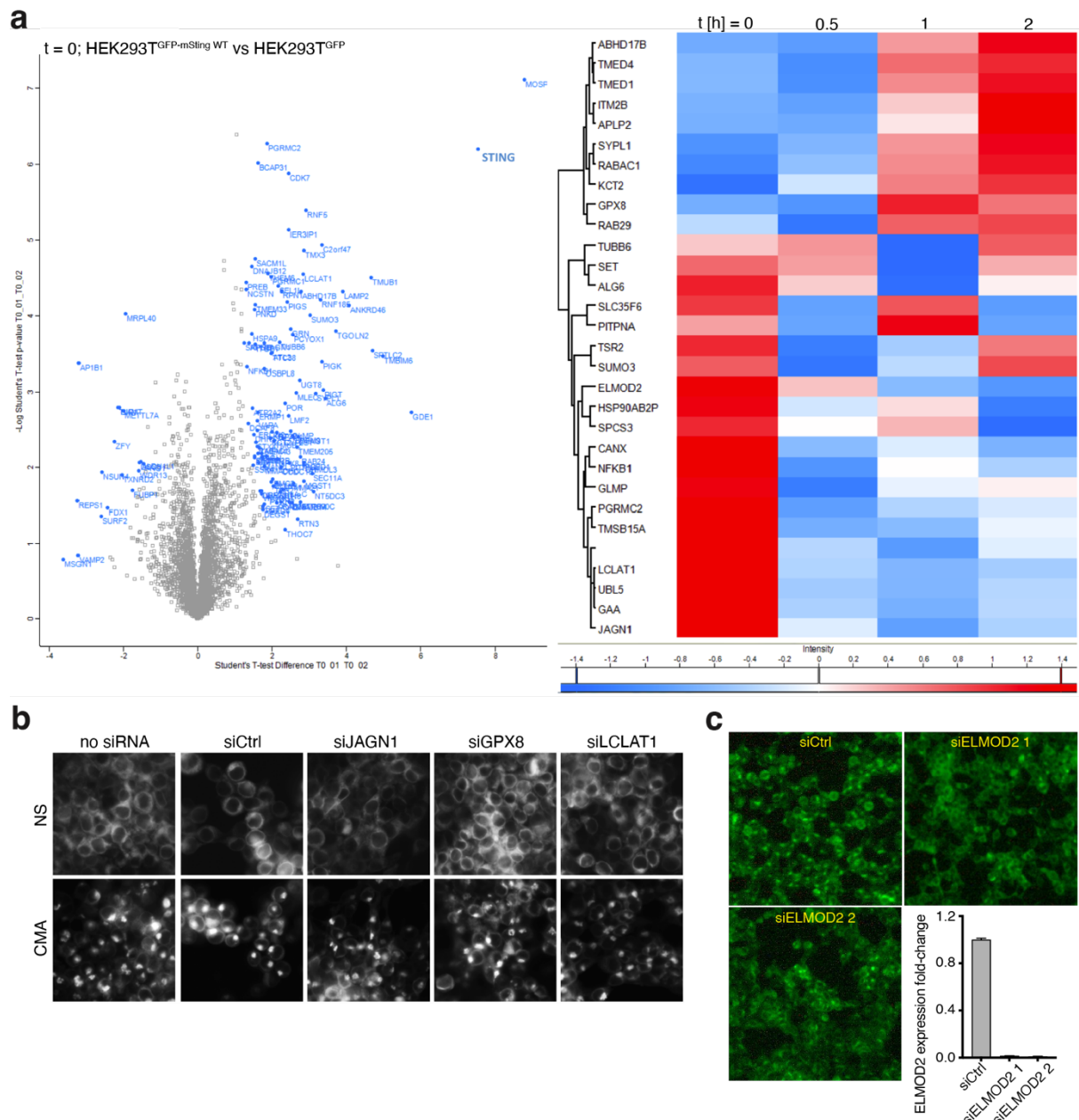


Figure 2.4 | MS/MS-screen and further validation of hits identify ELMOD2 as a partner of STING potentially involved in regulation its ER-to-Golgi trafficking. **a**, HEK293T^{GFP-mSting} WT and HEK293T^{GFP} were treated with 250 μ g/mL CMA and collected at four time points (t = 0, 0.5, 1, and 2 hours post-stimulation). Samples were lysed and a GFP-beads co-immunoprecipitation was performed. Interactants enriched in GFP-STING compared to GFP-only expressing cells were identified by MS/MS at all four time points, and those whose abundance was modified

during the course of the stimulation-triggered trafficking of STING were considered as potential hits. Left: volcano plot depicting the proteins significantly enriched in the GFP-STING cells compared to the GFP only one at $t = 0$. Right: heatmap listing the proteins that appear or disappear upon STING trafficking. Red, blue: enriched, respectively decreased, in GFP-STING versus GFP only samples. **b**, HEK293T^{GFP-mSTING WT} were treated for 3 days with siRNAs targeting the indicated proteins and then stimulated with 250 $\mu\text{g}/\text{mL}$ CMA for 3.5 hours before being imaged (IN Cell Analyzer 2200, 20x). Representative of $n = 2$ independent experiments with 2 distinct siRNAs per target. siCtrl – non-targeting control siRNA. **c**, HEK293T^{GFP-mSTING WT} were treated for 2.5 days with siCtrl or siELMOD2 1 or 2 and then stimulated with 250 $\mu\text{g}/\text{mL}$ CMA for 2 hours before imaging with a fluorescent light microscope (10x objective). Efficiency of ELMOD2 depletion by the siRNAs was assessed by RT-qPCR in the same cells. Representative of $n = 3$ independent experiments.

Further investigation revealed ELMOD2 as a poorly described Arl and Arf GAP¹⁷², a function compatible with playing a role in trafficking regulation. In addition, ELMOD2 had been previously associated both with antiviral response¹⁷³ and with familial idiopathic pulmonary fibrosis¹⁷⁴, a disease that exhibits symptoms similar to many interferonopathies, thus being compatible with STING-pathway-related dysregulation¹⁶¹. These previous discoveries combined with our screen and preliminary data led us to follow up on ELMOD2 to characterise its implication in the STING signalling pathway.

2.4 – ELMOD2 depletion impacts STING signalling at various levels and yields conflicting phenotypes

In order to better understand the link between ELMOD2 and STING, we looked at the impact of depleting ELMOD2 on downstream IFN I signalling. For this, we used a plasmid encoding for luciferase under the control of the IFN- β promoter. We co-transfected HEK293T cells with this plasmid and either mSting, human STING (hSTING) with cGAS, or TBK1 (positive control). We observed that silencing ELMOD2 before transfection drastically reduced luciferase signal in STING-stimulated cells compared to the TBK1 control (**Fig. 2.5a**). These results were compatible with a role played by ELMOD2 in STING trafficking regulation, as they indicated that ELMOD2 depletion impacted STING signalling upstream of TBK1 and hence at the level of STING. To verify that this effect was reproducible and biologically robust, we performed siRNA KD of ELMOD2 in several cell lines (**Fig. 2.5b**). We focused on p-STING and p-TBK1 as readouts for STING pathway activation, as these phosphorylation events take place directly after STING trafficking towards the Golgi and constitute the most proximal molecular indicators of pathway activation^{57,123}. Using cGAMP or dsDNA (90mer) as activators, we observed that ELMOD2 depletion decreased STING and TBK1 phosphorylation in activated human fibroblasts such as WI-38 cells (**Fig 2.5c**) or BJ cells (data not shown) as

well as in HeLa cells. While these results fit with the hypothesis that ELMOD2 regulated STING signalling, we also observed that, independently of STING activation status, ELMOD2 KD triggered signal transducer and activator of transcription 1 (STAT1) phosphorylation (**Fig 2.5c**). This raised concerns, as STAT1 phosphorylation is a marker of IFN receptor and Janus tyrosine kinase (JAK) activation and results in interferon stimulated genes (ISGs) production¹⁷⁵. Thus, silencing ELMOD2 might interfere with the STING-IFN axis at several levels, with potentially opposite effects (reduction of activation at the level of STING, but increase at the level of STAT1). Furthermore, to assess the impact of ELMOD2 on trafficking in other models, we transduced LL24 cells (human lung primary fibroblasts from healthy control patients) with our GFP-mSting WT construct and assessed CMA-triggered STING trafficking in those cells after ELMOD2 depletion. To our surprise, ELMOD2 KD did not restrict CMA-triggered STING trafficking in those cells, however we observed morphological changes in both stimulated and non-stimulated samples (**Fig. 2.5d**).

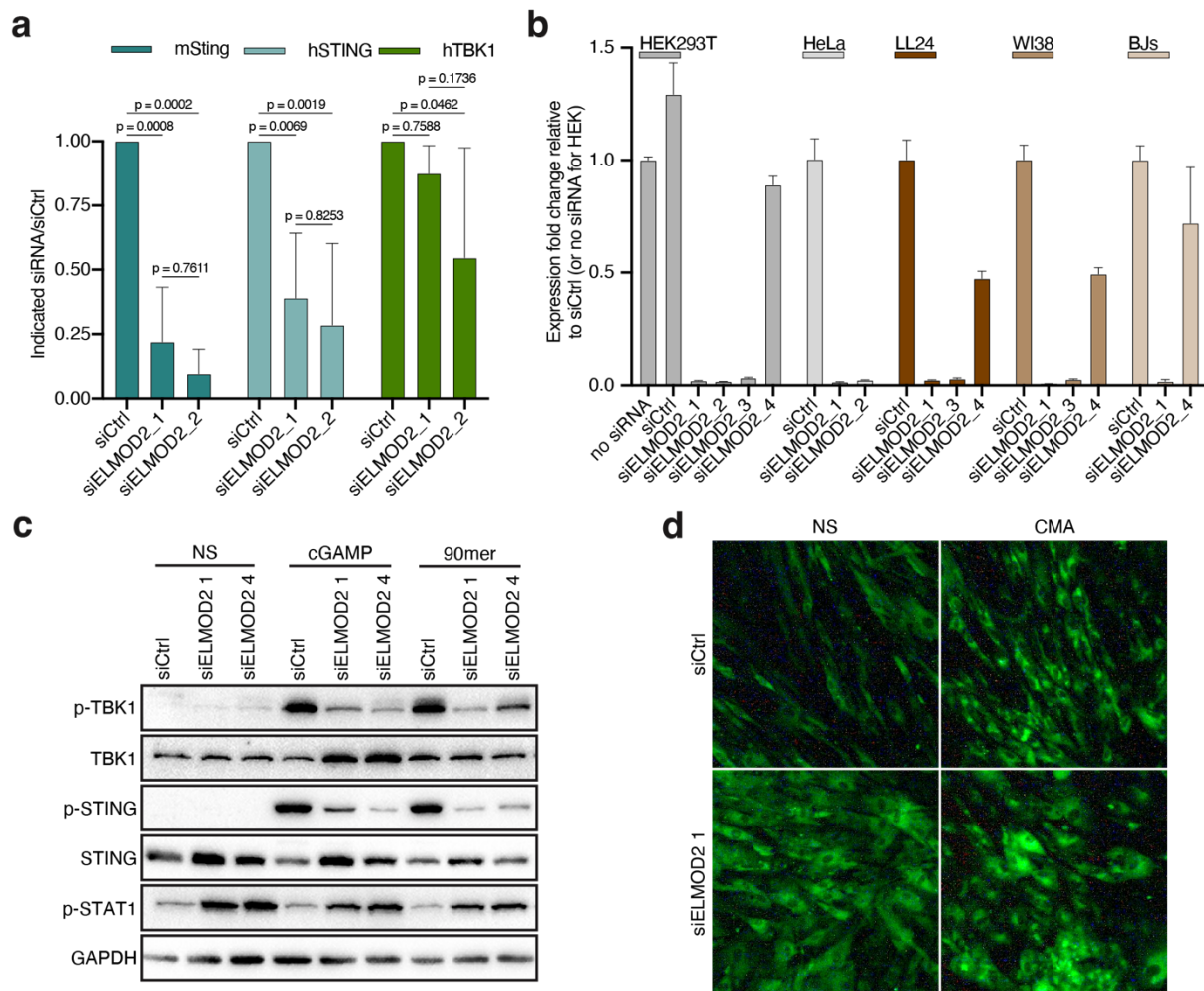


Figure 2.5 | ELMOD2 depletion influences STING-mediated downstream IFN I signalling. **a**, HEK293T were treated for 3 days with siCtrl or two different siELMOD2 and were then co-transfected with a plasmid encoding for luciferase under the IFN- β promoter together with the indicated stimulatory plasmids. Luciferase assay was performed the next morning. Mean \pm s.d of $n = 3$ independent experiment. Statistics from a 2-way ANOVA. **b**, Indicated cell lines were treated for 2.5 days with the several used siELMOD2, and ELMOD2 mRNA levels relative to corresponding siCtrl-treated cells were assessed by RT-qPCR. Mean \pm s.d. of $n = 3$ independent experiments or more for HEK293T and HeLa, 2 for LL24 and WI-38, and 1 for BJ cells. **c**, WI-38 cells were treated with indicated siRNAs for 3 days and stimulated 2 hours with cGAMP or 90mer. They were then immunoblotted against the indicated protein. GAPDH was used as loading control. Representative of $n = 3$ independent experiments (only 1 for p-STAT1). **d**, LL24 cells transduced to stably express GFP-mSting WT were treated for 3 days with siCtrl or siELMOD2 and then stimulated with 250 μ g/mL CMA for 2 hours before imaging with a fluorescent light microscope (10x objective). Representative images of only 1 experiment.

The variable phenotype across cell lines prompted us to further investigate our initial observation of the impact of ELMOD2 KD on CMA-triggered STING trafficking in HEK293T^{GFP-mSting WT} cells. Higher resolution imaging of the cells with a co-staining for the cis-Golgi marker GM130 led to two constatations. First, silencing of ELMOD2 via siELMOD2 1 failed at reproducing an efficient trafficking abolition and only triggered mild, if any, trafficking reduction. Second, while siELMOD2 2 indeed had an effect on trafficking, it also seemed to disrupt normal Golgi distribution, as GM130 staining was impacted (**Fig. 2.6a**). To observe the trafficking better and rule out artefacts created by the fixation process or time of observation, we live-imaged CMA-stimulated HEK293T^{GFP-mSting WT} cells. This confirmed that siELMOD2 1 had only very mild effects on trafficking (after 4 hours only), whereas siELMOD2 2 triggered a reduction, but no abrogation, of trafficking (**Fig 2.6b**). To confirm our initial findings, we used CRISPR-Cas9 to generate ELMOD2 knock-out (KO) HEK293T WT cells. After verifying that our KO was successful (**Fig. 2.6c**), we evaluated STING trafficking in these cells. We transfected them with either GFP-mSting (a transient overexpression which is sufficient for spontaneous pathway activation) or GFP-hSTING + cGAS. We detected normal trafficking in those cells one day post-transfection, reproducing the phenotype observed in HEK293T WT cells (**Fig. 2.6d**). Together, these data confirmed that ELMOD2 was dispensable for STING trafficking in our model. Therefore, while preliminary data strongly suggested a role for ELMOD2 in STING pathway regulation, further investigations were beyond the scope of our study and we chose to remain focussed on other aspects of STING trafficking.

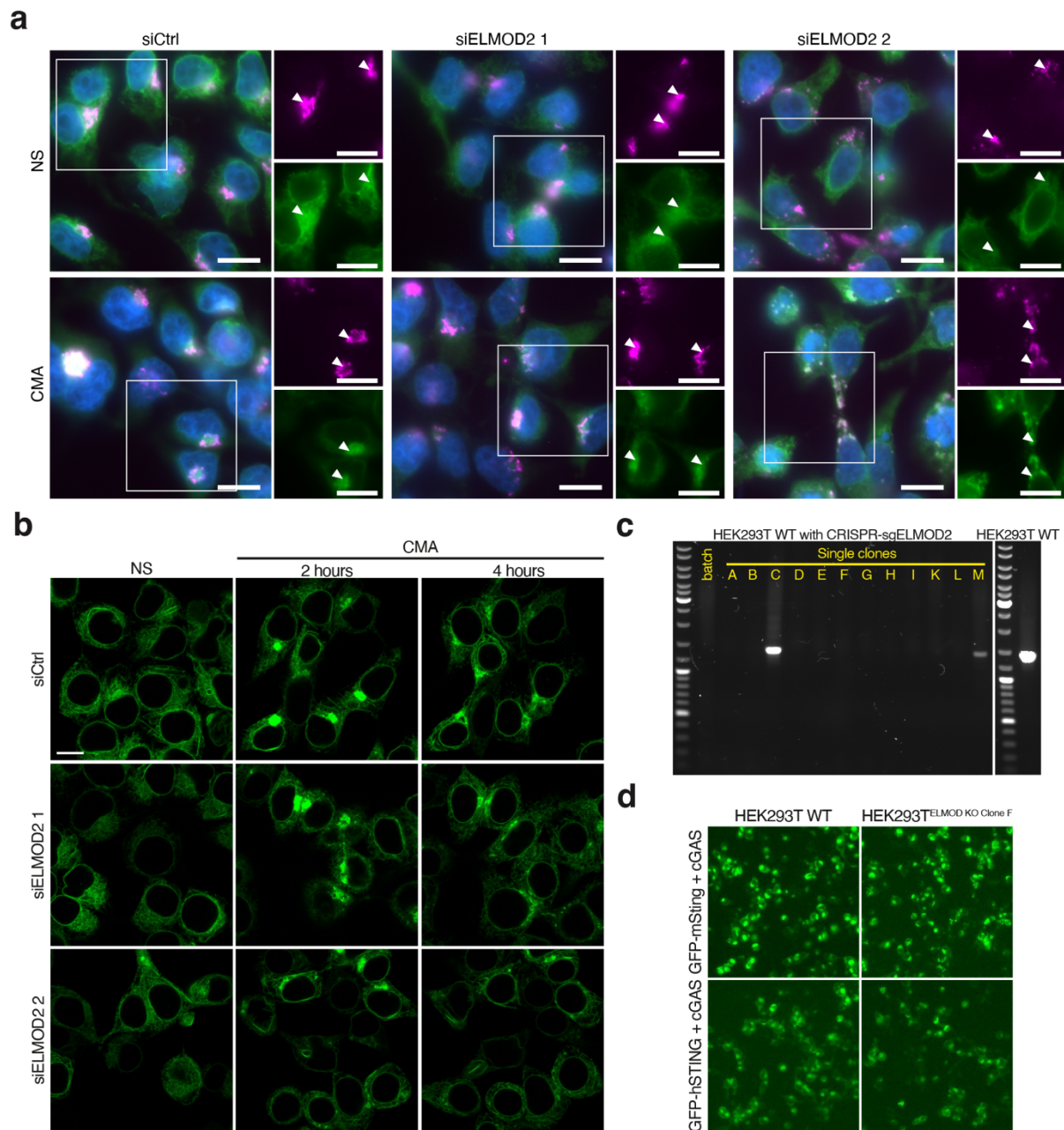


Figure 2.6 | High-resolution imaging of ELMOD2 KD cells show ambiguous results and ELMOD2 is dispensable for STING trafficking. **a**, HEK293T^{GFP-mSTING} WT were treated for 2 days with the indicated siRNAs and then stimulated with 250 $\mu\text{g}/\text{mL}$ CMA for 2 hours before fixation and staining with GM130 (cis-Golgi marker, pink) and Hoechst (nuclear dye, blue), and imaging with a fluorescent light Axioplan microscope (63x objective). Green is the signal of GFP-STING. Scale bars 10 μm . White arrows mark some GM130 positive regions. Representative of $n = 2$ independent experiments. **b**, HEK293T^{GFP-mSting} WT cells were treated for 3 days with the indicated siRNAs and then stimulated with 250 $\mu\text{g}/\text{mL}$ CMA for the indicated time. Images of live cells (green is GFP-STING) were taken before stimulation, cells were stimulated and placed back in the microscope and imaged after 2 and 4 hours on the same localisation. Images taken on a LSM700 confocal microscope (63x objective). Scale bar 10 μm . Representative of $n = 3$ independent experiments. **c**, Agarose electrophoresis gel of PCR-amplified ELMOD2 mRNA to test for success or not of ELMOD2 KO in various CRISPR-Cas9-generated clones in HEK293T cells. **d**, HEK293T WT or HEK293T^{ELMOD2} KO clone A were co-transfected with mSting or hSTING combined

with cGAS and imaged 1 day post-transfection with a fluorescent light microscope (10x objective) to assess GFP-STING trafficking. Representative of $n = 3$ independent experiments (for control and clone A shown here; the pooled CRISPR-Cas9-sgELMOD2 treated cells pre-clonal selection as well as 3 other KO clones were tested 1 to 2 times each and yielded the same trafficking phenotype upon STING + cGAS overexpression).

2.5 – STING C-terminal cytosolic head systematic mutagenesis helps mapping regions of STING important for trafficking regulation.

In our quest to understand STING trafficking regulation, we also investigated STING C-terminal cytosolic loop to determine which portions were involved in the proper regulation of its trafficking. For this, we performed an alanine-scanning (ala-scan): we applied site-directed mutagenesis to a GFP-hSTING WT plasmid to convert three-by-three all amino acids to alanine in the ligand-binding domain of STING (aa 157-370). We then systematically transfected those plasmids alone or combined with cGAS into HEK293T WT cells and imaged the cells to assess trafficking. This method led to the classification of each three-amino acid-mutant STING from the ala-scan: constructs trafficked either similarly to the WT protein, or had compromised trafficking, or were trafficking at rest. An important proportion (26/70) of the mutants exhibited unclear intermediary phenotypes, typically displaying mild trafficking at rest combined with reduction upon stimulation (**Fig. 2.7**). Nonetheless, our approach still led to the identification of regions of interest for STING trafficking regulation, and we could validate their relevance by considering available literature. For example, our ala-scan identified the 284-286AAA mutant as a constitutively trafficking, which fits with R284S being identified as a SAVI-causing STING mutant¹⁰³. Similarly, residues involved in binding of the ligand 2'3'-cGAMP have been identified among others around aa 239-242 and 260-263⁴⁹, while our ala-scan shows decrease or abrogation of trafficking for mutants 246-251 and 258-260. Together, this validates our screening method, and thus, our results offer important insights on key residues involved in ligand binding or STING trafficking regulation.

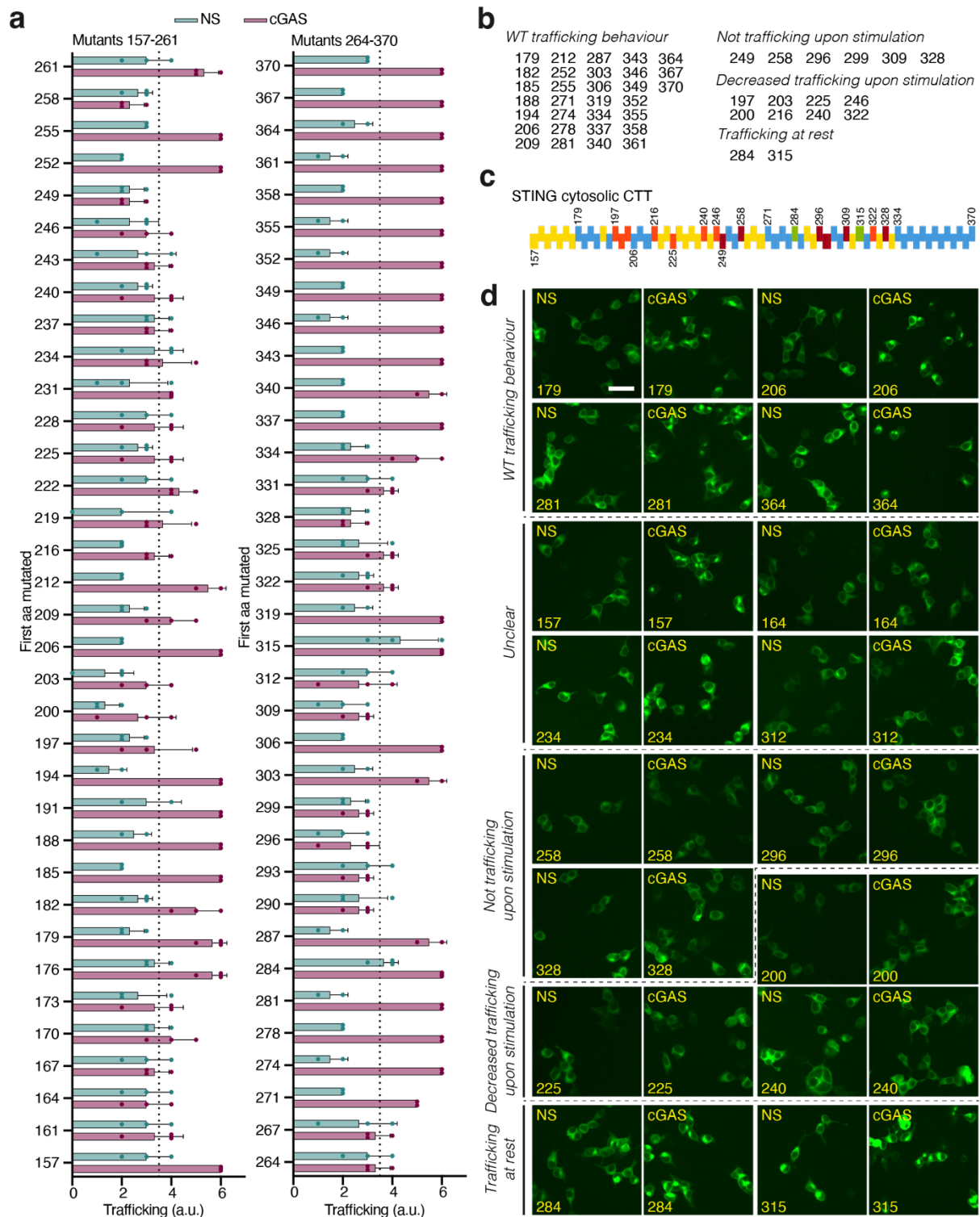


Figure 2.7 | Systematic three-by-three ala-scan of GFP-hSTING cytosolic C-terminal shows some regions crucial for trafficking regulation. HEK293T cells were transfected with all plasmids from the ala-scan of GFP-hSTING cytosolic C-terminal domain either alone or together with cGAS to activate trafficking, and imaged in the IN Cell Analyzer 2200 (20x objective, 6 fields of view per well, 2 wells per condition) 20 hours post-transfection, before blinded quantification of STING trafficking (arbitrary scale from 0 to 3 on 2 wells per condition, yielding a score between 0 and 6). This ala-scan microscopy screen was reproduced in $n = 3$ (all constructs with unclear or non-WT trafficking phenotypes) or $n = 2$ (all constructs with clearly WT trafficking phenotypes) independent

experiments. Numbers used to name the STING variants correspond to the first of the three amino acids mutated to alanine in each construct. **a**, Mean \pm standard error of the mean (s.e.m.) of the obtained trafficking scores. The dashed line represents a boundary arbitrarily set at 3.5, the empirical cut-off to distinguish trafficking from non-trafficking STING. **b**, Classification of the STING variants according to their trafficking scores. **c**, Schematic view of STING C-terminal cytosolic domain coloured according to this classification. Blue – trafficking phenotype similar to WT STING; green – trafficking without STING stimulus; red – decreased (light) or abolished (dark) trafficking upon stimulation; yellow – unclear phenotype. **d**, Example images for each category of STING variants from the microscopy ala-scan. Scale bar 40 μ m.

2.6 – Discussion

Although the data presented in this chapter were not published due to their preliminary nature, they nevertheless provide valuable insight into STING ER-to-Golgi trafficking and inform future experimentation into this challenging pathway.

First, the chemical screen, despite not allowing us to identify a clear hit specifically inhibiting STING trafficking, led to the optimisation of our high-throughput microscopy-based screening workflow, and, most importantly, the identification of several interesting trends. We observed that serotonin transporter inhibitors (compounds #93, #254, #343, #513) may act as CMA-competitors (**Fig. 2.3a-d**), and outcompete it for the binding pocket without triggering the conformational changes needed to activate STING. A second group of compounds, that consistently reduced, to a moderate degree, both trafficking and p-TBK1 (compounds #437, #656 and #986, **Fig. 2.3a, b, d-f**), provides very interesting, if incomplete, insight into STING regulation. Indeed, alone or with very low doses of CMA, these compounds seemed to trigger, rather than inhibit, trafficking, whereas at high concentrations of CMA, they were exclusively inhibitory (**Fig. 2.3d**). This “dual”, context-dependent, inhibitory-activating pattern might rely on very high affinity compounds whose binding induces a suboptimal STING dimer’s rearrangement, triggering limited trafficking and acting as weak agonists themselves. However, such dual compounds would become inhibitory with higher CMA doses, because they would still occupy the binding pocket and prevent binding of and activation by a lower affinity, more potent, agonist (here, CMA, but the concept could be the same with cGAMP or any other agonist sharing the same binding site). This “dose-dependent-dominant-negative”-like mode of action would be reminiscent of cyclic di-GMP, that can inhibit 2’3’-cGAMP-triggered activation despite being a STING agonist itself¹⁶. In sum, in both suggested modes of action, the inhibitory compounds would occupy the ligand-binding pocket of STING dimers without triggering the same conformation as CMA or cGAMP. This would either prevent trafficking (CMA-competitors), or, in case of high affinity “dual” compounds, set and maintain some level of trafficking despite variations of abundance of other agonists. These mechanisms

are speculative, and further experiments are necessary to know with certainty how these hit compounds are interfering with trafficking. However, whether the hypotheses raised by the observed phenotypes are verified or not, our findings are noteworthy within the context of the mode of action of STING chemical agonists. Indeed, most of them interact with the ligand-binding pocket of STING, but they do not all trigger the same dimer conformation^{46–49,164}. This means that some agonists could exhibit such a “dual”, behaviour. In future studies, it might be worth mixing STING agonists or combining them with DNA or cGAMP stimulation to see how they affect each other. In fact, a newly discovered STING agonist, which targets an allosteric transmembrane-located pocket of STING, has been shown to work synergistically with cGAMP to trigger oligomerisation and activation¹⁷⁶. Although this synergy between the two agonists is less surprising knowing that they have distinct binding sites, it exemplifies how investigation of two compounds simultaneously can bring interesting insights on STING activation and regulation. Another relevant outcome of our chemical screen is the “diffuse-dots” phenotype exhibited by nocodazole-triggered inhibition (**Fig. 2.2d**), whether for STING-specific or general trafficking, as assessed by RUSH. This showed that using different inhibitors (here, for example, BFA or nocodazole) blocks trafficking at different steps, and those distinct blocks can potentially be instructive regarding the sequence of mechanisms involved in trafficking modulation.

Second, our MS/MS-based STING interactome screen led to the identification of ELMOD2 (**Fig. 2.4**), which plays a complex role in STING regulation, influencing it at several levels across the STING-IFN I axis (**Fig. 2.4c** and **2.5a, c**): its depletion for example reduced trafficking and p-TBK1, but increased p-STAT1. The role of ELMOD2 in STING trafficking was less clear than initially expected and potentially very system-dependent (**Fig. 2.5d** and **2.6**). However, the evidence showing an impact of ELMOD2 depletion on either trafficking or TBK1 phosphorylation is concordant with the idea that this innate immune pathway is intricately linked with trafficking-regulated processes. Indeed, ELMOD2, as an Arl/Arf-GAP¹⁷², is very well placed to have an impact on cellular trafficking, a process governed by membrane and cytoskeleton remodelling, that depend heavily on GTPases and their associated GEFs and GAPs^{177,178}. In addition, after it was shown to be involved in familial idiopathic pulmonary fibrosis¹⁷⁴, its role in anti-viral response was also evaluated¹⁷³. It was shown that overexpression of ELMOD2 could increase basal IFN I signalling and that it was downregulated over the course of viral infections. These phenotypes were associated with TLR3¹⁷³, but the study did not include any STING-related experiments, and it is easy to speculate that the observed phenomena could be, at least partially, STING-dependent. Together, our results and previous studies involving ELMOD2 underline a complex link

between ELMOD2 and IFN I, with probable cross-talks with STING, as well as with other arms of IFN I signalling.

Altogether, our two screens underlined that STING ER-to-Golgi trafficking relies on processes central to the cell. As such, any interferences with the proteins or mechanisms involved in this trafficking have a broader impact on cellular state and signalling, rendering it complicated to focus exclusively on STING-trafficking-related phenotypes. This led us to take the opposite approach, and instead investigate trafficking from the perspective of STING by conducting a three-by-three amino acids ala-scan of STING C-terminal cytosolic domain. Combined with our initial GFP-mSting mutants (based on single points mutations in STING's transmembrane second cytosolic loop), this mutagenesis-based approach revealed some regions playing a crucial role in STING cellular localisation. Although we did not pursue the research further, these results, while preliminary, are strong and could be the basis for future investigation. Indeed, they align with the other concomitant discoveries in the field: we could identify residues previously described as important for 2'3'-cGAMP-binding⁴⁹ or linked to SAVI disease¹⁰³. In addition, we also pinpointed regions that have recently been highlighted through resolution of STING full-length structure⁵⁵. In fact, the cytosolic loop between transmembrane domain 2 and 3 (comprising E69 and R76) was shown to form, together with membrane proximal residues around aa 292-313, an interaction groove for STING N-terminal tail, while the regions around aa 228-239 and 249-250 were not resolved in the structure⁵⁵, probably indicating a link with conformational changes involved in STING regulation. Our three-by-three ala-scan had identified these regions as potentially important for STING trafficking (**Fig. 2.8**), validating the strategy. A next step would be to refine the scan's resolution by performing a one-by-one ala-scan together with a similar microscopy-screening strategy.

While we could have extended the above-mentioned studies or looked at other hits from the MS/MS screen in more details, we chose to redirect our energy towards understanding a different route STING takes through the cell upon activation, terminal Golgi-to-lysosomes trafficking, discussed in **Chapter 3**.

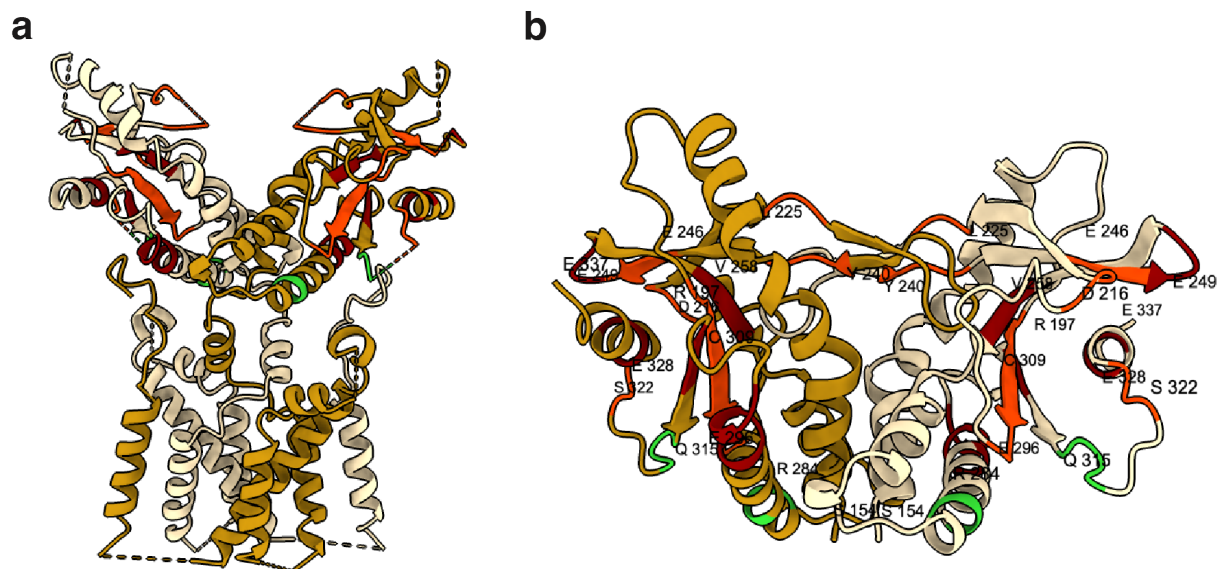


Figure 2.8 | Visualisation of STING's C-terminal domain regions identified in our ala-scan as important for signalling. **a, b,** Representation on STING structures of the regions identified in our ala-scan to either trigger STING trafficking at rest (green), or to decrease (red) or abolish (dark red) cGAS-dependent STING trafficking, as classified in Fig. 2.7c. Dashed lines represent unresolved regions. The two STING subunits forming the dimer are represented in white and brown, respectively. Images were generated in ChimeraX using **(a)** a side view of cryo-EM structure of full-length human STING dimer in the apo state (PDB accession code 6NT5)⁵⁵, or **(b)** a side of cGAMP-bound crystal structure of hSTING ligand-binding domain in complex with 2'3'-cGAMP (PDB accession code 4LOH)⁴⁹.

2.7 – Material and methods

Cell culture

HEK293T cells were a gift from Didier Trono (EPFL), originally purchased from ATCC (cat. no. SD-3515). HeLa (CCL-2) cells were purchased from Sigma-Aldrich. WI-38, LL24 and BJ cells were purchased from ATCC (CCL-75, CCL-151 and CRL-4001, respectively). HeLa, HEK293T, WI-38, BJs and all their derived lines were cultured in Dulbecco's Modified Eagle Medium (DMEM, Thermo Fisher Scientific, 41965039) supplemented with 10% (v/v) heat-inactivated fetal bovine serum (FBS) (Thermo Fisher Scientific, Gibco SKU, 10270106), 100 IU/ml penicillin-streptomycin (BioConcept, 4-01F00-H), 2 mM L-glutamine (Thermo Fisher Scientific, 25030024) and 1 mM sodium pyruvate (BioConcept, 5-60F00-H) at 37°C and at atmospheric O₂ and 5% CO₂. LL24 cells were cultured in Ham's F-12K medium (Thermo Fisher Scientific, 21127022) supplemented with 15% FBS, 100 IU/mL penicillin-streptomycin, and 1 mM sodium pyruvate at the same incubation conditions than above.

Stable cell lines

HEK293T^{GFP-mSting} (WT and STING variants) line were generated by infection with a pTJ lentiviral vector carrying corresponding GFP-mSting and a puromycin resistance gene. Cells were selected with puromycin (5 µg/mL) for 3-5 days and then expanded in antibiotics-free media and FACS-sorted into single clones. Plasmids used for transduction were mutated by point-directed mutagenesis to obtain the desired STING variants.

Cellular stimulation

Cells were stimulated for STING trafficking with several methods depending on the experiments, as indicated. The methods used are listed here:

- Direct addition in the culture medium of STING agonists CMA (10-carboxymethyl-9-acridanone, Sigma, 17927) or DMXAA (5,6-dimethylxanthenone-4-acetic acid, InvivoGen, tlr-dmx) at the indicated doses and durations;
- Transfection with 90mer (dsDNA, complementary strains, forward sequence is 5'-TACAGATCTACTAGTGATCTATGACTGATCTGTACATGATCTACATACAGATCTACTAGTGATCTATGACTGATCTGTACATGATCTACA-3') or with 2'3'-cGAMP using the transfection reagent Lipofectamine 2000 (Life Technologies, 11668019) according to the manufacturer's protocol and, if not specified otherwise, 1.5 µg of 90mer or 2.1 µL of cGAMP at 2.5 mM with 5 µL lipofectamine in 100 µL OptiMEM (LifeTechnologies, 31985047) total per 12-well plate well;
- Overexpression of stimulatory plasmids:
 - o pEFBos-hTBK1 (overexpression is sufficient to activate downstream IFN I),
 - o pEFBos-mSting (overexpression is sufficient to activate downstream IFN I, response can be increased by co-transfection of pEFBos-hcGAS),
 - o pEFBos-hSTING combined with pEFBos-hcGAS (co-expression triggers downstream IFN I);

These plasmids were transfected with the transfection reagent GeneJuice (NovaGen, 70967-6) according to the manufacturer's instructions, using, for one well of a 96-well plate, 0.5 µL of GeneJuice mixed in 10 µL OptiMEM total with 200 ng of TBK1 or mSting plasmids, or 190 ng of hSTING or mSting plasmids combined with 10 ng cGAS plasmid.

Trafficking visualisation by microscopy

Cells were observed with the indicated microscopes:

- when not specified: a table-top Zeiss Vert.A1 FL microscope equipped with an Axiocam ERc 5s and LD A-Plan 40x or 10x objectives;
- an upright Zeiss Axioplan 2 fluorescent light microscope equipped with a plan-apochromat objective (63x magnification 1.4 numerical aperture, oil immersion) and an AxioCam MRm camera;
- an inverted Zeiss AxioObserver Z1 confocal microscope also equipped with a plan-apochromat objective (63x magnification 1.4 numerical aperture, oil immersion) and an AxioCam MRm camera.
- a GE Healthcare IN Cell Analyzer 2200 automated microscope equipped with a 20x objective.

When not specified otherwise, cells expressing GFP-STING were directly observed live at the indicated time-points post-stimulation without prior fixation nor staining. Of note, all cells observed with the IN Cell Analyzer 2200 (except the ones used for the ala-scan screen displayed in Fig. 2.7) were dyed with the nuclear dye Draq5 (1 μ M in the experimental media for at least 30 min; Thermo Fisher Scientific, 62252).

Fixation and staining

The following cells were plated on glass slides pre-coated with poly-L-lysine, treated and stimulated as indicated, then fixed and stained as follows:

Fig. 2.1b: cells were fixed by incubation for 10 min in 2% paraformaldehyde in CBS buffer (10 mM MES pH 6.9, 138 mM KCl, 2 mM MgCl₂, 2 mM EGTA), washed twice with CBS, permeabilised with 0.1% saponin in PBS (Phosphate-buffered saline, Life Technologies, 10010015), washed again twice in CBS, blocked with 0.5% bovine serum albumin (BSA, Sigma, A7906) in PBS, incubated over the weekend in anti-GM130 (Alexa Fluor® 647 Mouse anti-GM130 Clone 35/GM130 (RUO), BD 558712) 1:100 in 0.1% saponin in CBS, washed twice with CBS and dyed with Hoechst 33342 (Sigma-Aldrich, B2261) 0.2 μ g/mL in CBS. Slides were mounted on coverslips and imaged on the LSM700 confocal microscope.

Fig. 2.6a: cells were fixed by incubation for 15 min in 2% paraformaldehyde in PBS, washed 3 times in PBS, permeabilised using Triton X-100 (Sigma) at 0.1% in PBS for 15 min, blocked 30 min with 5 % BSA in PBS, stained by overnight incubation with the above-described GM130 antibody diluted 1:100 in 5% BSA in PBS, washed twice more with PBS, dyed 5 min with Hoechst 33342 0.2 μ g/mL in PBS, rinsed once more with PBS and mounted on slides. They were imaged on the Axioplan microscope.

Prestwick small chemical compounds microscopy screen

In collaboration with the EPFL biomolecular screening facility (BSF), we established a protocol to screen the impact of the 1280 compounds of the Prestwick Chemical Library (with compounds available in the library in 2018, see exact list in the **Appendix**) on CMA-triggered STING trafficking.

Compounds' drops (maximum 50 nL) were robotically distributed in 96-well plates so that compounds' final concentration would be 10 μ M in the well filled with cells (final volume of 50 μ L). The first and last column on each plate (8 wells each) contained 50 nL of DMSO (negative control, no effect expected) and BFA to reach a final 2.5 μ M concentration (positive control, trafficking inhibition expected), respectively. All other compounds were present in duplicates, leading to a total of 32 plates, all prepared by the BSF facility. Upon screening, plates were thawed 1 hour before cell plating (20 000 HEK293T^{GFP-mSting} WT in 50 μ L media per well) with a multichannel pipet. Plates were left unmoved for 0.5 hour at room temperature to ensure homogenous cell distribution in the well, followed by 2 hours at 37°C for proper cellular adhesion. Then, with a multi-channel pipet, CMA at 250 μ g/mL final and Draq5 (nuclear stain) at 1 μ M final were added in 10 μ L (slightly diluting the compounds for the remaining time of the experiment). The plates were further incubated at 37°C. Images of the live cells were then taken sequentially 4 to 6 hours later with the IN Cell Analyzer 2200 microscope (20x objective, 9 fields of view per well, leading to 30 minutes of imaging per plate). To limit incubation time variation and long room-temperature processing time, the plates were processed as described above four-by-four during 4 days (two groups of plates per day). Plate plan was unknown to the experimenter (me) except for control wells. Duplicates for each compound were split over the different plate groups, one being in the first 16 plates and the second in the last 16 ones, ensuring independence.

Images were analysed using machine-learning-based pipelines in CellProfiler (including CellProfiler Analyst) and CellCognition softwares to classify the cells between trafficking or not, yielding a final readout in “% of trafficking cells per well”. The validity of the screening protocol was verified prior to launching the final screen by treating and processing a “Z’ plate” filled only with positive or negative controls (half each). Z’ score represents the signal to noise ratio of the screening. It is obtained by the formula:

$$Z' = 1 - 3 * (\sigma_{\text{positive}} + \sigma_{\text{negative}}) / |\mu_{\text{positive}} - \mu_{\text{negative}}|$$

where μ and σ represent the mean and the standard deviation, respectively, of the positive or negative controls, and the symbol “| ... |” refers to the absolute value.

Z’ can ideally oscillate between -1 and 1, values between 0.5 and 1 denoting a strong assay. Processing of the Z’ plate allowed us to test a few different options, and maximisation of the

Z' value for the whole plate led us to refine our image analysis pipeline: we decided to pre-process the images with the embedded 2D-deconvolution tool from the IN Cell Analyzer 2200 software and to work with classifier-based machine-learning. Implementing this type of analysis, we obtained a Z' score of 0.725 for this test plate, validating the strength of our controls as well as our assay setup and output parameter. During machine-learning algorithm refinement on the screen dataset, maximisation of the Z' score was used to further optimise our pipelines. The analysis workflows were based on the following steps: the programs were able to segment the cells using the Draq5 nuclear signal to identify nuclei and then localising the cytosol by extension around the nucleus using the GFP signal. Segmented cells were then classified between "trafficking" or "not trafficking" (with a third "undefined" category in the 3-class workflow) by classifier-based machine-learning algorithms. As an example, for the CellProfiler 2-class pipeline, to get this automated class attribution, we generated a training set composed of 10-20 images from the control wells, in which cells from the DMSO-wells were first classified as "trafficking" and cells from the BFA-wells as "non-trafficking". The classification was then manually adapted by visual inspection, and the obtained curated training set, containing 500-1000 cells per class, was used to train a machine-learning algorithm (we tested several possible algorithms and compared the obtained Z' scores). After empirical, Z' score-based, choice of the algorithm and refinement of the classification features retained by the software as useful to distinguish between our classes (selection of the relevant ones, linked with the GFP signal), we applied the analysis on the whole screen dataset. For this CellProfiler 2-class pipeline, we retained the Random Cut Forest classification algorithm, run with the following selected features (all linked with GFP signal): StdIntensity, MaxIntensity, MassDisplacement, LowerQuartileIntensity, MedianIntensity, StdIntensityEdge, UpperQuartileIntensity, MADIntensity, IntegratedIntensityEdge, MeanIntensity, IntegratedIntensity, MeanIntensityEdge). Similarly, 2 other pipelines were developed in CellCognition. The three final selected analysis pipelines yielded excellent overall Z' scores: 0.728 (CellProfiler 2-class, described above, designed by myself with the help of Fabien Kuttler from the BSF), 0.791 (CellCognition 2-class, designed by Fabien Kuttler) and 0.678 (CellCognition 3-class, designed by Fabien Kuttler). All plates of the screen also had their individual Z' score verified (one plate had a Z' score around 0.4, all others oscillated between 0.5 and 0.89), further validating our screening procedure.

The hits of these three analysis pipelines were then compared, combined and considered for visual inspection and validation before to focus on deeper characterisation.

RUSH (Retention Using Selective Hooks)

HEK293T were transduced with plasmids encoding for the RUSH system and selected by puromycin selection (3 days at 2 $\mu\text{g}/\text{mL}$). Used plasmids were gifts from Franck Perez: a plasmid containing a truncated mannosidase II within the RUSH system, Str-KDEL_ManII-SBP-EGFP (Addgene plasmid #65252) and a plasmid containing a truncated sialyltransferase within the RUSH system, Str-KDEL_ST-SBP-EGFP (Addgene plasmid #65267)¹⁷¹. The obtained HEK293T^{RUSH Man} or HEK293T^{RUSH ST} cells were plated and let to adhere 0.5 hour at room temperature followed by 2 hours at 37°C in compounds-pre-filled plates (as described for the Prestwick screen). Biotin was then added at 40 μM final (with Draq5 nuclear stain at 1 μM) to trigger selective hook release and allow trafficking of the GFP-tagged proteins towards the Golgi. 3 hours post-biotin addition, plates were imaged on the IN Cell Analyzer 2200 microscope (20x).

Trafficking quantification

Automated:

For images that yield a trafficking phenotype similar to the CMA-triggered trafficking of HEK293T^{GFP-mSting WT} cells used in the Prestwick-library screen described above, we could use the analysis scripts developed in CellProfiler for the screen to quantify the trafficking cells and get a % of trafficking cells in each well. This was possible for chemical agonists (CMA and DMXAA) that homogeneously activate trafficking in the well.

This automated trafficking assessment was used in Fig. 2.3d.

By eye:

For stimuli such as cGAS overexpression, as transfection is not homogenous and activation of trafficking appears to occur in patches of efficiently transfected cells in localised areas of the well, the algorithm used above was inconsistent. In addition, those stimulation performed with transfection were done on cells that had more adhesion time and were hence shaped differently, contributing to decrease classification algorithm's accuracy. Hence, for those experiments, quantification of trafficking was done in a blinded fashion using "human evaluation", i.e., observation and grading of each field of view of the well to credit each well with an arbitrary trafficking score oscillating between 0 (no trafficking cell), 1 (very little trafficking), 2 (less than half, but clear trafficking), or 3 (clear activation with more than half cells trafficking).

This "manual" or "by eye" assessment was used in Fig. 2.3b and Fig. 2.7 (ala-scan).

Acrylamide gel electrophoresis and immunoblotting (Western blot)

Cells were lysed in RIPA buffer (sodium deoxycholate 0.5% (w/v), Tris-hydroxymethyl-aminomethane 20 mM, NaCl 50 mM, MgCl₂ 1 mM, CaCl₂ 1 mM, Triton X-100 1% (v/v)) freshly supplemented with cOmplete™ Protease Inhibitor Cocktail (Roche). Samples were then digested for 10-15 min at 95°C after adding loading buffer Laemmli 1X (6X stock contains: 0.375 M Tris at pH 6.8, 8.3% (w/v) sodium dodecyl sulfate (SDS), 40% (v/v) glycerol, 0.06% (w/v) bromophenol blue and 20% (v/v) dithiothreitol (DTT)). They were loaded into 10% acrylamide gels suited for SDS-PAGE and run at 90 V for 5-15 min and then at 120-150V for about 1.5 hours (using a BioRad running chamber filled with running buffer: 10.08 g SDS, 30.3 g Tris-hydroxymethyl-aminomethane and 144 g glycine in 10 L water). The proteins were then transferred onto nitrocellulose membranes using a Trans-Blot Turbo cassette with the corresponding Turbo Transfer buffer (BioRad) according to manufacturer's instructions (pre-existing transfer protocol for mixed molecular weight was selected). Membranes were then blocked for 1 hour at room temperature in 4% milk (non-fat dry milk, Roth) in TBS-T (Tris-buffered saline-Tween, 50 mM Tris-Cl pH 7.5, 150 mM NaCl, and 0.1% (v/v) Tween 20), incubated with primary antibodies diluted in 5% BSA or milk in TBS-T overnight at 4°C, washed 3 times 5 min in TBS-T, incubated 1 hour at room temperature in horseradish peroxidase (HRP)-conjugated secondary antibodies diluted 1:5000 in 5% BSA in TBS-T, washed again 3 times 5 min in TBS-T and finally visualised using WesternBright ECL Spray-HRP Substrate (Advansta, K-12049-D50) and the ChemiDoc XRS BioRad Imager (with Image Lab software).

Primary antibodies used as loading controls: rabbit monoclonal anti-GAPDH (14C10) (Cell Signaling Technology, 2118, 1:1000 in 5% BSA in TBS-T), mouse monoclonal anti-β-actin (C4) (Santa Cruz, sc-47778, 1:5000 in 5% milk in TBS-T).

Other primary antibodies (diluted 1:1000 in 5% BSA in TBS-T): rabbit monoclonal anti-phospho-TBK1/NAK (Ser172) (D52C2) (Cell Signaling Technology, 5483), rabbit monoclonal anti-TBK1/NAK (D1B4) (Cell Signaling Technology, 3504), rabbit monoclonal anti-human phospho-STING (Ser366) (D7C3S) (Cell Signaling Technology, 19781), rabbit monoclonal anti-STING (D2P2F) (Cell Signaling Technology, 13647), anti-phospho-Stat1 (Tyr701) (58D6) (Cell Signaling Technology, 9167).

HRP-conjugated secondary antibodies (diluted 1:5000 in 5% BSA in TBS-T): donkey anti-rabbit IgG (H+L)-HRP (Jackson ImmunoResearch, 711-036-152), donkey anti-mouse IgG (H+L)-HRP (Jackson ImmunoResearch, 715-036-151).

siRNA-mediated protein knock-down

To silence the indicated proteins, cells were plated at a density of 200 000 HEK293T cells per 12-well plate (or similar confluency for other cell lines) and treated with 0.2 μ L of siRNA at 50 μ M and 3 μ L of Lipofectamine RNAiMAX transfection reagent (Invitrogen, 13778075) in 100 μ L OptiMEM total, following the manufacturer's protocol. The cells were then incubated 2-3 days (as indicated) and used for further experiments.

Used siRNAs (purchased from Thermo Fisher Scientific):

- negative control (non-targeting siRNA) siCtrl: Silencer™ Select Negative Control No. 2 siRNA, 4390847)
- siELMOD2 1: Silencer™ Select ref. s48678
- siELMOD2 2: Silencer™ Select ref. s110324
- siELMOD2 3: Silencer™ Select ref. s48679
- siELMOD2 4: Silencer™ Select ref. n339307
- siJAGN1 1: Silencer™ Select ref. s39100
- siJAGN1 2: Silencer™ Select ref. s39102
- siGPX8 1: Silencer™ Select ref. s54628
- siGPX8 2: Silencer™ Select ref. s54629
- siLCLAT1 1: Silencer™ Select ref. s48420
- siLCLAT1 2: Silencer™ Select ref. s48421

RT-qPCR

Cells were lysed in RLT buffer and RNA was extracted with a kit (Qiagen RNeasy Mini Kit, Cat. 74106), before reverse-transcription with the RevertAid First Strand cDNA synthesis Kit (Thermo Fisher Scientific) and analysis by RT-qPCR in triplicates using SYBR Green (Maxima SYBR Green/ROX qPCR Master Mix (2X), Thermo Fisher Scientific, K0223). All steps were performed according to the manufacturers' protocols. The qPCR reactions were run on a QuantStudio 7 Real-Time PCR system (Thermo Fisher Scientific). GAPDH was used as housekeeping gene for normalisation.

Used primers were the following: ELMOD2—forward: 5'-AAG GCG ACA CAT GTT GTT CA-3'—reverse: 5'-ACT GGC ATC CTT CTC AGG GT-3'; GAPDH—forward: 5'-GAG TCA ACG GAT TTG GTC GT-3'—reverse: 5'- GAC AAG CTT CCC GTT CTC AG-3'.

Luciferase assay

HEK293T cells were treated for 3 days with siCtrl or two distinct siELMOD2 and were then co-transfected with a plasmid encoding for luciferase under the IFN- β promoter (pIFN β -GLuc,

described in ref²⁰) together with the indicated stimulatory plasmids, using the transfection reagent GeneJuice (NovaGen, 70967-6) according to the manufacturer's instructions (per 96-well plate well, 100 ng of TBK1 or STING plasmids, 10 ng of cGAS plasmid (when present) and 25 ng of pIFN β -GLuc). Luciferase assay was performed the next morning by collecting the supernatant and measuring the activity of the gaussia luciferase in it thanks to the addition of the substrate coelenterazine (PJK GmbH) and subsequent luminescent detection.

HEK293T ELMOD2 KO cells generation (CRISPR-Cas9) and characterisation

To generate the needed CRISPR-Cas9 plasmid, a single guide RNA (sgRNA) targeting the second exon of ELMOD2 (after the start codon) was designed using the web tool CRISPOR¹⁷⁹ with default settings. The chosen sgRNA sequence was 5'-GGC TAT TAC GAC AGA TGA CT-3'. Hence, the ordered primers with cloning overlap sites were 5'-CACC GGC TAT TAC GAC AGA TGA CT-3' (sense) and 5'-AAAC AGT CAT CTG TCG TAA TAG CC-3' (antisense). Those primers were phosphorylated and annealed to be cloned into the Bpil-digested pSpCas9(BB)-2A-Puro (PX459) V2.0 plasmid (Addgene, 62988). This plasmid was a gift from Feng Zhang¹⁸⁰. The obtained plasmid could be used for CRISPR-Cas9 KO generation by direct transfection as described below.

HEK293T cells were plated in 6-well culture plates at about 80% confluency and transfected with the above described PX459-sgELMOD2 plasmid. Per well, 3.5 μ L Lipofectamine 2000 (LifeTechnologies, 11668019) and 1 μ g plasmid-DNA were each diluted in 125 μ L OptiMEM (LifeTechnologies, 31985047), mixed, incubated 5 minutes and added on top of the well. The next day, the culture media was replaced and cells were put under puromycin (5 μ g/mL) selection for 3 days. Surviving cells were expanded in antibiotics-free media and FACS-sorted into single clones.

Characterisation of the obtained clones were performed by genomic DNA extraction from cell lysates using the Extract-N-AmpTM Tissue PCR Kit (Sigma) according to the manufacturer's instructions. A classical PCR was then run on this total amplified genomic DNA with primers targeting exons 1 and 3 of the ELMOD2 gene, so that deletion caused by CRISPR in exon 2 would prevent PCR-amplification product to appear at the right size on an agarose electrophoresis gel. The used primers were: forward: 5'-GAC TTC CGG GTC GCG-3'; reverse: 5'- CTT ATT CTT GGA GTA TGT CAA GGA A-3', used with an annealing temperature of 60°C. PCR products were run on a 1% agarose gel in 1X UltraPureTM TAE buffer (Thermo Fisher Scientific, 15558026).

Alanine-scanning (ala-scan) of STING C-terminal cytosolic domain

Site-directed mutagenesis primers were designed to change three-by-three all amino acids of the STING C-terminal cytosolic domain to alanine. The needed primers were designed on the QuikChange Primer Design online tool developed by Agilent¹⁸¹. All plasmids were then obtained via mutagenesis PCR (using pEFBos GFP-hSTING WT as a template) and sequenced for verification.

HEK293T cells were then plated in 96-well plates and transfected using the GeneJuice transfectant reagent according to the manufacturer's protocol. The transfected plasmids were the ones from this GFP-hSTING ala-scan library, either alone or combined with cGAS plasmid. Per well, the amounts used were 200 ng of STING, combined with 5 ng of cGAS in the stimulated wells, with 0.5 μ L GeneJuice in a total of 45 μ L OptiMEM. 20 hours post-transfection, the cells were imaged on the IN Cell Analyzer 2200 microscope (20x). 6 fields of view per well (in 2 wells per condition in each experimental repeat) were imaged.

Trafficking evaluation of each construct was then performed "by eye", as described above, using the two available wells for each construct, yielding a trafficking score between 0 and 6.

Data analysis and figure assembly

Data were assembled and analysed combining the following softwares: Excel (Microsoft), Fiji, GraphPad PRISM (from v7 to v9.3.1) and Adobe Illustrator. Some images' panels were assembled using OMERO (v5.11.0)¹⁸².

2.8 – Contributions

Although I generated most data presented in **Chapter 2**, some experiments were partially or totally performed by colleagues or collaborators. Here is a list of these external contributions:

- Dr. Alexiane Decout, a postdoc in our lab at the time, worked together with me on several of the described projects, so that many experiments were shared between us. Her main contributions to the results presented in this chapter are the following: she generated the HEK293T^{GFP-mSting} cell lines (WT and mutants) first described in subchapter 2.1, prepared the samples for the MS/MS-screen described in subchapter 2.3 and worked together with me to investigate ELMOD2 as described in sub-chapter 2.4. In terms of results displayed in the figures above, she prepared and imaged the samples of Fig. 2.1b, ran the Western blots of Fig. 2.3f (on samples prepared by

myself), and performed part of the repeats of the experiments resulting in Fig. 2.5a and Fig. 2.5c.

- The Prestwick-library-based chemical screen described in sub-chapter 2.2 was designed with the help of the EPFL Biomolecular Screening Facility (BSF). The BSF prepared the used compounds-filled plates and Dr. Fabien Kuttler (from the BSF) wrote the machine learning scripts for CellCognition and the template of the script for CellProfiler used for image analysis.
- The MS/MS screen described in sub-chapter 2.3 was conducted by Anita Frauenstein, from Prof. Felix Meissner's laboratory at the Max Planck institute in Munich, on samples prepared in our lab by Alexiane Decout.

Chapter 3 – Clathrin-associated AP-1 controls termination of STING signalling

3.1 – Introductory remarks

Having gained some insights into initial STING ER-to-Golgi trafficking, we started building hypotheses about STING end-signalling and its trafficking from the Golgi to the lysosomes, one way by which it is degraded⁶². This shift of focus led to the second part of this thesis, results of which are described in Liu, Xu, Rivara et al., 2022, published very recently in *Nature* and where I am a co-first author¹³⁷. This chapter is hence named after and constituted by the accepted final pre-print version of our paper, adapted for this thesis.

My main responsibilities in this work were the following: generation of all in-house stable cell lines, many cell-based assays, all confocal and airyscan microscopy and analyses, experiments related to correlated light and electron microscopy (CLEM), including cell stimulation and light microscopy aspects, experiments related to sample preparation for stimulated emission depletion (STED) microscopy, extensive contribution to general experimental design and manuscript preparation.

3.2 – Main

Clathrin-associated AP-1 controls termination of STING signalling

Ying Liu^{1,4}, Pengbiao Xu^{1,4}, Sophie Rivara^{1,4}, Chong Liu¹, Jonathan Ricci¹, Xuefeng Ren², James H. Hurley^{2,3} & Andrea Ablasser¹

¹ Global Health Institute, Swiss Federal Institute of Technology Lausanne (EPFL), Lausanne, Switzerland

² Department of Molecular and Cell Biology and California Institute for Quantitative Biosciences, University of California, Berkeley, Berkeley, USA

³ Helen Wills Neuroscience Institute, University of California, Berkeley, Berkeley, USA

⁴ These authors contributed equally: Ying Liu, Pengbiao Xu, Sophie Rivara

Correspondence: andrea.ablasser@epfl.ch

3.2.1 – Abstract

Stimulator of interferon genes (STING) functions downstream of cyclic GMP-AMP synthase (cGAS) in DNA sensing or as a direct receptor for bacterial cyclic dinucleotides and small-molecules to activate immunity during infection, cancer, and immunotherapy^{19–24,47,48,111,164}. Precise regulation of STING is essential to ensure balanced immune responses and prevent detrimental autoinflammation^{99,110,112,183–185}. Upon activation, STING, a transmembrane protein, traffics from the endoplasmic reticulum (ER) to the Golgi, where its phosphorylation by the protein kinase TBK1 enables signal transduction^{56,57,118,123}. The mechanism that ends STING signalling at the Golgi remains unknown. Here we reveal that the adaptor protein complex-1 (AP-1) controls the termination of STING-dependent immune activation. We find that AP-1 sorts phosphorylated STING into clathrin-coated transport vesicles (CCVs) for delivery to the endo-lysosomal system where STING is degraded⁶². We identify a highly conserved dileucine motif in the cytosolic C-terminal tail (CTT) of STING that, jointly with TBK1-dependent CTT phosphorylation, dictates AP-1 engagement of STING. A 2.3 Å cryo-electron microscopy (EM) structure of AP-1 in complex with phospho-STING explains enhanced recognition of TBK1-activated STING. We show that suppression of AP-1 exacerbates STING-induced immune responses. Our results explain a structural mechanism of negative regulation of STING and establish that signalling initiation is inextricably associated with its termination to enable transient activation of immunity.

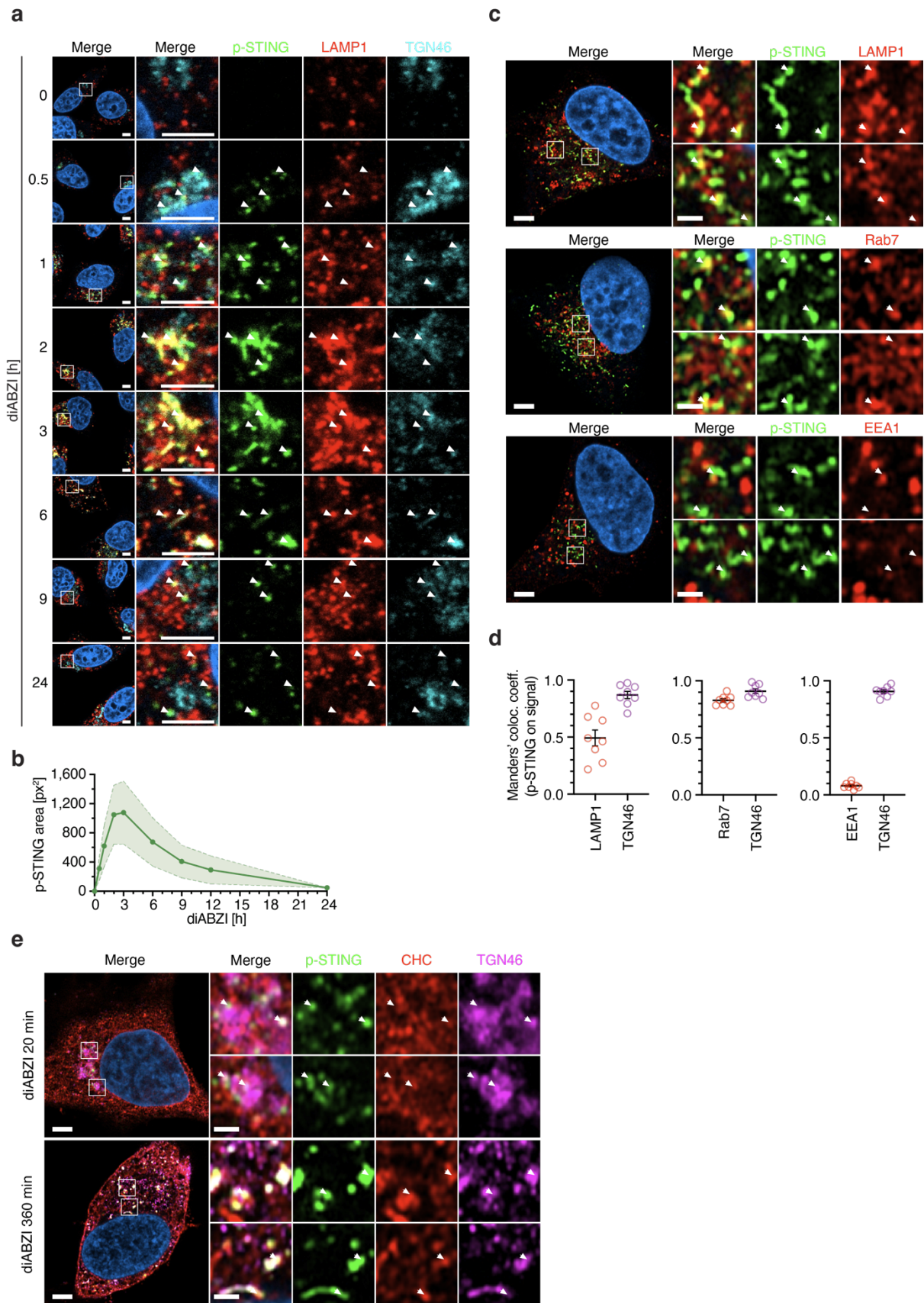
3.2.2 – Introduction

Following activation and ER exit, STING engages two bifurcating cellular effector pathways. The first pathway diverges along STING's transition to the Golgi and enables autophagy, an

ancestral antiviral function of STING, whereas the second pathway, launched from the Golgi, promotes the transcriptional activation of innate immune genes, an evolutionary more recent functional adaptation^{45,59}. Both pathways eventually converge at the lysosome, where STING is degraded^{58,59,62,139}. The initiation of STING's downstream transcription cascade is controlled by a multi-step process: it begins with the recruitment of TBK1, continues with the phosphorylation of STING by TBK1, and results in the engagement of IRF-3 by phosphorylated STING^{57,117,123,134}. STING bound IRF-3, in turn, is phosphorylated by TBK1, and translocates to the nucleus to regulate gene expression jointly with NF- κ B and other transcription factors. Through this cascade of molecular events, STING triggers a broad range of effector functions, most notably the expression of type I interferons (IFNs), proinflammatory cytokines, and co-stimulatory molecules. Owing to these favourable immunostimulatory properties, STING agonists are being developed for use as immunotherapeutics^{48,164,186}. However, to optimize robust immune activation while preventing immunopathology STING responses demand strict regulation. Here, we sought a mechanism that explains ending of STING-dependent immune signalling.

3.2.3 – Activated STING traffics from the Golgi to lysosomes via CCVs

We tracked activated STING (phosphorylated at S366; hereafter p-STING) (ref⁵⁷) along its intracellular traffic route by high resolution confocal and airyscan microscopy in HeLa cells. Extending prior findings^{62,123}, upon stimulation with the small-molecule agonist diABZI-C3 (hereafter diABZI) (ref⁴⁸), p-STING rapidly (~0.5 h) appeared at the *trans*-Golgi network (TGN) and then moved to LAMP1⁺ endo-lysosomal compartments before disappearing (**Extended Data Fig. 3.1a-d**). p-STING transited Rab7⁺ late endosomes, but did not co-localize with EEA1⁺, a marker of early endosomes (**Extended Data Fig. 3.1c, d**). Membrane traffic between the TGN and endocytic organelles can involve clathrin-coated transport vesicles (CCVs)¹⁴⁹. Interestingly, STING and p-STING were enriched in CCVs obtained from diABZI-stimulated cells, but not unstimulated cells (**Fig. 3.1a**). Further, p-STING co-localized with clathrin heavy chain, a defining component of CCVs, at TGN46⁺ compartments in activated cells (**Fig. 3.1b, c** and **Extended Data Fig. 3.1e**). Stimulated emission depletion (STED) super-resolution microscopy confirmed that p-STING is incorporated into small (~100 nm diameter) CCVs (**Fig. 3.1d** and **Extended Data Fig. 3.2a**). In correlated light and electron microscopy (CLEM) experiments, we observed that, upon activation, characteristic STING perinuclear foci localized to areas containing multiple CCVs (**Fig. 3.1e** and **Extended Data Fig. 3.2b, c**). Together, these results establish that CCVs can function as transport vehicles of activated STING.



Extended Data Fig. 3.1 | Intracellular trafficking of phospho-STING. a, b, Confocal imaging (a) or quantification of p-STING area in brightfield fluorescent microscopy images (b) of HeLa^{STING} cells stimulated for 0, 0.5, 1, 2, 3, 6,

9, 12 or 24 h with 1 μM diABZI. Cells were fixed and stained for TGN46 (*trans*-Golgi), p-STING and LAMP1 (endolysosomal compartment) as well as with Hoechst dye (nuclei, in dark blue). Mean \pm s.e.m. of $n = 3$ independent experiments with at least 84 fields of view each per condition. Scale bars, 4 μm . **c, d**, Airyscan imaging (**c**) of HeLa^{STING} cells stimulated for 2.5 h with 1 μM diABZI. Cells were fixed and stained for TGN46 (*trans*-Golgi, not shown here), p-STING and the indicated marker as well as with Hoechst dye (nuclei, in dark blue). Colocalization of p-STING with the indicated marker is quantified by Manders' colocalization coefficients (**d**). One representative cell is shown, and quantification is the mean \pm s.e.m. of $n = 8$ cells examined in 1 of 4 independent experiments. Scale bars, 4 μm in larger left panel, 1 μm in zoomed-in panels. **e**, Airyscan imaging of HeLa^{STING} cells stimulated for 20, 150 (see Fig. 3.1b) or 360 min with 1 μM diABZI. Cells were fixed and stained for TGN46 (*trans*-Golgi), p-STING and CHC (clathrins) as well as with Hoechst dye (nuclei, in dark blue). One representative cell is shown of at least $n = 6$ cells from 3 independent experiments. White arrows point at occurrences of p-STING. Scale bars, 4 μm in larger left panel, 1 μm in zoomed-in panels.

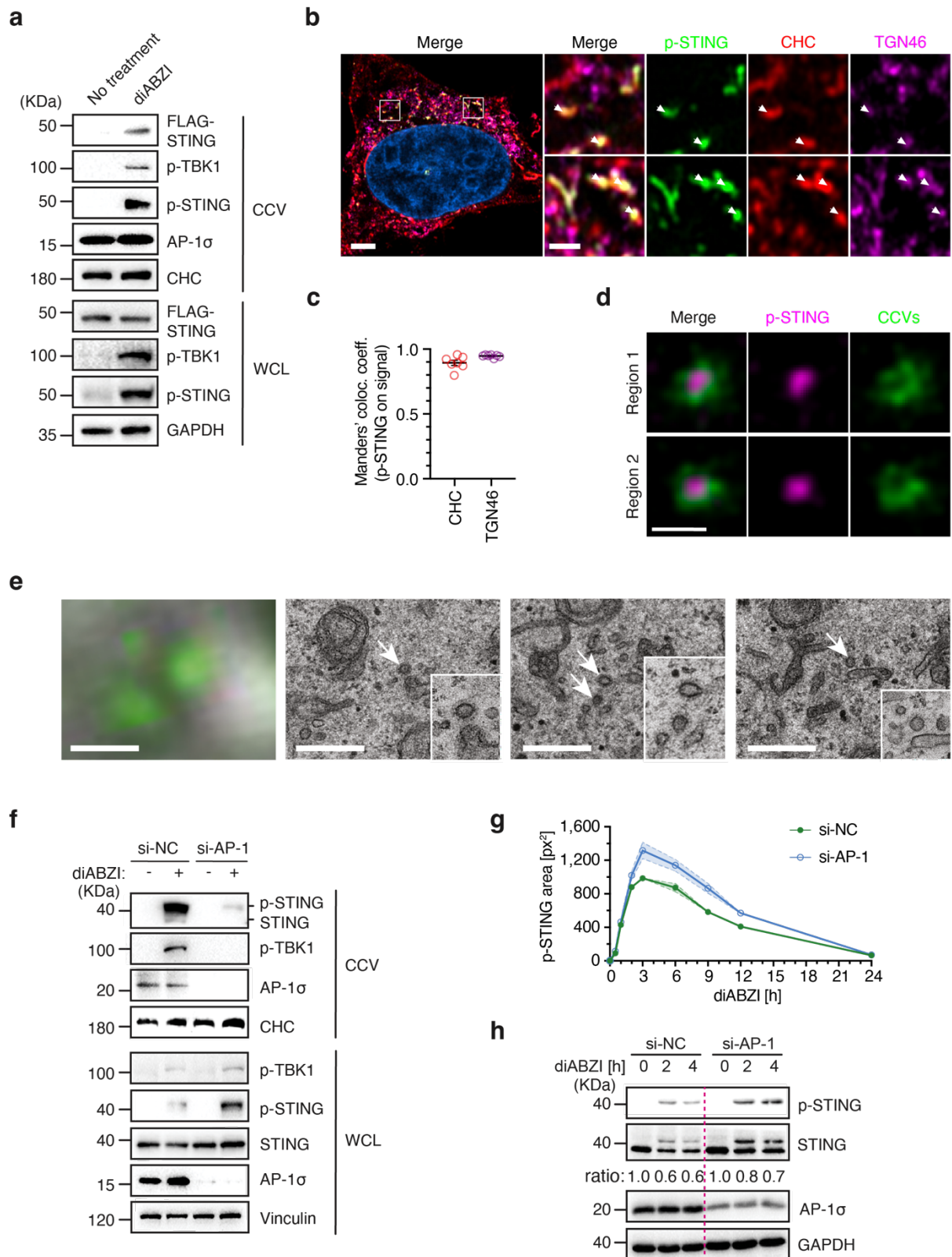
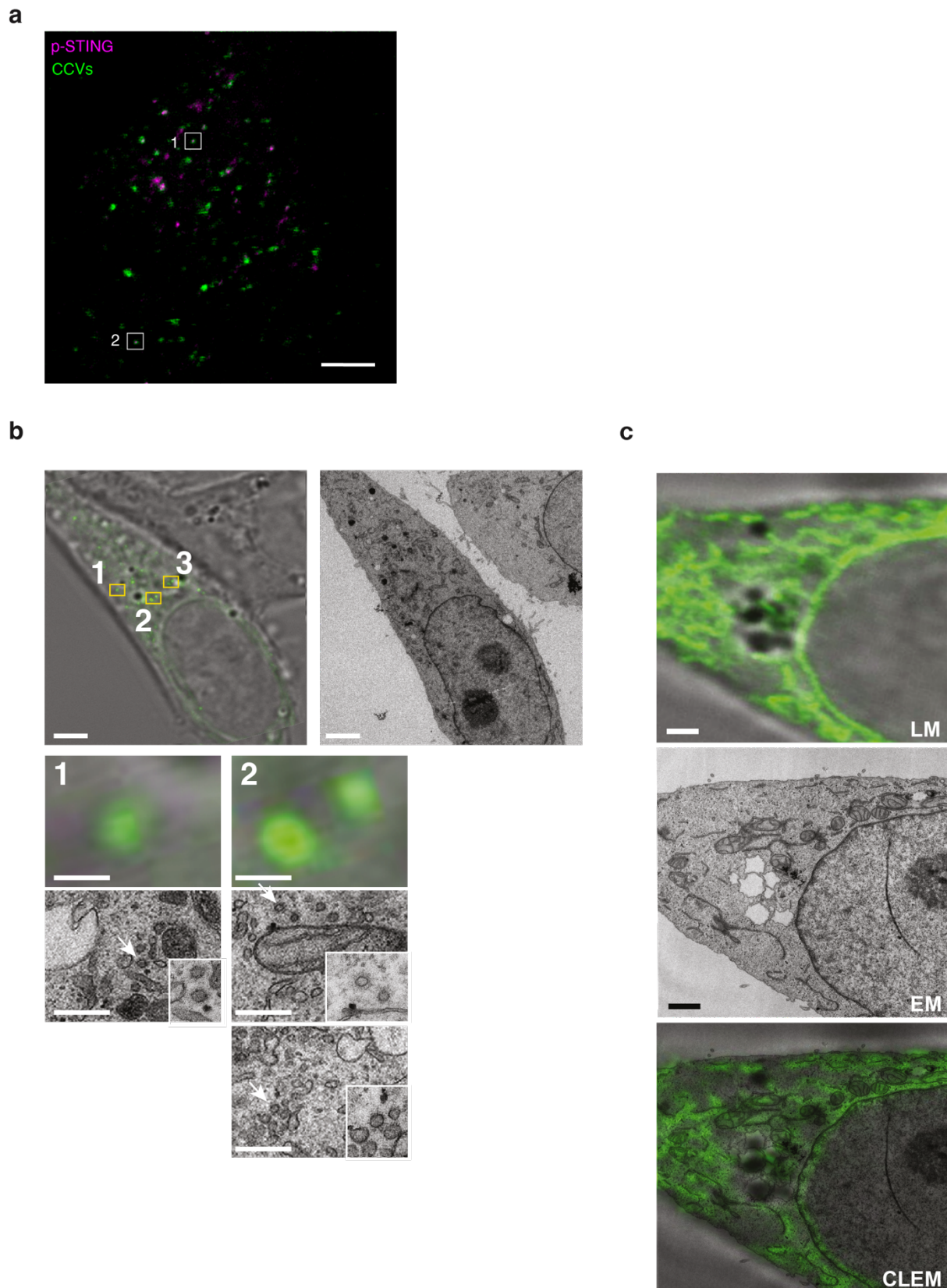


Fig. 3.1 | AP-1 loading of STING into CCVs at the TGN. a, Whole cell lysate (WCL) and clathrin coated vesicles (CCVs) fractions from HeLa^{STING} cells were analysed by Western blot. Clathrin heavy chain (CHC) and GAPDH were used as a loading and processing controls. **b**, Airyscan imaging of HeLa^{STING} cells stimulated with diABZI. One representative cell of $n = 7$ cells. White arrows point at occurrences of p-STING. Scale bars, 4 μm (left) or 1

μm (zoomed-in squares). **c**, Colocalization of p-STING with CHC described in **(b)** is quantified by Manders' colocalization coefficients. Mean \pm s.e.m. of $n = 7$ cells. **d**, STED images showing p-STING enclosed in CCVs from cells transfected with mCherry-clathrin and Flag-STING and stimulated with diABZI. Regions 1 and 2 are magnified from a large-field-of-view STED image (see Extended Data Fig. 3.2a). Scale bars, 200 nm. **e**, Correlative light and electron microscopy (CLEM) of HeLa^{GFP-STING} stimulated with diABZI. The shown images depict box 3 of Extended data Fig. 3.2b in airyscan microscopy (left) or EM at different Z-heights (three right panels). White arrows indicate CCVs. Scale bars, 0.5 μm . **f**, WCL and CCV fractions from HeLa cells treated with non-targeting control (NC) siRNA or AP-1 siRNA followed by stimulation with diABZI were analysed by Western blot. CHC was used as a loading control. **g**, Quantification of p-STING area in brightfield fluorescent microscopy images of HeLa^{STING} cells treated with siRNAs and stimulated with diABZI. Mean \pm s.e.m. of $n = 3$ independent experiments with 99 fields of view per condition. **h**, HeLa cells transfected with siRNAs and stimulated with diABZI were analysed by Western blot. Ratios of STING versus loading control (GAPDH) normalized to the 0 h of each condition. One representative of three (**a-c, h**) or two (**f**) independent experiments is shown.



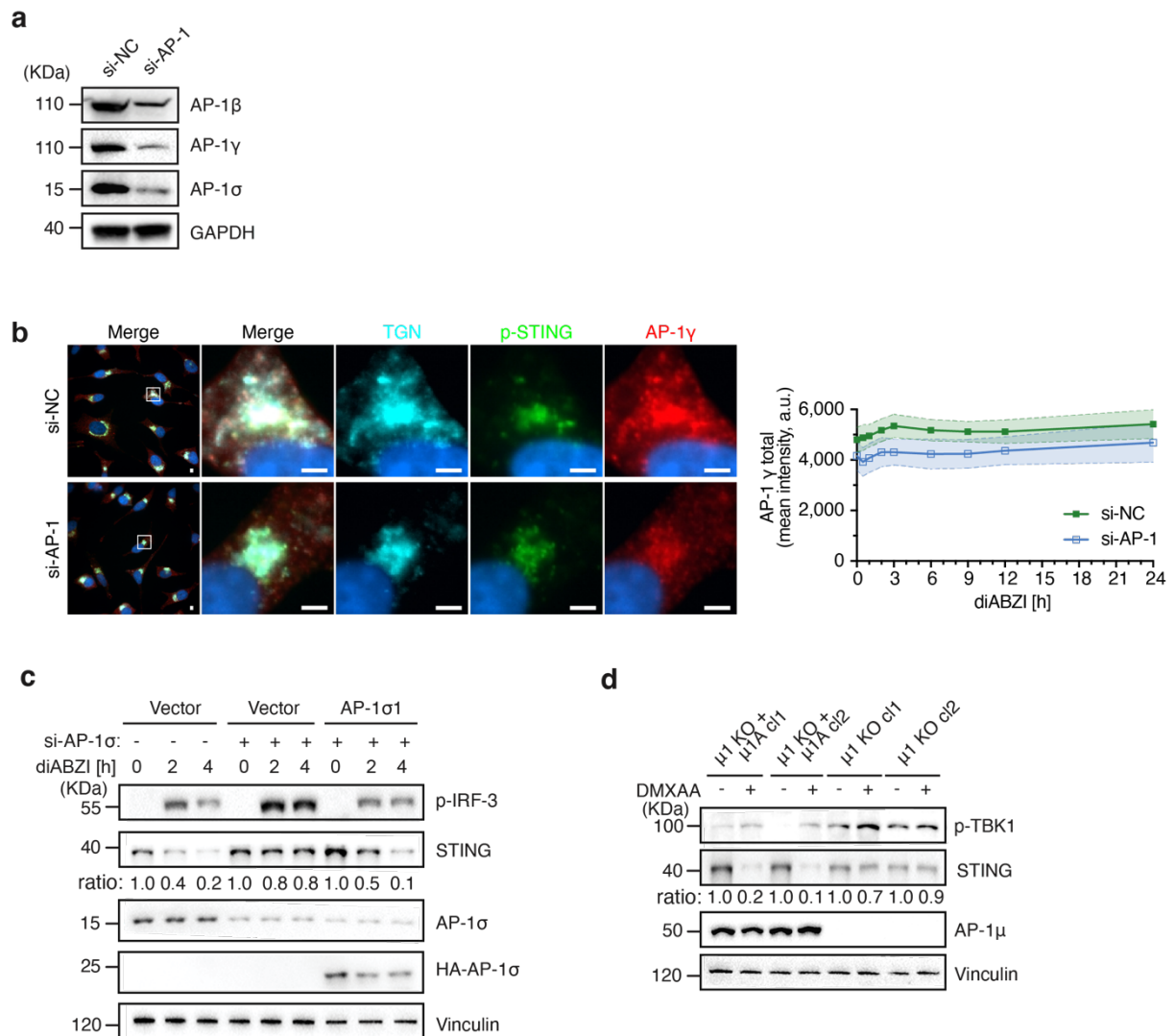
Extended Data Fig. 3.2 | Super-resolution imaging of STING in CCVs. **a**, Large-field-of-view STED image showing the co-localization of p-STING and CCVs. HeLa cGAS/STING double KO cells were transfected with mCherry-clathrin and Flag-STING. One day later they were stimulated with $1 \mu\text{M}$ diABZI for 2.5 hours and then fixed and stained for p-STING. Two representative events highlighted in the boxes were magnified (see Fig. 3.1d).

Scale bar, 2 μm . The image depicts $n = 1$ cell out of 62 cells imaged over the course of 2 independent experiments, including 25 cells showing clear colocalization and 3 exhibiting clathrin ring structures. **b, c**, Correlative light and electron microscopy (CLEM) of HeLa STING KO cells stably reconstituted with GFP-hSTING stimulated for 2.5 h with 1 μM diABZI (**b**) or left untreated (**c**). For the stimulated cell (**b**), some regions with accumulation of high GFP-STING intensity (yellow boxes) were re-imaged by EM in higher resolution at relevant Z-heights. Zoom-in and higher-resolution EM slices from box 3 is shown in Fig. 3.1e. LM – light microscopy (airyscan). EM – electron microscopy. CLEM – correlative light and electron microscopy. White arrows indicate CCVs. Scale bars in (**b**), 2 μm (un-zoomed top images) and 0.5 μm (zoom-in box images). Scale bars in (**c**), 1 μm . $n = 1$ out of 3 stimulated cells (**b**) and $n = 1$ out of 2 non-stimulated cells imaged from one sample per condition prepared for CLEM.

3.2.4 – AP-1 sorts STING into CCVs

Formation of CCVs relies on heterotetrameric adaptor protein (AP) complexes, which physically connect clathrin with transmembrane cargo proteins^{149,187,188}. The most prominent AP complex involved in cargo shuttling from the TGN to endo-lysosomes is AP-1, consisting of the four subunits $\beta 1$, γ , $\mu 1$, and $\sigma 1$ (ref¹⁸⁹). Notably, a knockdown of three AP-1 subunits (*AP1G1*, *AP1S1*, *AP1B1*) resulted in marked reduction of STING, p-STING and p-TBK1 within CCVs, whereas overall cellular levels of STING and p-STING were elevated (**Fig. 3.1f-h** and **Extended Data Fig. 3.3a**). Critically, STING trafficking from the ER to the TGN was not affected in AP-1-depleted cells (**Extended Data Fig. 3.3b**). We confirmed that a knockdown of the $\sigma 1$ subunit alone or genetic knockout of the $\mu 1$ subunit in mouse embryonic fibroblasts (MEFs) affected STING degradation and reintroducing the missing subunit restored decay of activated STING (**Extended Data Fig. 3.3c, d**)^{190,191}. These findings suggested a role for AP-1 in controlling activated STING by gating loading into CCVs.

Adaptor protein-dependent sorting requires direct engagement between the multimeric complex and its cargo on target membranes^{187,188}. Accordingly, p-STING co-localized with AP-1 at the TGN, and STING robustly bound the γ and $\sigma 1$ subunits of AP-1 upon activation (**Fig. 3.2a, b** and **Extended Data Fig. 3.4a**). STING associated with AP-1 in response to diverse cellular activators of STING, including dsDNA, cGAMP, and the physiological activator herpes simplex virus-1 (HSV-1), demonstrating that AP-1 recognition is an integral element of the cell biological regulation of STING (**Fig. 3.2c**).



Extended Data Fig. 3.3 | AP-1 associates with STING after activation. **a**, Western blot showing levels of AP-1 subunits after NC siRNA or AP-1 siRNA transfection in HeLa cells. GAPDH was used as a loading control. **b**, Brightfield fluorescent microscopy images and corresponding quantification of AP-1 γ signal intensity of HeLa^{STING} cells treated for 3 days with NC siRNA or AP-1 siRNA and then stimulated for 0, 0.5, 1, 2, 3, 6, 9, 12 or 24 h with 1 μ M diABZI. Cells were then fixed and stained for TGN46 (*trans*-Golgi), p-STING and AP-1 γ as well as with Hoechst dye (nuclei, in dark blue). Images shown here are from the 2 h time-points. Mean \pm s.e.m. of $n = 3$ independent experiments with 99 fields of view each per condition. Scale bars, 4 μ m. **c**, HeLa cGAS KO cells incubated with NC siRNA or siRNAs targeting AP-1 σ 1 and AP-1 σ 3 for 3 days and reconstituted with empty vector or HA-tagged AP-1 σ 1 were treated with 2.5 μ M diABZI for 0, 2, 4 h before analysis by Western blot. Vinculin was used as a loading control. **d**, AP-1 μ 1 KO MEFs and μ 1 KO + μ 1A MEFs were treated with 0.5 μ g/mL DMXAA for 2 h and analysed by Western blot. Vinculin was used as a loading control. One representative of three (**b**, **c**) or at least two (**a**, **c-d**) independent experiments is shown. Ratios of target proteins versus loading control normalized to the untreated sample of each condition (**c-d**).

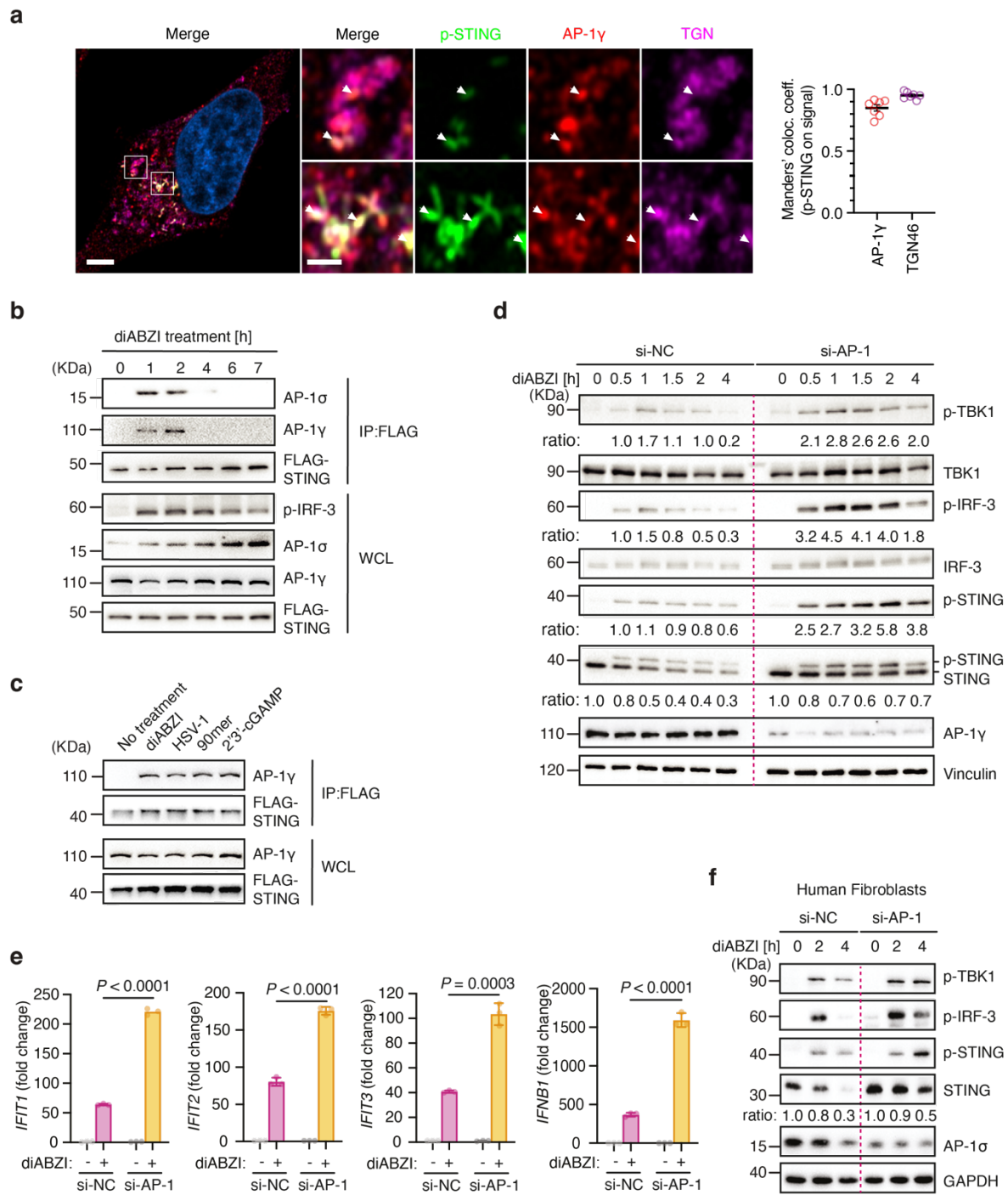
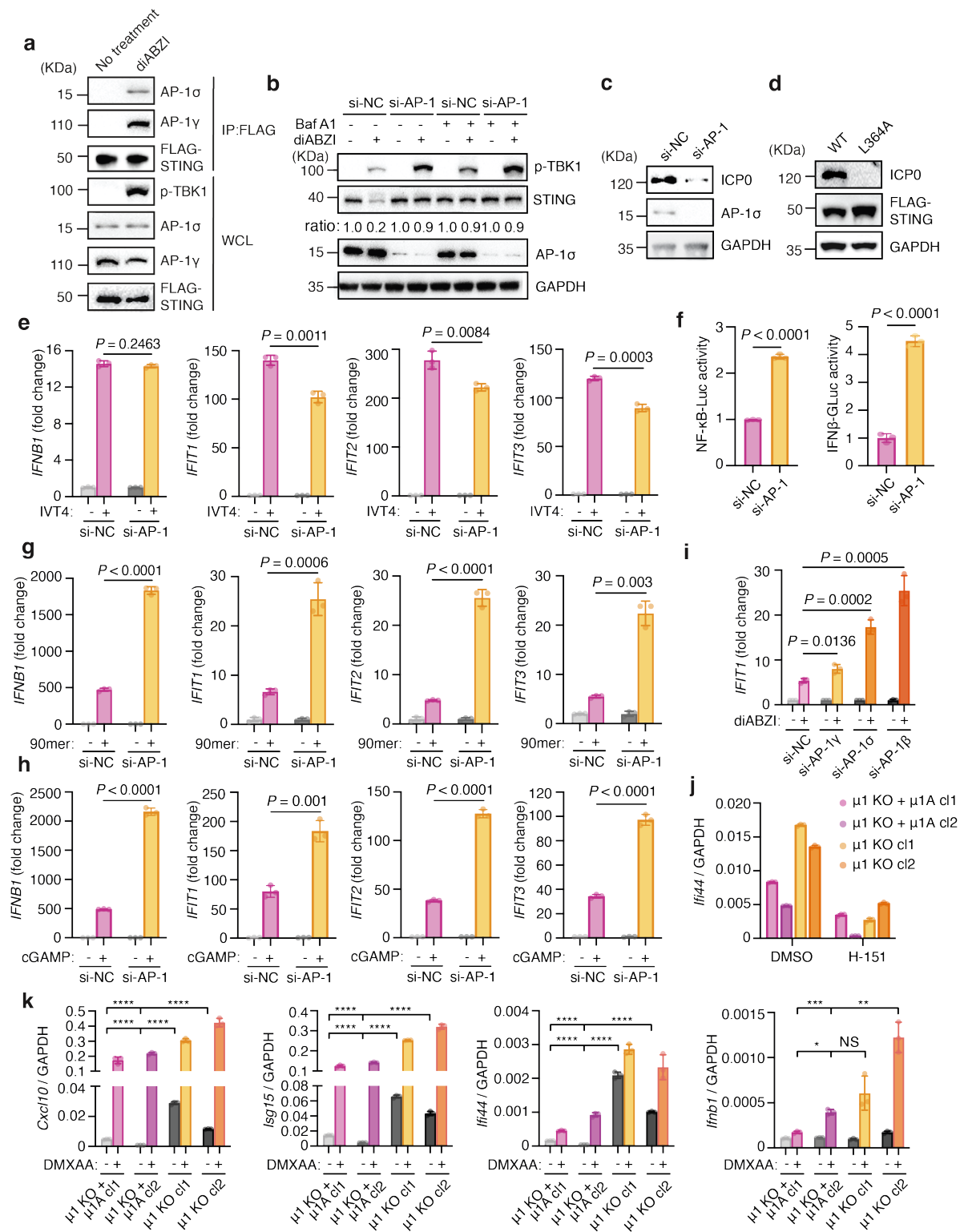


Fig. 3.2 | AP-1 binding directs STING degradation to limit immune activation. **a**, Airyscan imaging of HeLa^{STING} cells stimulated for 2.5 h with diABZI. Colocalization of p-STING with AP-1 γ is quantified by Manders' colocalization coefficients. One representative cell is shown, and quantification is the mean \pm s.e.m. of $n = 7$ cells from one out of 4 independent experiments. White arrows point at occurrences of p-STING. Scale bars, 4 μ m in larger left panel, 1 μ m in zoomed-in panels. **b**, HeLa^{STING} cells were stimulated with diABZI. After immunoprecipitation (IP) with anti-FLAG antibody, cells were analysed by Western blot. **c**, HeLa^{STING} cells were stimulated with diABZI for 2 h, infected with HSV-1 (MOI = 10) for 6 h or transfected with 90mer dsDNA (1 μ g) for 3 h or 1 μ M 2'3'-cGAMP for 6 h. After IP with anti-FLAG antibody samples were analysed by Western blot. **d**, HeLa cells transfected with siRNAs were stimulated with diABZI and were analysed by Western blot. Vinculin was used as a loading control. **e**, Induction of

IFNB1, *IFIT1*, *IFIT2*, *IFIT3* expression was assessed by RT-qPCR in HeLa cells transfected with siRNAs and treated with diABZI for 3 h. Ratios of *IFNB1*, *IFIT1*, *IFIT2*, *IFIT3* mRNA versus *GAPDH* mRNA normalized to the untreated groups of each condition. Data are mean \pm s.d. of three technical replicates. *P* values were obtained by two-tailed Student's *t*-test. **f**, WI-38 human fibroblasts transfected with siRNAs for 3 days were stimulated with diABZI and analysed by Western blot. GAPDH was used as a loading control. One representative of three (**a**, **d-f**) or two (**b**, **c**) independent experiments is shown. Ratios of target proteins versus loading control normalized to the 0 time-point of each condition (**d**, **f**).

3.2.5 – AP-1 restricts STING signalling

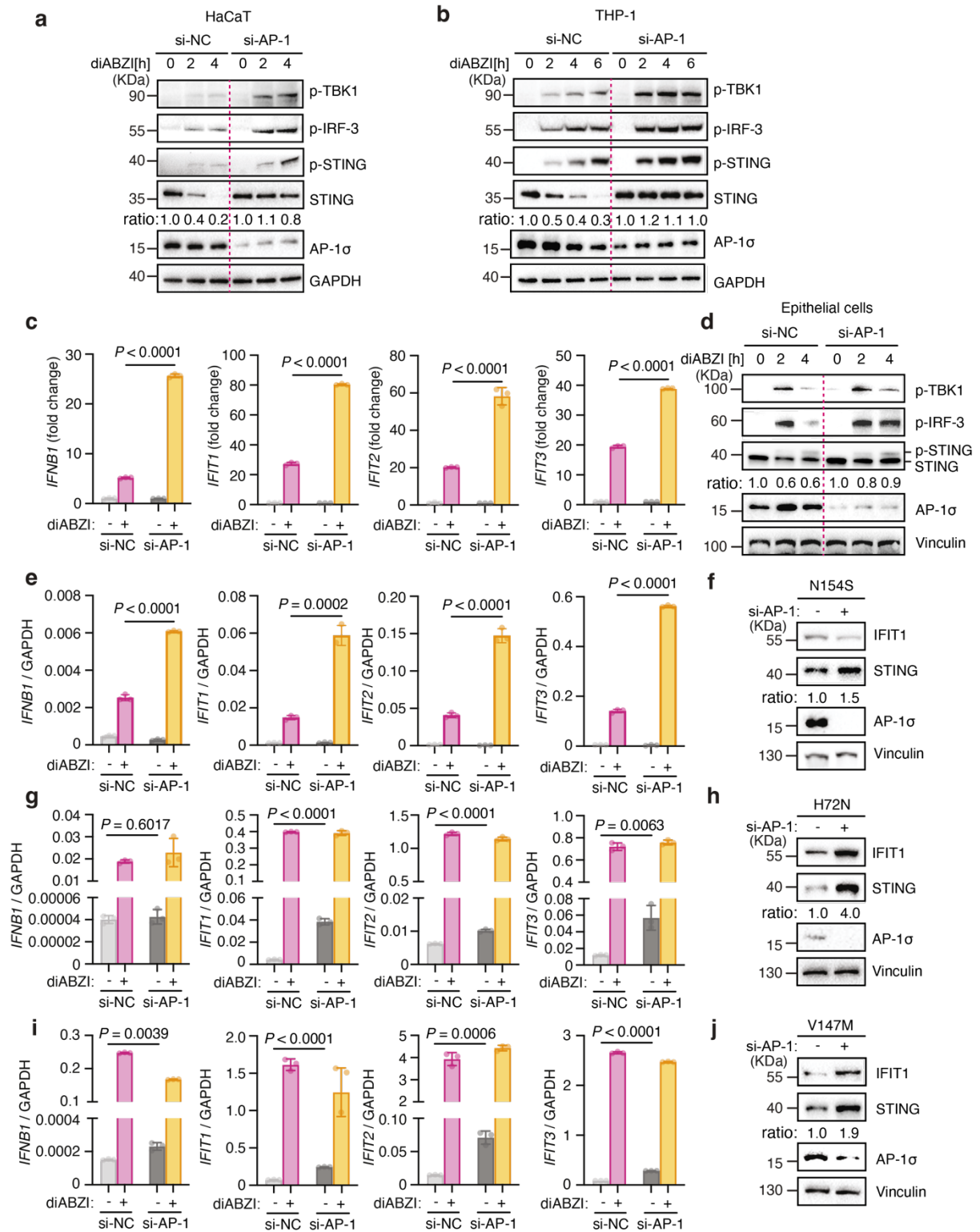
We next determined how disruption of AP-1 affects STING-dependent immune signalling. A knockdown of AP-1 potently augmented levels of p-TBK1 and p-IRF-3, in addition to p-STING, and prolonged signalling when compared to stimulated control cells (**Fig. 3.2d**). Blocking lysosomal acidification further boosted TBK1 activation in AP-1-depleted cells consistent with a model in which AP-1 functions as the initiator of signalling shut-down upstream of lysosomes (**Extended Data Fig. 3.4b**). Cells depleted for AP-1 displayed markedly increased type I IFN levels, which correlated with more potent inhibition of HSV-1 replication (**Fig. 3.2e** and **Extended Data Fig. 3.4c**). By contrast, AP-1 suppression mildly decreased type I IFN responses elicited by triphosphate RNA, a trigger for RIG-I-like helicases, demonstrating that AP-1-mediated negative regulation of innate immune activation is a specific feature of the STING signalling pathway (**Extended Data Fig. 3.4e**). Analysis of various cells, stimuli, and read-outs as well as single subunit knockdowns showed that AP-1-dependent restriction of type I IFN signalling is a universal mechanism of controlling STING activity (**Fig. 3.2f** and **Extended Data Figs. 3.4f-l** and **3.5a-d**). Stronger STING-dependent type I IFN responses were also apparent in μ 1A-deficient in MEFs compared to μ 1A-reconstituted counterparts (**Extended Data Fig. 3.4j, k**). In STING-associated vasculopathy with onset in infancy (SAVI), gain-of-function alleles of *STING1* cause constitutive type I IFN responses^{99,183}. AP-1 depletion in fibroblasts from SAVI patients with distinct hyperactive STING variants^{99,105} led to exaggerated type I IFN signalling and accumulation of STING (**Extended Data Fig. 3.5e-j**). Collectively, these results establish AP-1 as a critical and conserved mediator in balancing STING responses in various, biologically relevant contexts, and implicate AP-1 recruitment onto STING as the initiating event in immune signalling termination.



Extended Data Fig. 3.4 | AP-1 depletion boosts STING-dependent immune activation.

a, HEK293T cells transfected with FLAG-tagged STING^{WT} were treated with 2.5 μ M diABZI or left untreated for 2 h, immunoprecipitated (IP) with anti-FLAG antibody, and analysed by Western blot. **b**, HeLa cells transfected with NC siRNA or AP-1 siRNA for 3 days were treated with 20nM Baf A1 and 2.5 μ M diABZI for 2 h before analysed by Western blot. GAPDH was used as a loading control. **c**, HeLa cells incubated with NC siRNA or AP-1 siRNA for 3 days were infected with HSV-1 (MOI=5) for 14h and analysed by Western blot. GAPDH was used as a loading

control. **d**, HeLa cGAS/STING double KO cells transfected with FLAG-tagged STING^{WT}, STING^{L364A} were treated with 2.5 μ M diABZI for 2h were infected with HSV-1 (MOI=5) for 14h and analysed by Western blot. GAPDH was used as a loading control. **e**, mRNA levels of *IFNB1*, *IFIT1*, *IFIT2* and *IFIT3* in HeLa cells transfected with NC siRNA or AP-1 siRNA for 3 days and treated with 0.5 μ g/mL IVT4 were assessed by RT-qPCR. **f**, NF- κ B and IFN- β luciferase assay in HEK293T cells incubated with NC siRNA or AP-1 siRNA for 3 days, followed by transient expression of STING and stimulation with diABZI (2.5 μ M). **g**, Induction of *IFNB1*, *IFIT1*, *IFIT2*, *IFIT3* expression was assessed by RT-qPCR in HeLa cells transfected with NC siRNA or AP-1 siRNA for 3 days and then transfected with 1 μ g 90mer. **h**, Induction of *IFNB1*, *IFIT1*, *IFIT2*, *IFIT3* expression was assessed by RT-qPCR in HeLa cells transfected with NC siRNA or AP-1 siRNA for 3 days and then transfected with 1 μ M 2'3'-cGAMP. **i**, Induction of *IFIT1* expression was assessed by RT-qPCR in HeLa cells transfected with non-targeting control (NC) siRNA or AP-1 α , AP-1 β and AP-1 γ siRNA for 3 days and then treated with 1 μ M diABZI for 3 hours. **j**, mRNA levels of mouse *ifi44* in MEFs cells treated with DMSO or 2 μ M H-151 for 3 days were assessed by RT-qPCR. **k**, mRNA levels of mouse *Cxcl10*, *Isg15*, *ifi44*, *ifnb1* in MEFs cells treated with 40 μ g/mL DMXAA for 3 hours were assessed by RT-qPCR. One representative of three (**b**, **e-k**) or at least two (**a**, **c**, **d**) independent experiments is shown. For RT-qPCR experiments, ratios of *IFNB1*, *IFIT1*, *IFIT2*, *IFIT3* mRNA versus *GAPDH* mRNA normalized to the untreated groups of each condition. Mean \pm s.d. of three (**e-k**) technical replicates. *P* values based on two-tailed Student's *t*-tests (**e-i**, **k**). **P*<0.05, ***P*<0.01, ****P*<0.001, *****P*<0.0001 (**k**). Ratios of target proteins versus loading control normalized to the 0 time-point of each condition (**b**).



Extended Data Fig. 3.5 | AP-1 depletion boosts STING-dependent immune activation in different cell types. **a, b**, HaCaT cells (**a**) or THP-1 cells (**b**) transfected with NC siRNA or AP-1 siRNA for 3 days were treated with 2.5 μ M diABZI for indicated time and analysed by Western blot. GAPDH was used as a loading control. **c, d**, Human primary epithelial cells incubated with NC siRNA or AP-1 siRNA for 3 days were treated with 2.5 μ M diABZI and were analysed by RT-qPCR (**c**) and Western blot (**d**). Vinculin was used as a loading control. **e-j**, Fibroblast cells

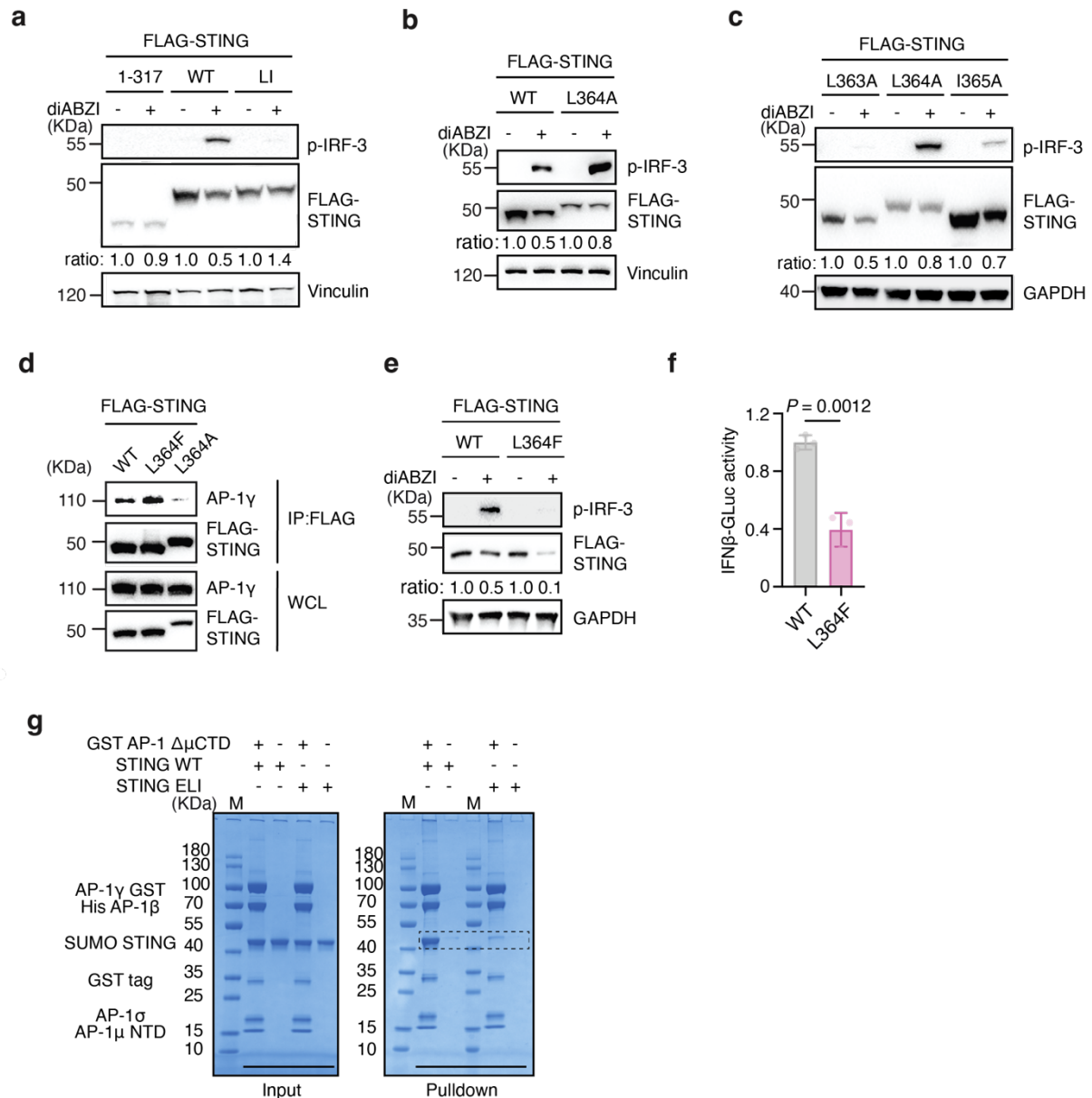
derived from SAVI patients characterized by *STING1* N154S mutation (**e-f**), H72N (**g-h**) or V147M (**i-j**) were incubated with NC siRNA or AP-1 siRNA for 3 days and then analysed by Western blot. Vinculin was used as a loading control in **f, h, j, e, g, i**. Induction of *IFNB1*, *IFIT1*, *IFIT2*, *IFIT3* expression was assessed by RT-qPCR in HeLa cells transfected with NC siRNA or AP-1 siRNA for 3 days and then stimulated with 1 μ M diABZI. Mean \pm s.d. of three (**c, e, g, i**) technical replicates. *P* values based on two-tailed Student's *t*-tests (**c, e, g, i**).

3.2.6 – Direct engagement of STING by AP-1

Adaptor protein interactions depend on the recognition of linear sorting signals in the cytosolic tail of transmembrane cargo proteins^{154,192,193}. Inspection of the cytosolic parts of STING revealed a highly conserved acidic dileucine-based consensus motif [D/E]xxxL[L/I] (x: any residue) located in the C-terminal tail (CTT; aa 336-379), juxtaposed to the PLPLRT/SD binding motif necessary for TBK1 recruitment and partially overlapping with the ϕ LxIS recruitment motif (ϕ : hydrophilic residue; x any residue) for IRF-3 (ref^{56,57,117,118}) (**Fig. 3.3a**). Strikingly, mutations of the two hydrophobic residues disrupted STING binding to AP-1 in activated cells, while mutation of the acidic residue alone had a negligible effect (**Fig. 3.3b**). A STING mutant devoid of the entire CTT also failed to bind AP-1 (**Fig. 3.3b**). As expected from the requirement of AP-1 for cargo loading, disruption of the LI motif abolished STING incorporation into CCVs and compromised subsequent degradation (**Fig. 3.3c** and **Extended Data Fig. 3.6a**). Moreover, neutralizing the hydrophobic leucine at position 364 (ExxxL) to alanine exaggerated type I IFN signalling, as shown by stronger IRF-3 phosphorylation and more potent inhibition of HSV-1 replication (**Extended Data Figs. 3.4d** and **3.6b**). Given that the isoleucine motif at position 365 (ExxxLI) is also required for the recruitment of IRF-3 onto STING (ϕ LxIS)^{57,117}, mutagenesis of this position abolished IRF-3 activation (**Extended Data Fig. 3.6c**). Analysing natural variants of STING, we identified a missense mutation, p.LL364LF, located in the ExxxLI motif reported for human cancer¹⁹⁴. Reconstitution experiments revealed that the L364F substitution increased STING binding to AP-1, accelerated STING degradation kinetics, and strongly impaired STING signalling activity (**Extended Data Fig. 3.6d-f**). Thus, unique substitutions within the ExxxLI motif influence type I IFN activation thresholds of human STING.

To directly probe STING dileucine recognition by AP-1, we reconstituted AP-1 target binding in vitro using the AP-1 core complex¹⁵³. Recombinant STING encompassing the ligand binding domain (LBD) including the CTT (LBD-STING) robustly interacted with Arf1-GTP activated AP-1 in pull-down assays¹⁵³, whereas a mutation of the STING dileucine motif (LBD-STING^{ELI}) was unable to bind AP-1 (**Fig. 3.3d**). Wild-type LBD-STING, but not LBD-STING^{ELI}, also bound a μ C-terminal domain truncated version of the AP-1 core, which mimics the open conformation of AP-1 and readily permits interaction with dileucine motifs in the absence of

allosteric activation by Arf-1 (**Extended Data Fig. 3.6g**) (ref^{195,196}). Together, these results reveal direct interaction between STING and the 'unlocked' activated AP-1 complex mediated by dileucine motif recognition.



Extended Data Fig. 3.6 I AP-1 binds to STING via a dileucine motif. **a**, HeLa cGAS/STING double KO cells transfected with FLAG-tagged STING^{WT}, STING¹⁻³¹⁷ or STING^{LI(L364A/I365A)} were treated or not with 2.5 μ M diABZI for 14 h and analysed by Western blot. Vinculin was used as a loading control. **b**, HeLa cGAS/STING double KO cells transfected with FLAG-tagged STING^{WT} or STING^{L364A} were treated or not with 2.5 μ M diABZI for 14 h and analysed by Western blot. Vinculin was used as a loading control. **c**, HeLa cGAS/STING double KO cells transfected with FLAG-tagged STING^{L363A}, STING^{L364A} or STING^{I365A} were treated or not with 2.5 μ M diABZI for 14 h and analysed by Western blot. GAPDH was used as a loading control. **d**, HEK293T cells transfected with FLAG-tagged STING^{WT}, STING^{L374A} or STING^{L374F} were treated with 2.5 μ M diABZI for 2 h, immunoprecipitated with anti-FLAG antibody, and analysed by Western blot. **e**, HeLa cGAS/STING double KO cells transfected with FLAG-

tagged STING^{WT} or STING^{L364F} were treated or not with 2.5 μ M diABZI for 14 h and analysed by Western blot. GAPDH was used as a loading control. **f**, IFN- β luciferase assay in HEK293T cells transfected with plasmids expressing indicated STING constructions and stimulated with diABZI (2.5 μ M). **g**, Glutathione Sepharose pull-down assays of LBD-STING^{WT} or LBD-STING^{ELI(E360A/L364A/I365A)} by GST-tagged AP-1 $\Delta\mu$ CTD core. One representative of three (**a-c**, **e-f**) or two (**d**, **g**) independent experiments is shown. Ratios of target proteins versus loading control normalized to the untreated sample of each condition (**a-c**, **e**). Mean \pm s.d. of three (**f**) technical replicates. *P* values based on two-tailed Student's *t*-tests (**f**).

3.2.7 – Phospho-regulation of STING binding AP-1

Owing to the positioning of the ExxxLI motif relative to the signalling elements for TBK1 and IRF-3 (see above; ref^{56,57,118}), simultaneous interactions between STING, TBK1, IRF-3, and AP-1, respectively, are physically impossible. Thus, we considered whether IRF-3 and TBK1 each could interfere with AP-1 recognition of STING. Whereas depletion of IRF-3 had no effect on STING binding to AP-1, TBK1 depletion strongly reduced binding, which suggested that rather than weakening, TBK1 enforces interaction between STING and AP-1 (**Fig. 3.3e**). In agreement with this finding, a truncated version of STING defective for TBK1 recruitment (STING^{LR}) (ref^{56,118}) was unable to bind AP-1 (**Extended Data Fig. 3.7a**). Further, TBK1 KO cells showed compromised degradation of activated STING and reconstitution studies and chemical inhibition of TBK1 by BX795 revealed that TBK1's impact on STING degradation depends on intact kinase activity (**Fig. 3.3f** and **Extended Data Fig. 3.7b, c**). We therefore hypothesized that TBK1-mediated phosphorylation might dictate interaction between STING and AP-1. Quantifying in vitro binding between STING and AP-1 showed that although unmodified LBD-STING bound to the open AP-1 core, in vitro phosphorylation of STING by TBK1 (p-LBD-STING) markedly increased the apparent affinity (**Fig. 3.3g** and **Extended Data Fig. 3.7d**). As expected, LBD-STING^{ELI} showed no binding, whereas a phospho-mimetic STING mutant¹¹⁸ increased binding affinity similar to the levels seen for in vitro phosphorylated STING (**Extended Data Fig. 3.7e, f**). Thus, TBK1-dependent phosphorylation is critical for regulating binding enhancement between STING and AP-1, which in the context of cells is important for efficient cargo recognition.

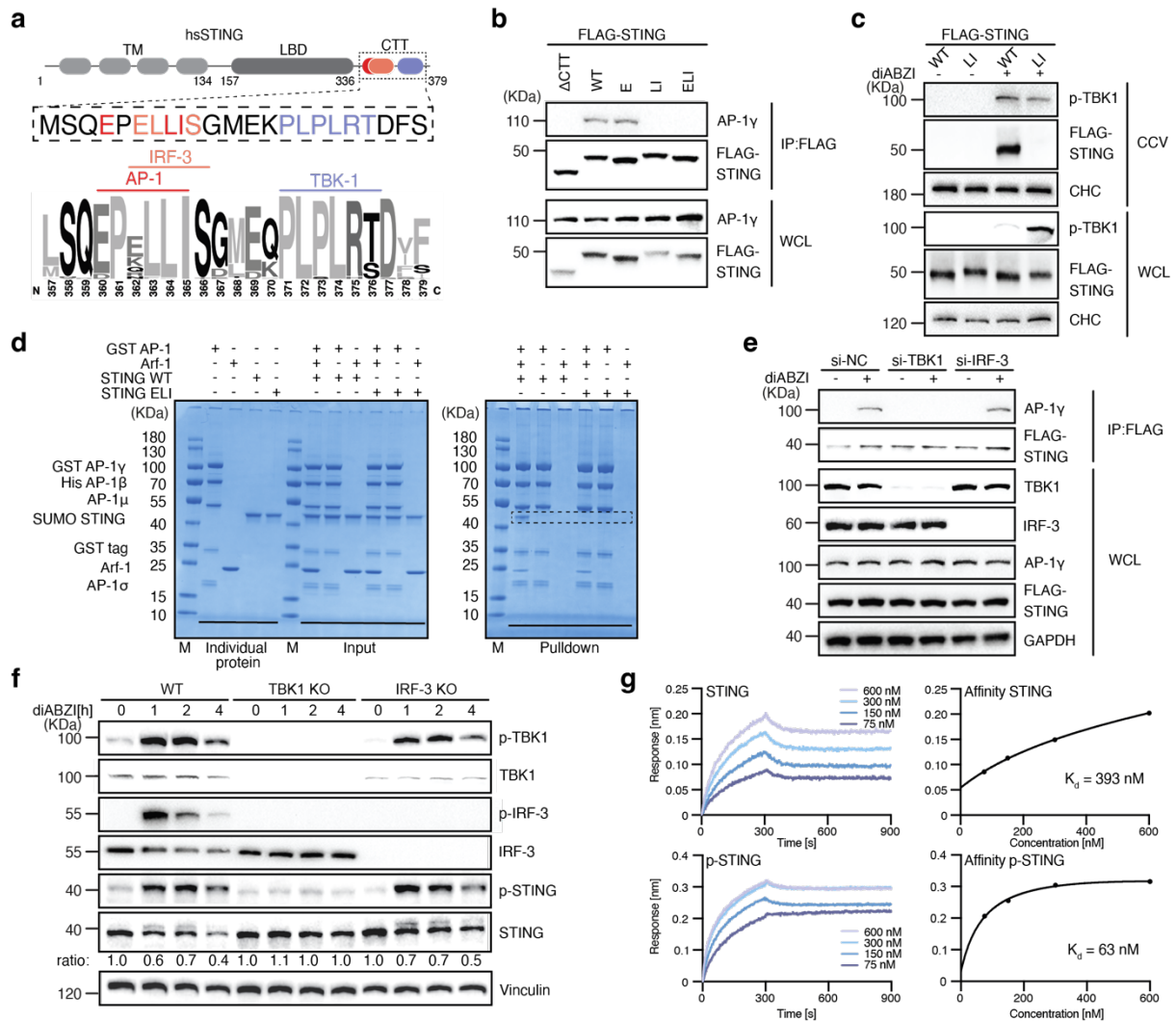
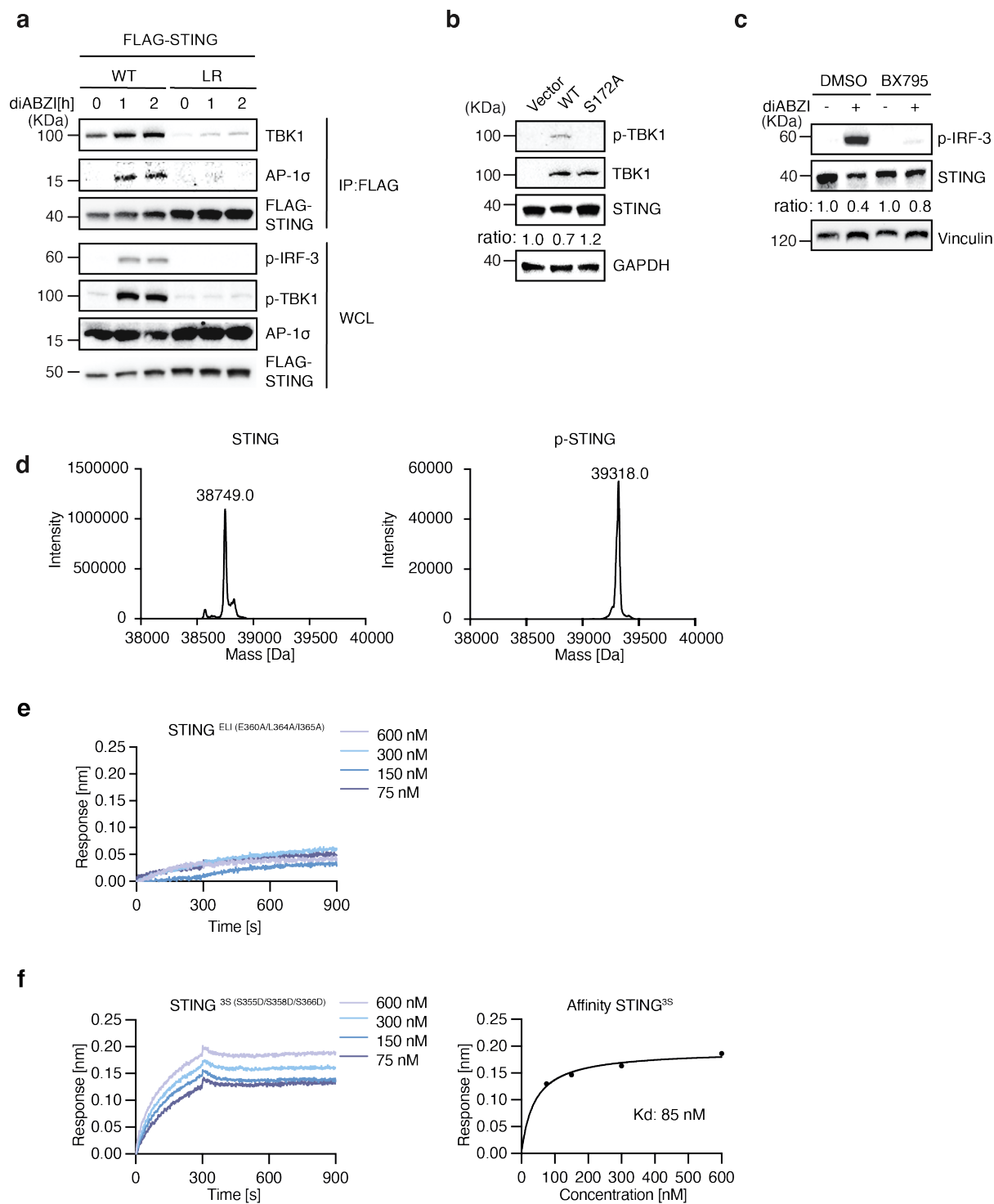


Fig. 3.3 | TBK1-dependent phosphorylation dictates STING binding to AP-1. **a**, Schematic diagram of C-terminal tail (CTT) of human STING and sequence logo of the CTT as indicated from 50 species are shown. **b**, HeLa STING KO cells transfected with FLAG-tagged STING^{ΔCTT(1-341)}, STING^{WT}, STING^{E(E360A)}, STING^{LI(L364A/I365A)} or STING^{ELI(E360A/L364A/I365A)} were treated with diABZI for 2 h. After IP with anti-FLAG antibody, samples were analysed by Western blot. **c**, WCL and extracted CCV fractions from HeLa STING KO cells reconstituted with FLAG-tagged STING^{WT} or STING^{LI(L364A/I365A)} and treated or not with diABZI were analysed by Western blot. CHC was used as a loading control. **d**, Glutathione Sepharose pull-down assays of LBD-STING^{WT} or LBD-STING^{ELI(E360A/L364A/I365A)} by GST-tagged AP-1 core with or without Arf-1. **e**, HeLa^{STING} cells transfected with NC siRNA or siRNA against TBK1 or IRF-3 were treated with or without diABZI. After IP with anti-FLAG antibody samples were analysed by Western blot. GAPDH was used as a loading control. **f**, HeLa WT cells, HeLa TBK1 KO cells, and HeLa IRF-3 KO cells stimulated with diABZI for 0, 1, 2 or 4 h were analysed by Western blot. Ratios of target proteins versus loading control normalized to the 0 time-point of each condition. Vinculin was used as a loading control. **g**, Bio-layer interferometry binding studies of LBD-STING or TBK1-phosphorylated LBD-STING (p-STING) with AP-1 $\Delta\mu$ CTD. One representative of at least three (**b**, **d**, **f**) or two (**c**, **e**, **g**) independent experiments is shown.

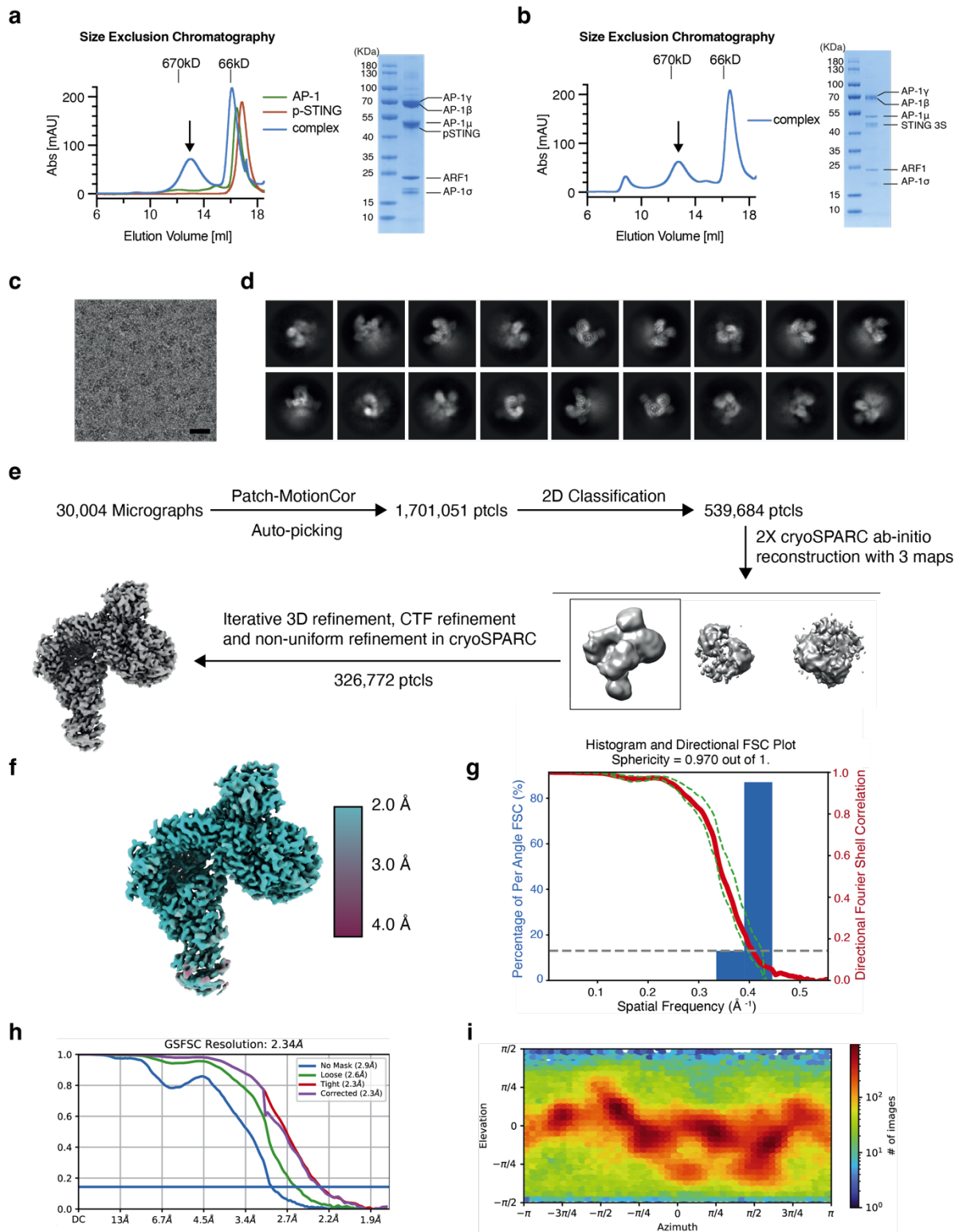


Extended Data Fig. 3.7 | STING-AP-1 interaction depends on TBK1-mediated phosphorylation. **a**, HeLa STING KO cells transfected with FLAG-tagged STING^{WT} or STING^{LR(L374A/I375A)} were treated with 2.5 μ M diABZI for 0, 1 or 2 h, immunoprecipitated with anti-FLAG antibody, and analysed by Western blot. **b**, HeLa TBK1 KO cells reconstituted with an empty plasmid or with plasmids expressing TBK1^{WT} or enzyme-dead TBK1^{S172A} were treated with 2.5 μ M diABZI for 2 h and analysed by Western blot. GAPDH was used as a processing control. **c**, HeLa cells pretreated with DMSO or 2 μ M BX795 for 24 h were stimulated with 2.5 μ M diABZI or not (2 h) and analysed by Western blot. Vinculin was used as a loading control. One representative of at least two (**a-c**) independent

experiments is shown. Ratios of target proteins versus loading control normalized to the untreated sample of each condition (b, c). d, Mass spectrometry detected molecular weight of SUMO LBD-STING and TBK1-phosphorylated LBD-STING (p-STING). e, Bio-layer interferometry binding studies of LBD-STING^{ELI(E360A/L364A/I365A)} with AP-1 ΔμCTD. f, Bio-layer interferometry binding studies of LBD-STING^{3S(S355D/S358D/S366D)} with AP-1 ΔμCTD. One representative of at least two (e, f) independent experiments is shown.

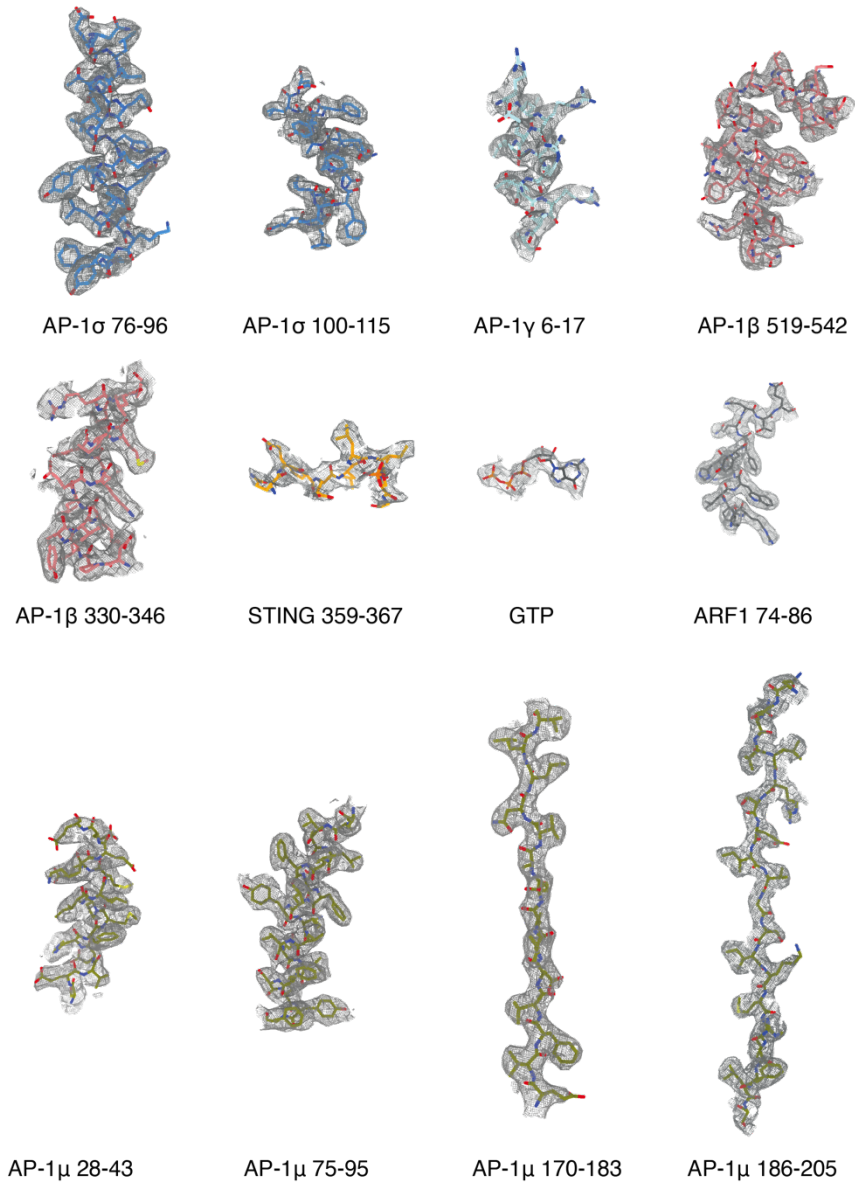
3.2.8 – Structure of the p-STING-AP-1-Arf1 complex

To define the mechanism underlying the enhanced recognition of p-STING by AP-1, we next determined the structure of the complex between the Arf1-activated AP-1 core and TBK1-phosphorylated LBD-STING (Fig. 3.4a, Extended Data Figs. 3.8 and 3.9 and Extended Data Table 1). A 2.3-Å-resolution cryo-EM reconstruction reveals that STING makes multiple contacts with AP-1 via its C-terminal unfolded loop (residue 359-367) (Fig. 3.4b-f). At the C-terminal portion of the loop, STING L364 and I365 of the ExxxLI sorting motif engage L65, F67, H85, V88, V98 of the σ subunit through hydrophobic interactions (Fig. 3.4e). At the N-terminal end of the loop, the carboxyl group of E360 contacts R15 of the γ subunit through an electrostatic interaction (Fig. 3.4e). Together these contacts anchor STING to AP-1 in a manner similar to previously described adaptor protein cargo peptide complexes^{195,197}. Notably, the phospho-moiety on S366 makes hydrogen bonds with a conserved basic patch formed by K60 and R61 of the σ subunit, which can function cooperatively with the dileucine motif interface to enforce binding between p-STING and AP-1 (Fig. 3.4f and Extended Data Fig. 3.10a). Binding studies validated that a K60/R61 substitution selectively reduced AP-1 binding of p-STING, but not native STING, consistent with the critical importance of these two acidic residues in specifying recognition of p-STING (Fig. 3.3g and Extended Data Fig. 3.10b). In cells, expression of a K60/R61 mutant or substitutions residues within the σ subunit essential for dileucine recognition abolished interaction between STING and AP-1^{157,197} (Fig. 3.4g and Extended Data Fig. 3.10c). Reciprocally, mutation of S366, but not S358, on STING compromised binding between STING and AP-1 and reduced STING sorting into CCVs (Fig. 3.4h, i). Together, these results demonstrate how a unique phosphorylation event within the C terminus of STING confers differential recognition by AP-1, and establish a generalizable mechanism for refining AP-1-based cargo selection through phospho-regulation.

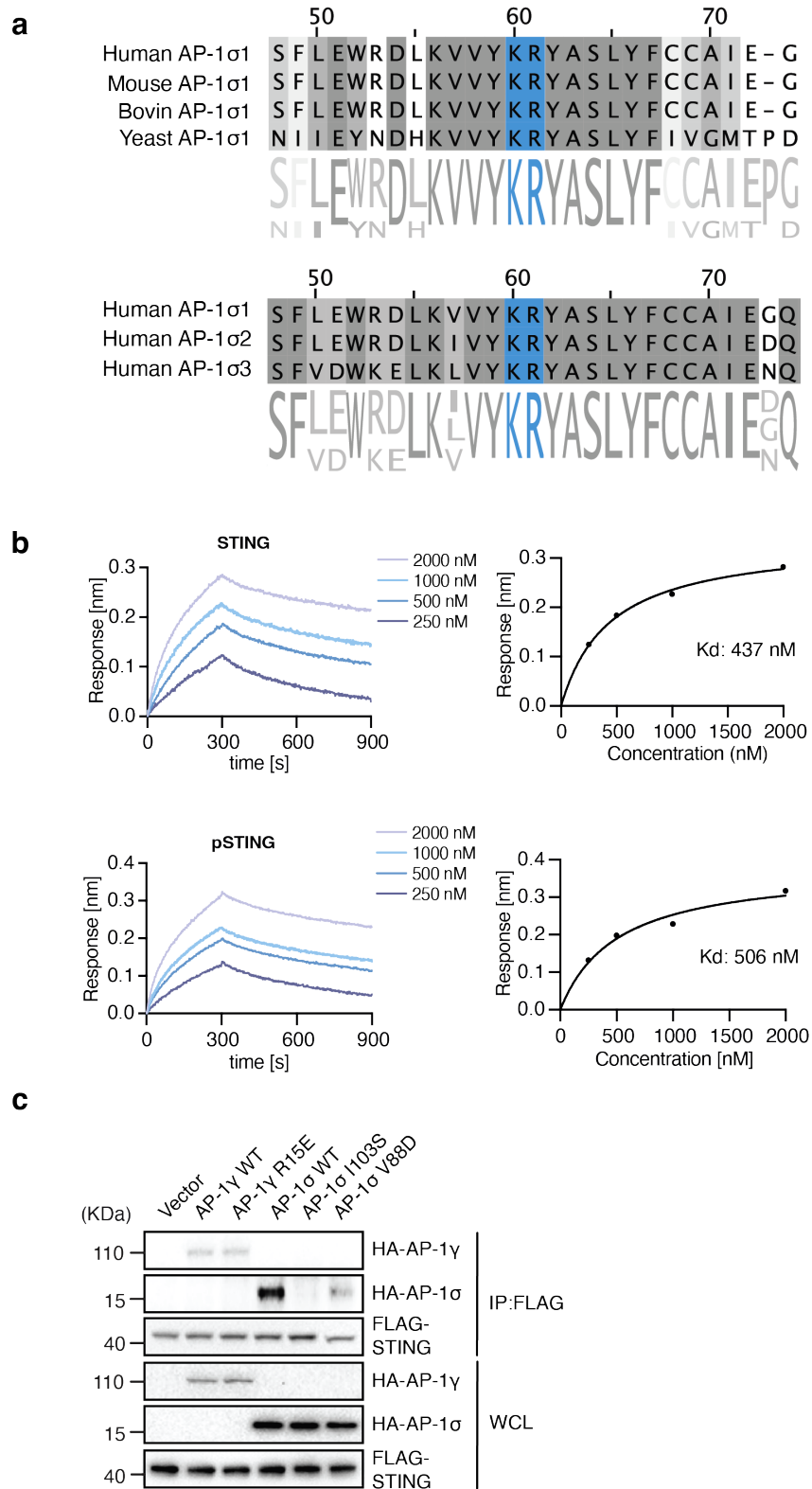


Extended Data Fig. 3.8 | Cryo-EM analysis of p-STING in complex with AP-1. **a**, Purification and SDS-PAGE analysis of AP-1 core in complex with p-STING and Arf-1. **b**, Purification and SDS-PAGE analysis of AP-1 core in complex with STING^{3S} (S355D/S358D/S366D). **c**, Representative micrograph of AP-1 p-STING complex in vitrified ice from 30,004 raw images. Scale bar, 30 nm. **d**, 2D class averages of AP-1 p-STING complex particles. Box size, 27 nm. **e**, Flowchart of data processing; see Methods for details. **f**, Final 3D reconstruction of the AP-1 p-STING complex, coloured according to the local resolution. **g**, 3D Fourier shell correlation of final 3D reconstruction of the AP-1 p-

STING complex. **h**, Corrected Gold-standard Fourier shell correlation curves of the AP-1 p-STING complex for the 3D electron microscopy reconstruction. **i**, Angular distribution of the AP-1 p-STING particles included in the final reconstruction. One representative of at least two (**a**, **b**) independent experiments is shown.



Extended Data Fig. 3.9 | Density maps and structural models of the AP-1 p-STING complex. The density maps (grey mesh) of AP-1 and p-STING contoured at 3σ . The protein structures fitted into the density map are shown by the stick models.



Extended Data Fig. 3.10 | pS366 of p-STING binds to a basic patch of AP-1 σ . **a**, Sequence alignment of AP-1 σ in different species and human σ subunit isomers. **b**, Bio-layer interferometry binding studies of LBD-STING or p-LBD-STING with AP-1 $\Delta\mu$ CTD σ^{KR} . **c**, HEK293T cells transfected with FLAG-tagged STING^{WT} and HA-tagged AP-1 γ^{WT} , γ^{R15E} , σ^{WT} , σ^{I103S} or σ^{V88D} , respectively, were treated with 2.5 μ M diABZI for 2 h, immunoprecipitated (IP) with anti-FLAG antibody and then analysed by Western blot. One representative of two (**b**, **c**) independent experiments is shown.

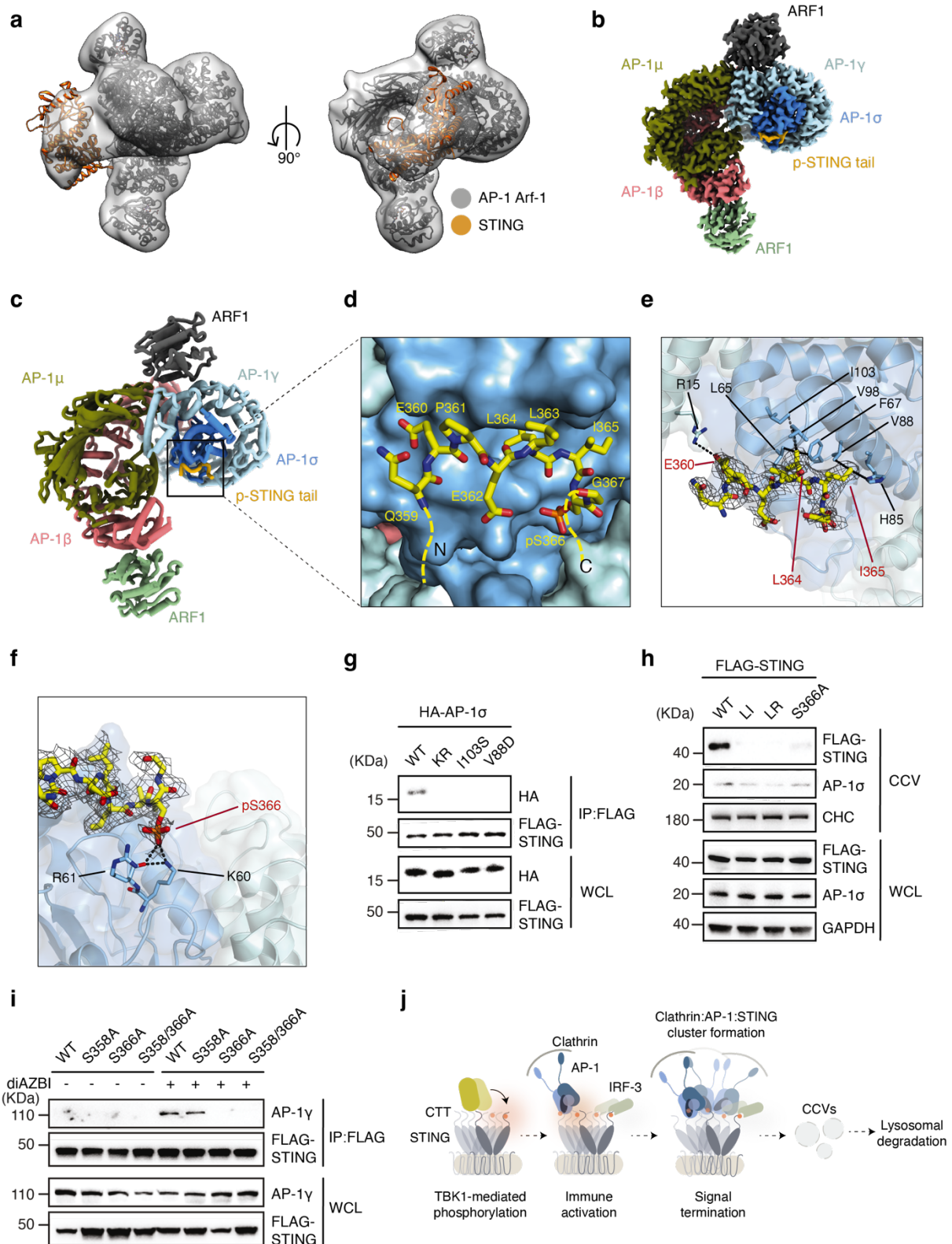


Fig. 3.4 | Structural basis for phosphoregulation of STING recognition by AP-1. **a**, Three-dimensional (3D) reconstructions of the complex in two different orientations. The atomic models of dimeric human LBD-STING (PDB 4KSY) and the AP-1 complex (PDB 6DFF) were fit into the maps (grey) through rigid-body docking. **b**, High-resolution 3D reconstruction from focused refinement on AP-1 core and p-STING tail at 2.34 Å resolution contoured at 3 σ . **c**, Ribbon representation of the AP-1 p-STING complex structure. **d-f**, Detailed views of the binding interface.

Potential hydrogen bonds and hydrophobic interactions are indicated with dotted lines. The density map (grey mesh) of p-STING tail is contoured at 3σ . **g**, HEK293T cells transfected with FLAG-tagged STING and HA-tagged AP-1- σ^{WT} or AP-1- σ mutants $\sigma^{KR(K60A/R61A)}$, σ^{I103S} , and σ^{V88D} were stimulated with diABZI for 2 h. Cell lysates were extracted, immunoprecipitated with anti-FLAG antibody, and analysed by Western blot. **h**, WCL and CCV fractions from untreated and diABZI treated HeLa STING KO cells reconstituted with FLAG-tagged STING^{WT} and indicated STING mutants STING^{L1}, STING^{LR(L374A/R375A)} or STING^{S358A} were analysed by Western blot. CHC and GAPDH were used as loading controls. **i**, HeLa STING KO cells reconstituted with FLAG-tagged STING and indicated STING mutants STING^{S358A}, STING^{S366A} or STING^{S358/366A} were stimulated with diABZI for 2 h or left untreated. After IP with anti-FLAG antibody samples were analysed by Western blot. **j**, Schematic diagram of AP-1 function in termination of STING signalling. One representative of at least three (**g-i**) independent experiments is shown.

3.2.9 – Discussion

Our results define a detailed mechanism underlying negative feedback-control of STING and, together with prior work^{56,57,62,118}, support a model for TGN-compartmentalized regulation of STING-dependent immune responses (**Fig. 3.4j**). First, STING oligomers bind TBK1 resulting in robust phosphorylation of STING CTTs to create a platform for interaction with downstream factors. Whereas signal activation is dictated by repeating cycles of IRF-3 recruitment, phosphorylation, and nuclear translocation, signal inactivation is controlled by AP-1 recognition, which regulates sorting of activated STING into nascent clathrin coats. Thus, initiation and shut-down of signal transduction at the Golgi are biochemically coupled, providing an elegant molecular strategy to self-limit immune activation induced by STING.

Our structural analysis revealed how remodelling of the primary dileucine binding motif via phosphorylation enables preferential recognition of the activated state of STING by AP-1. Coat formation is a highly cooperative process that depends on the clustering of a large number of discrete “adapted” cargos to efficiently cross-bridge clathrin triskelion and facilitate vesicle budding. Thus, even a relatively modest gain of affinity in the sorting interface, as provided by phosphorylation, can dramatically impact cargo selection at the cell level. Notably, prior work in the context of HIV-1 M-Nef has shown that a single phosphorylation event can function to repress dileucine motif and tetherin downregulation by AP-1¹⁹⁵. Thus, together with our finding this highlights an intriguing level of adaptability in which phosphorylation can be harnessed in opposing directions to refine dileucine binding and enable AP-1 to discriminate between distinct cargo states.

Despite high conservation in animals, the CTT only emerged in vertebrate STING to enable interferon-based immunity, which complements primordial antiviral effector functions, including autophagy and NF- κ B signalling^{34,45,198}. In a similar manner, the AP-1-mediated trafficking process dedicated to eliminate IFN-inducing STING, as we describe here, complements autophagy-mediated degradation of STING^{58,139}. The remarkable conservation

of the AP-1 recruitment motif in the STING CTT (**Fig. 3.3a**) suggests that, in vertebrates, acquisition of the type I IFN signalling module might have evolved together with its own integrated regulatory system.

In sum, by revealing a most upstream negative feedback mechanism, our work identifies a missing, but central piece for a more complete understanding of STING-dependent immunity, and may offer a new conceptual strategy to tune the immunogenic effect of STING for therapeutic interventions.

3.2.10 – Methods

Cell culture

HeLa (CCL-2) cells were obtained from Sigma-Aldrich. HEK 293T cells were a gift from Didier Trono (EPFL), originally purchased from ATCC (cat. no. SD-3515). THP-1 cells and WI-38 cells were obtained from ATCC. HaCaT cells were obtained from CLS. Primary human alveolar epithelial cells (epithelial cells) were obtained from a commercial supplier (Cell Biologics). MEFs (μ 1 KO cells and μ 1 KO cells reconstituted with μ 1A) were a gift from Peter Schu (University Medical Center Göttingen). Primary fibroblast cells from three SAVI patients were kindly provided by Raphaela Goldbach-Mansky (NIH). HeLa, HEK 293T, WI-38, HaCaT and primary fibroblast cells were cultured in Dulbecco's Modified Eagle Medium (DMEM, Thermo Fisher Scientific, 41965039) supplemented with 10% (v/v) heat-inactivated fetal bovine serum (FBS) (Thermo Fisher Scientific, Gibco SKU, 10270106), 100 IU/ml penicillin/streptomycin (BioConcept, 4-01F00-H), 2 mM L-glutamine (Thermo Fisher Scientific, 25030024) and 1 mM sodium pyruvate (BioConcept, 5-60F00-H) at 37°C and at atmospheric O₂ and 5% CO₂. THP-1 cells were cultured in RPMI 1640 Medium (Thermo Fisher Scientific, 21875091) supplemented with 10% FBS, 1x Penicillin-Streptomycin-L-Glutamine (Corning, 30-009-CI) and 1x 2-Mercaptoethanol (Gibco) at 37°C and at atmospheric O₂ and 5% CO₂. MEFs were cultured in Dulbecco's Modified Eagle Medium (DMEM, Thermo Fisher Scientific, 41965039) supplemented with 15% (v/v) heat-inactivated fetal bovine serum (FBS) (Thermo Fisher Scientific, Gibco SKU, 10270106), 100 IU/ml penicillin/streptomycin (BioConcept, 4-01F00-H), 1 mM sodium pyruvate (BioConcept, 5-60F00-H) at 37°C and at atmospheric O₂ and 5% CO₂. Primary human alveolar epithelial cells (epithelial cells) were cultured in complete human epithelial cell medium (Cell Biologics, H6621), according to the supplier's instructions. Cell lines were repeatedly tested for mycoplasma by PCR. No method of cell line authentication was used.

Plasmids

For CRISPR/Cas9 plasmids, single guide RNA (sgRNA) targeting TBK1, IRF-3, cGAS, AP1 σ 1 and STING were designed using the web tool CRISPOR¹⁷⁹. SgRNAs targeting TBK1, IRF-3 and cGAS, AP1 σ 1 were cloned in pSpCas9(BB)-2A-Puro (PX459) V2.0 plasmid (Addgene, 62988) while sgRNA targeting STING were cloned in pSpCas9(BB)-2A-GFP (PX458) plasmid (Addgene, 48138). Both plasmids are gifts from Feng Zhang¹⁸⁰. The pEF-Bos based STING truncations (1-341 and 1-317) and mutations (E360A, L1364/365AA, E1360/364/365AAA, L1374/375AA, L364A, L364F, I365A) were obtained by site-directed mutagenesis. pEF-Bos-human TBK1-Flag-His was a gift from Silvia Cerboni (Institute Curie, Paris). TBK1-S172A were generated by single amino acid mutation. pCDNA3-HA gamma adaptin 1 (AP1G1) (Addgene, 10712) were purchased from Addgene. pCDNA3-HA-AP1S1 were generated by inserting the coding sequences of AP1S1 flanked by 5' BamHI and 3' XhoI sites into the pCDNA3 vector. AP1G1 R15E, AP1S1 I103S and AP1S1 V88D were obtained by single amino acid mutagenesis. The primers used for plasmid constructions and sgRNA sequences are provided in Supplementary Table S1. Plasmids for NF- κ B-Luc (Promega, E8491) was purchased from Promega and for pIFN β -GLuc was previously described²⁰. All constructs were confirmed by DNA sequencing.

Stable cell lines

HeLa STING KO cells were obtained from F. Martinon¹⁹⁹. HeLa^{STING} cells and HeLa^{GFP-STING} cells were generated from HeLa STING KO by infection with a pTJ lentiviral vector carrying FLAG-STING or GFP-STING, respectively, and a puromycin resistance gene. Cells were selected with puromycin (2 μ g/mL). HeLa TBK1 KO cells and HeLa IRF3 KO cells, and HaCaT σ 1 KO were generated using CRISPR/Cas9 technology. Briefly, HeLa cells were plated in 6-wells culture plates at about 80% confluency and transfected. Per well, 3.5 μ L Lipofectamine 2000 (LifeTechnologies, 11668019) and 1 μ g plasmid-DNA were each diluted in 125 μ L OptiMEM (LifeTechnologies, 31985047), mixed, incubated 5 minutes and added on top of the well. The next day, the culture media was replaced and cells were put under puromycin (5 μ g/mL) selection for 3 days. Surviving cells were expanded in antibiotics-free media and FACS-sorted into single clones 3 days later. Growing clones were characterized by Western blotting and selected for absence of TBK1. HeLa cGAS/STING KO cells were generated using CRISPR/Cas9 technology. HeLa cells were transfected with pX459-sgcGAS plasmid for 24 h and then selected with puromycin for 3 days. Surviving cells were expanded in antibiotics-free media and then transfected with pX458-sgSTING plasmid in the same way for 3 days and sorted with FACS. The cells expressing GFP were maintained as HeLa cGAS/STING double

KO cells. Growing clones were characterized by Western blotting and selected for absence of cGAS and STING.

Transfection

For plasmid transfection, cells were transfected with plasmids and Lipofectamine™ 2000 Reagent (Invitrogen, 11668019) (for all imaging experiments) or GeneJuice transfection reagent (Millipore, 70967) (for all other experiments) following the manufacturer's respective protocols. For the siRNA knockdown, 3×10^4 cells were transfected with Lipofectamine RNAiMAX transfection reagent (Invitrogen, 13778075) and 40 pmol siRNA following the manufacturer's protocol followed by 3 days of incubation. Medium containing transfection reagents was replaced with fresh medium 6 h post transfection. Silencer select predesigned siRNAs (4390847), si-AP1G1 (s1143), si-AP1B1 (s1141), si-AP1S1 (s3115) and si-AP1S3 (s43490) were purchased from Thermo Fisher Scientific, si-IRF-3 and si-TBK1 were synthesized by MircoSynth. The sequences of siRNAs are provided in [Supplementary Table S1](#).

Stimulation of cells

Cells were treated with 2.5 μ M diABZI (Selleckchem, S8796) and collected at indicated timepoints. For cGAMP, 90mer and IVT4 stimulation, 0.1 μ M cGAMP (Invivogen), 0.2 μ g 90mer or 0.5 μ g IVT4 was transfected using Lipofectamine 2000 (Invitrogen, 11668019) according to the manufacturer's protocol and cells were incubated for 3 h. The DNA sequences of 90mer is provided in [Supplementary Table S1](#). Poly(I:C) (Invivogen) was added to the cell medium at a final concentration of 10 μ g/mL for 24 h. After infection with Herpes simplex virus-1 KOS strain (MOI=10), infected cells were incubated for 6 h. Pre-treatment with BX795 (MedChemExpress) was performed at 2 μ M for 24 h and pre-treatment with Bafilomycin A1 (Baf A1, Sigma) was performed at 20 nM for 1h. MEFs treated with 5 μ g/mL or 40 μ g/mL DMXAA (Invivogen) were collected 2h or 3h post-stimulation. For STING inhibition by H-151, H-151 (2 μ M) was added into cells every 24h for 3 days before cells were examined by RT-qPCR.

Antibodies

Primary antibodies used: mouse monoclonal anti-Vinculin (hVIN-1) (Sigma-Aldrich, V9264, immunoblot 1:5000), rabbit monoclonal anti-GAPDH (14C10) (Cell Signaling Technology, 2118, immunoblot 1:3000), mouse monoclonal anti-FLAG (M2) (Sigma-Aldrich, F1804, immunoblot 1:3000), rabbit monoclonal anti-human phospho-STING (Ser366) (D7C3S) (Cell

Signaling Technology, 19781, immunoblot 1:3000), rabbit monoclonal anti-phospho-TBK1/NAK (Ser172) (D52C2) (Cell Signaling Technology, 5483, immunoblot 1:1000), rabbit monoclonal anti-phospho-IRF-3 (Ser 386) (EPR2346) (Abcam, ab76493, immunoblot 1:1000), rabbit monoclonal anti-TBK1/NAK (D1B4) (Cell Signaling Technology, 3504, immunoblot 1:1000), rabbit polyclonal anti-TMEM173/STING (Proteintech, 19851-1-AP, immunoblot 1:1000), rabbit monoclonal anti-IRF-3 (D6I4C) (Cell Signaling Technology, 11904, immunoblot 1:1000), rabbit monoclonal anti-Clathrin Heavy Chain (P1663) (Cell Signaling Technology, 2410, immunoblot 1:500), mouse anti-Clathrin Heavy Chain Monoclonal Antibody (X22) (Thermo Fisher, # MA1-065, IF 1:100), rabbit polyclonal anti-AP1S1 (Thermo Fisher, PA5-63913, immunoblot 1:1000), rabbit polyclonal anti-AP1G1 (Thermo Fisher, PA5-65290, immunoblot 1:1000), rabbit polyclonal anti-AP1B1 (Sigma-Aldrich, HPA065226, immunoblot 1:1000), rabbit polyclonal anti-AP1M1 (Proteintech, 12112-1-AP, immunoblot 1:1000), mouse monoclonal anti-HSV-1 ICP0 (11060) (Santa Cruz, sc-53090, immunoblot 1:500), mouse monoclonal anti-HA.11 Epitope Tag (16B12) (Biolegend, MMS-101R, immunoblot 1:2000), mouse monoclonal γ -Adaptin (AP1G1) (100/3) (Sigma-Aldrich, A4200, IF 1:100), mouse monoclonal EEA1 (E9Q6G) (Cell Signaling, 48453, IF 1:100), mouse monoclonal LAMP1 (H4A3) (Abcam, ab25630, IF 1:100), rabbit monoclonal anti-human phospho-STING (Ser366) (D8K6H) (Cell Signaling Technology, #40818, IF 1:100, STED 1:50), mouse monoclonal Rab7 (E9O7E) (Cell Signaling Technology, 95746, IF 1:100), sheep polyclonal human-TGN46 (BioRad, AHP500G, IF 1:200). HRP-conjugated secondary antibodies used: Donkey anti-rabbit IgG (H+L)-HRP (Jackson ImmunoResearch, 711-036-152, immunoblot: 1:5000) and Donkey anti-mouse IgG (H+L)-HRP (Jackson ImmunoResearch, 715-036-151, immunoblot: 1:5000). Fluorescence-conjugated secondary antibodies used: Goat anti-Mouse IgG2a Cross-Adsorbed Secondary Antibody, Alexa Fluor 647-conjugated (Invitrogen, A-21241, IF 1:800), Donkey anti-Sheep IgG (H+L) Cross-Adsorbed Secondary Antibody, Alexa Fluor 488-conjugated (Invitrogen, A-11015, IF 1:800), Goat anti-Rabbit IgG (H+L) Cross-Adsorbed Secondary Antibody, Alexa Fluor 568-conjugated (Invitrogen, A-11011, IF 1:800), Goat anti-rabbit IgG F(ab) ATTO647N (H+L) (Hypermol,2318, IF 1:500). The details of antibodies are provided in [Supplementary Table S2](#).

Quantitative real-time PCR (RT-qPCR)

Cells were lysed in the RLT buffer (Qiagen). RNA was extracted following the manufacturer's protocol (Qiagen RNeasy Plant Mini Kit). RNA was reverse transcribed using RevertAid First Strand cDNA synthesis Kit (Thermo Fisher Scientific) and analysed by RT-qPCR in triplicates or quadruplicate using the ChamQ Universal SYBR qPCR Master Mix (Vazyme). The qPCR

reactions were run on a QuantStudio 7 Real-Time PCR system (Thermo Fisher Scientific). GAPDH was used as a housekeeping gene for normalization. Primer sequences are provided in [Supplementary Table S1](#).

Western blotting and Immunoprecipitation

Cells were harvested, quickly rinsed with 1x PBS, and lysed in lysis buffer (20 mM Tris pH 7.4, 0.5% Triton X-100, 150 mM NaCl, 1.5 mM MgCl₂, 2 mM EGTA, 2 mM DTT and 1x cComplete™ Protease Inhibitor Cocktail (Roche)) on ice for 30 min and centrifuged at 12,000 rpm, 4°C for 10 min. Supernatants were boiled with 4x loading buffer (200 mM Tris pH 6.8, 8% SDS, 40% glycerol, 0.4 M DTT, 0.4% Bromophenol blue) for 10 min. Proteins were resolved by SDS-PAGE using SurePAGE™ precast gels (GenScript) and transferred to nitrocellulose membranes using the Trans-Blot Turbo RTA Midi Nitrocellulose Transfer Kit (Bio-Rad) following the manufacturer's instructions. Membranes were blocked with 2% BSA + 1% milk in PBST (PBS + 0.05% Tween-20) at room temperature for 1 h and then incubated with the primary antibody (diluted in PBST) at 4°C overnight. After washing in PBST, membranes were incubated with the secondary antibody at room temperature for 1 h. Membranes were washed with PBST, visualized with Western Blotting Detection Reagent (advansta), and imaged with using the ChemiDoc XRS Biorad Imager and Image Lab Software. Band intensities were quantified using Fiji software (NIH). For immunoprecipitation, cells were seeded into 6-well plates and were transfected with indicated plasmids. 16 h post transfection, cells were lysed in lysis buffer on ice for 30 min and centrifuged at 12,000 rpm at 4°C for 10 min. Supernatants were transferred into new tubes and mixed with anti-FLAG M2 Magnetic beads (Sigma-Aldrich, M8823) at 4°C overnight on a rotator. After 3-6 washes with lysis buffer and 1-2 washes with cold 1x PBS, the beads were boiled with 1x loading buffer for 10 min. 20 µL samples were loaded into gel after short centrifugation, followed by SDS-PAGE and immunoblotting analysis.

Luciferase assay

HEK293T cells were plated into 96-well plates and transfected with non-targeting control or the combination of siRNAs targeting AP1G1, AP1S1 and AP1B1 for 3 days. Cells were transfected using GeneJuice transfection reagent (Millipore) with an IFN-β promoter–reporter plasmid (pIFNβ–GLuc) in combination with a STING-expressing plasmid (pEFBos-FLAG-STING). 16 h post transfection, cells were stimulated with fresh medium containing 2.5 µM diABZI for 6 h. Gaussia luciferase activity was measured in the supernatants using coelenterazine (PJK GmbH) as substrate. For the NF-κB promoter luciferase activity

measurement, cells were transfected with siRNAs as described before and then transfected using GeneJuice with a NF- κ B promoter-reporter plasmid (NF- κ B-Luc). After 16 h, cells were stimulated with fresh medium containing 2.5 μ M diABZI for 18 h. The promoter activity was determined using the Bright-Glo™ Luciferase Assay System (Promega). The expression of proteins was confirmed by immunoblotting. For the determination of viable cells number in culture, cells were seeded into a 96-well plate and were measured with CellTiter- Glo™ Luminescent Cell Viability Assay System (Promega) every 24h following the producer's instructions.

CCV extraction

CCV extraction was performed according to a protocol as described in ref²⁰⁰. Briefly, cells from one confluent 500 cm²-dish were treated with 2.5 μ M diABZI for 2 h and then rinsed with PBS twice. Cells were scrapped into 5 mL buffer A (0.1 M MES, pH 6.5, 0.2 mM EGTA, 0.5 mM MgCl₂) and homogenized by pipetting up and down for > 25 times using a 5-mL syringe with a 22-G needle attached. Cell lysates were centrifuged at 4,100 x g, 4°C for 32 min. Supernatants were moved into new tubes and treated with 50 μ g/mL ribonuclease A on ice for 30 min followed by centrifugation at 50'000 rpm, 4°C for 30 min using a Type 70 Ti rotor (Beckman Coulter). Pellets were resuspended in 300 μ L buffer A and mixed with an equal volume of buffer B (12.5% (w/v) Ficoll, 12.5% (w/v) sucrose in buffer A) followed by centrifugation at 20000 rpm, 4°C for 25 min. Supernatants were transferred into new tubes and diluted with four volumes of buffer A, and centrifuged at 40'000 rpm, 4°C for 30 min to obtain the CCV-enriched fraction.

Confocal microscopy: sample preparation

HeLa^{STING} cells were plated in CellCarrier-96 Ultra Microplates (Perkin Elmer, 6055302) at a density of 10,000 cells per well and let at least 5 h to adhere. Cells were then stimulated by adding diABZI at 1 μ M (MedChemExpress, HY-103665) for the indicated amount of time. In time-course experiments, cells were stimulated in a sequential fashion and fixed all at the same time. At the end of the stimulation, the wells were washed once with PBS, then cells were fixed adding paraformaldehyde 4% in CBS buffer (10 mM MES pH 6.9, 138 mM KCl, 2 mM MgCl₂, 2 mM EGTA) for 5-10 minutes at room temperature (RT). Cells were then washed 3 times at least 5 minutes in PBS before blocking for 1-2 h at RT with PBS supplemented with 0.1% (v/v) saponin and 5% (v/v) heat-inactivated FBS and later incubating overnight at 4°C with the primary antibodies diluted in staining solution (PBS supplemented with 0.1% (v/v) saponin) and 1% (w/v) bovine serum albumin (Sigma-Aldrich, A7906)). Antibodies and used

concentrations are listed in the [Supplementary Table S2](#). The cells were then washed with PBS 3 times 5 minutes and incubated for 1.5 h at RT in secondary antibodies diluted in staining solution. From then on, the plate was protected from light. Cells were washed twice more (5 min each) in PBS and incubated 30-60 minutes in Hoechst 33342 (Sigma-Aldrich, B2261) 0.2 $\mu\text{g}/\text{mL}$ in PBS. Cells were then put back into 100 μL PBS/well and either imaged directly or kept at 4°C until imaging. For experiments with KD of AP-1, HeLa^{STING} cells were plated (60,000 cells per well in a 6-wells plate) and let to adhere for 6-16 h. They were then transfected with siRNAs using Lipofectamine RNAiMax reagent (Thermo Fisher Scientific) according to the manufacturer's instructions. Silencer select predesigned siRNAs were purchased from Thermo Fisher Scientific: Negative Control (Cat.No. 4390847), or si-AP1G1 (s1143), si-AP1B1 (s1141) and si-AP1S1 (s3115), see details in [Supplementary Table S1](#). A total of 2 μL at 10 μM of siRNAs (equally split between the 3 siRNA for the siAP-1 wells) combined with 7 μL of lipofectamine RNAiMax reagent in 400 μL OptiMEM total was used per well. Media was changed after 6-16 h. 3 days after siRNA treatment, cells were replated into microscopy plates (10,000 cells/well) and the experiments were continued as described above for non-siRNA-treated cells.

Confocal microscopy: imaging and analysis

Fixed and stained 96-well plates were then imaged on two microscopes: a confocal Leica SP8 inverted microscope equipped with an HC PL APO 63x/1.40/oil (magnification/N.A./immersion) objective and HyD detectors, operated with the Leica LAS-X software; and a PerkinElmer Operetta CLS operated with the PerkinElmer Harmony software and equipped with an Andor Zyla 5.5 camera, and with an LD C Apochromat objective with magnification/N.A./immersion of 63x/1.4/water. Image analysis and quantifications were performed combining PerkinElmer Harmony (v4.9) and Fiji (v2.3.0) and data were further processed with KNIME (v4.3.2) and GraphPad PRISM 9 (v9.3.1). Images' panels were assembled using OMERO (v5.11.0)¹⁸². In more details, all depicted cell images were acquired with the Leica SP8 confocal microscope (63x), except for the images confirming that p-STING still accumulates at the TGN upon si-AP-1 (compared to si-NC), which are images captured on the Operetta (63x). Quantifications of p-STING total areas or AP1G1 intensity were calculated in Harmony software based on Operetta (63x) images.

Airyscan microscopy

HeLa^{STING} cells were plated in μ -Slide 8 well chamber slides (ibidi, 80826-IBI) at a density of 10,000 cells per well and let to adhere overnight. Cells were then stimulated by adding diABZI

at 1 μ M (MedChemExpress, HY-103665) for 0, 150 or 360 min (**Fig. 3.1b** depicts the 150 min time-point and **Extended Data Fig. 3.1e** the 0 and 360 min ones) or only 0 and 150 min (**Fig. 3.2a** and **Extended Data Fig. 3.1c, d**). In time-course experiments, cells were stimulated in a sequential fashion and fixed all at the same time. At the end of the stimulation, the wells were washed once with PBS, then cells were fixed adding paraformaldehyde 4% in CBS buffer (10 mM MES pH 6.9, 138 mM KCl, 2 mM $MgCl_2$, 2 mM EGTA) for 5-10 minutes at room temperature (RT). Cells were then washed 3 times at least 5 minutes in PBS before blocking for 1-2 h at RT with PBS supplemented with 0.1% (v/v) saponin and 5% (v/v) heat-inactivated FBS and later incubating overnight at 4°C with the primary antibodies diluted in staining solution (PBS supplemented with 0.1% (v/v) saponin) and 1% (w/v) bovine serum albumin (Sigma-Aldrich, A7906)). Antibodies and used concentrations are listed in the [Supplementary Table S2](#). The cells were then washed with PBS 3 times 5 minutes and incubated for 1.5 h at RT in secondary antibodies diluted in staining solution. From then on, the plate was protected from light. Cells were washed twice more (5 min each) in PBS and incubated 30-60 minutes in Hoechst 33342 (Sigma-Aldrich, B2261, blue on the depicted images) 0.2 μ g/mL in PBS. Cells were then put back into 200 μ L PBS/well and either imaged directly or kept at 4°C until imaging. Imaging was performed with a Zeiss LSM 980 Inverted microscope (Multi-purpose confocal with 32 Channels AiryScan, tPMT, widefield & brightfield capability) using the Plan-Apochromat 63x/1.40/oil (magnification/N.A./immersion) objective and the AiryScan mode and images were processed in the ZEN software using embedded AiryScan processing (3D-mode and “Normal” resolution). Image analysis and quantifications were performed with Fiji (v2.3.0). Colocalization analysis were performed on Fiji using the BIOP JACoP plugin with Otsu thresholding for all channels. Data were further processed with KNIME (v4.3.2) to combine them and remove cells with threshold values below 500 for p-STING (considered background) and results were then plotted with GraphPad PRISM 9 (v9.3.1). Images’ panels were assembled using OMERO (v5.11.0)¹⁸².

Correlative light and electron microscopy (CLEM)

HeLa^{GFP-STING} cells were plated in glass-bottom Petri dishes (MatTek, Cat. No. P35G-1.5-14-CGRD) with an alpha-numeric grid pattern at a density of 100,000 cells per dish and let to adhere overnight. They were stimulated by adding diABZI at 1 μ M (MedChemExpress, HY-103665) for 2.5 hours. They were then chemically fixed, with a buffered solution of 1 % glutaraldehyde and 2 % paraformaldehyde in 0.1 M phosphate buffer at pH 7.4. Dishes were then screened with light microscopy to identify cells of interest, which were imaged with both transmitted and fluorescence microscopy (AiryScan mode as described above) to record their

position on the grid. The cells were then washed thoroughly with cacodylate buffer (0.1M, pH 7.4), postfixed for 40 min in 1.0 % osmium tetroxide with 1.5% potassium ferrocyanide, and then 40 min in 1.0% osmium tetroxide alone. They were finally stained for 40 min in 1% uranyl acetate in water before being dehydrated through increasing concentrations of alcohol and then embedded in Durcupan ACM resin (Fluka, Switzerland). The dishes were then filled with 1 mm of resin and this was hardened for 18 hours in a 65°C oven. Cells of interest were then identified according to their position on the alpha-numeric grid, cut away from the rest of the material and glued to a blank resin block. Ultra-thin (50 nm thick) serial sections were cut through the entire cell with a diamond knife (Diatome) and ultramicrotome (Leica Microsystems, UC7), and collected onto single slot grids with a pioloform support film. These sections were further contrasted with lead citrate and uranyl acetate and images taken in a transmission electron microscope (FEI Company, Tecnai Spirit) with a digital camera (FEI Company, Eagle). To correlate the light microscopy images with the EM images and identify the exact position of the Centrin-1:GFP foci, fluorescent images were overlaid onto the electron micrographs of the same cell using the Photoshop software (Adobe).

STED

HeLa cGAS/STING double KO cells were plated in 3.5-cm glass-bottom Petri dishes (FluoroDish, WFD35-100) at a density of 100,000 cells per dish and let to adhere overnight. They were stimulated by adding diABZI at 1 μ M (MedChemExpress, HY-103665) for 2.5 hours. They were then transfected with plasmids containing Flag-hSTING and mCherry-clathrin (both in pEFBos mammalian expression plasmid) using Lipofectamine™ 2000 Reagent (Invitrogen, 11668019) according to the manufacturer's instructions. 1 μ g per plasmid and 4.5 μ L of lipofectamine in 250 μ L of OptiMEM (LifeTechnologies, 31985047) were used for one dish. The media was replaced with fresh culture media 6-hours post-transfection. The next day, the cells were stimulated by adding diABZI at 1 μ M (MedChemExpress, HY-103665) for 2.5 hours. They were then fixed and stained for phospho-STING as described for the AiryScan microscopy samples. STED images were acquired using a Leica SP8 STED 3X (Leica Micro-systems) equipped with a pulsed white light laser (WLL) as an excitation source and a 775 nm pulsed laser as depletion light source both for mCherry and ATTO647N. Samples were imaged with a 100 \times objective (Leica, HC APO CS2 100 \times /1.40/oil) using the LAS X software (Leica Microsystems). For excitation of the respective channels, the WLL was set to 587 nm for mCherry and 647 nm for ATTO647N. Hybrid spectral detectors were used to acquire the images with a final pixel size of 9.2 \times 9.2 nm. The detector time gates were set to 1.5-7.5 ns for mCherry and 0.5-6 ns for ATTO647N. Images were acquired as single planes

of 1,392 × 1,392 pixels, 600 lines per second, 32× line averaging for mCherry and 16× line averaging for ATTO647N. Deconvolution of STED images was done with Huygens Remote Manager v3.7, using the good's roughness maximum likelihood estimation with 60 iterations and signal-to-noise ratio equal to 2 until it reached a quality threshold of 0.03.

Protein expression and purification

6His-TEVsite-Hs Arf1 (17-181)-Q71L in pHis2 vector was expressed in BL21 (DE3) bacteria (Sigma-Aldrich, #CMC0014). A single colony was inoculated in a culture flask with 100 mL LB with Ampicillin (100 µg/mL) and incubated with shaking (200 rpm, Infors-HT Multitron) at 37°C overnight as preculture. Large scale expression of the protein was started the next day by pouring 100 mL of preculture in a 5 L Erlenmeyer flask containing 2 L of LB with Ampicillin (100 µg/mL). The cells were grown until the Optic Density 600 reached 0.7. Expression was then induced by adding isopropyl β-D-1-thiogalactopyranoside (IPTG) to a final concentration of 0.5 mM while transferring the culture in an 18°C shaking incubator overnight. The bacteria was then harvested by centrifugation, solubilized in HisTrap buffer A (20 mM HEPES, 500 mM NaCl, 20 mM Imidazole, 1 mM DTT, 5% Glycerol, pH 7.5) supplemented with AEBSF and cOmplete protease inhibitors (Roche), lysed by sonication, cleared by 20'000 x g centrifugation, then passed through a 5 mL nickel immobilized metal affinity chromatography column (Cytiva, HisTrap HP, #17524802) on an FPLC system. The protein of interest was eluted with buffer B (20 mM HEPES, 500 mM NaCl, 500 mM Imidazole, 1 mM DTT, 5% Glycerol, pH 7.5). Arf1 was then purified by Size Exclusion Chromatography through a Superdex 75 Hiload 16/600 column (Cytiva #28-9893-33). The cDNA of human LBD-STING (139-379) was cloned into a pET-28 vector with an N-terminal His6-SUMO tag. LBD-STING was expressed in *Escherichia coli* BL21 (DE3) with 0.4 mM IPTG induction overnight at 16 °C. The cell pellet was lysed by sonication and purified on a Ni-NTA column in 50 mM Tris at pH 8.0, 350 mM NaCl, 20 mM imidazole, and 0.5 mM phenylmethanesulfonyl fluoride (PMSF). The protein was eluted with buffer containing 50 mM Tris at pH 8.0, 350 mM NaCl and 300 mM imidazole, and then loaded onto a Superdex 75 HiLoad 16/600 column (Cytiva #28-9893-33) in PBS. The sample fractions were pooled and proteins were quantified by molar absorption measurements. All mutants were generated using a PCR-based technique with appropriate primers and confirmed by DNA sequencing. The mutant STING proteins were expressed and purified in the same way as the wild-type STING. His-tagged AP-1β 1-584, GST-tagged AP-1γ 1-595, AP-1μ 1-423 and AP-1σ 1-154 were cloned into pST44 vector and referred to as AP-1 core. His-tagged AP-1β 1-584, GST-tagged AP-1γ 1-595, AP-1μ 1-142 and AP-1σ 1-154 were cloned into pST44 vector and referred to as AP-1 ΔμCTD. The AP-1

core complex in pST44 vector was expressed in BL21 (DE3) (Sigma-Aldrich, #CMC0014). A single colony was inoculated in a culture flask with 400 mL LB with Ampicillin (100 $\mu\text{g}/\text{mL}$) and incubated with shaking (200 rpm, Infors-HT Multitron) at 37°C overnight as preculture. Large scale expression of the complex (8L total: 2 L in four 5-L Erlenmeyer flask) was started the next day by pouring 100 mL of preculture in 2 L of Auto Induction Media Terrific Broth (Formedium, #AIMTB0210) with Ampicillin (100 $\mu\text{g}/\text{mL}$). Flasks were incubated with shaking at 37°C for 6h, then incubated at 18°C overnight. The cells were then harvested by centrifugation (4000 x g, 15 min). A cell pellet of 2 L expression culture was transferred in a Falcon 50-mL tube. The 2 L expression cells were solubilized in PBS with 1 mM DTT, 1 mM EDTA and 2% glycerol at pH 7.5, supplemented with AEBSF and cOmplete protease inhibitors, then lysed by sonication. The cell lysate was clarified by centrifugation followed by 0.45 μm filtration. The supernatant was first purified on a glutathione-Sepharose 4B 5-mL column (Cytiva #28401748) on a FPLC system (Cytiva Äktä Pure). After TEV cleavage at 4°C overnight in a 3500MW cut-off dialysis tubing against PBS with 5% glycerol at pH 7.5, the sample was passed through a Superose 6 HiLoad 16/600 Size Exclusion Chromatography column (Cytiva # 29323952) equilibrated in PBS with 2% glycerol at pH 7.5, to remove the TEV protease as well as free GST. When used for GST pull-down, TEV cleavage was skipped and the pool of GST-AP-1 eluate was directly loaded on the Size Exclusion Chromatography column. AP-1 $\Delta\mu\text{CTD}$ was expressed and purified in the same way as AP-1 core.

In vitro phosphorylation of SUMO-STING 139-379 by TBK1

The recombinant SUMO-STING stock protein was diluted in assay buffer containing 20 mM Tris, 25 mM MgCl_2 , 2 mM EDTA, 4 mM EGTA and 1 mM DTT at pH 7.5, supplemented with phosphatase inhibitor cocktails and protease inhibitors. The pH was controlled before and after addition in the sample of 10 mM ATP. TBK1 (MRC PPU Reagents, #DU12469) was added at a ratio of 1:20 (w/w) TBK1:STING. The reaction was performed at 4°C overnight. The sample was loaded on a Superdex 200 Increase 10/300 GL Size Exclusion Chromatography column (Cytiva, #28990944) to purify phosphorylated SUMO-STING from the other reagents. The phosphorylation assay was monitored by LC-ESI-MS.

GST pull-down assay

For AP1-ARF1 pull-down, 30 μg GST-tagged AP1 complex, 10 μg ARF1 and 10 μg LBD-STING were mixed together or individually in 40 μL pull-down buffer (PBS supplemented with 2 mM MgCl_2 , 1 mM GTP, 2 mM TCEP). The mixture was incubated overnight on ice. 30 μL Glutathione Sepharose beads (Cytiva) were incubated with the mixture for 30 min at 4°C.

Excess proteins were washed off the beads using 200 μ L pull-down buffer each time for four times. 20 μ L 5x SDS loading buffer was added to the resin and the mixture was boiled for 5 min. The samples were then centrifuged briefly. 5 μ L of supernatant were analysed by SDS-PAGE. The protein bands were visualized by Coomassie blue staining. For AP1 $\Delta\mu$ CTD pull-down, 30 μ g GST-tagged AP1 $\Delta\mu$ CTD complex and 10 μ g LBD-STING were mixed together or individually in 40 μ L PBS supplemented with 2 mM TCEP. The mixture was incubated overnight on ice. 30 μ L Glutathione Sepharose beads (Cytiva) were incubated with the mixture for 30 min at 4°C. Excess proteins were washed off the beads using 200 μ L PBS each time for four times. 20 μ L 5x SDS loading buffer were added to the resin and the mixture was boiled for 5 min. The samples were then centrifuged briefly. 5 μ L of supernatant were analysed by SDS-PAGE. The protein bands were visualized by Coomassie blue staining.

Bio-layer interferometry

BLI analyses were performed at 25 °C using a GatorPrime biosensor system (GatorBio) with Streptavidin probes (GatorBio, 160002). STING, STING mutants or p-STING were mixed with biotin (EZ-Link-NHS-LC-LC-Biotin, Thermo Fisher Scientific) at a molar ratio of three biotins to one STING and incubated at room temperature for 30 min, and then excess biotin was removed by using a desalting column (PD 10, Cytiva). Biotinylated STING (10 μ g / mL) was immobilized onto the Streptavidin biosensor (GatorBio, 18-5019) for 1 min. The tips were washed with PBS buffer for 2 min to obtain a baseline reading, then the biosensors were dipped into wells containing the various concentrations of AP-1 $\Delta\mu$ CTD or its mutant for 5 min, which was followed by a 10-min buffer wash to allow the dissociation of molecules from the sensor. Data analysis was performed with GraphPad PRISM 9 using a standard 1:1 binding model. Two independent experiments were performed for each sample.

Cryo-EM data acquisition

2 mg GST-tag cleaved AP-1 core complex were incubated with 2 mg ARF1 for 30 minutes at room temperature in PBS supplemented with 2 mM $MgCl_2$, 1 mM GTP and 2 mM TCEP. 2 mg p-STING was then added, and the mixture was incubated on ice overnight. Excess ARF1 and p-STING were removed with a Superose 6 increase 10/300 GL column (Cytiva) in PBS. The AP-1-ARF1-p-STING complex fraction was collected and concentrated to 0.8 mg/mL. Aliquots of 3 μ L of AP-1-ARF1-p-STING complexes were loaded onto glow-discharged holey carbon grids (Electron Microscopy Sciences, Q250AR1.3, Quantifoil, Au, R 1.2/1.3, 300 mesh). Grids were blotted for 4 s and plunged frozen in liquid ethane using a Vitrobot at 4 °C and with 100% humidity. Grids were screened for particle presence and ice quality on a TFS

Glacios microscope (200 kV), and the best grids were transferred to TFS Titan Krios G4. Cryo-EM data was collected using TFS Titan Krios G4 transmission electron microscope (TEM), equipped with a Cold-FEG on a Falcon IV detector in electron counting mode. Falcon IV gain references were collected just before data collection. Data was collected with TFS EPU v2.12.1 using aberration-free image shift protocol (AFIS), recording 8 micrographs per ice hole. Movies were recorded at a magnification of 270 kx, corresponding to the 0.45 Å pixel size at the specimen level, with defocus values ranging from -0.8 to -1.8 µm. Exposures were adjusted automatically to 60 e⁻/Å² total dose, resulting in an exposure time of approximately 3 seconds per movie. In total, 30,004 micrographs in EER format were collected.

Cryo-EM data processing

Motion correction was performed on raw stacks without binning using the cryoSPARC implementation of motion correction. 1,701,051 particles were template-based automatically picked and particles were binned by a factor of 4. Two rounds of 2D classification were performed, resulting in a particle set of 539,684 particles. 2D classification of particles showed that the relative orientation between STING and AP-1 was highly variable. Selected particles resulting from the 2D classification were used for ab-initio reconstruction. After 2 rounds of ab-initio reconstruction, 326,772 particles were selected based on STING densities. The particles were re-centered and re-extracted by a binning factor of 2. The particles were subjected to iterative CTF refinement and non-uniform refinement in cryoSPARC to 2.34 Å. The reported resolutions are based on the gold-standard Fourier shell correlation 0.143 criterion. Local resolution variations were estimated using cryoSPARC.

Model building and refinement

AP-1-ARF1-p-STING model was generated using a published AP-1-ARF1-tetherin Nef structure (PDB 6DFF). The AP-1-ARF1 model after removing tetherin Nef ligand was docked into the cryo-EM map in Chimera and fine-tuned by manual adjustment with Coot. The p-STING tail was docked against the cryo-EM map in Coot and the whole model was refined in Phenix. Several loop regions of AP-1, ARF1 and p-STING were manually adjusted to fit into the map using Coot. The model was refined in real space again in Phenix. All structure figures were made by UCSF Chimera, UCSF ChimeraX, and PyMOL.

3.2.11 – Additional paper sections

Acknowledgments

We are grateful to N. Jordan for technical assistance and members of the Ablasser lab for helpful discussions. We thank P. Schu for sharing μ 1A-deficient MEFs and their complemented counterparts. We thank R. Goldbach-Mansky for providing fibroblasts from SAVI patients. We thank the EPFL BiImaging & Optics Core Facility, in particular N. Chiaruttini, R. Guiet, T. Laroche, and C. Stoffel, for support on imaging and data processing. We are also grateful to the EPFL Biological Electron Microscopy Core Facility, in particular G. Knott, S. Rosset and J. Blanc, for performing the electron microscopy and alignments of the CLEM experiment. Cryo-EM data acquisition was performed at the Dubochet Center for Imaging, Lausanne, CH and we are grateful to A. Myasnikov, B. Beckert, S. Nazarov, and E. Uchikawa. The work was funded by grants to A. A. from the Swiss National Science Foundation (310030_188759), the Dr. Josef Steiner Cancer Research Foundation, the European Union's Horizon 2020 Research and Innovation program grant agreement (grant no: 804933, ImAgine), the Leenaards Foundation, the Fondation Acteria, and the U.S. National Institutes of Health grant R01 AI 120691 to J.H.H. P. X. and C.L. are supported by EMBO Post-doctoral Fellowships (ALTF 184-2021 and ALTF 88-2022).

Data availability

Full scans for all western blots and the in-gel fluorescence images are provided in Supplementary Figure 1. The three-dimensional cryo-EM density map is deposited into the Electron Microscopy Data Bank (EMDB) under accession number EMD-14312. The coordinate is deposited in the Protein Data Bank (PDB) with accession number 7R4H. Source data are available.

Author contributions

Experiments were designed, conducted, and analysed by Y.L., P.X., S.R., C.L., and J.R. Cell experiments and confocal and airyscan microscopy studies were carried out by Y.L. and S.R. Cryo-EM structural experiments and analysis was performed by P.X. STED image acquisition and analysis was performed by C.L. Biochemical experiments were performed by P.X. and J.R. X.R. and J. H. shared materials for adaptor protein complex in vitro reconstitution and provided helpful advice for biochemical studies. A.A. conceived and supervised the work and wrote the manuscript. All authors contributed to editing of the manuscript and support the conclusions.

Chapter 4 – Global discussion and perspectives

4.1 – Summary and significance of findings

The cGAS-STING pathway has been identified as the main cytosolic DNA sensing pathway and as such constitutes a key element of our innate immune defence. In addition to being involved in resistance against several pathogens or immune detection of tumours¹⁰, when dysregulated, the pathway can be associated with autoinflammatory diseases. The classical examples of cGAS-STING-related autoinflammatory disorders are severe interferonopathies (e.g., Aicardi–Goutières syndrome, SAVI, or COPA syndrome), but diseases with a less clear pathogenesis, such as systemic lupus erythematosus, Parkinson’s disease and other motor diseases also exhibit a partial IFN I signature¹⁸. The crucial involvement of IFN I in general, and cGAS-STING in particular, in human health has fostered a lot of research. The work presented in this thesis unveils some previously unknown mechanisms involved in STING regulation, in particular elements relative to STING trafficking and its spatiotemporal localisation in the cell upon pathway activation.

The initial question we decided to address regarding this topic was how STING ER-to-Golgi trafficking is regulated and how it can be modulated. When we first started investigating this, no key STING ER-anchor or trafficking stimulator had been identified^{115,116}, and it was merely suspected that oligomerisation might play a role. COPII players’ ability to mediate STING ER-to-Golgi trafficking was also not yet confirmed^{116,144}, and retrograde shuttling via COPI was not known^{107–110}. The first chemical inhibitor of STING activation was about to be published by our group¹²⁴, and, knowing that its mechanism of action targeted Golgi-based palmitoylation, we aimed to further investigate the upstream molecular events linking ligand-binding with trafficking and the impact mutations in STING could have. The two initial experimental strategies we followed in parallel were a chemical inhibition microscopy screen and a mass spectrometry-based interactome screen. These complementary approaches aimed at simultaneously identifying critical STING regulatory partners and their role in trafficking, as well as potentially uncovering novel, fast to implement strategies to modulate this shuttling mechanism. Furthermore, we also performed an ala-scan on STING to directly identify key regulatory regions that were important for trafficking regulation. As described in **Chapter 2** of this thesis, these different projects could shed light on some interesting techniques, information about regulatory mechanisms and key residues of STING. However, our data regarding STING ER-to-Golgi trafficking remain preliminary and should only be used to contribute to the design of future research projects, or be further elaborated upon for stronger claims of mechanistic discoveries.

As a second part of trying to understand how STING localisation was regulated and its implication for the pathway, we interrogated how late-stage trafficking of STING, namely from the Golgi onwards, could impact signalling and its termination. Indeed, the exact mechanisms underlying STING terminal trafficking and signalling shut down remained quite mysterious. Diverse reports mentioned the role of autophagy and proposed an ultimate lysosomal degradation^{59,62}, but there was a lack of a precise understanding of the fate of p-STING oligomers between their phosphorylation by TBK1 at the Golgi and their reported terminal presence and degradation in endolysosomal compartments. The work presented in **Chapter 3** of this thesis describes precisely a mechanism leading to STING signal termination by transport of activated p-STING at the Golgi towards the endolysosomal degradation system via AP-1-mediated loading into CCVs¹³⁷.

During the course of this research, several central discoveries were also made by others in the cGAS-STING community. For example, the elucidation of STING full-length structure by cryogenic electron microscopy (cryo-EM), alone or in complex with TBK1^{55,56}, provided valuable insights into STING conformational changes and their causes and consequences for pathway activation as well as trafficking. These discoveries, paralleled with the identification of additional critical binding partners^{115,116} and deeper understanding of STING ER-Golgi shuttle mechanisms^{16,107–109}, greatly contributed to a better knowledge of STING initial trafficking. On the other hand, little progress was made regarding pathway termination, and in this perspective, the work described in **Chapter 3** represents a significant advance in the field. Not only does it unravel a key regulatory mechanism by which STING can be transported towards lysosomes to terminate its signalling, but it also underlines again the place of tight feedback regulation in innate immunity. In addition, it points towards the need to co-evolve activating and inhibitory mechanisms simultaneously in order to maintain an efficient yet not harmful immune defence.

4.2 – Perspectives

4.2.1 – Implications of STING regulation by conformation and localisation changes

Interestingly, most of the newly uncovered mechanisms impacting STING regulation are directly linked with STING conformation, aggregation state and trafficking, three elements that appear closely related with each other. Indeed, either trafficking leads to STING being modified as a result of reaching compartments or areas where the necessary partners are operating, or PTMs are required for trafficking to occur, or a mix of both. In any case, whether regulatory PTMs (e.g., palmitoylation at the Golgi or phosphorylation at the TGN) are a

consequence of STING's movements, or whether they are a prerequisite to trigger these, it has become clear that the sensor's cellular localisation determines its activity status. This had been emphasised by the relationship between STING overactivation and its accumulation at the Golgi in SAVI and COPA syndrome¹⁸, and our latest discoveries on STING degradation and pathway termination confirm it. Indeed, decreasing STING Golgi-to-lysosome transport by depleting AP-1 enhances downstream signalling. These elements point towards a model in which STING subcellular localisation appears essential and sometimes sufficient for activation. Further insights are given by the observed need for STING palmitoylation for IFN I signalling. This was verified by downstream pathway blockade either when using a general palmitoylation inhibitor¹²³, or when adding a STING-specific inhibitor that functions by covalently binding STING cysteine 91 and preventing its palmitoylation¹²⁴. In both cases, downstream signalling is hindered despite STING being located at the Golgi^{123,124}. This later point fits a hypothesis in which the link between STING localisation and its activity is based on essential (and sufficient) PTMs along its intracellular route that can only occur in given subcellular regions. This could either be because the involved partners are only active in those regions, or because the local environment allows for proper SMOC assembly and associated efficient signal transduction. If verified, this model, merged together with the published literature and results discussed in this thesis, would be compatible with the following regulatory sequence of STING. STING would be activated by conformational changes and aggregation at the ER, where the first SMOC composed of STING dimers able to attract STEEP and COPII components would launch efficient trafficking to the Golgi. There, palmitoylation would occur, allowing further transport to the TGN or re-organisation of the oligomers, forming clusters qualitatively distinct from the ones found at the ER, as also proposed by Taguchi et al¹²⁵. The constituted structures would assimilate with a second SMOC, able to efficiently recruit TBK1, which could in turn start a phosphorylation cascade. This would initiate IRF3 recruitment—and IFN I signalling—and other TBK1-dependent or independent responses—such as NF-κB activation or autophagy. Simultaneously, it would also initiate the shutdown of signalling, via AP-1 recruitment and loading into CCVs targeted to the lysosomes for degradation. These sequential SMOCs are a particularly convenient mode of activation for STING. Indeed, its signalling steps involve cooperative processes (vesicle formation and need for a platform regrouping the actors of the phosphorylation cascade) that need clustering to become active at relevant levels and see their efficacy exponentially boosted.

Besides unveiling mechanistic details of STING activation, these discoveries and the associated hypotheses also underline the important notion of successive signalling hubs with distinct localisation, that can integrate various signals along the way and act as checkpoints

where responses can be adapted or modulated if needed. This notion challenges, to a small degree, the more classical view of regulatory proteins as drivers of pathway activation or inhibition. Here, we find regulation to depend on maintaining STING on its dedicated path, where the correct spatiotemporal location of binding partners is crucial to perform the needed PTMs to achieve optimal regulation. Thus, rather than a partner-dependent regulation, we have a localisation-dependence, and partners, such as TBK1 and IRF3, can process or be recruited by STING upon proper delivery to the Golgi. In this vision, the cell constitutes a well-regulated factory environment where product flows determine the next steps, but regulators themselves are more passively involved. This is obviously a simplification, since each of those regulatory proteins in turn has its own regulatory pathway. However, focusing on the dynamics of individual proteins by looking at their conformational and localisation changes and at how these are impacted by and impact other signalling proteins or networks might be a valuable perspective. This strategy can indeed provide a good global picture of the regulatory mechanisms at play, nicely complementing a more traditional step-by-step pathway approach. In the case of STING, close tracking allows to turn the sequential pathway into a flow of interconnected, partially concomitant events constantly branching with other signalling axes. It also sheds light on structural specificities, such as the CTT, that appear critical in determining the equilibrium between the different possible downstream responses along the pathway.

4.2.2 – What evolution tells us about STING

Another complementary approach that can be crucial for orienting research about cGAS-STING in particular and innate immunity in general is to consider evolutionary clues. This has been discussed and shown by others as well as by the work presented in this thesis. Indeed, lack of conservation and sudden apparition of some sequences in STING CTT have been shown to correlate with acquisition of new functionalities of the pathway, such as DNA detection-associated IFN I signalling arising in vertebrates or increased NF- κ B signalling found in zebrafish¹³⁵. Simultaneously, some conserved regions can inform us about crucial motifs or amino acids, such as the CTT-localised TBK1, IRF3 and AP-1 recruitment motifs, that are conserved across mammals^{57,118,137}. Similarly, highly conserved amino acids in the “neck” dimerization interface of STING (near aa 141-156) or in the second transmembrane cytosolic loop (E69 and R76) happen to be critical for trafficking, and hence activity, of STING⁵⁵. In addition to pinpointing interesting regions of the protein, evolution can make acquisition of modules apparent, such as the above-mentioned mammalian CTT motifs or zebrafish NF- κ B-enhancing cassette. This allows for insights into protein regulation, the

system's versatility, as well as about which modifications are possible. Indeed, with such interconnected and complex networks, evolution can be hindered, because changing one element at a time is at risk of disturbing the balance of the whole system. Hence, quite often, at least two evolutionary traits seem to be selected for together, or an evolutionary difference is accompanied by a drastic shift of protein or pathway use. This can be observed in the increased NF- κ B signalling in zebrafish coming with an impaired IRF3 recruitment motif compared to mammalian STING¹³⁵, or in the probable co-selection of IRF3 and AP-1 recruitment motifs in mammalian STING facilitated by their direct proximity (see **Chapter 3**). Another example is found in bats, which have a mutation in the highly conserved S358 of their STING CTT allowing them to coexist with viruses without overactivation of their innate immune response¹³⁸.

Interestingly, the pieces of work described above and the present thesis emphasise how STING appears simultaneously evolutionarily conserved and highly modular. It indeed seems that evolution of STING is driven by acquisition or loss of complete “packages”, coming with embedded positive and negative regulatory mechanisms, as observed for the mammalian IFN I induction of zebrafish NF- κ B cassette extensively discussed above. Considering this, it is tempting to propose that this modularity, best imaged by the architecture of STING CTT with its subsequent motifs, is in fact a core characteristic shared by PRRs across our innate immunity. This intriguing hypothesis has been explored by Tan and Kagan, who designed a nature-inspired “SMOC-like nanomachine”²⁰¹. They used synthetic biology to combine TLR and STING signalling features: they fused the IRF3 recruitment motif of STING CTT, ϕ LxIS (ϕ : hydrophilic residue; x any residue; also found on other innate immune proteins such as TRIF and MAVS), to MyD88, the adaptor forming myddosomes downstream of activated TLRs. They could show that such synthetic PRRs responded to TLR-ligands by producing IFN I in addition to their usual response²⁰¹, underlying the flexibility and modularity of innate immune signalling throughout evolution.

Another aspect apparent in the work presented in this thesis is how proteins involved in STING trafficking appear to be central for the cell and linked with its viability. This is true for all identified trafficking partners (all proteins directly or not involved with COPII-, COPI- and AP-1-mediated trafficking, see **Chapters 1.5** and **3**) and confirmed by the difficulty in finding compounds or hits whose action solely block STING trafficking without disrupting the cell's homeostasis, as enforced by the results of the screens we present in **Chapter 2** of this thesis. This makes sense in an evolutionary perspective, as cGAS-STING appears so central that uncontrolled mutations or regulation changes could quickly prove very detrimental. One could hypothesise that, by governing cGAS-STING regulation via central, almost architectural

constituents of the cellular organisation, cells prevent their survival or proliferation in case of drastic changes, ensuring some degree of stability of the pathway at the population level. This is reminiscent of the rationale behind tumour suppressor genes, that typically govern multiple central cellular activities such as cell cycle checkpoints or DNA damage response pathways and can block them upon detection of sustained hyperproliferative signals or abnormal stress factors²⁰².

4.2.3 – STING dysregulation as a powerful tool to understand homeostatic regulation

While interfering with cGAS-STING is an intervention that needs to be carefully evaluated, it has been done successfully in several cases. One of the promising uses of cGAS-STING modulation is the use of STING activation, whether via administration of CDN analogues or of chemical agonists to boost immunity in tumours^{48,111,164} or as vaccine adjuvant¹⁶⁰. These examples show that, despite it being central for our cellular homeostasis, modulating the cGAS-STING pathway can, when done properly, offer great therapeutic benefit. This is also true in the cases of several interferonopathies. In those diseases, the outcome of pathway dysregulation is an aberrant IFN I response harming the host. For example, dampening downstream signalling by JAK inhibition has been shown to lead to a highly beneficial clinical outcome in SAVI patients. However, the downside of this downstream intervention is a broader immune suppression as well as only partial symptom relief (as some STING-dependent, IFN I/JAK-independent symptoms persist)¹⁸. These problems might be overcome by the use of more targeted therapies, such as the specific STING palmitoylation inhibitor H-151 (ref¹²⁴), acting directly at the STING level (in SAVI or COPA syndrome), leaving alternative nucleic acid sensing pathways unaffected and hopefully blocking all-STING-related aberrant inflammation.

In parallel to direct clinical relevance, study of cGAS-STING through the prism of interferonopathies' pathogenesis is a powerful tool for improving our fundamental understanding of the pathway and deciphering the exact mechanisms involved in its regulation. For example, the variable level of penetrance of some interferonopathies informs us about heterogeneity of the pathway under homeostatic conditions and tissues or cellular variability. This can in turn expose the roles and requirements for specific signalling partners whose distribution varies between cells. By looking at what can dysregulate STING, and what treatment restores which associated functions, we can thus uncover one by one the building blocks that are crucial to the complex regulatory network of STING.

Conversely, by closely following STING upon activation and tracking its partners, we can discover potential STING regulators that had been associated with diseases of unknown

mechanistic source. In this case, we can explore potential causative links between STING signalling and the observed symptoms. In this thesis, we identified two such proteins. First, ELMOD2, that was associated with familial idiopathic pulmonary fibrosis¹⁷⁴. Secondly, we uncovered the critical role of AP-1 in STING signalling termination. Interestingly, loss-of-function mutations in all three possible isoforms of AP-1 σ 1 subunit (A/B/C, encoded by *AP1S1*, *AP1S2* and *AP1S3*, respectively) are associated with genetic disorders. Indeed, *AP1S1* or *AP1S2* biallelic mutations cause severe diseases: the MEDNIK (mental retardation, enteropathy, deafness, peripheral neuropathy, ichthyosis, and keratoderma) multisystem disorder, or various neurodevelopmental syndromes (Fried syndrome, Pettigrew syndrome, and X-linked syndromic mental retardation type 59), respectively¹⁴⁰. The last subunit, encoded by *AP1S3*, has been found to carry monoallelic mutations in some patients affected by pustular psoriasis¹⁴⁰. While the central role of AP-1 in vesicular transport implies that these syndromes are probably multifactorial, investigating the role of STING and the potential impact of STING inhibitors on patient cells or mice models might prove relevant. Of note, in the paper presented in **Chapter 3**, when silenced AP-1 σ 1 subunits (σ 1A and σ 1C, referred to as subunits σ 1 and σ 3), we observed an increase in STING-dependent IFN I signalling (**Extended Data Fig. 3.4i**). Furthermore, transfection of *AP1S1* (subunit σ 1A) could rescue the decrease in STING degradation and associated increase in STING signalling caused by silencing of AP-1 σ 1A and σ 1C subunits (**Extended Data Fig. 3.3c**). While knock-down of the subunits is not directly comparable with disease-associated mutations, the pathogenic alleles might exhibit a similar phenotype. Together, this further confirms that exploring the role of STING in AP-1-associated diseases could be a promising avenue of research.

4.2.4 – The advantages and limits of microscopy-based approaches in studying STING

Closely following and monitoring STING upon activation is crucial to better understand the pathway, and can only be achieved by combining several approaches, including traditional cell signalling studies and assays, but also microscopy, biochemistry or structural biology. In the present thesis, microscopy has been used extensively as an investigative tool. We developed GFP-STING reporter cell lines and multiple staining methods to visualise over-expressed STING and several relevant cellular compartments. Among the characteristics that make microscopy invaluable to study signalling and trafficking of STING are the ability to observe whole cells and populations as well as to follow the evolution of distribution of STING over time. An aspect that could have been developed further and holds great promise is live cell imaging, especially in high resolution. Indeed, although this requires the use of reporter cell lines and/or markers suitable for live cell imaging, this allows the observation of STING in

cells that have not been fixed nor permeabilised, reducing the risks of imaging artefacts. In addition, we can observe the exact trajectory of STING, and therefore not only see the final localisation of STING's cellular pool at a given time point, but which path was taken and what steps lead to this relocation. A key factor that could have helped to refine the knowledge about this pathway would have been to follow live p-STING (rather than total STING) to obtain extra information about the distinct fate of an activated STING molecule over a resting one in live cells. However, this would have required the development of fluorescent-probes sensitive to STING phosphorylation, a technical challenge that was beyond the scope of this work.

Another method that we used was to combine microscopy with screening approaches. While we used this strategy in our chemical and, to some extent, ala-scan screenings, implementing this type of approach with higher resolution microscopy could bring further discoveries. This is even more true as current progress in machine learning-based image analysis can greatly power up microscopy-based assays. Many models and hypotheses (concerning the importance of key residues for conformation-induced clustering and/or trafficking, impact of potential PTMs or partners, or exact mode of action of modulatory chemical compounds) could indeed be investigated with high resolution microscopy-based screens. In fact, preliminary data obtained in our ala-scan shed light on STING regions that are of definite interest, and higher screening resolution (i.e., better spatial and temporal resolution, but also amino acids resolution, using one-by-one rather than three-by-three amino acid mutation) could help in precisely pinpointing key residues and hinting towards the exact mechanisms behind the observed regulatory changes. Taken together with subsequent in vitro structural or conformational validation experiments, this type of approach—not so distant from what we did in the research presented in **Chapter 3**—could prove a powerful approach to explore the subtle fine-tuning involved in precise STING regulation.

Another related approach that might prove promising is to combine recently developed super-high resolution microscopy technologies such as DNA-PAINT, that can reach a single molecule resolution²⁰³, with the activity and trafficking assays used here, to elucidate STING's cellular fate. This would add precise information about oligomerisation status to the spatial data usually available through microscopy, rendering the approach particularly fit to study STING, where trafficking and clustering are both essential for one another and for downstream activation. Co-staining of putative partners would be the next step to design a study allowing an in-detail comprehension of how diverse elements come together to build the well-constructed regulatory network of STING. Of course, microscopy is time- and resources-consuming and, the higher the resolution, the lower the throughput. As such, high-resolution strategies are more amenable to later-stage projects, with specific targets and spatiotemporal

frames in mind. However, the right method applied to the right problem could allow to capture precise cellular mechanisms in a straight-forward fashion.

4.2.5 – Open questions and how to address them

Among all the aspects covered by our study and discussed in this thesis, several elements pave the way for potential further research. One such element is related to identified key point mutations. Indeed, conserved amino acids in the initial secondary transmembrane domain cytosolic loop (E69 and R76) identified as required for trafficking in our hands have later been shown in the work of others to be key in STING regulation⁵⁵. However, why these exact sites are key remains unknown, and further conformational-, localisation- or aggregation-related data could help answer this question. In our studies about ELMOD2, we obtained preliminary data indicative of a potential STING-ELMOD2 interaction that was reduced when working with the non-trafficking mutant STING R76A. If confirmed, such a mechanism could be an example of how mixing data from trafficking, interactome, and activity screens can reveal a regulation mechanism by pinpointing the exact residue responsible for an interaction that is crucial to trigger trafficking. To elaborate further in this direction, we had also initiated preliminary research into the ability of small GTPases and associated GAPs and GEFs to impact STING trafficking. While we did not pursue these experiments further, they could prove very informative, in particular if combined with interaction tests using point-mutants shown to have hyper- or hypo-trafficking phenotypes. A few such mutants have been described (SAVI or non-trafficking ones), and more could be obtained from our three-by-three ala-scan, by refining the results to identify single-point mutations similarly affecting trafficking. Therefore, combining study of point-mutations, interactions, and trafficking appears likely to constitute an efficient and interesting angle to collect regulatory information about STING.

Another promising approach is to tackle new open questions, that seem broader, less mechanisms-centred and rather conceptual for now. One of those revolves around the exact degradation occurring once STING reaches the lysosomes. Indeed, while we uncovered that CCVs transport STING to the lysosomes, how this transport finally culminates in multivesicular body formation remains unknown. Furthermore, how STING ends up transported on the intra-lysosomal side of the lysosomes while being oriented towards the cytosol at the Golgi would also be an interesting mechanism to investigate. To add to the potential models, Chu et al. identified another protein, Niemann-Pick type C1 (NPC1), as a co-factor acting as lysosomal adaptor for STING transport¹⁸⁵. Interestingly, NPC1 has recently been shown to be able to regulate clathrin dynamics upon viral entry²⁰⁴, suggesting that it might be acting sequentially to or in parallel with AP-1. All these results and the questions they raise are exciting milestones

on the road towards a more exhaustive and comprehensive understanding of STING signalling. They might also prove clinically relevant, since control of STING degradation is an interesting therapeutic option, as exemplified by the enhanced cGAMP-triggered anti-tumour response observed in mice co-treated with the lysosomal inhibitor bafilomycin A⁶².

Staying in the field of STING terminal degradation, the parallels and interconnections between AP-1-clathrin-mediated STING degradation or autophagosome-mediated one is also of great interest. Indeed, we did collect some preliminary data indicating that, while decreasing STING degradation and increasing its signalling, AP-1 depletion also had a tendency to increase LC3B lipidation, an indicator of autophagy. This could indicate that blocking one cellular path followed by STING upon activation might re-route some of the adaptor on other paths, with potential implications on the duration and type of downstream immune signalling.

Another interesting observation is that the WD40 domain, a tryptophan rich-region known to play a role in protein-protein interactions and found to be implicated in the formation of a number of cellular networks' hubs²⁰⁵, can be found both in α -COP and in ATG16L. These two proteins have been cited as interactants of STING at the ERGIC or Golgi, to help it traffic back to the ER, or direct it towards formation of non-canonical autophagosomes, respectively^{108,159}. A mutation in the WD40 domain of α -COP prevented recognition of SURF4, the adaptor necessary to recruit STING, blocking its retrograde trafficking¹⁰⁸. In the case of ATG16L, details of the proteins at play remain unknown, but STING somehow depends on the WD40 domain of ATG16L to directly activate LC3B lipidation to trigger autophagy, with no need for other canonical autophagy proteins. In addition, surprisingly, the constituted autophagosomes have a single membrane and the concomitant LC3B lipidation depends on V-ATPase, indicating that this autophagy mechanism is distinct from the ones classically triggering double-membrane autophagosomes¹⁵⁹. Here again, a more thorough examination of those exact mechanisms first brings more questions than answers, but the WD40 domain and other potential STING interactants harbouring it warrant further investigation.

4.2.6 – Concluding remarks

To conclude this work, I would like to reflect on the global trends emerging from the findings in this thesis, other published works as well as the speculative mechanisms discussed here. A main concrete element that seems clearer than ever is the extent to which structure, conformation and localisation are related and key to STING regulation. This has implications both for our understanding of regulatory innate immune networks and their dynamics as well as for which tools and approaches to prioritise when studying them. Indeed, the work described above underlines how attention to molecular details leads us to specific mutations

or sequences that in turn direct us towards understanding of evolution, modularity and essence of the studied pathways.

Furthermore, understanding fundamental pathways is crucial, as each new discovery brings not only ideas for potential new therapeutic approaches, but also leads to the identification of interconnection with other cellular networks and to an improved comprehension of how and why some mechanisms are so intricately intertwined. One of the main paradigms arising in innate immunity is the realisation that seemingly specific pathways can not only respond to their primary activator, but also integrate a huge diversity of potential stimuli branching along signal transduction, making them excellent sentinels of the cell. This militia-like behaviour of innate immune sensors is facilitated by regulatory mechanisms implicating components involved in the maintenance of normal cellular activity and homeostasis, such as trafficking machinery and the GTPase networks. The cross-over between basic cell maintenance and innate immune signalling had already been uncovered for inflammasomes, that can be activated in response to GTPases inactivation²⁰⁶ or metabolic perturbations²⁰⁷. In the research discussed above, we and others show that cGAS-STING is also regulated by GTPases and other endogenous central trafficking components. These systems, that ensure interspersed regulatory checkpoints along innate immune pathways, put the light back on the evolution of cellular signalling in general and innate immune signalling in particular. A strategy seems to emerge, in which embedding a given pathway in multiple central mechanisms serves both as an evolutionary safeguard mechanism and as a way to broaden as much as possible the dangers and disruptions to homeostasis that our cells can sense.

Acknowledgements

This section is a dangerous one, because so many people would deserve to be mentioned here, and I don't see by which miracle I would not forget someone while writing the next paragraphs. In case this happens, and so that no-one is completely forgotten, I want to start these acknowledgments by thanking everyone who, in one way or another, contributed to the present thesis or supported me during these past five years. That was the easy part. Now let's dig a bit deeper.

First of all, I would like to thank my thesis supervisor, Prof. Andrea Ablasser. I am grateful that you introduced me to the world of innate immunity by opening the doors of your lab to me when I was just freshly out of my bachelor studies, and by recommending me to my master thesis' lab, the Latz lab at the institute of innate immunity of Bonn, in Germany. I am also thankful that you provided me with the opportunity to pursue my PhD in your lab. You were always passionate about the projects and the science behind them, showing how to persevere and never abandon, even when facing unexpected challenges and drawbacks along the road. These five years allowed me to develop not only my technical skills, but also my ability to think a project through, to react to and solve unexpected issues, my assiduity, my resilience and my capacity to strive. These traits will undoubtedly be assets for me both as a scientist and as a human being.

Next, I am grateful to all jury members, Prof. David Suter, Dr. Carina de Oliveira Mann, Prof. Petr Broz and Prof. Giovanni D'Angelo, who kindly agreed to offer some of their time to read through my manuscript and attend my thesis defence. Thank you very much!

I would also like to thank my PhD mentor, Prof. Alex Persat, as well as all the other professors of the Global Health Institute (GHI) that I had the opportunity to interact with. Special thanks to Prof. Bruno Lemaître, who acted as the GHI director for most of my PhD, had me as a teaching assistant for a memorable SHS exam session and never failed to start nice discussions at the coffee machine! Other people who were never far away were Sonia, Cécile and Sonja, the lab, institute and doctoral school administrators. Thanks for your help, frequent smiles, and also the non-administrative conversations! And special thanks to Cécile for the coffee and milk!

A PhD does not start suddenly, out of the blue. This is why I also want to thank all the professors who have had me in their labs, as well as PhDs and postdocs who trained me along the way and allowed me to grow as a scientist when I was just beginning to discover what research was.

But most of all, a PhD is far from being a lonely road. It would not have been possible for me to achieve what I achieved in the past five years without the support of my colleagues, friends and family.

I cannot express the extent of my gratitude to all the colleagues I was lucky enough to work alongside in the Ablasser lab during my PhD. If my memory is good enough, they are, by order of appearance (!): Fatih, Simone, Selene, Nathalie, Baptiste, Nicole, Maria-Luna, Alexiane, Marilena, Natasha, Victoria, Jo, Pauline, Flavie, Paola, Paula, Jihen, Ying, Bing, Pengbiao, Alex K., Chong, Alex H., Céline and Lingyun! Thanks to all of you for making the lab the lab!

Alex H., it was a pleasure welcoming you in the sacred yoghurt trio! Thanks for your last-minute help, for pushing for social events, for all the conversations, lunches (sandwiches!), laughs and good mood, and for making me realise how old I was!

Alex K., I have to start by thanking you for your immense help in proof-reading this thesis. I honestly don't know how I would have managed without your English and structural insights, but mostly without your support. Besides this, I could not have wished for a better "new" neighbour to spend my last year and a bit in the bay with! Thanks for the conversations about everything and nothing, the good mood, for training my artistic imagination with your dot plots and mostly for being extremely supportive in all aspects of my final PhD year!

Alexiane, thanks for your mentoring in the early (and not-so-early!) days of my PhD life, the Jedi-ness, all the shared Holycows and pizzas, climbing sessions, music sessions, and above all, thanks for the endless conversations about science, about art, about the lab, about the nerdiest possible topics, about life. I am glad we got to meet and happy that we can keep in touch!

Baptiste, I will miss (well, I miss already!) the sudden happiness your live microscopy could bring, calling you for lunch across the lab, your constant questioning and discussing of all projects, the dumb jokes we would share... I would almost miss your music and whistling in the lab! You brought me a lot scientifically, and you have opened the BIOP's doors to me, which was invaluable. But besides all, I will remember your laughter, the shared videos, the extensive moral support in so many occasions, and your good mood (and your messy hair!).

Céline, thanks for the shared lunches, laughs and conversations, and for always being super smiling, motivated for social activities, empathetic and supportive!

Chong, it was a pleasure getting to share some microscopy experiments with you. Thanks for always being ready to help, and thanks for smiling all day long!

Fatih, you are far more than a scientific encyclopedia, but you *are* a scientific encyclopedia! Thanks for all your pieces of advice, but mostly, for your scientific and non-scientific wisdom, your enigmatic smile, your cunning humour and your empathy!

Flavie, it was great having you in the lunch team, discussing and laughing together, and getting to know each other! Thanks for your time spent in the lab!

Jihen, thank you for the year spent working together, for the bike rides, the good mood even late in the evening, the memorable puzzling sessions, the countless pizza-crash evenings, and mostly all the discussions, fun or deep, that we shared. Above all, thanks for your immense empathy! I'll be back for a pizza soon!

Jo, thanks for sharing the night sessions with me! I have been really happy to work with you, but also to confront our visions of life, of art, or to simply share dumb jokes with you. Thanks for all the late evening conversations and shared experimental frustration!

Lingyun, I did not really get to know you, because I was writing this thesis during the few weeks we shared in the lab, but thanks for being a smiling and nice new desk neighbour!

Marilena, the list is long, I am going to shorten it, but I know that you know how invaluable your support has been during my five years of PhD. I could not have wished for a better PhD buddy and desk neighbour. Thanks for all the time shared running, singing, eating, crying, discussing science, discussing life. On a very concrete note, thanks for your proofreading of parts of this thesis. On a deeper one, thanks for believing in me and making me believe in myself too. Thanks for your Christmas reminders, for the timely hot chocolates, for allowing me to practice my German, for all the "you can do it" or "scroll-scroll-scroll" moments, for the infinite number of silent supportive smiles... Thanks for striving and thriving with me, thanks for being you!

Natasha, thanks for all the conversations, the lighter and the deeper ones, the jokes, the support, the empathy... Thanks for sharing my taste for art, for sharing our experiences as PhDs, for the mutual help, advice and support. We've known each other for a while, but I guess we both learned a lot about ourselves (and each other!) during that PhD. Thanks for walking that path alongside me! I'll miss our little PhD coffee breaks, we need to somehow proceed with them!

Nathalie, thanks for your help on so many little things, your tricks and advice here and there, sharing your experience, but mostly thanks for all the shared meals, conversations and laughs, and for always being extremely supportive, helpful and kind to me!

Paola, thank you so much for the time spent together. Our little PhD coffee-groups were always uplifting and helping to take a step back or find motivation again. I am glad I got

to know you, practice my German with you, laugh with you and cry with you! Thanks for everything!

Paula, it was great getting to know you! Thanks for the time shared together at lunch, the weekend in the mountains, all the conversations, good laughs and good mood!

Pauline, just thank you. Making a list is ridiculous, but here are the first things coming to my mind: I will deeply miss your culinary skills (yes, well, it *has to* be put first!), your constant smile and uplifting mood, the shared meals, jokes, gossips, your “plans” for me, but also our deeper conversations... Thank you for the empathy and real support you provided me with every time I needed it (and you would know that it was more than once!), and thank you for having so actively contributed to making the lab a better place for everyone, scientifically too, but mostly on the human level! We need to keep in touch, and I don't say that (just) for the gluten-free cakes. Thanks for always being a heart-warming little sun in my daily life!

Ying, it was a pleasure getting to know you and working with you. I really liked how we often started chatting about project-related stuff in cell culture and ended-up discussing general life-related topics at our desks or at the cafeteria! Thanks for your experimental help, but mostly for always being very nice and supportive with me!

The lab is not a closed space, so I also had the chance to interact with lots of other EPFL colleagues! I would like to express my deepest gratitude to all GHI members, as well as to our non-GHI neighbours from the Deplancke lab! You have all contributed to build a great atmosphere in the SV third floor!

Special thanks to our great neighbours from the Blokesch lab, and in particular to Leo, for your contagious good mood and smile and your amazing positivity, as well as to Natalia, Nina, Alexis and Céline, for all the nice moments shared in or out of the lab and the several supportive conversations!

A big thank you also goes to the Lemaître team, and in particular to Thomas (we won't share the same coffee machine anymore, but we still need to go sailing!), Alexia (keep that smile, you are almost there too!), Faustine, Asya, Sam, and Mark and Hannah, for all the nice shared moments and conversations.

I am also very grateful to the McKinney people. Thank you Ophélie for all the little coffee-chats, our shared time as PhD reps, and your general mood and ability to make me take a step back! Thomas, I don't know if you realise the extent to which you contributed to my PhD. I'll never thank you enough for your support when I was down. You kept me on track and helped me find my positivity back. Thank you so much for your help, motivational speeches and empathy! And thank you also for all the other, normal, very nice shared

conversations! Suzanne, I also want to thank you for all the nice moments and discussions we shared, and for your amazing and contagious enthusiasm for seemingly everything!

Special thanks also go to the Persat lab! Thank you all for adopting me at several Happy hours, and thanks in particular to Lorenzo, Xavier, Alice, Zaïnebe, Sourabh, Tania, and Lucas for all the nice shared moments and conversations. Tamara, I am not forgetting you, you're coming later, but thanks for letting me in in the Persat family!

My list of special GHI thanks would not be complete without mentioning Raphaël, from the Cole lab. I might be speaking of ancient times, but I never forgot how your presence around the cafeteria and corridors of the GHI always brought sunshine and good mood! Thanks a lot!

Finally, I'd like to thank other people around SV who contributed to make those 5 years special:

Thank you to the whole BIOP team, and in particular to Nico and Romain, for providing super efficient scientific help and advice, but also great mood;

Huge thank you to Barbara Grisoni, who accompanied me along my whole EPFL journey, not only as my first practical course professor in Bachelor, my advisor for the iGEM project, and the first professor to have me as an SV teaching assistant at the beginning of my PhD, but also as someone always ready to discuss with me and provide advice and support!

My gratitude also goes to all other SV people who accompanied me along my PhD, with scientific support or simply smiles and uplifting talks, or both: all the ADSV team; Kelvin and Florence from the protein facility; all the flow cytometry team, the BioEM and BSF teams (in particular Fabien); the magasin, solution preparation and laverie teams; all the Ornithorynque team, and in particular Stéphane, all the cooks who made the effort to feed me gluten free dishes, and Lassina, the most positive tray-man in the world (your smile really brightened my daily lunch for 2.5 years!).

Some previous colleagues have had an influence on me beyond our shared lab time, either because of what they taught me, or because they became true friends, most often both. In that respect, I would like to thank all the Latzies, who made my master thesis unforgettable and forged my love for research, in particular Matt, who taught me so much during my master thesis, and Christina and Marta, who offered not only invaluable scientific help, but also indefectible moral support, infinite conversation topics and friendships that last up to this day! Finally, my gratitude also goes to my very first colleagues, from the Auwerx and TES crews, and in particular to Alessia, Adrienne and especially Elena, my first ever supervisor, who became not just the first PhD student I really got to know, but also a true friend who continued

offering support and sharing nice moments until the end of my own PhD adventure, and, I am sure, beyond!

Another key aspect of my PhD was linked with science outreach and communication. I want to thank all people who opened my eyes to these fields and gave me the opportunity to realise how beautiful and important sci-comm can be! Along this amazing journey, the most memorable experience was definitely my participation to *Ma thèse en 180 secondes*. A most heartfelt thank you to all organisers and participants to the Swiss final, it's always a great pleasure to go grab a drink with you! A not less warm thank you to the delegations and organisers who took part in the international final in Montréal, and in particular to all my fellow finalists, to Cassandre, who took care of us the whole week, and to all people, too numerous to be named, I shared drinks, sightseeing, and deep, insightful conversations with. Being part of this group changed me for the best, as did the whole adventure. My deepest gratitude thus also goes to Denis, Anouk and Farnaz, who made this possible in the first place and accompanied me to Montréal.

Despite how it feels after a PhD, I also have a life outside of science, and it is full of important people. For the sake of the length of this acknowledgements section that is getting out of control, I will try to keep it short, but some cannot go without being at least mentioned!

I want to express my deepest gratitude to Chloé. Your friendship is invaluable, to the point that you are family. You know better than anyone how to bring me back on earth when needed, you are always there for me, ready to listen, offering to go in the mountains, taking me in holidays, inviting me over, changing my mind, helping me to put things in perspective, discussing life and discussing everything, anything, literally just discussing all the time... You helped keeping me sane (as much as possible!) during this PhD, even made me a god-mother along the way, and continuously brightened my mood. Thank you so much for this and for everything else!

Similarly, but differently, because we are humans, I express my equally deep gratitude to Léa. I could not have survived these five years without your support and friendship. You were always there (or on the phone!) when I needed to cry, you listened to my problems, helped me, made me feel better. Thanks for all the endless (really!) conversations, the sailing, the chilling, the worrying, the laughing, the playing, the singing, the travelling, the cooking, the talking, the everything-ing... You too were more than crucial in maintaining my mental health

and general mood, and a simple “thank you” expresses only very weakly the extent of my gratitude!

I also want to say a huge thank you to Tamara. Our PhDs definitely strengthened our friendship, and that’s something I am deeply happy about. I cannot tell you how much you have helped over the past five years. Thanks for all the walking, discussing and laughing! My head is full of all the great memories we now share, from chill evenings on sofas to late evenings on campus (in the lab or not!), from shared meals to shared rooms, from moments of tears to moments of joy! Thank you for everything we shared and will continue sharing in the future!

Another person in this list is Elodie. Thanks for all the crazy, ultra-nerdy evenings, the tons of vocal messages, the deep conversations, the geographical or Sherlock-related fun-fact sharing (yep, this is very precise!), the laughs, your capacity to put more or less everything in perspective, your good mood and your enormous support, whether I needed someone to complain to, chill or just bring food!

My gratitude also goes to Emmanuel and Marina, for all the singing, the board game playing, the sailing, the escapes, the shared passion for les Cowboys, the brunches and other shared meals, the puns, the travels, the discussions... Thanks for all the cherished memories I share with you, for your kindness, your support, your humour... your trustworthy friendship!

I also want to thank Maud for our deep, long-lasting friendship. The trust we have in each other is one of the most reassuring things I got to experience in life. I am so grateful to know that you are always there if I need you! Thanks for all the discussions and good memories that we managed scattering along the years despite our too busy timetables!

Another long-lasting and precious friendship I would like to mention is the one with Maude. Thanks for all the discussions about everything and nothing, for making life sound so straightforward, for being super supportive. And thank you for all the times you and Julie had me over, for the swimming, the paddling, the grilling and the chilling!

I would also like to mention other friends that have each been regularly there for me to share nice meals, deep conversations or good laughs. Thanks to Prisca, Florence, Raphaël (aka le gars du bateau), Mathilde, the other choir people, Coralie and all the theatre group, Jenni, Florence, and so many others...

Finally (not really, but almost), I would like to thank all my flatmates! If I kept track correctly (and it could well not be the case), I have had 20 different flatmates over the course of my PhD. All of them endured living with me, whether for just 6 weeks or 9 years, so they could all, to various degrees, taste the highs and lows of my PhD mood. Because they

supported or at least tolerated me, I would like to thank, by order of appearance again, Arthur, Leana, Chloé, Didier, Joshua, Jaspreet, Alex, Jerem, Jo, Hamid, Tamara, Julie, Ana, Matteo, Davide, Saverio, Luca, Nicola, Marco and Ludo.

From this list, I need to thank in particular Arthur and Ana (and now Eloïse!), who saved me from my dark moods on so many occasions, made me laugh, eat and drink, discussed with me, went through confinement with me, chilled with me, and, let's admit it publicly, fed me very often. You really feel like family, thank you so much!

I also want to dedicate special thanks to Julie, Alex, Davide, Luca and Nico, who, each in their own fashion, helped me strive through my PhD, keep going forward, stay positive and maintain my good mood. Thanks to all of you for the shared meals, discussions, games, and general good mood!

I have been telling myself “this one is the last one” for seven pages, and I still feel like I could go on for hours and hours. However, I do need to hand out this thesis at some point, so I'll finish with the most “ready-to-go” ever formula: last but not least, I would like to thank my family. This is—really, for once— going to be short, because I know that you know how much you mean to me, and I can hear some of you telling me to wrap it up and go get some sleep... My deepest gratitude goes to all my cousins, aunts and uncles, to Brigitte, to Oma and to Grand-mère. Simplement merci. Quant à maman, papa, Clément, Anouk et Lune... There is no fitting word to express my love, the value and importance of your presence and support along the years... Merci, GWB et haut les trompes!

References

1. Murphy, K., Travers, P., Walport, M. & Janeway, C. *Janeway's immunobiology*. (Garland Science, 2012).
2. Lemaitre, B., Nicolas, E., Michaut, L., Reichhart, J.-M. & Hoffmann, J. A. The Dorsoventral Regulatory Gene Cassette *spätzle/Toll/cactus* Controls the Potent Antifungal Response in *Drosophila* Adults. *Cell* **86**, 973–983 (1996).
3. Aderem, A. & Ulevitch, R. J. Toll-like receptors in the induction of the innate immune response. *Nature* **406**, 782–787 (2000).
4. Akira, S. & Takeda, K. Toll-like receptor signalling. *Nat. Rev. Immunol.* **4**, 499–511 (2004).
5. Kawasaki, T. & Kawai, T. Toll-Like Receptor Signaling Pathways. *Front. Immunol.* **5**, (2014).
6. Geijtenbeek, T. B. H. & Gringhuis, S. I. Signalling through C-type lectin receptors: shaping immune responses. *Nat. Rev. Immunol.* **9**, 465–479 (2009).
7. Chen, G., Shaw, M. H., Kim, Y.-G. & Nuñez, G. NOD-Like Receptors: Role in Innate Immunity and Inflammatory Disease. *Annu. Rev. Pathol. Mech. Dis.* **4**, 365–398 (2009).
8. Martinon, F., Burns, K. & Tschopp, J. The Inflammasome: A Molecular Platform Triggering Activation of Inflammatory Caspases and Processing of proIL- β . *Mol. Cell* **10**, 417–426 (2002).
9. Schroder, K. & Tschopp, J. The Inflammasomes. *Cell* **140**, 821–832 (2010).
10. Ablasser, A. & Hur, S. Regulation of cGAS- and RLR-mediated immunity to nucleic acids. *Nat. Immunol.* **21**, 17–29 (2020).
11. Hornung, V. *et al.* AIM2 recognizes cytosolic dsDNA and forms a caspase-1-activating inflammasome with ASC. *Nature* **458**, 514–518 (2009).
12. Lugrin, J. & Martinon, F. The AIM2 inflammasome: Sensor of pathogens and cellular perturbations. *Immunol. Rev.* **281**, 99–114 (2018).
13. Unterholzner, L. *et al.* IFI16 is an innate immune sensor for intracellular DNA. *Nat. Immunol.* **11**, 997–1004 (2010).
14. Kagan, J. C., Magupalli, V. G. & Wu, H. SMOCs: supramolecular organizing centres that control innate immunity. *Nat. Rev. Immunol.* **14**, 821–826 (2014).
15. Du, M. & Chen, Z. J. DNA-induced liquid phase condensation of cGAS activates innate immune signaling. *Science* **361**, 704–709 (2018).
16. Ergun, S. L., Fernandez, D., Weiss, T. M. & Li, L. STING Polymer Structure Reveals Mechanisms for Activation, Hyperactivation, and Inhibition. *Cell* **178**, 290–301.e10 (2019).
17. Wu, J. & Chen, Z. J. Innate Immune Sensing and Signaling of Cytosolic Nucleic Acids. *Annu. Rev. Immunol.* **32**, 461–488 (2014).
18. Crow, Y. J. & Stetson, D. B. The type I interferonopathies: 10 years on. *Nat. Rev. Immunol.* 1–13 (2021) doi:10.1038/s41577-021-00633-9.
19. Wu, J. *et al.* Cyclic GMP-AMP is an endogenous second messenger in innate immune signaling by cytosolic DNA. *Science* **339**, 826–830 (2013).
20. Ablasser, A. *et al.* cGAS produces a 2'-5'-linked cyclic dinucleotide second messenger that activates STING. *Nature* **498**, 380–384 (2013).
21. Gao, P. *et al.* Cyclic [G(2',5')pA(3',5')p] is the metazoan second messenger produced by DNA-activated cyclic GMP-AMP synthase. *Cell* **153**, 1094–1107 (2013).

22. Ishikawa, H. & Barber, G. N. STING is an endoplasmic reticulum adaptor that facilitates innate immune signalling. *Nature* **455**, 674–678 (2008).
23. Burdette, D. L. *et al.* STING is a direct innate immune sensor of cyclic di-GMP. *Nature* **478**, 515–518 (2011).
24. Diner, E. J. *et al.* The Innate Immune DNA Sensor cGAS Produces a Noncanonical Cyclic Dinucleotide that Activates Human STING. *Cell Rep.* **3**, 1355–1361 (2013).
25. Saitoh, T. *et al.* Atg9a controls dsDNA-driven dynamic translocation of STING and the innate immune response. *Proc. Natl. Acad. Sci. U. S. A.* **106**, 20842–20846 (2009).
26. Dobbs, N. *et al.* STING Activation by Translocation from the ER Is Associated with Infection and Autoinflammatory Disease. *Cell Host Microbe* **18**, 157–168 (2015).
27. Balka, K. R. & De Nardo, D. Molecular and spatial mechanisms governing STING signalling. *FEBS J.* **288**, 5504–5529 (2021).
28. Ishikawa, H., Ma, Z. & Barber, G. N. STING regulates intracellular DNA-mediated, type I interferon-dependent innate immunity. *Nature* **461**, 788–792 (2009).
29. Sagulenko, V. *et al.* AIM2 and NLRP3 inflammasomes activate both apoptotic and pyroptotic death pathways via ASC. *Cell Death Differ.* **20**, 1149–1160 (2013).
30. Zhang, Z. *et al.* The helicase DDX41 senses intracellular DNA mediated by the adaptor STING in dendritic cells. *Nat. Immunol.* **12**, 959–965 (2011).
31. Takaoka, A. *et al.* DAI (DLM-1/ZBP1) is a cytosolic DNA sensor and an activator of innate immune response. *Nature* **448**, 501–505 (2007).
32. Sun, L., Wu, J., Du, F., Chen, X. & Chen, Z. J. Cyclic GMP-AMP Synthase Is a Cytosolic DNA Sensor That Activates the Type I Interferon Pathway. *Science* **339**, 786–791 (2013).
33. Civril, F. *et al.* Structural mechanism of cytosolic DNA sensing by cGAS. *Nature* **498**, 332–337 (2013).
34. Kranzusch, P. J., Lee, A. S.-Y., Berger, J. M. & Doudna, J. A. Structure of human cGAS reveals a conserved family of second-messenger enzymes in innate immunity. *Cell Rep.* **3**, 1362–1368 (2013).
35. Xie, W. *et al.* Human cGAS catalytic domain has an additional DNA-binding interface that enhances enzymatic activity and liquid-phase condensation. *Proc. Natl. Acad. Sci. U. S. A.* **116**, 11946–11955 (2019).
36. Zhang, X. *et al.* The cytosolic DNA sensor cGAS forms an oligomeric complex with DNA and undergoes switch-like conformational changes in the activation loop. *Cell Rep.* **6**, 421–430 (2014).
37. Li, X. *et al.* Cyclic GMP-AMP synthase is activated by double-stranded DNA-induced oligomerization. *Immunity* **39**, 1019–1031 (2013).
38. The Human Protein Atlas. <https://www.proteinatlas.org/>.
39. Holleufer, A. *et al.* Two cGAS-like receptors induce antiviral immunity in *Drosophila*. *Nature* **597**, 114–118 (2021).
40. Slavik, K. M. *et al.* cGAS-like receptors sense RNA and control 3'2'-cGAMP signalling in *Drosophila*. *Nature* **597**, 109–113 (2021).
41. Kranzusch, P. J. *et al.* Ancient Origin of cGAS-STING Reveals Mechanism of Universal 2',3' cGAMP Signaling. *Mol. Cell* **59**, 891–903 (2015).
42. Whiteley, A. T. *et al.* Bacterial cGAS-like enzymes synthesize diverse nucleotide signals. *Nature* **567**, 194–199 (2019).
43. Cohen, D. *et al.* Cyclic GMP-AMP signalling protects bacteria against viral infection. *Nature* **574**, 691–695 (2019).

44. Wu, X. *et al.* Molecular evolutionary and structural analysis of the cytosolic DNA sensor cGAS and STING. *Nucleic Acids Res.* **42**, 8243–8257 (2014).
45. Margolis, S. R., Wilson, S. C. & Vance, R. E. Evolutionary Origins of cGAS-STING Signaling. *Trends Immunol.* **38**, 733–743 (2017).
46. Cavlar, T., Deimling, T., Ablasser, A., Hopfner, K.-P. & Hornung, V. Species-specific detection of the antiviral small-molecule compound CMA by STING. *EMBO J.* **32**, 1440–1450 (2013).
47. Pan, B.-S. *et al.* An orally available non-nucleotide STING agonist with antitumor activity. *Science* **369**, eaba6098 (2020).
48. Ramanjulu, J. M. *et al.* Design of amidobenzimidazole STING receptor agonists with systemic activity. *Nature* **564**, 439–443 (2018).
49. Gao, P. *et al.* Structure-function analysis of STING activation by c[G(2',5')pA(3',5')p] and targeting by antiviral DMXAA. *Cell* **154**, 748–762 (2013).
50. Gao, P. *et al.* Binding-pocket and lid-region substitutions render human STING sensitive to the species-specific drug DMXAA. *Cell Rep.* **8**, 1668–1676 (2014).
51. Morehouse, B. R. *et al.* STING cyclic dinucleotide sensing originated in bacteria. *Nature* **586**, 429–433 (2020).
52. Martin, M., Hiroyasu, A., Guzman, R. M., Roberts, S. A. & Goodman, A. G. Analysis of *Drosophila* STING Reveals an Evolutionarily Conserved Antimicrobial Function. *Cell Rep.* **23**, 3537–3550.e6 (2018).
53. Sun, W. *et al.* ERIS, an endoplasmic reticulum IFN stimulator, activates innate immune signaling through dimerization. *Proc. Natl. Acad. Sci. U. S. A.* **106**, 8653–8658 (2009).
54. Ouyang, S. *et al.* Structural analysis of the STING adaptor protein reveals a hydrophobic dimer interface and mode of cyclic di-GMP binding. *Immunity* **36**, 1073–1086 (2012).
55. Shang, G., Zhang, C., Chen, Z. J., Bai, X. & Zhang, X. Cryo-EM structures of STING reveal its mechanism of activation by cyclic GMP–AMP. *Nature* **567**, 389–393 (2019).
56. Zhang, C. *et al.* Structural basis of STING binding with and phosphorylation by TBK1. *Nature* **567**, 394–398 (2019).
57. Liu, S. *et al.* Phosphorylation of innate immune adaptor proteins MAVS, STING, and TRIF induces IRF3 activation. *Science* **347**, aaa2630 (2015).
58. Konno, H., Konno, K. & Barber, G. N. Cyclic Dinucleotides Trigger ULK1 (ATG1) Phosphorylation of STING to Prevent Sustained Innate Immune Signaling. *Cell* **155**, 688–698 (2013).
59. Gui, X. *et al.* Autophagy induction via STING trafficking is a primordial function of the cGAS pathway. *Nature* **567**, 262–266 (2019).
60. Liu, D. *et al.* STING directly activates autophagy to tune the innate immune response. *Cell Death Differ.* **26**, 1735–1749 (2019).
61. Hopfner, K.-P. & Hornung, V. Molecular mechanisms and cellular functions of cGAS–STING signalling. *Nat. Rev. Mol. Cell Biol.* **21**, 501–521 (2020).
62. Gonugunta, V. K. *et al.* Trafficking-Mediated STING Degradation Requires Sorting to Acidified Endolysosomes and Can Be Targeted to Enhance Anti-tumor Response. *Cell Rep.* **21**, 3234–3242 (2017).
63. Crow, Y. J. Type I interferonopathies: a novel set of inborn errors of immunity. *Ann. N. Y. Acad. Sci.* **1238**, 91–98 (2011).
64. Crow, Y. J. *et al.* Mutations in the gene encoding the 3'-5' DNA exonuclease TREX1 cause Aicardi-Goutières syndrome at the AGS1 locus. *Nat. Genet.* **38**, 917–920 (2006).

65. Crow, Y. J. *et al.* Mutations in genes encoding ribonuclease H2 subunits cause Aicardi-Goutières syndrome and mimic congenital viral brain infection. *Nat. Genet.* **38**, 910–916 (2006).
66. Stetson, D. B., Ko, J. S., Heidmann, T. & Medzhitov, R. Trex1 prevents cell-intrinsic initiation of autoimmunity. *Cell* **134**, 587–598 (2008).
67. Kawane, K. *et al.* Chronic polyarthritis caused by mammalian DNA that escapes from degradation in macrophages. *Nature* **443**, 998–1002 (2006).
68. Krieg, A. M. CpG Motifs in Bacterial DNA and Their Immune Effects. *Annu. Rev. Immunol.* **20**, 709–760 (2002).
69. O'Neill, L. A. J. Sensing the Dark Side of DNA. *Science* **339**, 763–764 (2013).
70. Liu, H. *et al.* Nuclear cGAS suppresses DNA repair and promotes tumorigenesis. *Nature* **563**, 131–136 (2018).
71. Boyer, J. A. *et al.* Structural basis of nucleosome-dependent cGAS inhibition. *Science* **370**, 450–454 (2020).
72. Cao, D., Han, X., Fan, X., Xu, R.-M. & Zhang, X. Structural basis for nucleosome-mediated inhibition of cGAS activity. *Cell Res.* **30**, 1088–1097 (2020).
73. Kujirai, T. *et al.* Structural basis for the inhibition of cGAS by nucleosomes. *Science* **370**, 455–458 (2020).
74. Michalski, S. *et al.* Structural basis for sequestration and autoinhibition of cGAS by chromatin. *Nature* **587**, 678–682 (2020).
75. Pathare, G. R. *et al.* Structural mechanism of cGAS inhibition by the nucleosome. *Nature* **587**, 668–672 (2020).
76. Zhao, B. *et al.* The molecular basis of tight nuclear tethering and inactivation of cGAS. *Nature* **587**, 673–677 (2020).
77. Guey, B. *et al.* BAF restricts cGAS on nuclear DNA to prevent innate immune activation. *Science* **369**, 823–828 (2020).
78. Zhong, L. *et al.* Phosphorylation of cGAS by CDK1 impairs self-DNA sensing in mitosis. *Cell Discov.* **6**, 26 (2020).
79. Seo, G. J. *et al.* Akt Kinase-Mediated Checkpoint of cGAS DNA Sensing Pathway. *Cell Rep.* **13**, 440–449 (2015).
80. Li, T. *et al.* Phosphorylation and chromatin tethering prevent cGAS activation during mitosis. *Science* **371**, eabc5386 (2021).
81. Wang, Z. *et al.* PCV2 targets cGAS to inhibit type I interferon induction to promote other DNA virus infection. *PLoS Pathog.* **17**, e1009940 (2021).
82. Chen, M. *et al.* TRIM14 Inhibits cGAS Degradation Mediated by Selective Autophagy Receptor p62 to Promote Innate Immune Responses. *Mol. Cell* **64**, 105–119 (2016).
83. Hu, M.-M. *et al.* Sumoylation Promotes the Stability of the DNA Sensor cGAS and the Adaptor STING to Regulate the Kinetics of Response to DNA Virus. *Immunity* **45**, 555–569 (2016).
84. Cui, Y. *et al.* SENP7 Potentiates cGAS Activation by Relieving SUMO-Mediated Inhibition of Cytosolic DNA Sensing. *PLoS Pathog.* **13**, e1006156 (2017).
85. Xia, P. *et al.* Glutamylation of the DNA sensor cGAS regulates its binding and synthase activity in antiviral immunity. *Nat. Immunol.* **17**, 369–378 (2016).
86. Wang, Y. *et al.* Inflammasome Activation Triggers Caspase-1-Mediated Cleavage of cGAS to Regulate Responses to DNA Virus Infection. *Immunity* **46**, 393–404 (2017).
87. Ablasser, A. *et al.* Cell intrinsic immunity spreads to bystander cells via the intercellular transfer of cGAMP. *Nature* **503**, 530–534 (2013).

88. Bridgeman, A. *et al.* Viruses transfer the antiviral second messenger cGAMP between cells. *Science* **349**, 1228–1232 (2015).
89. Gentili, M. *et al.* Transmission of innate immune signaling by packaging of cGAMP in viral particles. *Science* **349**, 1232–1236 (2015).
90. Luteijn, R. D. *et al.* SLC19A1 transports immunoreactive cyclic dinucleotides. *Nature* **573**, 434–438 (2019).
91. Ritchie, C., Cordova, A. F., Hess, G. T., Bassik, M. C. & Li, L. SLC19A1 Is an Importer of the Immunotransmitter cGAMP. *Mol. Cell* **75**, 372-381.e5 (2019).
92. Li, L. *et al.* Hydrolysis of 2'3'-cGAMP by ENPP1 and design of nonhydrolyzable analogs. *Nat. Chem. Biol.* **10**, 1043–1048 (2014).
93. Zhou, C. *et al.* Transfer of cGAMP into Bystander Cells via LRRC8 Volume-Regulated Anion Channels Augments STING-Mediated Interferon Responses and Anti-viral Immunity. *Immunity* **52**, 767-781.e6 (2020).
94. Lahey, L. J. *et al.* LRRC8A:C/E Heteromeric Channels Are Ubiquitous Transporters of cGAMP. *Mol. Cell* **80**, 578-591.e5 (2020).
95. Chen, X. *et al.* Regulation of Anion Channel LRRC8 Volume-Regulated Anion Channels in Transport of 2'3'-Cyclic GMP-AMP and Cisplatin under Steady State and Inflammation. *J. Immunol. Baltim. Md 1950* **206**, 2061–2074 (2021).
96. Concepcion, A. R. *et al.* The volume-regulated anion channel LRRC8C suppresses T cell function by regulating cyclic dinucleotide transport and STING-p53 signaling. *Nat. Immunol.* **23**, 287–302 (2022).
97. Eaglesham, J. B., Pan, Y., Kupper, T. S. & Kranzusch, P. J. Viral and metazoan poxins are cGAMP-specific nucleases that restrict cGAS-STING signalling. *Nature* **566**, 259–263 (2019).
98. Eaglesham, J. B., McCarty, K. L. & Kranzusch, P. J. Structures of diverse poxin cGAMP nucleases reveal a widespread role for cGAS-STING evasion in host-pathogen conflict. *eLife* **9**, e59753 (2020).
99. Liu, Y. *et al.* Activated STING in a Vascular and Pulmonary Syndrome. *N. Engl. J. Med.* **371**, 507–518 (2014).
100. Melki, I. *et al.* Disease-associated mutations identify a novel region in human STING necessary for the control of type I interferon signaling. *J. Allergy Clin. Immunol.* **140**, 543-552.e5 (2017).
101. Saldanha, R. G. *et al.* A Mutation Outside the Dimerization Domain Causing Atypical STING-Associated Vasculopathy With Onset in Infancy. *Front. Immunol.* **9**, 1535 (2018).
102. Patel, S. & Jin, L. TMEM173 variants and potential importance to human biology and disease. *Genes Immun.* (2018) doi:10.1038/s41435-018-0029-9.
103. Konno, H. *et al.* Pro-inflammation Associated with a Gain-of-Function Mutation (R284S) in the Innate Immune Sensor STING. *Cell Rep.* **23**, 1112–1123 (2018).
104. Keskitalo, S. *et al.* Novel TMEM173 Mutation and the Role of Disease Modifying Alleles. *Front. Immunol.* **10**, (2019).
105. Lin, B. *et al.* A novel STING1 variant causes a recessive form of STING-associated vasculopathy with onset in infancy (SAVI). *J. Allergy Clin. Immunol.* **146**, 1204-1208.e6 (2020).
106. Rivara, S. & Ablasser, A. COPA silences STING. *J. Exp. Med.* **217**, e20201517 (2020).
107. Lepelley, A. *et al.* Mutations in COPA lead to abnormal trafficking of STING to the Golgi and interferon signaling. *J. Exp. Med.* **217**, e20200600 (2020).
108. Deng, Z. *et al.* A defect in COPI-mediated transport of STING causes immune dysregulation in COPA syndrome. *J. Exp. Med.* **217**, e20201045 (2020).
109. Mukai, K. *et al.* Homeostatic regulation of STING by retrograde membrane traffic to the ER. *Nat. Commun.* **12**, 61 (2021).

110. Steiner, A. *et al.* Activation of STING due to COPI-deficiency. 2020.07.09.194399 Preprint at <https://doi.org/10.1101/2020.07.09.194399> (2020).
111. Chin, E. N. *et al.* Antitumor activity of a systemic STING-activating non-nucleotide cGAMP mimetic. *Science* **369**, 993–999 (2020).
112. Decout, A., Katz, J. D., Venkatraman, S. & Ablasser, A. The cGAS–STING pathway as a therapeutic target in inflammatory diseases. *Nat. Rev. Immunol.* **21**, 548–569 (2021).
113. Ogawa, E., Mukai, K., Saito, K., Arai, H. & Taguchi, T. The binding of TBK1 to STING requires exocytic membrane traffic from the ER. *Biochem. Biophys. Res. Commun.* **503**, 138–145 (2018).
114. Luo, W.-W. *et al.* iRhom2 is essential for innate immunity to DNA viruses by mediating trafficking and stability of the adaptor STING. *Nat. Immunol.* **17**, 1057–1066 (2016).
115. Srikanth, S. *et al.* The Ca²⁺ sensor STIM1 regulates the type I interferon response by retaining the signaling adaptor STING at the endoplasmic reticulum. *Nat. Immunol.* **20**, 152–162 (2019).
116. Zhang, B. *et al.* STEEP mediates STING ER exit and activation of signaling. *Nat. Immunol.* **21**, 868–879 (2020).
117. Zhao, B. *et al.* Structural basis for concerted recruitment and activation of IRF-3 by innate immune adaptor proteins. *Proc. Natl. Acad. Sci.* **113**, E3403–E3412 (2016).
118. Zhao, B. *et al.* A conserved PLPLRT/SD motif of STING mediates the recruitment and activation of TBK1. *Nature* **569**, 718–722 (2019).
119. Zhang, J., Hu, M.-M., Wang, Y.-Y. & Shu, H.-B. TRIM32 Protein Modulates Type I Interferon Induction and Cellular Antiviral Response by Targeting MITA/STING Protein for K63-linked Ubiquitination*. *J. Biol. Chem.* **287**, 28646–28655 (2012).
120. Wang, Q. *et al.* The E3 Ubiquitin Ligase AMFR and INSIG1 Bridge the Activation of TBK1 Kinase by Modifying the Adaptor STING. *Immunity* **41**, 919–933 (2014).
121. Zhong, B. *et al.* The Ubiquitin Ligase RNF5 Regulates Antiviral Responses by Mediating Degradation of the Adaptor Protein MITA. *Immunity* **30**, 397–407 (2009).
122. Wang, Y. *et al.* TRIM30α Is a Negative-Feedback Regulator of the Intracellular DNA and DNA Virus-Triggered Response by Targeting STING. *PLoS Pathog.* **11**, e1005012 (2015).
123. Mukai, K. *et al.* Activation of STING requires palmitoylation at the Golgi. *Nat. Commun.* **7**, 11932 (2016).
124. Haag, S. M. *et al.* Targeting STING with covalent small-molecule inhibitors. *Nature* **559**, 269–273 (2018).
125. Taguchi, T., Mukai, K., Takaya, E. & Shindo, R. STING Operation at the ER/Golgi Interface. *Front. Immunol.* **12**, (2021).
126. Wu, J. & Yan, N. No Longer A One-Trick Pony: STING Signaling Activity Beyond Interferon. *J. Mol. Biol.* **434**, 167257 (2022).
127. Liu, Y. *et al.* Inflammation-Induced, STING-Dependent Autophagy Restricts Zika Virus Infection in the Drosophila Brain. *Cell Host Microbe* **24**, 57-68.e3 (2018).
128. Yamashiro, L. H. *et al.* Interferon-independent STING signaling promotes resistance to HSV-1 in vivo. *Nat. Commun.* **11**, 3382 (2020).
129. Wu, J., Dobbs, N., Yang, K. & Yan, N. Interferon-Independent Activities of Mammalian STING Mediate Antiviral Response and Tumor Immune Evasion. *Immunity* **53**, 115-126.e5 (2020).
130. Cerboni, S. *et al.* Intrinsic antiproliferative activity of the innate sensor STING in T lymphocytes. *J. Exp. Med.* **214**, 1769–1785 (2017).
131. Hou, Y. *et al.* Non-canonical NF-κB Antagonizes STING Sensor-Mediated DNA Sensing in Radiotherapy. *Immunity* **49**, 490-503.e4 (2018).

132. Bakhoun, S. F. *et al.* Chromosomal instability drives metastasis through a cytosolic DNA response. *Nature* **553**, 467–472 (2018).
133. Abe, T. & Barber, G. N. Cytosolic-DNA-mediated, STING-dependent proinflammatory gene induction necessitates canonical NF- κ B activation through TBK1. *J. Virol.* **88**, 5328–5341 (2014).
134. Balka, K. R. *et al.* TBK1 and IKK ϵ Act Redundantly to Mediate STING-Induced NF- κ B Responses in Myeloid Cells. *Cell Rep.* **31**, 107492 (2020).
135. de Oliveira Mann, C. C. *et al.* Modular Architecture of the STING C-Terminal Tail Allows Interferon and NF- κ B Signaling Adaptation. *Cell Rep.* **27**, 1165–1175.e5 (2019).
136. Yum, S., Li, M., Fang, Y. & Chen, Z. J. TBK1 recruitment to STING activates both IRF3 and NF- κ B that mediate immune defense against tumors and viral infections. *Proc. Natl. Acad. Sci. U. S. A.* **118**, e2100225118 (2021).
137. Liu, Y. *et al.* Clathrin-associated AP-1 controls termination of STING signalling. *Nature* 1–7 (2022) doi:10.1038/s41586-022-05354-0.
138. Xie, J. *et al.* Dampened STING-Dependent Interferon Activation in Bats. *Cell Host Microbe* **23**, 297–301.e4 (2018).
139. Prabakaran, T. *et al.* Attenuation of cGAS-STING signaling is mediated by a p62/SQSTM1-dependent autophagy pathway activated by TBK1. *EMBO J.* **37**, e97858 (2018).
140. Dell’Angelica, E. C. & Bonifacino, J. S. Coatopathies: Genetic Disorders of Protein Coats. *Annu. Rev. Cell Dev. Biol.* **35**, 131–168 (2019).
141. Roth, T. F. & Porter, K. R. YOLK PROTEIN UPTAKE IN THE OOCYTE OF THE MOSQUITO AEDES AEGYPTI. L. *J. Cell Biol.* **20**, 313–332 (1964).
142. Zanetti, G. *et al.* The structure of the COPII transport-vesicle coat assembled on membranes. *eLife* **2**, e00951 (2013).
143. Hutchings, J., Stancheva, V., Miller, E. A. & Zanetti, G. Subtomogram averaging of COPII assemblies reveals how coat organization dictates membrane shape. *Nat. Commun.* **9**, 4154 (2018).
144. Ran, Y. *et al.* YIPF5 Is Essential for Innate Immunity to DNA Virus and Facilitates COPII-Dependent STING Trafficking. *J. Immunol.* **203**, 1560–1570 (2019).
145. Watkin, L. B. *et al.* COPA mutations impair ER-Golgi transport and cause hereditary autoimmune-mediated lung disease and arthritis. *Nat. Genet.* **47**, 654–660 (2015).
146. Waters, M. G., Serafini, T. & Rothman, J. E. ‘Coatomer’: a cytosolic protein complex containing subunits of non-clathrin-coated Golgi transport vesicles. *Nature* **349**, 248–251 (1991).
147. Serafini, T. *et al.* ADP-ribosylation factor is a subunit of the coat of Golgi-derived COP-coated vesicles: a novel role for a GTP-binding protein. *Cell* **67**, 239–253 (1991).
148. Jackson, L. P. *et al.* Molecular Basis for Recognition of Dilysine Trafficking Motifs by COPI. *Dev. Cell* **23**, 1255–1262 (2012).
149. Kirchhausen, T., Owen, D. & Harrison, S. C. Molecular structure, function, and dynamics of clathrin-mediated membrane traffic. *Cold Spring Harb. Perspect. Biol.* **6**, a016725 (2014).
150. Ungewickell, E. & Branton, D. Assembly units of clathrin coats. *Nature* **289**, 420–422 (1981).
151. Fotin, A. *et al.* Molecular model for a complete clathrin lattice from electron cryomicroscopy. *Nature* **432**, 573–579 (2004).
152. Wang, Y. J. *et al.* Phosphatidylinositol 4 phosphate regulates targeting of clathrin adaptor AP-1 complexes to the Golgi. *Cell* **114**, 299–310 (2003).

153. Ren, X., Farias, G. G., Canagarajah, B. J., Bonifacino, J. S. & Hurley, J. H. Structural Basis for Recruitment and Activation of the AP-1 Clathrin Adaptor Complex by Arf1. *Cell* **152**, 755–767 (2013).
154. Ohno, H. *et al.* Interaction of Tyrosine-Based Sorting Signals with Clathrin-Associated Proteins. *Science* **269**, 1872–1875 (1995).
155. Mattera, R., Farias, G. G., Mardones, G. A. & Bonifacino, J. S. Co-assembly of viral envelope glycoproteins regulates their polarized sorting in neurons. *PLoS Pathog.* **10**, e1004107 (2014).
156. Janvier, K. *et al.* Recognition of dileucine-based sorting signals from HIV-1 Nef and LIMP-II by the AP-1 gamma-sigma1 and AP-3 delta-sigma3 hemicomplexes. *J. Cell Biol.* **163**, 1281–1290 (2003).
157. Mattera, R., Boehm, M., Chaudhuri, R., Prabhu, Y. & Bonifacino, J. S. Conservation and diversification of dileucine signal recognition by adaptor protein (AP) complex variants. *J. Biol. Chem.* **286**, 2022–2030 (2011).
158. Nassour, J. *et al.* Autophagic cell death restricts chromosomal instability during replicative crisis. *Nature* **565**, 659–663 (2019).
159. Fischer, T. D., Wang, C., Padman, B. S., Lazarou, M. & Youle, R. J. STING induces LC3B lipidation onto single-membrane vesicles via the V-ATPase and ATG16L1-WD40 domain. *J. Cell Biol.* **219**, e202009128 (2020).
160. Van Herck, S., Feng, B. & Tang, L. Delivery of STING agonists for adjuvanting subunit vaccines. *Adv. Drug Deliv. Rev.* **179**, 114020 (2021).
161. Frémond, M.-L. & Crow, Y. J. STING-Mediated Lung Inflammation and Beyond. *J. Clin. Immunol.* **41**, 501–514 (2021).
162. Glück, S. *et al.* Innate immune sensing of cytosolic chromatin fragments through cGAS promotes senescence. *Nat. Cell Biol.* **19**, 1061–1070 (2017).
163. Sladitschek-Martens, H. L. *et al.* YAP/TAZ activity in stromal cells prevents ageing by controlling cGAS–STING. *Nature* **607**, 790–798 (2022).
164. Corrales, L. *et al.* Direct Activation of STING in the Tumor Microenvironment Leads to Potent and Systemic Tumor Regression and Immunity. *Cell Rep.* **11**, 1018–1030 (2015).
165. Harding, S. M. *et al.* Mitotic progression following DNA damage enables pattern recognition within micronuclei. *Nature* **548**, 466–470 (2017).
166. Sivick, K. E. *et al.* Magnitude of Therapeutic STING Activation Determines CD8+ T Cell-Mediated Anti-tumor Immunity. *Cell Rep.* **25**, 3074–3085.e5 (2018).
167. Pantelidou, C. *et al.* PARP Inhibitor Efficacy Depends on CD8+ T-cell Recruitment via Intratumoral STING Pathway Activation in BRCA-Deficient Models of Triple-Negative Breast Cancer. *Cancer Discov.* **9**, 722–737 (2019).
168. Hansen, A. L., Mukai, K., Schopfer, F. J., Taguchi, T. & Holm, C. K. STING palmitoylation as a therapeutic target. *Cell. Mol. Immunol.* **16**, 236–241 (2019).
169. Prestwick Chemical Library®: 1520 drugs mainly FDA-approved. *Prestwick Chemical Libraries* <https://www.prestwickchemical.com/screening-libraries/prestwick-chemical-library/>.
170. Peyroche, A. *et al.* Brefeldin A Acts to Stabilize an Abortive ARF–GDP–Sec7 Domain Protein Complex: Involvement of Specific Residues of the Sec7 Domain. *Mol. Cell* **3**, 275–285 (1999).
171. Boncompain, G. *et al.* Synchronization of secretory protein traffic in populations of cells. *Nat. Methods* **9**, 493–498 (2012).
172. Bowzard, J. B., Cheng, D., Peng, J. & Kahn, R. A. ELMOD2 is an Arl2 GTPase-activating protein that also acts on Arfs. *J. Biol. Chem.* **282**, 17568–17580 (2007).

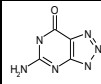
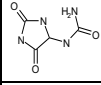
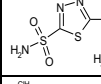
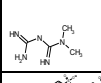
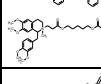
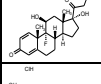
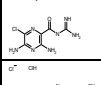
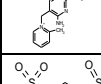
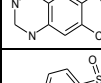
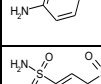
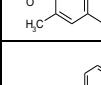
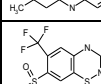
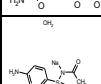
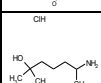
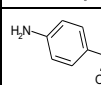
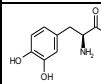
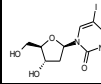
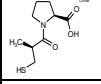
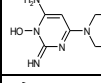
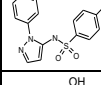
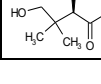

173. Pulkkinen, V. *et al.* ELMOD2, a candidate gene for idiopathic pulmonary fibrosis, regulates antiviral responses. *FASEB J. Off. Publ. Fed. Am. Soc. Exp. Biol.* **24**, 1167–1177 (2010).
174. Hodgson, U. *et al.* ELMOD2 is a candidate gene for familial idiopathic pulmonary fibrosis. *Am. J. Hum. Genet.* **79**, 149–154 (2006).
175. Darnell, J. E., Kerr, I. M. & Stark, G. R. Jak-STAT pathways and transcriptional activation in response to IFNs and other extracellular signaling proteins. *Science* **264**, 1415–1421 (1994).
176. Lu, D. *et al.* Activation of STING by targeting a pocket in the transmembrane domain. *Nature* **604**, 557–562 (2022).
177. Randazzo, P. A. & Hirsch, D. S. Arf GAPs: multifunctional proteins that regulate membrane traffic and actin remodelling. *Cell. Signal.* **16**, 401–413 (2004).
178. Thomas, L. L. & Fromme, J. C. Extensive GTPase crosstalk regulates Golgi trafficking and maturation. *Curr. Opin. Cell Biol.* **65**, 1–7 (2020).
179. Concordet, J.-P. & Haeussler, M. CRISPOR: intuitive guide selection for CRISPR/Cas9 genome editing experiments and screens. *Nucleic Acids Res.* **46**, W242–W245 (2018).
180. Ran, F. A. *et al.* Genome engineering using the CRISPR-Cas9 system. *Nat. Protoc.* **8**, 2281–2308 (2013).
181. QuickChange Primer Design. <https://www.agilent.com/store/primerDesignProgram.jsp>.
182. Allan, C. *et al.* OMEERO: flexible, model-driven data management for experimental biology. *Nat. Methods* **9**, 245–253 (2012).
183. Jeremiah, N. *et al.* Inherited STING-activating mutation underlies a familial inflammatory syndrome with lupus-like manifestations. *J. Clin. Invest.* **124**, 5516–5520 (2014).
184. McCauley, M. E. *et al.* C9orf72 in myeloid cells suppresses STING-induced inflammation. *Nature* **585**, 96–101 (2020).
185. Chu, T.-T. *et al.* Tonic prime-boost of STING signalling mediates Niemann–Pick disease type C. *Nature* **596**, 570–575 (2021).
186. Corrales, L., McWhirter, S. M., Dubensky, T. W. & Gajewski, T. F. The host STING pathway at the interface of cancer and immunity. *J. Clin. Invest.* **126**, 2404–2411 (2016).
187. Owen, D. J., Collins, B. M. & Evans, P. R. Adaptors for clathrin coats: structure and function. *Annu. Rev. Cell Dev. Biol.* **20**, 153–191 (2004).
188. Traub, L. M. & Bonifacino, J. S. Cargo recognition in clathrin-mediated endocytosis. *Cold Spring Harb. Perspect. Biol.* **5**, a016790 (2013).
189. Heldwein, E. E. *et al.* Crystal structure of the clathrin adaptor protein 1 core. *Proc. Natl. Acad. Sci.* **101**, 14108–14113 (2004).
190. Zizioli, D. *et al.* Early embryonic death of mice deficient in gamma-adaptin. *J. Biol. Chem.* **274**, 5385–5390 (1999).
191. Meyer, C. *et al.* μ 1A-adaptin-deficient mice: lethality, loss of AP-1 binding and rerouting of mannose 6-phosphate receptors. *EMBO J.* **19**, 2193–2203 (2000).
192. Doray, B., Lee, I., Knisely, J., Bu, G. & Kornfeld, S. The γ/σ 1 and α/σ 2 Hemicomplexes of Clathrin Adaptors AP-1 and AP-2 Harbor the Dileucine Recognition Site. *Mol. Biol. Cell* **18**, 1887–1896 (2007).
193. Chaudhuri, R., Lindwasser, O. W., Smith, W. J., Hurley, J. H. & Bonifacino, J. S. Downregulation of CD4 by human immunodeficiency virus type 1 Nef is dependent on clathrin and involves direct interaction of Nef with the AP2 clathrin adaptor. *J. Virol.* **81**, 3877–3890 (2007).
194. Konno, H. *et al.* Suppression of STING signaling through epigenetic silencing and missense mutation impedes DNA damage mediated cytokine production. *Oncogene* **37**, 2037–2051 (2018).

195. Morris, K. L. *et al.* HIV-1 Nefs Are Cargo-Sensitive AP-1 Trimerization Switches in Tetherin Downregulation. *Cell* **174**, 659-671.e14 (2018).
196. Jia, X. *et al.* Structural basis of HIV-1 Vpu-mediated BST2 antagonism via hijacking of the clathrin adaptor protein complex 1. *eLife* **3**, e02362 (2014).
197. Kelly, B. T. *et al.* A structural explanation for the binding of endocytic dileucine motifs by the AP2 complex. *Nature* **456**, 976–979 (2008).
198. Margolis, S. R. *et al.* The cyclic dinucleotide 2'3'-cGAMP induces a broad antibacterial and antiviral response in the sea anemone *Nematostella vectensis*. *Proc. Natl. Acad. Sci.* **118**, e2109022118 (2021).
199. Di Micco, A. *et al.* AIM2 inflammasome is activated by pharmacological disruption of nuclear envelope integrity. *Proc. Natl. Acad. Sci.* **113**, E4671–E4680 (2016).
200. Hirst, J. *et al.* Distinct and Overlapping Roles for AP-1 and GGAs Revealed by the “Knocksideways” System. *Curr. Biol.* **22**, 1711–1716 (2012).
201. Tan, Y. & Kagan, J. C. Innate Immune Signaling Organelles Display Natural and Programmable Signaling Flexibility. *Cell* **177**, 384-398.e11 (2019).
202. Sherr, C. J. Principles of Tumor Suppression. *Cell* **116**, 235–246 (2004).
203. Schnitzbauer, J., Strauss, M. T., Schlichthaerle, T., Schueder, F. & Jungmann, R. Super-resolution microscopy with DNA-PAINT. *Nat. Protoc.* **12**, 1198–1228 (2017).
204. Li, G. *et al.* NPC1-regulated dynamic of clathrin-coated pits is essential for viral entry. *Sci. China Life Sci.* **65**, 341–361 (2022).
205. Stirnimann, C. U., Petsalaki, E., Russell, R. B. & Müller, C. W. WD40 proteins propel cellular networks. *Trends Biochem. Sci.* **35**, 565–574 (2010).
206. Xu, H. *et al.* Innate immune sensing of bacterial modifications of Rho GTPases by the Pyrin inflammasome. *Nature* **513**, 237–241 (2014).
207. Próchnicki, T. & Latz, E. Inflammasomes on the Crossroads of Innate Immune Recognition and Metabolic Control. *Cell Metab.* **26**, 71–93 (2017).

Appendix

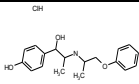
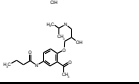
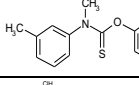
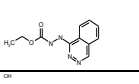
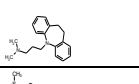
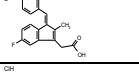
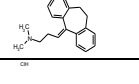
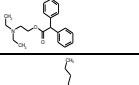
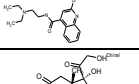
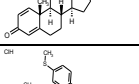
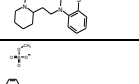
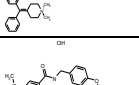
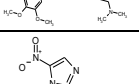
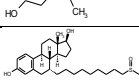
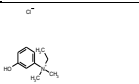
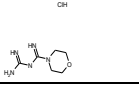
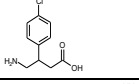
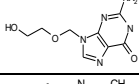
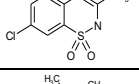
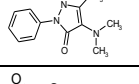
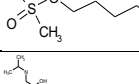
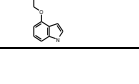

Documents appended are:

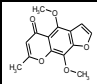
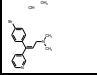
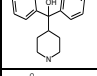
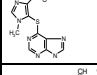
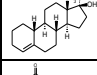
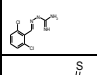
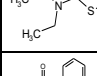
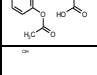
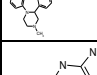
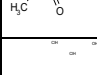
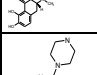
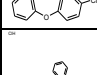
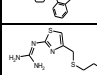
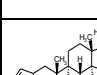
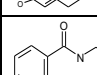
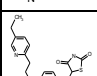
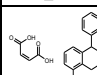
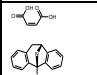
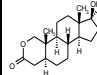
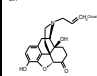
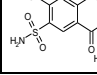

- The catalogue of the Prestwick chemical library listing all compounds (Prestwick identifier, name, CAS number, structural information) used in the chemical screening described in section 2.2 of this thesis;
- My required Curriculum Vitae.

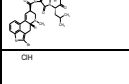
Prestw-number	Structure	Chemical name	CAS number	Mol weight structure	Smiles code	IUPAC name
Prestw-1		Azaguanine-8	134-58-7	152.12	<chem>c12/N=C(\NC(c1nn[nH]2)=O)/N</chem>	5-Amino-3H-[1,2,3]triazolo[4,5-d]pyrimidin-7-ol
Prestw-2		Allantoin	97-59-6	158.12	<chem>N1C(NC(C1=O)NC(=O)N)=O</chem>	(2,5-Dioxo-4-imidazolidinyl) urea
Prestw-3		Acetazolamide	59-66-5	222.25	<chem>c1(S(=O)(=O)N)sc(nn1)NC(=O)C</chem>	N-(5-sulfamoyl-1,3,4-thiadiazol-2-yl)acetamide
Prestw-4		Metformin hydrochloride	1115-70-4	165.63	<chem>C(NC(=N)N)(=N)N(C)C</chem>	1-carbamimidamido-N,N-dimethylmethanimidamide
Prestw-5		Atracurium besylate	64228-81-5	1243.51	<chem>[N+](C1C2C(Cc(c(c2)OC)OC)CC1)Cc1cc(c(cc1)OC)OC)(CCC(=O)O)CCCCOC(Cc1N+)(C1C2C(Cc(c(c2)OC)OC)OC)C1)Cc1cc(c(cc1)OC)OC)C(=O)C</chem>	2,2'-(1,5-Pentanediyloxybis[3-oxo-3,1-propanediyl])bis[1-(3,4-dimethoxybenzyl)-6,7-
Prestw-6		Isoflupredone acetate	338-98-7	420.48	<chem>[C@]12([C@@](C(COC(=O)C)=O)[C@]1([C@]1([C@@]([C@@]3(C=C/C(C=C3)=O)CC1)C)([C@H](C2)O)F)[H])[H])O)C</chem>	(11beta)-9-Fluoro-11,17-dihydroxy-3,20-dioxopregna-1,4-dien-21-yl acetate
Prestw-7		Amiloride hydrochloride dihydrate	17440-83-4	302.12	<chem>c1(nc(c(nc1N)N)Cl)C(NC(=N)N)=O</chem>	3,5-diamino-N-(aminoiminomethyl)-6-chloro-, monohydrochloride
Prestw-8		Amprolium hydrochloride	137-88-2	315.25	<chem>[n+](C1C2C(Cc(c(c2)CCC)N)C)C)cccc1</chem>	1-[(4-Amino-2-propyl-5-pyrimidinyl)methyl]-2-methylpyridinium chloride
Prestw-9		Hydrochlorothiazide	58-93-5	297.74	<chem>S1(c2cc(S(=O)(=O)N)c(cc2NCN1)Cl)(=O)=O</chem>	6-Chloro-3,4-dihydro-2H-1,2,4-benzothiazine-7-sulfonamide 1,1-dioxide, 6-Chloro-7-sulfamyl-3,4-dihydro-
Prestw-10		Sulfaguanidine	57-67-0	214.25	<chem>S(NC(=N)N)(c1ccc(N)cc1)(=O)=O</chem>	4-amino-N-[amino(imino)methyl]benzene sulfonamide
Prestw-11		Meticrane	1084-65-7	275.35	<chem>S1(c2cc(S(=O)(=O)N)c(cc2CCCC1)C(=O)=O</chem>	6-methylthiochromane-7-sulfonamide 1,1-dioxide
Prestw-12		Benzonatate	104-31-4	603.76	<chem>c1c(ccc1)C(OCCOC)=O)NCCCC</chem>	2,5,8,11,14,17,20,23,26-Nonaaoxaoctacosan-28-yl-p-(butylamino) benzoate
Prestw-13		Hydroflumethiazide	135-09-1	331.29	<chem>S1(c2cc(S(=O)(=O)N)c(C(F)F)cc2NCN1)(=O)=O</chem>	1,1-dioxo-6-(trifluoromethyl)-3,4-dihydro-2H-1S(6),2,4-benzothiaziazine-7-sulfonamide
Prestw-14		Sulfacetamide sodic hydrate	6209-17-2	254.24	<chem>S(N(C(=O)C)[Na])(c1ccc(N)cc1)(=O)=O</chem>	N-(p-Aminobenzenesulfonyl)acetamide
Prestw-15		Heptaminol hydrochloride	543-15-7	181.71	<chem>C(O)(CCCC(N)C)C</chem>	6-amino-2-methyl-2-heptanol hydrochloride
Prestw-16		Sulfathiazole	72-14-0	255.32	<chem>S(Nc1nccs1)(c1ccc(N)cc1)(=O)=O</chem>	4-amino-N-(1,3-thiazol-2-yl)benzene-1-sulfonamide
Prestw-17		Levodopa	59-92-7	197.19	<chem>C([C@H](Cc1cc(c(cc1)O)O)N)(=O)O</chem>	(S)-2-Amino-3-(3,4-dihydroxyphenyl)propanoic acid
Prestw-18		Idoxuridine	54-42-2	354.10	<chem>N1(C(NC(C=C1)I)=O)O[C@@H]1O[C@@H]([C@H](C1)O)CO</chem>	1-(2-Deoxy-beta-D-ribofuranosyl)-5-iodouracil
Prestw-19		Captopril	62571-86-2	217.29	<chem>N1(C([C@@H](CS)C)=O)[C@H](C(=O)O)CCC1</chem>	((2S)-1-[3-Mercapto-2-methylpropionyl]-L-proline)
Prestw-20		Minoxidil	38304-91-5	209.25	<chem>N=1/C(N/(C=C1C1N1CCCC1)/N)O)=N</chem>	6-(1-Piperidinyl)-2,4-pyrimidinediamine 3-oxide
Prestw-21		Sulfaphenazole	526-08-9	314.37	<chem>S(Nc1n(ncc1)c1cccc1)(c1ccc(N)cc1)(=O)=O</chem>	4-amino-N-(1-phenyl-1H-pyrazol-5-yl)benzene-1-sulfonamide
Prestw-22		Panthenol (D)	81-13-0	205.26	<chem>C([C@@H](C(CO)C)C)O(=O)NCCCCO</chem>	(R)-2,4-Dihydroxy-3,3-dimethylbutyric 3-hydroxypropylamide

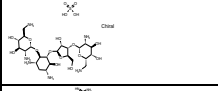
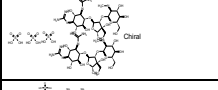
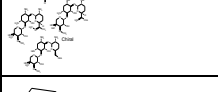
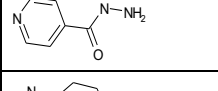
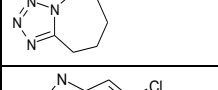
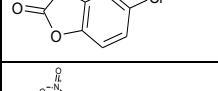
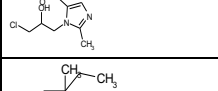
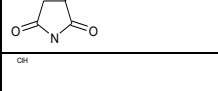
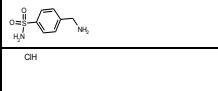
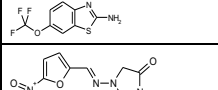
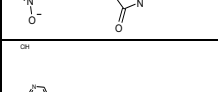
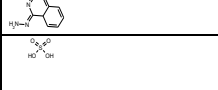
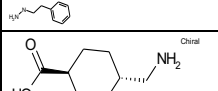
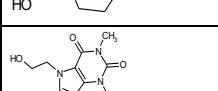
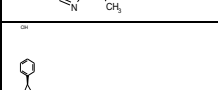
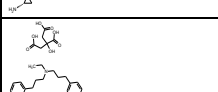
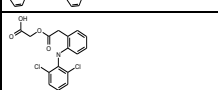
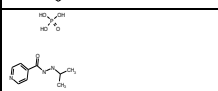
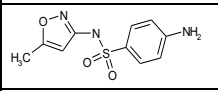
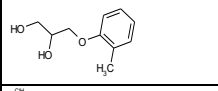
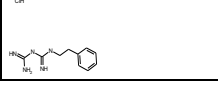

Prestw-23		Sulfadiazine	68-35-9	250.28	<chem>S(Nc1ncccn1)(c1ccc(N)cc1)(=O)=O</chem>	4-amino-N-(pyrimidin-2-yl)benzene-1-sulfonamide
Prestw-24		Norethynodrel	68-23-5	298.43	<chem>C=1\2/[C@@]3([C@]([C@]4[C@@]([C@]([C#C](CC4)O)(CC3)C)[H])(CC1C1CC(=O)CC2)[H])[H]</chem>	(8S,9S,13S,14S,17S)-17-ethynyl-17-hydroxy-13-methyl-1,2,4,6,7,8,9,11,12,14,15,16-dodecahydrocyclopenta[a]ph
Prestw-25		Thiamphenicol	15318-45-3	356.23	<chem>S(c1ccc([C@H]([C@H](NC(C(Cl)Cl)=O)CO)O)cc1)(=O)(=O)C</chem>	2,2-dichloro-N-[(1R,2R)-1,3-dihydroxy-1-(4-methanesulfonylphenyl)propan-2-yl]acetamide
Prestw-26		Cimetidine	51481-61-9	252.34	<chem>c1(nc[nH]c1C)CSCC/N=C(NC#N)/NC</chem>	(Z)-1-cyano-2-methyl-3-(2-[[5-methyl-1H-imidazol-4-yl)methyl]sulfanyl]ethyl)guanidine
Prestw-27		Doxylamine succinate	562-10-7	388.47	<chem>C(c1ncccc1)(c1cccc1)(OCCN(C)C)C</chem>	N,N-dimethyl-2-(1-phenyl-1-pyridin-2-ylethoxy)ethanamine butanedioate
Prestw-28		Ethambutol dihydrochloride	1070-11-7	277.24	<chem>N([C@@H](CO)CC)CCN[C@@H](CO)CC</chem>	(2R,2'R)-2,2'-(1,2-Ethanediyliimino)di(1-butanol) dihydrochloride
Prestw-29		Antipyrine	60-80-0	188.23	<chem>C1(N(N(C(=C1)C)C)c1cccc1)=O</chem>	1,5-dimethyl-2-phenylpyrazol-3-one
Prestw-30		Antipyrine, 4-hydroxy	1672-63-5	204.23	<chem>C1(\C(=C(N(N1c1cccc1)C)\C)O)=O</chem>	4-hydroxy-1,5-dimethyl-2-phenylpyrazol-3-one
Prestw-31		Chloramphenicol	56-75-7	323.13	<chem>[N+](c1ccc([C@H]([C@H](NC(C(Cl)Cl)=O)CO)O)cc1)([O-])=O</chem>	2,2-Dichloro-N-[(1R,2R)-1,3-dihydroxy-1-(4-nitrophenyl)-2-propanyl]acetamide
Prestw-32		Epirizole	18694-40-1	234.26	<chem>n1(c2nc(cc(n2)C)OC)c(cc(n1)C)OC</chem>	4-methoxy-2-(5-methoxy-3-methylpyrazol-1-yl)-6-methylpyrimidine
Prestw-33		Diprophylline	479-18-5	254.25	<chem>c12c(C(N(C(N1C)=O)C)=O)n(cn2)CC(O)CO</chem>	7-(2,3-dihydroxypropyl)-1,3-dimethyl-2,3,6,7-tetrahydro-1H-purine-2,6-dione
Prestw-34		Triamterene	396-01-0	253.27	<chem>c12c(nc(c(n1)N)c1cccc1)c(nc(n2)N)N</chem>	2,4,7-Triamino-6-phenylpteridine
Prestw-35		Dapsone	80-08-0	248.31	<chem>S(c1ccc(N)cc1)(c1ccc(N)cc1)(=O)=O</chem>	4-[(4-aminobenzene)sulfonyl]aniline
Prestw-36		Troleandomycin	2751-09-9	813.99	<chem>[C@@]12[C]([C@@H]([C@H]([C@H]([C@H]OC([C@@H]([C@H]([C@@H]([C@@H](O[C@H]3[C@@H]([C@H]([C@H](C[C@H](O3)C)N(C)C)OC(=O)C[C@H](C1)C)C)O[C@@H1O[C@H]([C@@H]([C@H]([C@H]([C@H]1OC)OC(=O)C)C)C)=O)</chem>	
Prestw-37		Pyrimethamine	58-14-0	248.72	<chem>n1c(c(c(nc1N)CC)c1ccc(cc1)Cl)N</chem>	5-(4-Chlorophenyl)-6-ethyl-2,4-pyrimidinediamine
Prestw-38		Hexamethonium dibromide dihydrate	55-97-0	398.22	<chem>[N+](CCCCC[N+](C)(C)C)(C)C</chem>	Hexane-1,6-bis[trimethylammonium bromide]
Prestw-39		Diflunisal	22494-42-4	250.20	<chem>c1(cc(c2c(cc(c2)F)F)ccc1O)C(=O)O</chem>	5-(2,4-difluorophenyl)-2-hydroxybenzoic acid
Prestw-40		Niclosamide	50-65-7	327.13	<chem>[N+](c1cc(c(NC(c2c(ccc(c2)Cl)O)=O)cc1)Cl)([O-])=O</chem>	5-chloro-N-(2-chloro-4-nitrophenyl)-2-hydroxybenzamide
Prestw-41		Procaine hydrochloride	51-05-8	272.78	<chem>C(c1ccc(N)cc1)(=O)OCCN(CC)CC</chem>	2-(Diethylamino)ethyl 4-aminobenzoate hydrochloride
Prestw-42		Moxisylyte hydrochloride	964-52-3	315.84	<chem>c1(cc(c(cc1OCCN(C)C)C)OC(=O)C)C(C)C</chem>	4-[2-(Dimethylamino)ethoxy]-5-isopropyl-2-methylphenyl acetate hydrochloride
Prestw-43		Betazole hydrochloride	138-92-1	184.07	<chem>n1[nH]ccc1CCN</chem>	2-(1H-Pyrazol-3-yl)ethanamine dihydrochloride
Prestw-44		Isoxicam	34552-84-6	335.34	<chem>S1(N(\C(=C(c2c1cccc2)/O)/C(Nc1noc(c1)C)=O)C(=O)=O)=O</chem>	4-Hydroxy-2-methyl-N-(5-methyl-3-isoxazolyl)-2H-1,2-benzothiazine-3-carboxamide 1,1-dioxide

Prestw-45		Naproxen	22204-53-1	230.27	<chem>c1(cc2c(cc(cc2)OC)cc1)C(C(=O)O)C</chem>	[S(+)-2-(6-Methoxy-2-naphthyl)propionic acid]
Prestw-46		Naphazoline hydrochloride	550-99-2	246.74	<chem>C1(=N/CCN1)Cc1c2c(ccc1)cccc2</chem>	2-(1,8a-Dihydro-1-naphthalenylmethyl)-4,5-dihydro-1H-imidazole hydrochloride
Prestw-47		Ticlopidine hydrochloride	53885-35-1	300.25	<chem>c12c(scc1)CCN(C2)Cc1c(Cl)cccc1</chem>	Hydrogen chloride - 5-(2-chlorobenzyl)-4,5,6,7-tetrahydrothieno[3,2-c]pyridine
Prestw-48		Dicyclimine hydrochloride	67-92-5	345.96	<chem>C1(C(=O)OCCN(CC)CC)(C2CCCC2)CCCC1</chem>	2-(Diethylamino)ethyl 1,1'-bi(cyclohexyl)-1-carboxylate hydrochloride
Prestw-49		Amyleine hydrochloride	532-59-2	271.79	<chem>C(OC(CN(C)C)(CC)C(=O)c1cccc1</chem>	1-(Dimethylamino)-2-methyl-2-butanyl benzoate hydrochloride
Prestw-50		Lidocaine hydrochloride	73-78-9	270.81	<chem>c1(NC(=O)CN(CC)CC)c(ccc1C)C</chem>	N-(2,6-Dimethylphenyl)-N2,N2-diethylglycinamide hydrochloride
Prestw-1795		Mupirocin	12650-69-0	500.64	<chem>CC(=CC(=O)OCCCCCCCC(=O)O)CC1OCC(C(C1O)O)CC1C(C(C(C)O)C)O1</chem>	9-[(E)-4-[(2S,3R,4R,5S)-5,4-dihydroxy-5-[[[(2S,3S)-3-[(2S,3S)-3-hydroxybutan-2-yl]oxycarbonyl]amino]butano-2-yl]oxy]butano-2-yl]oxy]nonanoic acid
Prestw-52		Carbamazepine	298-46-4	236.28	<chem>N1(C(=O)N)c2c(C=C/c3c1cccc3)cccc2</chem>	(5H-Dibenz[b,f]azepine-5-carboxamide)
Prestw-53		Triflupromazine hydrochloride	1098-60-8	388.89	<chem>N1(c2c(Sc3c1cccc3)ccc(C(F)(F)F)c2)CCCN(C)C</chem>	N,N-dimethyl-3-[2-(trifluoromethyl)phenothiazin-10-yl]propan-1-amine hydrochloride
Prestw-54		Mefenamic acid	61-68-7	241.29	<chem>c1(c(Nc2c(c(ccc2)C)C)cccc1)C(=O)O</chem>	2-(2,3-dimethylphenyl)aminobenzoic acid
Prestw-55		Acetohexamide	968-81-0	324.40	<chem>S(NC(NC1CCCC1)=O)(c1ccc(C(=O)C)cc1)C(=O)O</chem>	4-Acetyl-N-[(cyclohexylamino)carbonyl]benzenesulfonamide
Prestw-56		Sulpiride	15676-16-1	341.43	<chem>S(c1cc(C(NCC2N(CCC2)CC)=O)c(cc1)OC)C(=O)O)N</chem>	(±)-5-(aminosulfonyl)-N-[(1-ethylpyrrolidin-2-yl)methyl]-2-methoxybenzamide
Prestw-57		Benoxinate hydrochloride	5987-82-6	344.89	<chem>C(c1cc(c(cc1)N)OCCCC(=O)OCCN(CC)CC</chem>	2-(diethylamino)ethyl 4-amino-3-butoxybenzoate hydrochloride
Prestw-58		Oxethazaine	126-27-2	467.66	<chem>C(N(C(Cc1cccc1)C)C)C)CN(CC(N(C(Cc1cccc1)C)C)C)C(=O)CCO=O</chem>	2,2'-(2-hydroxyethylimino)bis[N-(1,1-dimethyl-2-phenylethyl)-N-methylacetamide]
Prestw-59		Pheniramine maleate	132-20-7	356.43	<chem>C(CCN(C)C)(c1ncccc1)c1cccc1</chem>	N,N-dimethyl-3-phenyl-3-pyridin-2-ylpropan-1-amine (Z)-but-2-enedioic acid
Prestw-60		Tolazoline hydrochloride	59-97-2	196.68	<chem>C1(=N/CCN1)Cc1cccc1</chem>	2-benzyl-4,5-dihydro-1H-imidazole hydrochloride
Prestw-61		Morantel tartrate	26155-31-7	370.43	<chem>C=1(N(CCC1N)C)C=C1c1c(ccs1)C</chem>	1-Methyl-2-[(E)-2-(3-methyl-2-thienyl)vinyl]-1,4,5,6-tetrahydropyrimidine 2,3-dihydroxysuccinate
Prestw-62		Homatropine hydrobromide (R,S)	51-56-9	356.26	<chem>N1([C@]2[C@H](OC(C3CCCC3)O)=O)C[C@@]1(CC2)[H])[H]C</chem>	[(1S,5R)-8-methyl-8-azabicyclo[3.2.1]octan-3-yl] 2-hydroxy-2-phenylacetate hydrobromide
Prestw-63		Nifedipine	21829-25-4	346.34	<chem>C=1(C(C(=C/N/C1)C)C)C(=O)OC)c1c([N+](=O)=O)cccc1)C(=O)OC</chem>	dimethyl 2,6-dimethyl-4-(2-nitrophenyl)-1,4-dihydropyridine-3,5-dicarboxylate
Prestw-64		Chlorpromazine hydrochloride	69-09-0	355.33	<chem>N1(c2c(Sc3c1cccc3)ccc(c2)Cl)CCCN(C)C</chem>	(2-Chloro-10[3-dimethylamino-propyl]phenothiazine)
Prestw-65		Diphenhydramine hydrochloride	147-24-0	291.82	<chem>C(c1cccc1)(c1cccc1)OCCN(C)C</chem>	(N-[2-Diphenylmethoxyethyl]-N,N-dimethylamine) hydrochloride
Prestw-66		Minaprine dihydrochloride	25953-17-7	371.31	<chem>n1nc(cc1NCCN1CCOCC1)C)c1cccc1</chem>	4-methyl-N-(2-morpholin-4-ylethyl)-6-phenylpyridazin-3-amine dihydrochloride
Prestw-67		Miconazole	22916-47-8	416.14	<chem>c1(c(cc(cc1)Cl)Cl)C(Cn1ncc1)OCc1c(cc(cc1)Cl)Cl</chem>	1-[2-(2,4-dichlorophenyl)-2-[(2,4-dichlorophenyl)methoxy]ethyl]imidazole

Prestw-68		Isoxsuprine hydrochloride	579-56-6	337.85	<chem>N(C(C(c1ccc(cc1)O)O)C)C(COc1ccccc1)C</chem>	4-[1-hydroxy-2-(1-phenoxypropan-2-ylamino)propyl]phenol hydrochloride
Prestw-69		Acebutolol hydrochloride	34381-68-5	372.90	<chem>c1(c(OCC(CNC(C)C)O)ccc(NC(=O)CCC)c1)C(=O)C</chem>	N-{3-Acetyl-4-[2-hydroxy-3-(isopropylamino)propoxy]phenyl}butanamide hydrochloride
Prestw-70		Tolnaftate	2398-96-1	307.42	<chem>C(N(c1cc(ccc1)C)C)(O(c1cc2c(cc1)cccc2)=S</chem>	O-naphthalen-2-yl N-methyl-N-(3-methylphenyl)carbamothioate
Prestw-71		Todralazine hydrochloride	3778-76-5	268.70	<chem>c1(nccc2c1cccc2)NNC(=O)OCC</chem>	ethyl N-(phthalazin-1-ylamino)carbamate hydrochloride
Prestw-72		Imipramine hydrochloride	113-52-0	316.88	<chem>N1(c2c(CCC3c1cccc3)cccc2)CCCN(C)C</chem>	3-(5,6-dihydrobenzo[b][1]benzazepin-11-yl)-N,N-dimethylpropan-1-amine hydrochloride
Prestw-73		Sulindac	38194-50-2	356.42	<chem>C1(\C=C(/c2c1ccc(c2)F)CC(=O)O)C)=C/c1ccc(S(=O)C)cc1</chem>	2-[(3Z)-6-fluoro-2-methyl-3-[(4-methylsulfinylphenyl)methylidene]inden-1-yl]acetic acid
Prestw-74		Amitriptyline hydrochloride	549-18-8	313.87	<chem>C1(\c2c(CCC3c1cccc3)cccc2)=C/CCN(C)C</chem>	3-(10,11-Dihydro-5H-dibenzo[a,d]cyclohepten-5-ylidene)-N,N-dimethyl-1-propanamine hydrochloride
Prestw-75		Adiphenine hydrochloride	50-42-0	347.89	<chem>C(C(c1ccccc1)c1cccc1)(=O)OCCN(CC)CC</chem>	2-(diethylamino)ethyl 2,2-diphenylacetate hydrochloride
Prestw-76		Dibucaine	85-79-0	343.47	<chem>c1(C(=O)NCCN(CC)CC)c2c(nc(c1)OCCCC)cccc2</chem>	2-butoxy-N-[2-(diethylamino)ethyl]quinoline-4-carboxamide
Prestw-77		Prednisone	53-03-2	358.44	<chem>[C@]12([C@@](C(=O)CO)(CC[C@]1([C@]1([C@@]([C@@]1)3(\C=C/C(\C=C3)=O)CC1)C)(C(C2)=O)[H])[H])O)C</chem>	(8S,9S,10R,13S,14S,17R)-17-hydroxy-17-(2-hydroxyacetyl)-10,13-dimethyl-6,7,8,9,12,14,15,16,10-[2-(1-methylpiperidin-2-yl)ethyl]-2-methylsulfonylphenothiazine hydrochloride
Prestw-78		Thioridazine hydrochloride	130-61-0	407.04	<chem>N1(c2c(Sc3c1cccc3)ccc(c2)SC)CCC1N(C)CCCC1</chem>	10-[2-(1-methylpiperidin-2-yl)ethyl]-2-methylsulfonylphenothiazine hydrochloride
Prestw-79		Diphepanil methylsulfate	62-97-5	389.52	<chem>[N+](CC/C=C(/c2ccccc2)c2cccc2)/CC1)(C)C</chem>	4-benzhydrylidene-1,1-dimethylpiperidin-1-ium methyl sulfate
Prestw-80		Trimethobenzamide hydrochloride	554-92-7	424.93	<chem>c1(cc(C(NC2ccc(cc2)OCCN(C)C)=O)cc1OC)OC)OC</chem>	N-[[4-[2-(dimethylamino)ethoxy]phenyl]methyl]-3,4,5-trimethoxybenzamide
Prestw-81		Metronidazole	443-48-1	171.16	<chem>c1(n(c(nc1)C)CCO)[N+](O)=O</chem>	2-(2-methyl-5-nitro-1H-imidazol-1-yl)ethan-1-ol
Prestw-1424		Fulvestrant	129453-61-8	606.79	<chem>[C@]12([C@](CC[C@]3([C@]1([C@@H](Cc1c3ccc(c1)O)CCCCCCCCS(=O)CCCC(C(F)(F)F)(F)F)[H])[H])([C@H](CC2)O)C)I)H</chem>	(7R,8R,9S,13S,14S,17S)-13-methyl-7-[9-(4,4,5,5,5-pentafluoropentyl)sulfinyl]non
Prestw-83		Edrophonium chloride	116-38-1	201.70	<chem>[N+](c1cc(O)ccc1)(CC)(C)C</chem>	ethyl-(3-hydroxyphenyl)-dimethylazanium chloride
Prestw-84		Moroxidine hydrochloride	3160-91-6	207.66	<chem>C(NC(=N)N)(N1CCOCC1)=N</chem>	N-(diaminomethylidene)morpholine-4-carboximidamide hydrochloride
Prestw-85		Baclofen (R,S)	1134-47-0	213.67	<chem>C(CC(c1ccc(cc1)Cl)CN)(=O)O</chem>	4-amino-3-(4-chlorophenyl)butanoic acid
Prestw-86		Acyclovir	59277-89-3	225.21	<chem>c1/2c(ncn1COCCO)C(N/C(=N2)/N)=O</chem>	2-amino-9-((2-hydroxyethoxy)methyl)-1H-purin-6(9H)-one
Prestw-87		Diazoxide	364-98-7	230.67	<chem>S1(N/C(=N)C2c1cc(cc2)Cl)/C(=O)=O</chem>	7-chloro-3-methyl-4H-1,2,4-benzothiadiazine 1,1-dioxide
Prestw-88		Amidopyrine	58-15-1	231.30	<chem>C1(\C=C(/N(N1c1cccc1)C)C)N(C)C)=O</chem>	4-Dimethylamino-1,5-dimethyl-2-phenylpyrazol-3-one
Prestw-1179		Busulfan	55-98-1	246.30	<chem>S(=O)(=O)(OCCCCOS(=O)(=O)C)C</chem>	4-methylsulfonyloxybutyl methanesulfonate
Prestw-90		Pindolol	13523-86-9	248.33	<chem>c12c([nH]cc1)cccc2OCC(CNC(C)C)O</chem>	(RS)-1-(1H-indol-4-yloxy)-3-(isopropylamino)propan-2-ol

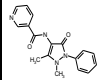
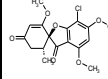
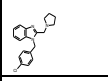
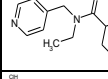
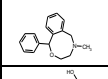
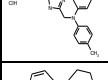
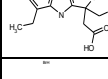
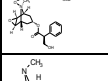
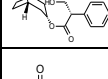
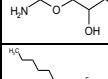
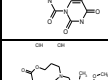
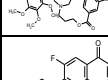
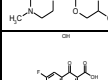
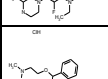
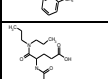
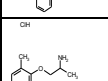
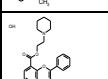
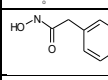
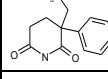
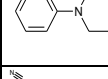
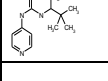
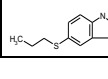

Prestw-91		Khellin	82-02-0	260.25	<chem>c12c(c(c3c(c1OC)cc3)OC)O1C(=C/C2=O)C</chem>	4,9-Dimethoxy-7-methylfuro[3,2-g]chromen-5-one
Prestw-92		Zimelidine dihydrochloride monohydrate	61129-30-4	408.17	<chem>C(=C1CN(C)C)(c1ccc(cc1)Br)/c1cnccc1</chem>	(Z)-3-(4-bromophenyl)-N,N-dimethyl-3-pyridin-3-ylprop-2-en-1-amine hydrate dihydrochloride
Prestw-93		Azacyclonol	115-46-8	267.37	<chem>C(c1cccc1)(c1cccc1)(C1CCNCC1)O</chem>	Diphenyl(piperidin-4-yl)methanol
Prestw-94		Azathioprine	446-86-6	277.27	<chem>c1(c(Sc2c3c([nH]cn3)ncn2)n(cn1)C)[N+](O)=O</chem>	6-[(1-methyl-4-nitro-1H-imidazol-5-yl)sulfanyl]-7H-purine
Prestw-95		Lynestrenol	52-76-6	284.45	<chem>[C@]12([C@]([C@]3([C@@]([C@@]4(C(C3)=C/CCC4)[H])(CC1)[H])([H])(CC[C@]2(C#C)O)[H])C</chem>	(8R,9S,10R,13S,14S,17R)-17-ethynyl-13-methyl-2,3,6,7,8,9,10,11,12,14,15,16-dodecahydro-1H-
Prestw-96		Guanabenz acetate	23256-50-0	291.14	<chem>c1(c(Cl)cccc1Cl)C=N/C(=N)N</chem>	1-(2,6-Dichlorobenzylideneamino)guanidine acetate
Prestw-97		Disulfiram	97-77-8	296.54	<chem>C(SSC(=S)N(CC)CC)(=S)N(CC)CC</chem>	N,N-diethyl[(diethylcarbamothioyl)disulfanyl]carbothioamide
Prestw-98		Acetylsalicylic acid	530-75-6	300.27	<chem>C(c1c(OC(=O)C)cccc1)(Oc1c(C(=O)O)cccc1)=O</chem>	2-(2-acetoxybenzoyl)oxybenzoic acid
Prestw-99		Mianserine hydrochloride	21535-47-7	300.83	<chem>N12C(c3c(Cc4c1cccc4)cccc3)CN(CC2)C</chem>	1,2,3,4,10,14b-Hexahydro-2-methyl-dibenzo[c,f]pyrazino[1,2-a]azepine hydrochloride
Prestw-100		Nocodazole	31430-18-9	301.33	<chem>c1(nc2c([nH]1)ccc(C(c1sc1)=O)c2)NC(=O)OC</chem>	Methyl (5-(2-thienylcarbonyl)-1H-benzimidazole-2-yl)-carbamate
Prestw-101		R(-) Apomorphine hydrochloride hemihydrate	41372-20-7	625.60	<chem>[C@@]12(c3c(c4c(C1)ccc(c4O)O)cccc3CCN2C)[H].[C@@]12(c3c(c4c(C1)ccc(c4O)O)cccc3CCN2C)[H]</chem>	(6aR)-6-Methyl-5,6,6a,7-tetrahydro-4H-dibenzo[de,g]quinoline-10,11-diol hydrochloride hydrate
Prestw-102		Amoxapine	14028-44-5	313.79	<chem>C1(=N)c2c(Oc3c1cc(cc3)Cl)cccc2)/N1CCNCC1</chem>	8-chloro-6-piperazin-1-ylbenzo[b][1,4]benzoxazepine
Prestw-103		Cyproheptadine hydrochloride	969-33-5	323.87	<chem>C1(/c2c(1C=C/c3c1cccc3)cccc2)=C1/CCN(CC1)C</chem>	4-(5H-dibenzo[a,d]cyclohepten-5-ylidene)-1-methylpiperidine hydrochloride
Prestw-104		Famotidine	76824-35-6	337.45	<chem>S(NC(=N)CCSCc1nc(N=C(N)N)sc1)(=O)(=O)N</chem>	3-[2-(diaminomethylideneamino)-1,3-thiazol-4-ylmethylsulfanyl]-N'-
Prestw-105		Danazol	17230-88-5	337.47	<chem>[C@]12(C=C/C3C1Cno3)CC[C@@]1([C@@]2(CC[C@]2([C@]1(CC[C@]2(C#C)O)[H])C)[H])C</chem>	(1S,2R,13R,14S,17R,18S)-17-ethynyl-2,18-dimethyl-7-oxa-6-azapentacyclo[11.7.0.0.0.2.10.
Prestw-106		Nicorandil	65141-46-0	211.18	<chem>[N+](O)=OCCNC(c1cnccc1)=O</chem>	2-[(pyridin-3-ylcarbonyl)amino]ethyl nitrate
Prestw-1314		Pioglitazone	111025-46-8	356.45	<chem>N1C(SC(C1=O)Cc1ccc(cc1)O)CCc1ncc(cc1)CC)=O</chem>	5-[[4-[2-(5-ethylpyridin-2-yl)ethoxy]phenyl]methyl]-1,3-thiazolidine-2,4-dione
Prestw-108		Nomifensine maleate	32795-47-4	354.41	<chem>c12c(C(CN(C1)C)c1cccc1)cccc2N</chem>	2-methyl-4-phenyl-3,4-dihydro-1H-isoquinolin-8-amine (Z)-but-2-enedioic acid
Prestw-109		Dizocilpine maleate	77086-22-7	337.38	<chem>[C@]12(N[C@@H]([C@]1c3c1cccc3)C)c2cccc1C</chem>	[5R,10S]-[+]-5-methyl-10,11-dihydro-5H-dibenzo[a,d]cyclohepten-5,10-imine maleate
Prestw-1192		Oxandrolone	53-39-4	306.45	<chem>[C@]12([C@@]3([C@]([C@]4([C@@]([C@]([C@]4(O)C)(CC3)C)[H])(CC[C@]1(C(CO2)=O)[H])([H])C</chem>	(1S,3aS,3bR,5aS,9aS,9bS,11aS)-1-hydroxy-1,9a,11a-trimethyl-2,3,3a,3b,4,5,5a,6,9,9b,10,1
Prestw-111		Naloxone hydrochloride	357-08-4	363.84	<chem>[C@]123[C@@]4([C@H](N(CC1)CC=C)C)c1c2c(O[C@H]3C(C4)=O)c(cc1)O)O</chem>	(4R,4aS,7aR,12bS)-4a,9-dihydroxy-3-prop-2-enyl-2,4,5,6,7a,13-hexahydro-1H-4,12-methanobenzofuro[3,2-
Prestw-112		Metolazone	17560-51-9	365.84	<chem>N1(C(c2c(NC1)cc(c(S(=O)(=O)N)c2)Cl)=O)c1c(C)cccc1</chem>	7-chloro-2-methyl-3-(2-methylphenyl)-4-oxo-1,2-dihydroquinazolin-6-sulfonamide

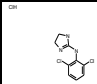
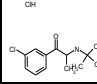
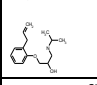
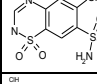
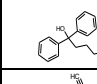
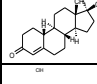
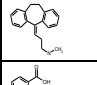
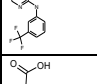
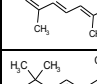
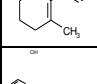
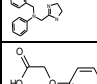
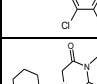
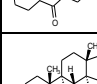
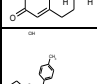
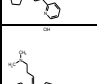
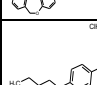
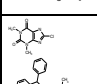
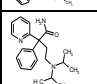
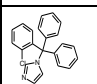
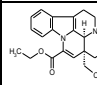
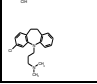

Prestw-113		Ciprofloxacin hydrochloride monohydrate	93107-08-5	385.83	<chem>C=1(C(c2c(N(C1)C1CC1)cc(c2)F)N1CCNCC1)=O)C(=O)O</chem>	1-cyclopropyl-6-fluoro-4-oxo-7-piperazin-1-ylquinoline-3-carboxylic acid hydrate hydrochloride
Prestw-114		Ampicillin trihydrate	7177-48-2	403.46	<chem>N12[C@@H]([C@@H](C1=O)NC([C@@H](c1cccc1)N)=O)SC([C@@H]2C(=O)O)C)C</chem>	(2S,5R,6R)-6-[(2R)-2-amino-2-phenylacetamido]-3,3-dimethyl-7-oxo-4-thia-1-azabicyclo[3.2.0]heptane-2-
Prestw-115		Haloperidol	52-86-8	375.87	<chem>C1(CCN(CC1)CCCC(c1ccc(cc1)F)=O)(c1ccc(cc1)Cl)O</chem>	4-[4-(4-chlorophenyl)-4-hydroxypiperidin-1-yl]-1-(4-fluorophenyl)butan-1-one
Prestw-116		Naltrexone hydrochloride dihydrate	16676-29-2	413.90	<chem>[C@]123[C@@]4([C@H](N(CC5CC5)CC1)Cc1c2c(O[C@@H]3C(CC4)=O)c(cc1)O)O</chem>	(4R,4aS,7aR,12bS)-3-(cyclopropylmethyl)-4a,9-dihydroxy-2,4,5,6,7a,13-hexahydro-1H-4,12-
Prestw-117		Chlorpheniramine maleate	113-92-8	390.87	<chem>C(CCN(C)C)(c1ccc(cc1)Cl)c1ncccc1</chem>	[3-(4-chlorophenyl)-3-(pyridin-2-yl)propyl]dimethylamine
Prestw-118		Nalbuphine hydrochloride	23277-43-2	393.91	<chem>[C@]123[C@@]4([C@H](N(CC1)CC1)CCCC1)Cc1c2c(O[C@@H]3[C@H](CC4)O)c(cc1)O)O</chem>	(4R,4aS,7S,7aR,12bS)-3-(cyclobutylmethyl)-1,2,4,5,6,7,7a,13-octahydro-4,12-methanobenzofuro[3,2-
Prestw-119		Picotamide monohydrate	80530-63-8	394.43	<chem>c1(C(NCc2cnccc2)=O)cc(C(NCc2cnccc2)=O)ccc1OC</chem>	4-methoxy-1-N,3-N-bis(pyridin-3-ylmethyl)benzene-1,3-dicarboxamide hydrate
Prestw-120		Triamcinolone	124-94-7	394.44	<chem>[C@]12([C@]([C@@H](C1C@]1([C@]1([C@@]([C@@]3(C=C/C(C=C3)=O)CC1)C)([C@H](C2)O)F)[H])H)O)(C(=O)CO)O)C</chem>	(8S,9R,10S,11S,13S,14S,16R,17S)-9-fluoro-11,16,17-trihydroxy-17-(2-hydroxyacetyl)-10,13-
Prestw-121		Bromocryptine mesylate	22260-51-1	750.72	<chem>N12[C@@]([O[C@]([C1=O)NC([C@@H]1C=C/3c4c5c(c[nH]c5ccc4)Br)C[C@]3(N(C1)C)[H])=O)C)C)([C@]1(N(C([C@@H]2CC(C)C)=O)CCC1)[H])O</chem>	(5'a)-2-Bromo-12'-hydroxy-2'-(1-methylethyl)-5'-(2-methylpropyl)ergotaman-3',6',18-trione mesylate
Prestw-1471		Amfepramone hydrochloride	90-84-6	241.76	<chem>C(C(N(CC)C)C)(=O)c1cccc1</chem>	2-(diethylamino)-1-phenylpropan-1-one
Prestw-123		Dehydrocholic acid	81-23-2	402.54	<chem>[C@]12([C@]([C@]3([C@@]([C@@]4([C@]([CC3=O)C(=O)CC4)[H])C)(C(=O)[H])H)CC[C@@H]2[C@@H](CCC(=O)O)C)[H]C</chem>	(4R)-4-[(5S,8R,9S,10S,13R,14S,17R)-10,13-dimethyl-3,7,12-trioxo-
Prestw-1184		Tioconazole	65899-73-2	387.72	<chem>c1(c(scc1)Cl)COC(c1c(cc(cc1)Cl)Cl)Cn1cncc1</chem>	1-[2-[(2-chlorothiophen-3-yl)methoxy]-2-(2,4-dichlorophenyl)ethyl]imidazole
Prestw-125		Perphenazine	58-39-9	403.98	<chem>N1(c2c(Sc3c1cccc3)ccc(c2)Cl)CCCN1CCN(CC1)CCO</chem>	2-[4-[3-(2-chloro-10H-phenothiazin-10-yl)propyl]piperazin-1-yl]ethanol
Prestw-126		Mefloquine hydrochloride	51773-92-3	414.78	<chem>c12nc(C(F)(F)F)cc(c1cccc2C(F)(F)F)C1NCCCC1O</chem>	(S)-[2,8-bis(trifluoromethyl)quinolin-4-yl]-[(2R)-piperidin-2-yl]methanol hydrochloride
Prestw-127		Isoconazole	27523-40-6	416.14	<chem>c1(COC(c2c(cc(cc2)Cl)Cl)Cn2cncc2)c(Cl)cccc1Cl</chem>	1-[2-(2,4-dichlorophenyl)-2-[(2,6-dichlorophenyl)methoxy]ethyl]imidazole
Prestw-128		Spironolactone	52-01-7	416.58	<chem>[C@]12(C=C/C(=O)CC1)C[C@H]([C@@]1([C@@]2[C@@]2([C@]1(C[C@]21)CC[C@]21OC(=O)CC1)[H])C)[H])S(=O)C</chem>	S-[(7R,8R,9S,10R,13S,14S,17R)-10,13-dimethyl-3,5'-dioxospiro[2.6,7,8,9,11,12,11'-[2-(4-methylpiperazin-1-yl)acetyl]-5H-pyrido[2,3-b][1,4]benzodiazepin-6-one dihydrochloride
Prestw-129		Pirenzepine dihydrochloride	29868-97-1	424.33	<chem>N1(c2c(C(Nc3c1nccc3)=O)cccc2)C(CN1CCN(CC1)C)=O</chem>	(S)-[2,8-bis(trifluoromethyl)quinolin-4-yl]-[(2R)-piperidin-2-yl]methanol hydrochloride
Prestw-130		Dexamethasone acetate	1177-87-3	434.51	<chem>[C@]12([C@]([C@]3([C@@]([C@@]4([C@]([C=C/C(C=C4)=O)CC3)C)([C@H](C1)O)F)[H])C)[C@H]([C@@]2[C@@]2([C@]1(C[C@]21)CC[C@]21OC(=O)CC1)[H])C</chem>	[(8S,9R,10S,11S,13S,14S,16R,17R)-9-fluoro-11,17-dihydroxy-10,13,16-trimethyl-
Prestw-131		Glipizide	29094-61-9	445.54	<chem>S(NC(NC1CCCC1)=O)(c1ccc(cc1)CCNC(c1ncc(nc1)C)=O)=O</chem>	N-[2-[4-(cyclohexylcarbamoylsulfamoyl)phenyl]ethyl]-5-methylpyrazine-2-
Prestw-132		Loxapine succinate	27833-64-3	445.91	<chem>C1(=Nc2c(Oc3c1cc(cc3)Cl)cccc2)/N1CCN(CC1)C</chem>	8-chloro-6-(4-methylpiperazin-1-yl)benzo[b][1,4]benzoxazine butanedioic acid
Prestw-133		Hydroxyzine dihydrochloride	2192-20-3	447.84	<chem>N1(C(c2ccc(cc2)Cl)c2cccc2)CCN(CC1)CCOCCO</chem>	2-[2-[4-[(4-chlorophenyl)phenylmethyl]piperazin-1-yl]ethoxy]ethanol dihydrochloride
Prestw-134		Diltiazem hydrochloride	33286-22-5	450.99	<chem>[C@@H]1(C(N(c2c(S[C@H]1c1ccc(cc1)OC)cccc2)CCN(C)C)=O)OC(=O)C</chem>	[(2S,3S)-5-[2-(dimethylamino)ethyl]-2-(4-methoxyphenyl)-4-oxo-2,3-dihydro-1,5-benzothiazepin-3-

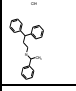
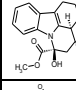
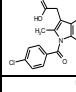
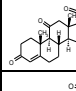
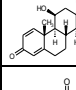
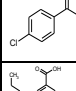
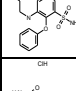
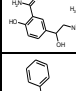
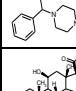
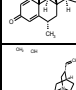
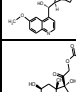
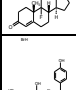
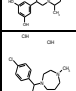
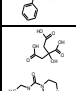
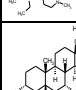
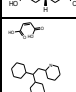
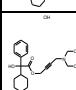
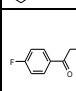
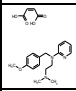
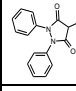
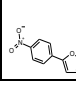

Prestw-158		Neomycin sulfate	1405-10-3	712.73	<chem>[C@@H]1([C@H](O[C@@H]2[C@@H]([C@H]([C@@H]([C@H](O2)CN)O)O)N)[C@H](C[C@H]([C@@H]1O)N)N)O[C@H]1[C@@H]([C@H](O[C@@H]2[C@@H]([C@H]([C@@H]([C@H]([C@@H]([C@H](O2)CN)O)O)N)[C@H](O1)CO)O</chem>	
Prestw-159		Dihydrostreptomycin sulfate	5490-27-7	1461.43	<chem>N(C1C(OC(C1O)O)CO)OC2C(OC(C2O)CO)C)OC3C(C(C(C3O)O)NC(=N)N)O)NC(=N)N)C</chem>	1,1'-[(1R,2R,3S,4R,5R,6S)-4-((5-Deoxy-2-O-[2-deoxy-2-(methylamino)-alpha-L-glucopyranosyl]-3-C-
Prestw-160		Gentamicine sulfate	1405-41-0	1488.81	<chem>N(C1C(COC(C1O)OC2C(CC(C(C2O)OC3OC(CCC3N)C)NC)N)N)O)C)C</chem>	2-[[4,6-diamino-3-((3-amino-6-[1-(methylamino)ethyl]oxan-2-yl)oxy)-2-hydroxycyclohexyl]oxy]-5-
Prestw-161		Isoniazid	54-85-3	137.14	<chem>C(=O)c1ccncc1)NN</chem>	pyridine-4-carbohydrazide
Prestw-162		Pentylenetetrazole	54-95-5	138.17	<chem>n1nn2c(n1)CCCC2</chem>	6,7,8,9-Tetrahydro-5H-tetrazolo[1,5-a]azepine
Prestw-163		Chlorzoxazone	95-25-0	169.57	<chem>C1(Nc2c(O1)ccc(c2)Cl)=O</chem>	(5-Chloro-2-hydroxybenzoxazole)
Prestw-164		Omidazole	16773-42-5	219.63	<chem>c1(n(c(nc1)C)CO)C(Cl)[N+](=[O-])=O</chem>	1-(3-Chloro-2-hydroxypropyl)-2-methyl-5-nitroimidazole
Prestw-165		Ethosuximide	77-67-8	141.17	<chem>N1C(C(CC1=O)(CC)C)=O</chem>	2-Ethyl-2-methylsuccinimide
Prestw-166		Mafenide hydrochloride	138-37-4	222.69	<chem>S(c1ccc(cc1)CN)(=O)(=O)N</chem>	4-(Aminomethyl)benzenesulfonamide hydrochloride
Prestw-167		Riluzole hydrochloride	not available	270.66	<chem>c1(nc2c(s1)cc(OC(F)(F)F)cc2)N</chem>	2-Amino-6-trifluoromethoxybenzothiazole
Prestw-168		Nitrofurantoin	67-20-9	238.16	<chem>C1(NC(CN1/N=C/c1oc([N+](=[O-])=O)cc1)=O)=O</chem>	1-[(Z)-{(5-nitrofurane-2-yl)methylidene}amino]imidazolidine-2,4-dione
Prestw-169		Hydralazine hydrochloride	304-20-1	196.64	<chem>C1(\N=N/C=C/2\1C=C/C=C2)=N\N</chem>	phthalazin-1-ylhydrazine hydrochloride
Prestw-170		Phenelzine sulfate	156-51-4	234.28	<chem>N(N)CCc1ccccc1</chem>	2-phenylethylhydrazine sulfuric acid
Prestw-171		Tranexamic acid	1197-18-8	157.21	<chem>C([C@H]1CC[C@@H](CC1)CN)(=O)O</chem>	4-(aminomethyl)cyclohexane-1-carboxylic acid
Prestw-172		Etofylline	519-37-9	224.22	<chem>c12c(C(N(C(N1)=O)C)=O)n(cn2)CCO</chem>	1,3-Dimethyl-7-(BETA-hydroxyethyl-xanthine
Prestw-173		Tranlycypromine hydrochloride	1986-47-6	169.66	<chem>[C@@H]1(C[C@@H]1N)c1ccccc1</chem>	2-phenylcyclopropan-1-amine hydrochloride
Prestw-174		Alverine citrate salt	5560-59-8	473.57	<chem>N(CCCc1ccccc1)(CCc1ccccc1)CC</chem>	N-ethyl-3-phenyl-N-(3-phenylpropyl)propan-1-amine 2-hydroxypropane-1,2,3-tricarboxylic acid
Prestw-175		Aceclofenac	89796-99-6	354.19	<chem>N(c1c(Cl)cccc1Cl)c1c(CC(=O)OCC(=O)O)cccc1</chem>	2-[2-[2-(2,6-dichloroanilino)phenyl]acetyl]oxyacetic acid
Prestw-176		Iproniazide phosphate	305-33-9	277.22	<chem>C(NNC(C)C)(=O)c1ccncc1</chem>	N'-propan-2-ylpyridine-4-carbohydrazide phosphoric acid
Prestw-177		Sulfamethoxazole	723-46-6	253.28	<chem>S(Nc1noc(c1)C)(c1ccc(N)cc1)(=O)=O</chem>	4-Amino-N-(5-methyl-1,2-oxazol-3-yl)benzenesulfonamide
Prestw-178		Mephesisin	59-47-2	182.22	<chem>O(c1c(C)cccc1)CC(O)CO</chem>	3-(2-methylphenoxy)propane-1,2-diol
Prestw-179		Phenformin hydrochloride	834-28-6	241.73	<chem>N(C(=N)NCCc1ccccc1)C(=N)N</chem>	1-(diaminomethylidene)-2-(2-phenylethyl)guanidine hydrochloride

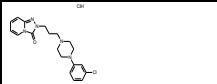
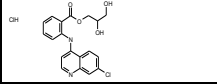


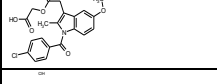

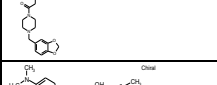
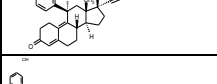

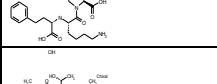
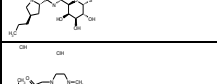
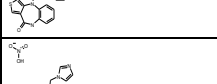
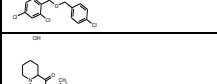
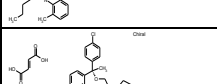
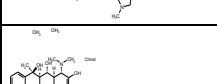
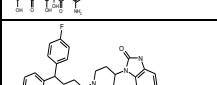
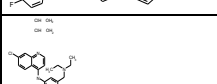
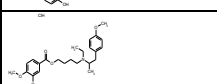
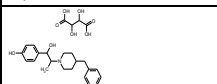
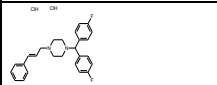
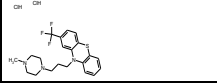

Prestw-180		Flutamide	13311-84-7	276.22	<chem>c1(C(F)(F)F)c([N+](O)=O)ccc(NC(=O)C(C)C)c1</chem>	2-methyl-N-[4-nitro-3-(trifluoromethyl)phenyl]propanamide
Prestw-181		Ampyrone	83-07-8	203.25	<chem>C1(C=C/N(N1c1ccccc1)C)C)N=O</chem>	4-Amino-1,5-dimethyl-2-phenyl-1,2-dihydro-3H-pyrazol-3-one
Prestw-182		Levamisole hydrochloride	16595-80-5	240.76	<chem>C/12=N/[C@H](CN1CCS2)c1ccccc1</chem>	(6S)-6-phenyl-2,3,5,6-tetrahydroimidazo[2,1-b][1,3]thiazole hydrochloride
Prestw-183		Pargyline hydrochloride	306-07-0	195.69	<chem>C(#C)CN(Cc1ccccc1)C</chem>	N-benzyl-N-methylprop-2-yn-1-amine hydrochloride
Prestw-184		Methocarbamol	532-03-6	241.25	<chem>C(=O)OCC(COc1c(OC)cccc1)O)N</chem>	[2-hydroxy-3-(2-methoxyphenoxy)propyl] carbamate
Prestw-185		Aztreonam	78110-38-0	435.44	<chem>N1(C[C@H]([C@@H]1C)NC(/C/c1nc(sc1)N)=N)OC(C(=O)O)(C)C)=O)S(=O)(=O)O</chem>	(2S,3S)-3-[(2Z)-2-(2-azaniumyl-1,3-thiazol-4-yl)-2-[(1-carboxy-1-methylethoxy)imino]acetamidate]-3,3-dimethyl-6-[[3-(2-chlorophenyl)-5-methyl-3-phenyl-4-isoxazolyl]carbonyl]amino]-7-oxo-4-thia-
Prestw-186		Cloxacillin sodium salt	642-78-4	457.87	<chem>N12[C@@]([C@@H](C1=O)NC(c1c(noc1C)c1c(Cl)cccc1)=O)(SC([C@@H]2C(O)=O)(C)C)[H]</chem>	[2S (2a, 5a, 6b)]-3,3-Dimethyl-6-[[3-(2-chlorophenyl)-5-methyl-3-phenyl-4-isoxazolyl]carbonyl]amino]-7-oxo-4-thia-
Prestw-187		Catharanthine	2468-21-5	336.44	<chem>[C@]12(c3c4c([nH]3)cccc4)CC[N@]3[C@@]1(C=C/[C@@](C2)(C3)[H])CC)[H]C(=O)OC</chem>	Methyl (2alpha,5beta,6alpha)-3,4-didehydrobogamine-18beta-carboxylate
Prestw-188		Pentolinium bitartrate	52-62-0	538.60	<chem>[N+]1(CCCCC[N+]2(C)CCCC2)C)CCCC1</chem>	1-methyl-1-[5-(1-methylpyrrolidin-1-ium-1-yl)pentyl]pyrrolidin-1-ium
Prestw-189		Aminopurine, 6-benzyl	1214-39-7	225.25	<chem>c12c(nc[nH]1)ncn2Nc1ccccc1</chem>	N-benzyl-7H-purin-6-amine
Prestw-190		Tolbutamide	64-77-7	270.35	<chem>S(NC(=O)NCCCC)(c1ccc(cc1)C(=O)=O</chem>	1-butyl-3-(4-methylphenyl)sulfonylurea
Prestw-191		Midodrine hydrochloride	3092-17-9	290.75	<chem>c1(c(ccc(c1)OC)OC)C(CNC(=O)CN)O</chem>	2-amino-N-[2-(2,5-dimethoxyphenyl)-2-hydroxyethyl]acetamide hydrochloride
Prestw-192		Thalidomide	50-35-1	258.24	<chem>N1(C(c2c(C1=O)cccc2)=O)C1C(NC(=O)CC1)=O</chem>	(RS)-2-(2,6-dioxopiperidin-3-yl)isoindole-1,3-dione
Prestw-193		Oxolinic acid	14698-29-4	261.24	<chem>C=1(C(c2c(N(C1)CC)cc1c(c2)OCO1)=O)C(=O)O</chem>	5,8-Dihydro-5-ethyl-8-oxo-1,3-dioxolo[4,5-g]quinoline-7-carboxylic acid
Prestw-194		Nimesulide	51803-78-2	308.31	<chem>S(Nc1c(cc([N+](O-)=O)cc1)Oc1ccccc1)(=O)=O)C</chem>	N-(4-nitro-2-phenoxyphenyl)methanesulfonamide
Prestw-1231		Asenapine maleate	85650-56-2	401.85	<chem>[C@]12([C@](c3c(Oc4c1cc(cc4)Cl)cccc3)(CN(C2)C)[H])[H]</chem>	(3aRS,12bRS)-5-Chloro-2,3,3a,12b-tetrahydro-2-methyl-1H-dibenz[2,3:6,7]oxepino[4,5-
Prestw-196		Pentoxifylline	6493-05-6	278.31	<chem>c12c(C(N(C(N1)C=O)CCCC(=O)C)=O)n(cn2)C</chem>	3,7-dimethyl-1-(5-oxohexyl)purine-2,6-dione
Prestw-197		Metaraminol bitartrate	33402-03-8	467.39	<chem>c1([C@H]([C@@H](N)C)O)cc(O)ccc1</chem>	3-[(1R,2S)-2-amino-1-hydroxypropyl]phenol (2R,3R)-2,3-dihydroxybutanedioic acid
Prestw-198		Salbutamol	18559-94-9	239.32	<chem>c1(cc(ccc1O)C(CNC(C)C)O)CO</chem>	4-[2-(tert-butylamino)-1-hydroxyethyl]-2-(hydroxymethyl)phenol
Prestw-199		Prilocaine hydrochloride	1786-81-8	256.78	<chem>C(Nc1c(C)cccc1)(=O)C(NCCC)C</chem>	N-(2-methylphenyl)-2-(propylamino)propanamide hydrochloride
Prestw-200		Camptothecin (S,+)	7689-03-4	348.36	<chem>N12C(c3c(C1)cc1c(n3)cccc1)=C/C1=C(C2=O)/COC([C@]1(O)CC)=O</chem>	(S)-4-ethyl-4-hydroxy-1H-pyrano[3',4':6,7]indolizino[1,2-b]quinoline-3,14-(4H,12H)-dione
Prestw-201		Ranitidine hydrochloride	66357-59-3	350.87	<chem>[N+](/C=C/N(C)NCCSCc1oc(cc1)CN(C)C)([O-])=O</chem>	(E)-1-N'-[2-[[5-[[dimethylamino)methyl]furan-2-yl]methylsulfanyl]ethyl]-1-N-methyl-2-nitroethene-1,1-


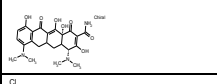
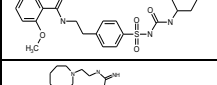
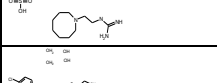
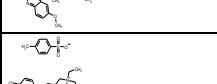
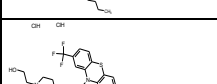
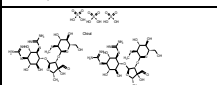
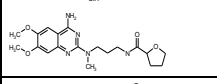
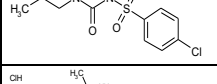
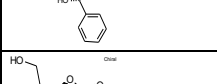
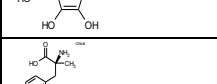
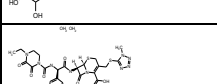
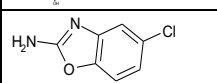

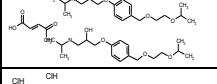
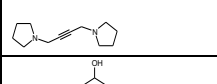
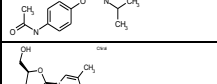
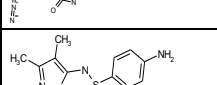
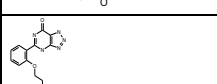



Prestw-202		Tiratricol, 3,3',5-triiodothyroacetic acid	51-24-1	621.94	<chem>c1(cc(cc1)CC(=O)O)O)c1cc(cc1)O</chem>	2-[4-(4-hydroxy-3-iodophenoxy)-3,5-diiodophenyl]acetic acid
Prestw-203		Flufenamic acid	530-78-9	281.24	<chem>C(c1cc(Nc2c(C(=O)O)cccc2)ccc1)(F)(F)F</chem>	2-[3-(trifluoromethyl)aniino]benzoic acid
Prestw-204		Flumequine	42835-25-6	261.26	<chem>C1(=C1N2c3c(C(=O)O)cc(cc3CCC2)F)/C(=O)O</chem>	9-Fluoro-5-methyl-1-oxo-6,7-dihydro-1H,5H-pyrido[3,2,1-ij]quinoline-2-carboxylic acid
Prestw-205		Tolfenamic acid	13710-19-5	261.71	<chem>c1(c(Nc2c(c(Cl)ccc2)C)cccc1)C(=O)O</chem>	2-[(3-Chloro-2-methylphenyl)amino]benzoic acid
Prestw-206		Meclofenamic acid sodium salt monohydrate	6385-02-0	336.15	<chem>c1(Nc2c(C([O-])=O)cccc2)c(c(ccc1Cl)C)Cl</chem>	2-[(2,6-Dichloro-3-methylphenyl)amino]benzoic acid sodium salt
Prestw-1181		Tibolone	5630-53-5	312.46	<chem>C1/12=C/C[C@H]([C@]3([C@]4([C@@]([C@](#C)(CC4)O)CC[C@]13[H])C)[H])C)CC(=O)CC2</chem>	(7R,8R,9S,13S,14S,17R)-17-ethynyl-17-hydroxy-7,13-dimethyl-1,2,4,6,7,8,9,11,12,14,15,16-
Prestw-208		Trimethoprim	738-70-5	290.32	<chem>n1c(c(Cc2cc(c(c2)OC)OC)C)nc1N)N</chem>	5-[(3,4,5-trimethoxyphenyl)methyl]pyrimidine-2,4-diamine
Prestw-209		Metoclopramide monohydrochloride	7232-21-5	336.26	<chem>c1(cc(c(c1)Cl)N)OC(C(=O)NCCN(CC)CC</chem>	4-amino-5-chloro-N-[2-(diethylamino)ethyl]-2-methoxybenzamide
Prestw-210		Fenbendazole	43210-67-9	299.35	<chem>c1(nc2c([nH]1)ccc(c2)Sc1cccc1)NC(=O)OC</chem>	Methyl 5-phenylthio-1H-benzimidazol-2-ylcarbamate
Prestw-211		Piroxicam	36322-90-4	331.35	<chem>S1(N(C=C(/c2c1cccc2)O))C(Nc1ncccc1=O)C(=O)=O</chem>	4-Hydroxy-2-methyl-N-(2-pyridinyl)-2H-1,2-benzothiazine-3-carboxamide 1,1-dioxide
Prestw-212		Pyrantel tartrate	33401-94-4	356.40	<chem>C=1(N(CCC/N1)C)C=C/c1sccc1</chem>	Dihydroxysuccinic acid-1-methyl-2-[(E)-2-(2-thienyl)vinyl]-1,4,5,6-
Prestw-213		Fenspiride hydrochloride	5053-08-7	296.80	<chem>C1(OC2(CCN(CC2)CCc2cccc2)CN1)=O</chem>	8-(2-Phenylethyl)-1-oxa-3,8-diazaspiro[4.5]decan-2-one
Prestw-214		Gemfibrozil	25812-30-0	250.34	<chem>C(C(CCCOc1c(ccc(c1)C)C)(C)C(=O)O</chem>	5-(2,5-dimethylphenoxy)-2,2-dimethylpentanoic acid
Prestw-215		Mefexamide hydrochloride	3413-64-7	316.83	<chem>C(=O)(NCCN(CC)CC)COc1ccc(cc1)OC</chem>	p-Methoxyphenoxyacetic acid 2-(diethylamino)ethylamide
Prestw-216		Tiapride hydrochloride	51012-33-0	364.89	<chem>S(c1cc(C(=O)NCCN(CC)CC)c(cc1)OC(=O)(=O)C</chem>	N-[2-(diethylamino)ethyl]-2-methoxy-5-methylsulfonylbenzamide hydrochloride
Prestw-217		Mebendazole	31431-39-7	295.30	<chem>c1(nc2c([nH]1)ccc(C(=O)c1cccc1)c2)NC(=O)OC</chem>	methyl N-(6-benzoyl-1H-benzimidazol-2-yl)carbamate
Prestw-218		Fenbufen	36330-85-5	254.29	<chem>C(c1ccc(cc1)c1cccc1)(=O)CCC(=O)O</chem>	4-oxo-4-(4-phenylphenyl)butanoic acid
Prestw-219		Ketoprofen	22071-15-4	254.29	<chem>C(c1cc(C(C(=O)O)C)ccc1)(=O)c1cccc1</chem>	2-(3-benzoylphenyl)propanoic acid
Prestw-220		Indapamide	26807-65-8	365.84	<chem>S(c1cc(C(NN2c3c(CC2C)cccc3)=O)ccc1Cl)(=O)(=O)N</chem>	4-chloro-N-(2-methyl-2,3-dihydroindol-1-yl)-3-sulfamoylbenzamide
Prestw-221		Norfloxacin	70458-96-7	319.34	<chem>C=1(C(c2c(N(/C1)CC)cc(c2)F)N1CCNCC1)=O)/C(=O)O</chem>	1-ethyl-6-fluoro-4-oxo-7-(piperazin-1-yl)-4,4-dihydroquinoline-3-carboxylic acid
Prestw-222		Antimycin A	1397-94-0	548.64	<chem>C1(C(O[C@H]([C@@H]([C@H](C(O[C@@H]1)C)=O)CC(CCC)OC(=O)CC(C)C)C(=O)NC(c1c(c(NC(=O)[H])ccc1)O)=O</chem>	3-methylbutanoate de (2R,6S,7R,8R)-3-[(3-formamido-2-hydroxybenzoyl)amino]-8-
Prestw-223		Xylometazoline hydrochloride	1218-35-5	280.84	<chem>c1(c(cc(cc1)C)C(C)C)C1=NCN1</chem>	2-[(4-tert-butyl-2,6-dimethylphenyl)methyl]-4,5-dihydro-1H-imidazole hydrochloride
Prestw-224		Oxymetazoline hydrochloride	2315-02-8	296.84	<chem>c1(c(c(c(c1)C)C/C1=N/CCN1)O)C(C)C</chem>	6-tert-butyl-3-(4,5-dihydro-1H-imidazol-2-ylmethyl)-2,4-dimethylphenol hydrochloride

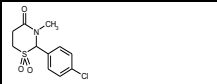
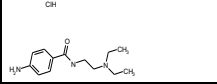
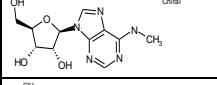
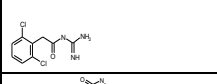
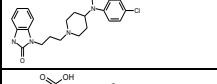
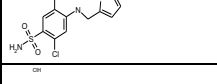
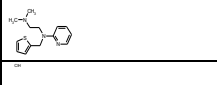
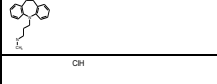
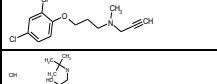
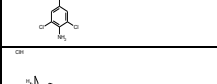
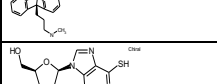
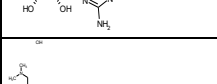
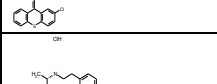
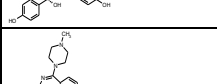
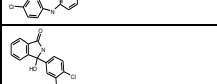
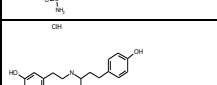
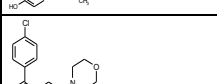
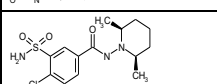
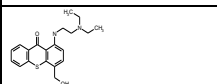
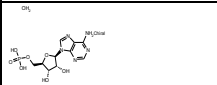


Prestw-225		Nifenazone	2139-47-1	308.34	<chem>C=1/C(N(N(C1C)C)c1cccc1)=O)NC(c1cccc1)=O</chem>	N-(1,5-dimethyl-3-oxo-2-phenylpyrazol-4-yl)pyridine-3-carboxamide
Prestw-226		Griseofulvin	126-07-8	352.77	<chem>[C@]12(C(c3c(O1)c(cc3OC)OC)Cl)=O)/C=C\C(C[C@H]2C)=O)OC</chem>	(2S,5'R)-7-chloro-3',4,6-trimethoxy-5'-methylspiro[1-benzofuran-2,4'-cyclohex-2-ene]-1',3-dione
Prestw-227		Clemizole hydrochloride	1163-36-6	362.31	<chem>c1(n(c2c(n1)cccc2)Cc1ccc(Cl)cc1)CN1CCCC1</chem>	1-[(4-chlorophenyl)methyl]-2-(pyrrolidin-1-ylmethyl)benzimidazole hydrochloride
Prestw-228		Tropicamide	1508-75-4	284.36	<chem>C(C(c1cccc1)CO)(N(Cc1cccc1)CC)=O</chem>	N-ethyl-3-hydroxy-2-phenyl-N-(pyridin-4-ylmethyl)propanamide
Prestw-229		Nefopam hydrochloride	23327-57-3	289.81	<chem>c12C(OCCN(Cc1cccc2)C)c1cccc1</chem>	5-methyl-1-phenyl-1,3,4,6-tetrahydro-2,5-benzoxazine hydrochloride
Prestw-230		Phentolamine hydrochloride	73-05-2	317.82	<chem>N(c1cc(O)ccc1)(C1C1=N1CCN1)c1ccc(cc1)C</chem>	3-[N-(4,5-dihydro-1H-imidazol-2-ylmethyl)-4-methylanilino]phenol hydrochloride
Prestw-231		Etodolac	41340-25-4	287.36	<chem>c12[nH]c3c(c1)CCOC2(CC(=O)O)CC)cccc3CC</chem>	2-(1,8-diethyl-4,9-dihydro-3H-pyrano[3,4-b]indol-1-yl)acetic acid
Prestw-232		Scopolamin-N-oxide hydrobromide	6106-81-6	400.27	<chem>[C@]12([C@@](O1)([C@]1([N+](C@@]2(C[C@H](C1)OC([C@@H](c1cccc1)CO)=O)[H])([O-])C)[H])[H])</chem>	
Prestw-233		Hyoscyamine (L)	101-31-5	289.38	<chem>N1([C@@]2(C[C@@H](OC([C@H](c3cccc3)CO)=O)C[C@]1(CC2)[H])[H])C</chem>	
Prestw-234		Chlorphensin carbamate	886-74-8	245.66	<chem>C(=O)OCC(COC1ccc(Cl)cc1)O)N</chem>	[3-(4-chlorophenoxy)-2-hydroxypropyl] carbamate
Prestw-1771		Carmofur	61422-45-5	257.27	<chem>N1(C(NC(C=C1)F)=O)C(=O)NCCCCC</chem>	5-fluoro-N-hexyl-2,4-dioxypyrimidine-1-carboxamide
Prestw-236		Dilazep dihydrochloride	20153-98-4	677.63	<chem>c1(c(cc(C(=O)O)CCCN2CCN(CCC2)CCOC(c2cc(c(c2)OC)OC)OC)=O)cc1OC)OC</chem>	3-[4-{3-(3,4,5-trimethoxybenzoyloxypropyl)-1,4-diazepan-1-yl}propyl 3,4,5-trimethoxybenzoate
Prestw-237		Ofloxacin	82419-36-1	361.38	<chem>N12c3c(c(cc3C(C=C1)C(=O)O)=O)F)N1CCN(CC1)C)OCC2C</chem>	9-Fluoro-3-methyl-10-(4-methyl-1-piperazinyl)-7-oxo-2,3-dihydro-7H-[1,4]oxazinof[2,3,4-j]quinoline
Prestw-238		Lomefloxacin hydrochloride	98079-52-8	387.82	<chem>C=1/C(c2c(N(C1)CC)c(c(N1CC(NCC1)C)c(c2)F)F)=O)\C(=O)O</chem>	1-ethyl-6,8-difluoro-7-(3-methylpiperazin-1-yl)-4-oxo-1,4-dihydroquinoline-3-carboxylic acid
Prestw-239		Orphenadrine hydrochloride	341-69-5	305.85	<chem>c1(C(c2cccc2)OCCN(C)C)c(C)cccc1</chem>	N,N-dimethyl-2-[(2-methylphenyl)phenylmethoxy]ethanamine hydrochloride
Prestw-240		Proglumide	6620-60-6	334.42	<chem>C(C(NC(=O)c1cccc1)CCC(=O)O)(N(CCC)CCC)=O</chem>	4-benzamido-5-(dipropylamino)-5-oxopentanoic acid
Prestw-241		Mexiletine hydrochloride	5370-01-4	215.73	<chem>c1(OCC(N)C)c(ccc1)C</chem>	1-(2,6-dimethylphenoxy)propan-2-amine hydrochloride
Prestw-242		Flavoxate hydrochloride	3717-88-2	427.93	<chem>c12O\C=C(/C(c1cccc2C(=O)OCCN1CCCC1)=O)C)c1cccc1</chem>	2-piperidin-1-ylethyl 3-methyl-4-oxo-2-phenylchromene-8-carboxylate hydrochloride
Prestw-243		Bufexamac	2438-72-4	223.27	<chem>C(=O)(NO)Cc1ccc(cc1)OCCCC</chem>	2-(4-butoxyphenyl)-N-hydroxyacetamide
Prestw-244		Glutethimide, para-amino	125-84-8	232.28	<chem>C1(NC(=O)CCC1(c1ccc(N)cc1)CC)=O</chem>	3-(4-aminophenyl)-3-ethylpiperidine-2,6-dione
Prestw-245		Dropropizine (R,S)	17692-31-8	236.32	<chem>N1(CCN(CC(O)CO)CC1)c1cccc1</chem>	3-(4-phenylpiperazin-1-yl)propane-1,2-diol
Prestw-246		Pinacidil	85371-64-8	245.33	<chem>C(=N(C#N))/(NC(C(C)C)C)Nc1cccc1</chem>	1-cyano-2-(3,3-dimethylbutan-2-yl)-3-pyridin-4-ylguanidine
Prestw-247		Albendazole	54965-21-8	265.34	<chem>c1(nc2c([nH]1)ccc(c2)SCCC)NC(=O)OC</chem>	methyl N-(6-propylsulfanyl-1H-benzimidazol-2-yl)carbamate

Prestw-248		Clonidine hydrochloride	4205-91-8	266.56	<chem>C1(NC2c(Cl)cccc2Cl)=N/CCN1</chem>	N-(2,6-dichlorophenyl)-4,5-dihydro-1H-imidazol-2-amine hydrochloride
Prestw-249		Bupropion hydrochloride	31677-93-7	276.21	<chem>C(c1cc(Cl)ccc1)C(NC(C)C)C)C=O</chem>	2-(tert-butylamino)-1-(3-chlorophenyl)propan-1-one hydrochloride
Prestw-250		Alprenolol hydrochloride	13707-88-5	285.82	<chem>O(c1c(CC=C)cccc1)CC(CNC(C)C)O</chem>	1-(propan-2-ylamino)-3-(2-prop-2-enylphenoxy)propan-2-ol hydrochloride
Prestw-251		Chlorothiazide	58-94-6	295.72	<chem>S1(c2cc(S(=O)(=O)N)c(cc2N=C/N1)Cl)(=O)=O</chem>	(6-Chloro-2H-1,2,4-benzothiazine-7-sulfonamide 1,1-dioxide)
Prestw-252		Diphenidol hydrochloride	3254-89-5	345.92	<chem>C(c1cccc1)(c1cccc1)(O)CCCN1CCCC1</chem>	1,1-diphenyl-4-piperidin-1-ylbutan-1-ol hydrochloride
Prestw-253		Norethindrone	68-22-4	298.43	<chem>[C@]12([C@]([C@]3([C@@]([C@@]4(C=C/C(=O)CC4)CC3)[H])(CC1)[H])([H])(CC[C@]2(C#C)O)[H])C</chem>	(8R,9S,10R,13S,14S,17S)-17-ethynyl-17-hydroxy-13-methyl-1,2,6,7,8,9,10,11,12,14,15,16-tetrahydro-4H-cyclohepta[1,2-b:1',1'-f][7]annulen-11-ylidene)-N-methylpropan-1-amine hydrochloride
Prestw-254		Nortriptyline hydrochloride	894-71-3	299.85	<chem>C1(c2c(CCC3c1cccc3)cccc2)=C1CCNC</chem>	3-(5,6-dihydroindolizin-2-ylidene)-N-methylpropan-1-amine hydrochloride
Prestw-255		Niflumic acid	4394-00-7	282.22	<chem>c1(c(C(=O)O)cccn1)Nc1cc(C(F)(F)F)ccc1</chem>	2-[3-(trifluoromethyl)anilino]pyridine-3-carboxylic acid
Prestw-256		Isotretinoin	4759-48-2	300.44	<chem>C1(/C=C/C(=C/C=C/C(=O)O)/C)C=C(\CCCC1(C)C)/C</chem>	(2Z,4E,6E,8E)-3,7-dimethyl-9-(2,6,6-trimethylcyclohexen-1-yl)nona-2,4,6,8-tetraenoic acid
Prestw-257		Retinoic acid	302-79-4	300.44	<chem>C1(/C=C/C(=C/C=C/C(=O)O)/C)C=C(\CCCC1(C)C)/C</chem>	(2E,4E,6E,8E)-3,7-dimethyl-9-(2,6,6-trimethylcyclohexen-1-yl)nona-2,4,6,8-tetraenoic acid
Prestw-258		Antazoline hydrochloride	2508-72-7	301.82	<chem>N(C/C1=N/CCN1)(Cc1cccc1)c1cccc1</chem>	N-benzyl-N-(4,5-dihydro-1H-imidazol-2-yl)methylaniline hydrochloride
Prestw-259		Ethacrynic acid	58-54-8	303.14	<chem>c1(c(c(c(OCC(=O)O)cc1)Cl)Cl)C(C=C)CC=O</chem>	2-[2,3-dichloro-4-(2-methylidenebutanoyl)phenoxy]acetic acid
Prestw-260		Praziquantel	55268-74-1	312.42	<chem>N1(C(=O)C2CCCC2)CC2N(C1=O)CCc1c2cccc1</chem>	2-(Cyclohexylcarbonyl)-1,2,3,6,7,11b-hexahydro-4H-pyrazino[2,1-a]isoquinolin-4-one
Prestw-261		Ethisterone	434-03-7	312.46	<chem>[C@]12(C=C/C(=O)CC1)CC[C@@]1([C@@]2(CC[C@@]2([C@]1(CC[C@]2(C#C)O)[H])C)[H])C</chem>	(8R,9S,10R,13S,14S,17R)-17-ethynyl-17-hydroxy-10,13-dimethyl-2,6,7,8,9,11,12,14,15,16-tetrahydro-4H-cyclohepta[1,2-b:1',1'-f][7]annulen-11-ylidene)-N-methylpropan-1-amine hydrochloride
Prestw-262		Triprolidine hydrochloride	550-70-9	314.86	<chem>C=C/CN1CCCC1)/(c1ccc(cc1)C)/c1ncccc1</chem>	2-[(E)-1-(4-methylphenyl)-3-pyrrolidin-1-ylprop-1-enyl]pyridine hydrochloride
Prestw-263		Doxepin hydrochloride	1229-29-4	315.85	<chem>C1(/c2c(OCC3c1cccc3)cccc2)=C1CCN(C)C</chem>	(3-Dibenz(b,c)oxepin 11(6H)ylidene-N,N-dimethylpropanamine) hydrochloride
Prestw-264		Dyclonine hydrochloride	536-43-6	325.88	<chem>N1(CCC(c2ccc(cc2)O)CCCC)O)CCCC1</chem>	1-(4-butoxyphenyl)-3-piperidin-1-ylpropan-1-one hydrochloride
Prestw-265		Dimenhydrinate	523-87-5	469.98	<chem>C(c1cccc1)(c1cccc1)OCCN(C)C</chem>	2-benzhydryloxy-N,N-dimethylethanamine 8-chloro-1,3-dimethyl-7H-purine-2,6-dione
Prestw-266		Disopyramide	3737-09-5	339.48	<chem>C(C(=O)N)(CCN(C(C)C)C(C)C)(c1ncccc1)c1cccc1</chem>	4-[di(propan-2-yl)amino]-2-phenyl-2-pyridin-2-ylbutanamide
Prestw-267		Clotrimazole	23593-75-1	344.85	<chem>C(n1ncc1)(c1c(Cl)cccc1)(c1cccc1)c1cccc1</chem>	1-[(2-chlorophenyl)-diphenylmethyl]imidazole
Prestw-268		Vinpocetine	42971-09-5	350.46	<chem>n1/2c3c(c4c1cccc4)CCN1[C@]3([C@]([C=C/C(=O)OC)C](CCC1)CC)[H]</chem>	ethyl (15S,19S)-15-ethyl-1,11-diazapentacyclo[9.6.2.0^2,7.0^8,18.0^15,19]nonadeca-2,4,6,8(18),16-pentaene-
Prestw-269		Clomipramine hydrochloride	17321-77-6	351.32	<chem>N1(c2cc(ccc2CCc2c1cccc2)Cl)CCCN(C)C</chem>	(3-Chloro-10,11-dihydro-N,N-dimethyl-5H-dibenz[b,f]azepine-5-propanamine) hydrochloride

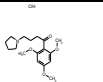
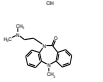
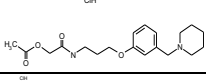
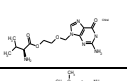
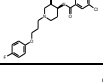
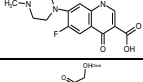
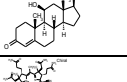
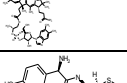
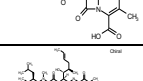
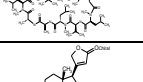
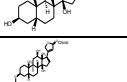
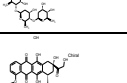
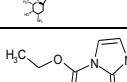
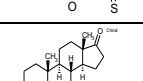
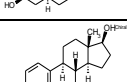
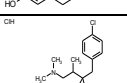
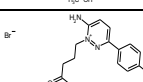
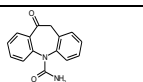
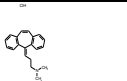
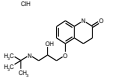
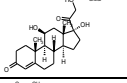
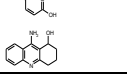

Prestw-270		Fendiline hydrochloride	13636-18-5	351.92	<chem>C(c1cccc1)(c1cccc1)CCNC(c1cccc1)C</chem>	3,3-diphenyl-N-(1-phenylethyl)propan-1-amine hydrochloride
Prestw-271		Vincamine	1617-90-9	354.45	<chem>n12[C@]([C@]3([C@]4(c1c(c1c2cccc1)CCN4CCC3)[H])CC)(C(=O)OC)O</chem>	(3alpha,14beta,16alpha)-14,15-dihydro-14-hydroxybumamenine-14-carboxylic acid methyl ester
Prestw-272		Indomethacin	53-86-1	357.80	<chem>n1(c(c(c2c1ccc(c2)OC)CC(=O)O)C)C(c1ccc(cc1)Cl)=O</chem>	2-[1-(4-chlorobenzoyl)-5-methoxy-2-methylindol-3-yl]acetic acid
Prestw-273		Cortisone	53-06-5	360.45	<chem>[C@]12([C@@](C(=O)CO)(CC[C@]1([C@]1([C@@](C@@@]3(\C=C/C(=O)CC3)\CC1)C)(C(C2)=O)[H])[H]O)C</chem>	(8S,9S,10R,13S,14S,17R)-17-hydroxy-17-(2-hydroxyacetyl)-10,13-dimethyl-
Prestw-274		Prednisolone	50-24-8	360.45	<chem>[C@]12([C@@](C(=O)CO)(CC[C@]1([C@]1([C@@](C@@@]3(\C=C/C(=O)CC3)\CC1)C)(C(C2)=O)[H])[H]O)C</chem>	(8S,9S,10R,11S,13S,14S,17R)-11,17-dihydroxy-17-(2-hydroxyacetyl)-10,13-dimethyl-
Prestw-275		Fenofibrate	49562-28-9	360.84	<chem>C(C(Oc1ccc(C(c2ccc(cc2)Cl)=O)cc1)(C)C)(OC(C)C)=O</chem>	propan-2-yl 2-[4-(4-chlorobenzoyl)phenoxy]-2-methylpropanoate
Prestw-276		Bumetanide	28395-03-1	364.42	<chem>S(c1c(c(cc1)C(=O)O)NCCCC)Oc1cccc1(=O)=O)N</chem>	3-(butylamino)-4-phenoxy-5-sulfamoylbenzoic acid
Prestw-277		Labetalol hydrochloride	32780-64-6	364.88	<chem>c1(cc(cc1)O)C(CNC(Cc1cccc1)C)O)C(=O)N</chem>	2-hydroxy-5-[1-hydroxy-2-(4-phenylbutan-2-ylamino)ethyl]benzamide hydrochloride
Prestw-278		Cinnarizine	298-57-7	368.53	<chem>N1(C(c2cccc2)c2cccc2)CCN(CC1)C/C=C/c1cccc1</chem>	1-benzhydryl-4-[(E)-3-phenylprop-2-enyl]piperazine
Prestw-279		Methylprednisolone, 6-alpha	83-43-2	374.48	<chem>[C@]12([C@@](C(=O)CO)(CC[C@]1([C@]1([C@@](C@@@]3(\C=C/C(=O)CC3)\CC1)C)(C(C2)=O)[H])[H]O)C</chem>	(6S,8S,9S,10R,11S,13S,14S,17R)-11,17-dihydroxy-17-(2-hydroxyacetyl)-6,10,13-trimethyl-
Prestw-280		Quinidine hydrochloride monohydrate	6151-40-2	378.90	<chem>N12[C@@]([C@H](C3c4c(nc3)ccc(c4)OC)O)C(C@@)([C@H](C1)C=C)(CC2)[H][H]</chem>	(S)-[(2R,4S,5R)-5-ethenyl-1-azabicyclo[2.2.2]octan-2-yl]- (6-methoxyquinolin-4-yl)methanol hydrate
Prestw-281		Fludrocortisone acetate	514-36-3	422.50	<chem>[C@]12([C@@](C(COC(=O)C)=O)(CC[C@]1([C@]1([C@@](C@@@]3(\C=C/C(=O)CC3)\CC1)C)(C(C2)=O)[H])[H]O)C</chem>	[[8S,9R,10S,11S,13S,14S,17R]-9-fluoro-11,17-dihydroxy-10,13-dimethyl-3-oxo-5-[1-hydroxy-2-[1-(4-hydroxyphenyl)propan-2-ylamino]ethyl]benzene-1,3-diol hydrobromide
Prestw-282		Fenoterol hydrobromide	1944-12-3	384.27	<chem>c1(cc(cc1)O)C(CNC(Cc1ccc(cc1)O)C)O</chem>	5-[1-hydroxy-2-[1-(4-hydroxyphenyl)propan-2-ylamino]ethyl]benzene-1,3-diol hydrobromide
Prestw-283		Homochlorcyclizine dihydrochloride	1982-36-1	387.78	<chem>N1(C(c2ccc(cc2)Cl)c2cccc2)CCN(CCC1)C</chem>	1-[4-(4-chlorophenyl)phenylmethyl]-4-methyl-1,4-diazepane-1,4-dium dichloride
Prestw-284		Diethylcarbamazine citrate	1642-54-2	391.42	<chem>C(N1CCN(CC1)C)(N(CC)CC)=O</chem>	(N,N-Diethyl-4-methyl-piperazine carboxamide) Citrate Salt
Prestw-285		Chenodiol	474-25-9	392.58	<chem>[C@]12([C@@](C(=O)O)(CC[C@]1([C@]1([C@@](C@@@]3(\C=C/C(=O)CC3)\CC1)C)(C(C2)=O)[H])[H]O)C</chem>	(4R)-4-[(3R,5S,7R,8R,9S,10S,13R,14S,17R)-3,7-dihydroxy-10,13-dimethyl-
Prestw-286		Perhexiline maleate	6724-53-4	393.57	<chem>C(CC1NCCCC1)(C1CCCC1)C1CCCC1</chem>	2-(2,2-dicyclohexylethyl)piperidine (Z)-but-2-enedioic acid
Prestw-287		Oxybutynin chloride	1508-65-2	393.96	<chem>C(C(=O)OCC#CCN(CC)CC)(c1cccc1)(C1CCCC1)O</chem>	4-(diethylamino)but-2-ynyl 2-cyclohexyl-2-hydroxy-2-phenylacetate hydrochloride
Prestw-288		Spiperone	749-02-0	395.48	<chem>C12(N(CNC1=O)c1cccc1)CCN(CC2)CCCC(c1ccc(cc1)F)=O</chem>	8-[4-(4-fluorophenyl)-4-oxobutyl]-1-phenyl-1,3,8-triazaspiro[4.5]decan-4-one
Prestw-289		Pyrilamine maleate	59-33-6	401.47	<chem>N(c1ncccc1)(Cc1ccc(cc1)OC)CCN(C)C</chem>	N'-[(4-methoxyphenyl)methyl]-N,N-dimethyl-N'-pyridin-2-ylethane-1,2-diamine (Z)-but-2-enedioic acid
Prestw-290		Sulfipyrazone	57-96-5	404.49	<chem>N1(N(C(C1=O)CCS(=O)C)cccc1)C)O)c1cccc1)c1ccc</chem>	4-[2-(benzenesulfinyl)ethyl]-1,2-diphenylpyrazolidine-3,5-dione
Prestw-291		Dantrolene sodium salt	14663-23-1	336.24	<chem>N1=C(N(CC1=O)N=C/c1cc(cc1)ccc([N+](=[O-])=O)cc1)[O-]</chem>	3-[(E)-[5-(4-nitrophenyl)furan-2-yl]methylideneamino]-5-oxo-4H-imidazol-2-olate sodium

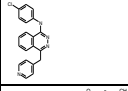
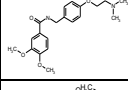
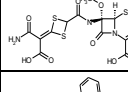
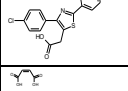
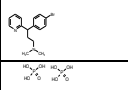
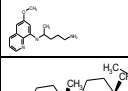
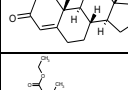
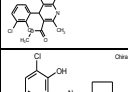
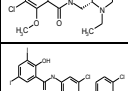
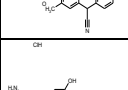
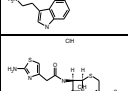
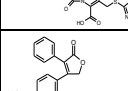
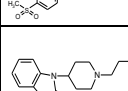
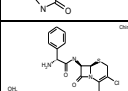
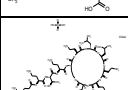
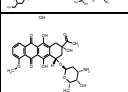
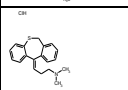
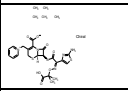
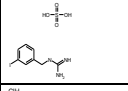
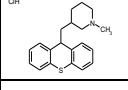
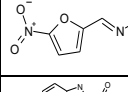
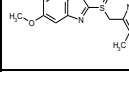

Prestw-292		Trazodone hydrochloride	25332-39-2	408.33	<chem>N1/C(N(N=C1\C/C=C=C2)CCCN1CCN(c2cc(Cl)ccc2)CC1)=O</chem>	2-[3-[4-(3-chlorophenyl)piperazin-1-yl]propyl]-[1,2,4]triazolo[4,3-a]pyridin-3-one hydrochloride
Prestw-293		Glafenine hydrochloride	65513-72-6	409.27	<chem>c1(C(OCC(O)CO)=O)c(Nc2c3c(cc(cc3)Cl)nc2)cccc1</chem>	2,3-dihydroxypropyl 2-[(7-chloroquinolin-4-yl)amino]benzoate hydrochloride
Prestw-294		Pimethixene maleate	13187-06-9	409.51	<chem>C1/(c2c(Sc3c1cccc3)cccc2)=C1/CCN(CC1)C</chem>	1-methyl-4-thioxanthen-9-ylidene-piperidine (Z)-but-2-enedioic acid
Prestw-295		Pergolide mesylate	66104-23-2	410.60	<chem>c1c2c3c([C@@]4([C@](N(C[C@@H](C4)CSC)CCC)(C1)[H])[H])cccc3[nH]c2</chem>	(6aR,9R,10aR)-9-(methylsulfanylmethyl)-7-propyl-6,6a,8,9,10,10a-hexahydro-4H-indolo[4,3-
Prestw-296		Acemetacin	53164-05-9	415.83	<chem>n1(c(c(c2c1ccc(c2)OC)CC(=O)OCC(=O)O)C)c1ccc(cc1)Cl=O</chem>	2-[2-[1-(4-chlorobenzoyl)-5-methoxy-2-methylindol-3-yl]acetyl]oxyacetic acid
Prestw-297		Benzydamine hydrochloride	132-69-4	345.88	<chem>n1(nc(c2c1cccc2)OCCCN(C)C)c1cccc1</chem>	3-(1-benzylindazol-3-yl)oxy-N,N-dimethylpropan-1-amine hydrochloride
Prestw-298		Fipexide hydrochloride	34161-23-4	425.32	<chem>N1(C(CO2ccc(Cl)cc2)=O)CCN(Cc2cc3c(OCO3)cc2)CC1</chem>	1-[4-(1,3-benzodioxol-5-ylmethyl)piperazin-1-yl]-2-(4-chlorophenoxy)ethanone hydrochloride
Prestw-299		Mifepristone	84371-65-3	429.61	<chem>C1/12=C13/C(=C(C=O)CC3)/CC[C@]1([C@]1([C@](C[C@@]2(c2ccc(N(C)C)cc2)[H])([C@](C#CC)(CC1)O)C)[H])H</chem>	11beta-(4-Dimethyl-amino)-phenyl-17beta-hydroxy-17-(1-propynyl)-estra-4,9-dien-3-
Prestw-300		Diperodon hydrochloride	537-12-2	433.94	<chem>C(Nc1cccc1)(OC(CN1CCC1)COC(Nc1cccc1)=O)=O</chem>	[2-(phenylcarbamoyloxy)-3-piperidin-1-ylpropyl] N-phenylcarbamate hydrochloride
Prestw-301		Lisinopril	83915-83-7	441.53	<chem>N1(C([C@@H](N[C@H](C=O)CCc2cccc2)CCCN)=O)[C@H](C(=O)O)CCC1</chem>	(2S)-1-[(2S)-6-amino-2-[[[(1S)-1-carboxy-3-phenylpropyl]amino]hexanoyl]pyrrolidine-2-carboxylic acid
Prestw-302		Lincomycin hydrochloride	859-18-7	443.01	<chem>[C@@H]1(O[C@H]([C@@H]([C@H]([C@H]1O)O)O)S[C]([C@H](NC([C@H]1N(C[C@@H](C1)CCC)C=O)[C@H](O)C</chem>	(4R)-N-[(1R,2R)-2-hydroxy-1-[(2R,3R,4S,5R,6R)-3,4,5-trihydroxy-6-(methylsulfanyl)oxan-2-
Prestw-303		Telenzepine dihydrochloride	147416-96-4	443.40	<chem>N1(c2c(C(Nc3c1cccc3)=O)csc2C)C(CN1CCN(CC1)C)=O</chem>	1-methyl-10-[2-(4-methylpiperazin-1-yl)acetyl]-5H-thieno[3,4-b][1,5]benzodiazepin-4-one
Prestw-304		Econazole nitrate	24169-02-6	444.70	<chem>c1(c(cc(c1)Cl)Cl)C(Cn1cncc1)OCc1ccc(Cl)cc1</chem>	(1-[2-(4-Chlorophenyl)methoxy]-2-(2,4-dichlorophenyl)ethyl]-1H-imidazole nitrate)
Prestw-305		Bupivacaine hydrochloride	18010-40-7	324.90	<chem>C(Nc1c(ccc1C)C)(C1N(CCCC)CCCC1)=O</chem>	1-butyl-N-(2,6-dimethylphenyl)piperidine-2-carboxamide hydrochloride
Prestw-306		Clemastine fumarate	14976-57-9	459.97	<chem>[C@@](c1ccc(cc1)Cl)(c1cccc1)(OCC[C@H]1N(CCC1)C)C</chem>	(2R)-2-[2-[(1R)-1-(4-chlorophenyl)-1-phenylethoxy]ethyl]-1-methylpyrrolidine (E)-but-2-
Prestw-307		Oxytetracycline dihydrate	6153-64-6	496.48	<chem>[C@@]112([C@]([C@@H](C=C/C1=O)C(=O)N)O)N(C)C([C@H]([C@]1(C=C2)O)C(c2c([C@]1(O)C)cccc2O=O)[H])O</chem>	2-Naphthacene-carboxamide, 4-(dimethylamino)-1,4,4a,5,5a,6,11,12a-octahydro-3,5,6,10,12,12a-
Prestw-308		Pimozide	2062-78-4	461.56	<chem>C1(N(c2c(N1)cccc2)C1CCN(CC1)CCCC(c1ccc(cc1)F)c1ccc(cc1)F)=O</chem>	3-[1-[4,4-bis(4-fluorophenyl)butyl]piperidin-4-yl]-1H-benzimidazol-2-one
Prestw-309		Amodiaquin dihydrochloride dihydrate	6398-98-7	464.82	<chem>c1c2c(Nc3cc(c(cc3)O)CN(CC)CC)ccnc1cc(cc2)Cl</chem>	4-[(7-chloroquinolin-4-yl)amino]-2-(diethylaminomethyl)phenol dihydrate dihydrochloride
Prestw-310		Mebeverine hydrochloride	2753-45-9	466.02	<chem>C(c1cc(c(cc1)OC)OC(=O)O)CCCCN(C(Cc1ccc(cc1)OC)C)CC</chem>	4-ethyl-[1-(4-methoxyphenyl)propan-2-yl]amino]butyl 3,4-dimethoxybenzoate
Prestw-311		Ifenprodil tartrate	23210-58-4	475.54	<chem>N1(C(C(c2ccc(cc2)O)O)C)CCC(Cc2cccc2)CC1</chem>	4-[2-(4-benzylpiperidin-1-yl)-1-hydroxypropyl]phenol (2R,3R)-2,3-dihydroxybutanedioate
Prestw-312		Flunarizine dihydrochloride	30484-77-6	477.43	<chem>N1(C(c2ccc(cc2)F)c2ccc(cc2)F)CCN(CC1)C/C=C/c1cccc1</chem>	1-[Bis(4-fluorophenyl)methyl]-4-(3-phenyl-2-propenyl)-piperazine dihydrochloride
Prestw-313		Trifluoperazine dihydrochloride	440-17-5	480.43	<chem>N1(c2c(Sc3c1cccc3)ccc(C(F)(F)F)c2)CCCN1CCN(CC1)C</chem>	10-[3-(4-methylpiperazin-1-yl)propyl]-2-(trifluoromethyl)phenothiazine dihydrochloride

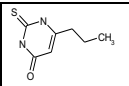
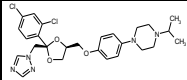
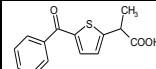
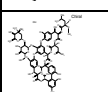
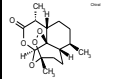
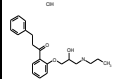
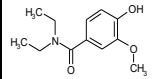
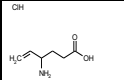
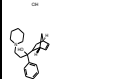
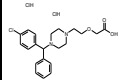
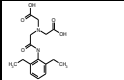
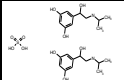
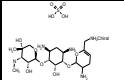
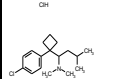
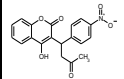
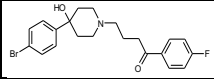
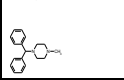
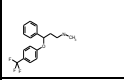
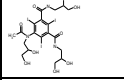
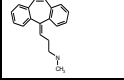
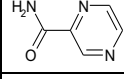
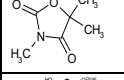
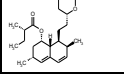
Prestw-314		Enalapril maleate	76095-16-4	492.53	<chem>N1(C(C@@H)(N(C@H)(C(=O)O)CCc2cccc2)C)=O)C@H](C(=O)O)CCC1</chem>	(2S)-1-[(2S)-2-[(2S)-1-ethoxy-1-oxo-4-phenylbutan-2-yl]amino]propanoyl]pyrrolidine-2-carboxylic acid (Z)-but-2-
Prestw-315		Minocycline hydrochloride	13614-98-7	493.95	<chem>[C@]12/C=C/C(C4c(c(ccc4O)N(C)C)CC3CC1[C@H](C=C(C2=O)C(=O)N)O)N(C)C(=O)O)O</chem>	[amino(hydroxy)methylidene]-4,7-bis(dimethylamino)-10,11,12a-trihydroxy-5-chloro-N-(4-[N-(cyclohexylcarbamoyl)sulfamoyl]phenethyl)-2-methoxybenzamide
Prestw-316		Glibenclamide	10238-21-8	494.01	<chem>S(NC(NC1CCCC1)=O)(c1ccc(cc1)CCNC(c1ccc(c1)Cl)OC)=O(=O)=O</chem>	(cyclohexylcarbamoyl)sulfamoyl]phenethyl)-2-methoxybenzamide
Prestw-317		Guanethidine sulfate	60-02-6	494.70	<chem>C(=N)(NCCN1CCCCC1)N.C(=N)(NCCN1CCCCC1)N</chem>	2-[2-(azocan-1-yl)ethyl]guanidine sulfuric acid
Prestw-318		Quinacrine dihydrochloride hydrate	69-05-6	508.92	<chem>c1(c2c(nc3c1ccc(c3)Cl)ccc(c2)OC)NC(CCCN(CC)CC)C</chem>	6-Chloro-9-(4-diethylamino-1-methylbutyl)amino-2-methoxyacridine dihydrochloride hydrate
Prestw-319		Clofilium tosylate	92953-10-1	510.18	<chem>[N+](CC)(CC)(CCCCC)CCCCc1ccc(Cl)cc1</chem>	4-(4-chlorophenyl)butyl-diethyl-heptylazanium 4-methylbenzenesulfonate
Prestw-320		Fluphenazine dihydrochloride	146-56-5	510.45	<chem>N1(c2c(Sc3c1cccc3)ccc(C(F)(F)F)c2)CCCN1CCN(CC1)CCO</chem>	4-[3-[2-(Trifluoromethyl)-10H-phenothiazin-10-yl]-1-piperazine]ethanol dihydrochloride
Prestw-321		Streptomycin sulfate	3810-74-0	1457.40	<chem>N(C1C(OC(C(C1O)CO)OC2C(OC(C2O)C=O)C)OC3C(C(C(C3O)O)NC(=N)N)O)NC(=N)N)C</chem>	1,1'-[1(2R,3S,4R,5R,6S)-4-((5-Deoxy-2-O-[2-deoxy-2-(methylamino)-alpha-D-glucopyranosyl]-3-C-fomyl-N-[3-(4-amino-6,7-dimethoxyquinazolin-2-yl)-methylamino]propyl]oxolane-2-carboxamide hydrochloride
Prestw-322		Alfuzosin hydrochloride	81403-68-1	425.92	<chem>n1c(nc2c(c1N)cc(c(c2)OC)OC)N(CCCNC(C1OCCC1)=O)C</chem>	dimethoxyquinazolin-2-yl)-methylamino]propyl]oxolane-2-carboxamide hydrochloride
Prestw-323		Chlorpropamide	94-20-2	276.74	<chem>S(NC(=O)NCCC)(c1ccc(cc1)Cl)(=O)=O</chem>	(1-[p-Chlorobenzenesulfonyl]-3-propylurea)
Prestw-324		Phenylpropanolamine hydrochloride	154-41-6	187.67	<chem>[C@H](c1ccccc1)([C@H](N)C)O</chem>	2-amino-1-phenylpropan-1-ol hydrochloride
Prestw-325		Ascorbic acid	50-81-7	176.13	<chem>C1(=C([C@H](OC1=O)[C@@H](O)CO)O)O</chem>	(5R)-5-[(1S)-1,2-dihydroxyethyl]-3,4-dihydroxy-2,5-dihydrofuran-2-one
Prestw-326		Methyldopa (L-)	555-30-6	211.22	<chem>[C@](C(=O)O)(Cc1cc(c(cc1)O)O)(N)C</chem>	(2S)-2-amino-3-(3,4-dihydroxyphenyl)-2-methylpropanoic acid
Prestw-327		Cefoperazone dihydrate	not available	681.71	<chem>N1\2C([C@]([C@]1(S)C(C=C2)C(=O)O)CS)C1n(nnn1)C([H])(N)(C@H)(NC(N1C(C(N(CC1)CC)=O)=O)O)c1ccc(cc1)O)=O)[H]=O</chem>	(6R,7R)-7-[[[(2R)-2-[(4-ethyl-2,3-dioxypiperazine-1-carbonyl)amino]-2-(4-hydroxyphenyl)acetyl]amino]-
Prestw-328		Zoxazolamine	61-80-3	168.58	<chem>n1c(oc2c1cc(cc2)Cl)N</chem>	5-Chloro-1,3-benzoxazol-2-amine
Prestw-329		Tacrine hydrochloride	1684-40-8	234.73	<chem>c1(c2c(nc3c1cccc3)CCCC2)N</chem>	1,2,3,4-tetrahydroacridin-9-amine hydrochloride
Prestw-330		Bisoprolol fumarate	104344-23-2	766.98	<chem>N(CC(CO)c1ccc(cc1)COCCOC(C)O)C(C)C.N(CC(CO)c1ccc(cc1)COCCOC(C)O)C(C)C</chem>	(RS)-1-[4-[[2-(1-Methylethoxy)ethoxy]methyl]phenoxy]-3-[[1-(1-methylethyl)amino]propan-2-
Prestw-331		Tremorine dihydrochloride	51-73-0	265.23	<chem>C(#CCN1CCCC1)CN1CCCC1</chem>	1-(4-pyrrolidin-1-ylbut-2-ynyl)pyrrolidine dihydrochloride
Prestw-332		Practolol	6673-35-4	266.34	<chem>C(Nc1ccc(OCC(CNC(C)C)O)cc1)(=O)C</chem>	N-[4-[2-hydroxy-3-(propan-2-ylamino)propoxy]phenyl]acetamide
Prestw-333		Zidovudine, AZT	30516-87-1	267.25	<chem>N1(C(NC(C=C1)C(=O)O)O)C[C@@H]1OC@H(C1)N=[N+]=[N-]CO</chem>	1-[(2R,4S,5S)-4-azido-5-(hydroxymethyl)oxolan-2-yl]-5-methylpyrimidine-2,4-dione
Prestw-334		Sulfisoxazole	127-69-5	267.31	<chem>S(Nc1c(c(no1)C)C)(c1ccc(N)cc1)(=O)=O</chem>	4-amino-N-(dimethyl-1,2-oxazol-5-yl)benzene-1-sulfonamide
Prestw-335		Zaprinast	37762-06-4	271.28	<chem>c12c(C(N=C(N1)c1c(OCCC)cccc1)=O)[nH]nn2</chem>	1,4-Dihydro-5-(2-propoxyphenyl)-7H-1,2,3-triazolo[4,5-d]pyrimidine-7-one

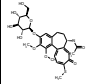
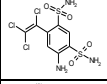
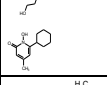
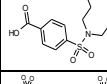
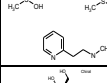
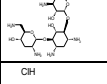
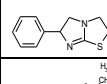
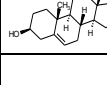
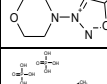
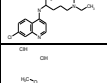
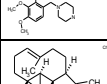
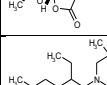
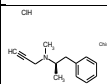
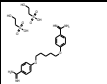
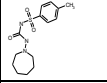
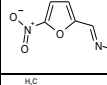
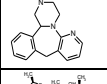
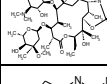
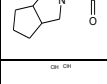
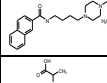
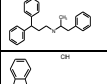
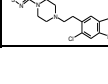

Prestw-336		Chlormezanone	80-77-3	273.74	<chem>S1(C(N(C(CC1=O)C)c1ccc(cc1)Cl)(=O)=O</chem>	2-(4-chlorophenyl)-3-methyl-1,1-dioxo-1,3-thiazinan-4-one
Prestw-337		Procainamide hydrochloride	614-39-1	271.79	<chem>C(c1ccc(N)cc1)(=O)NCCN(CC)CC</chem>	4-amino-N-(2-(diethylamino)ethyl)benzamide hydrochloride
Prestw-338		N6-methyladenosine	1867-73-8	281.27	<chem>n1([C@H]2[C@@H]([C@@H]([C@H](O2)CO)O)O)c2c(nc1)C</chem>	(2R,3S,4R,5R)-2-(hydroxymethyl)-5-[6-(methylamino)purin-9-yl]oxolane-3,4-diol
Prestw-339		Guanfacine hydrochloride	29110-48-3	282.56	<chem>N(C(=N)N)C(Cc1c(Cl)cccc1Cl)=O</chem>	N-(diaminomethylidene)-2-(2,6-dichlorophenyl)acetamide hydrochloride
Prestw-340		Domperidone	57808-66-9	425.92	<chem>C1(N(c2c(N1)cc(cc2)Cl)C1CCN(CC1)CCCN1C(Nc2c1cc(cc2)=O)=O</chem>	6-chloro-3-[1-[3-(2-oxo-3H-benzimidazol-1-yl)propyl]piperidin-4-yl]-1H-benzimidazol-2-one
Prestw-341		Furosemide	54-31-9	330.75	<chem>S(c1cc(c(cc1Cl)N)Cc1occc1)C(=O)O)(=O)(=O)N</chem>	5-[Aminosulfonyl]-4-chloro-2-[(2-furanylmethyl)amino]benzoic acid
Prestw-342		Methapyrilene hydrochloride	135-23-9	297.85	<chem>N(c1ncccc1)(Cc1sccc1)CCN(C)C</chem>	N,N-dimethyl-N'-pyridin-2-yl-N'-(thiophen-2-ylmethyl)ethane-1,2-diamine hydrochloride
Prestw-343		Desipramine hydrochloride	58-28-6	302.85	<chem>N1(c2c(CCc3c1cccc3)cccc2)CCNC</chem>	3-(5,6-dihydrobenzo[b][1]benzazepin-11-yl)-N-methylpropan-1-amine hydrochloride
Prestw-344		Clorgyline hydrochloride	17780-75-5	308.64	<chem>C(#C)CN(CCCOc1c(ccc1)Cl)Cl)C</chem>	3-(2,4-dichlorophenoxy)-N-methyl-N-prop-2-ynylpropan-1-amine hydrochloride
Prestw-345		Clenbuterol hydrochloride	21898-19-1	313.66	<chem>c1(c(cc(cc1Cl)C(CNC(C)C)O)Cl)N</chem>	1-(4-amino-3,5-dichlorophenyl)-2-(tert-butylamino)ethanol hydrochloride
Prestw-346		Maprotiline hydrochloride	10347-81-6	313.87	<chem>[C@@]12(c3c([C@](c4c1cccc4)(CC2)[H])cccc3)CCNC</chem>	3-(9,10-ethanoanthracen-9(10H)-yl)-N-methylpropan-1-amine hydrochloride
Prestw-347		Thioguanosine	85-31-4	299.31	<chem>n1(c2c(nc1)c(nc(n2)N)S)[C@H]1[C@@H]([C@@H]([C@H](O1)CO)O)O</chem>	2-amino-1H-purine-6(7H)-thione
Prestw-348		Chlorprothixene hydrochloride	6469-93-8	352.33	<chem>C1(/c2c(Sc3c1cccc3)ccc(c2)Cl)=C1CCN(C)C</chem>	(3Z)-3-(2-chlorothioxanthene-9-ylidene)-N,N-dimethylpropan-1-amine hydrochloride
Prestw-349		Ritodrine hydrochloride	23239-51-2	323.82	<chem>[C@@H](c1ccc(cc1)O)([C@@H](NCCc1ccc(cc1)O)C)O</chem>	4-[2-[[[1S,2R]-1-hydroxy-1-(4-hydroxyphenyl)propan-2-yl]amino]ethyl]phenol hydrochloride
Prestw-350		Clozapine	5786-21-0	326.83	<chem>C1(=Nlc2c(Nc3c1cccc3)ccc(c2)Cl)/N1CCN(CC1)C</chem>	3-chloro-6-(4-methylpiperazin-1-yl)-5H-benzo[b][1,4]benzodiazepine
Prestw-351		Chlorthalidone	77-36-1	338.77	<chem>C1(NC(c2c1cccc2)=O)c1cc(S(=O)(=O)N)(cc1)Cl)O</chem>	(RS)-2-chloro-5-(1-hydroxy-3-oxo-2,3-dihydro-1H-isoindol-1-yl)benzene-1-sulfonamide
Prestw-352		Dobutamine hydrochloride	49745-95-1	337.85	<chem>c1(c(ccc1)CCNC(CCc1ccc(cc1)O)C)O)O</chem>	4-[2-[4-(4-hydroxyphenyl)butan-2-ylamino]ethyl]benzene-1,2-diol hydrochloride
Prestw-353		Moclobemide	71320-77-9	268.75	<chem>C(c1ccc(cc1)Cl)(=O)NCCN1CCOCC1</chem>	4-chloro-N-(2-morpholin-4-ylethyl)benzamide
Prestw-354		Clopamide	636-54-4	345.85	<chem>S(c1cc(C(NN2[C@H](CCC[C@H]2C)C)=O)ccc1Cl)(=O)(=O)N</chem>	4-chloro-N-(2,6-dimethylpiperidin-1-yl)-3-sulfamoylbenzamide
Prestw-355		Hycanthone	3105-97-3	356.49	<chem>c12c(Sc3c(C1=O)cccc3)c(ccc2NCCN(CC)CC)CO</chem>	1-(2-Diethylaminoethylamino)-4-(hydroxymethyl)-9-thioxanthone
Prestw-356		Adenosine 5'-monophosphate monohydrate	18422-05-4	365.24	<chem>n1([C@H]2[C@@H]([C@@H]([C@H](O2)COP(=O)(O)O)O)c2c(nc1)c(ncn2)N</chem>	[(2R,3S,4R,5R)-5-(6-aminopurin-9-yl)-3,4-dihydroxoxolan-2-yl]methyl dihydrogen phosphate
Prestw-357		Amoxicillin	26787-78-0	365.41	<chem>N12[C@@H]([C@@H]([C1=O)NC([C@@H](c1ccc(cc1)O)N)=O)SC([C@@H]2C(=O)O)C)C</chem>	(2S,5R,6R)-6-[(2R)-2-amino-2-(4-hydroxyphenyl)acetyl]amino-3,3-dimethyl-7-oxo-4-thia-1-

Prestw-1603		Pemirolast potassium	100299-08-9	266.31	<chem>C=1(c2[n-nnn2]/C(N2/C(=N1)/C(=C1C=C2)/C)=O</chem>	9-methyl-3-(1,2,3-triaza-4-azanidacyclopenta-2,5-dien-5-yl)pyrido[1,2-a]pyrimidin-4-one potassium
Prestw-359		Dextromethorphan hydrobromide monohydrate	6700-34-1	370.33	<chem>[C@]123c4c(C[C@@H]([C@]1(CCCC2)[H])N(CC3)C)cc(c4)OC</chem>	(9S,13S,14S)-3-Methoxy-17-methylmorphinan hydrobromide
Prestw-360		Droperidol	548-73-2	379.44	<chem>C1(N(C2=C/C/CN(CC2)CCCC(c2ccc(cc2)F)=O)c2c(N1)cc(c2)=O</chem>	3-[1-[4-(4-fluorophenyl)-4-oxobutyl]-3,6-dihydro-2H-pyridin-4-yl]-1H-benzimidazol-2-one
Prestw-361		Bambuterol hydrochloride	81732-46-9	403.91	<chem>C(Oc1cc(OC(N(C)C)=O)cc(c1)C(CNC(C)C)C)O)(N(C)C)=O</chem>	5-[(RS)-2-[(1,1-dimethylethylamino)-1-hydroxyethyl]-1,3-phenylene bis(dimethylcarbamate)]
Prestw-362		Betamethasone	378-44-9	392.47	<chem>[C@]12([C@]([C@]3([C@@]([C@@]4(C=C(C(C=C4)=O)CC3)C)([C@H](C1)O)F)[H])([C@@H]([C@@]2(C(=O)CO)O)C)[H])C</chem>	(8S,9R,10S,11S,13S,14S,16S,17R)-9-fluoro-11,17-dihydroxy-17-(2-hydroxyacetyl)-10,13,16-N-(7S)-1,2,3,10-tetramethoxy-9-oxo-5,6,7,9-tetrahydrobenzo[a]heptalen-7-yl]acetamide
Prestw-363		Colchicine	64-86-8	399.45	<chem>C=1\2/C(=C1/C(=C1)O)C(=O)/[C@@H](NC(=O)C)C(Cc1c2c(c(c1)OC)OC)OC</chem>	benzyl N-[[[6aR,9S,10aR)-4,7-dimethyl-6,6a,8,9,10,10a-hexahydroindolo[4,3-fg]quinoline-9-
Prestw-364		Metergoline	17692-51-2	403.53	<chem>c12c3c([C@@]4([C@](N(C)C@H(C4)CNC(=O)OCc4cccc4)C(1)[H])[H])cccc3n(c2)C</chem>	(4R)-4-(ethylamino)-2-(3-methoxypropyl)-1,1-dioxo-3,4-dihydrothieno[3,2-e]thiazine-6-sulfonamide
Prestw-365		Brinzolamide	138890-62-7	383.51	<chem>S1(c2c(cc(s2)S(=O)(=O)N)[C@H](CN1CCCOC)NCC)(=O)=O</chem>	4-(2-amino-3,5-dibromophenyl)methylamino]cyclohexan-1-ol hydrochloride
Prestw-366		Ambroxol hydrochloride	23828-92-4	414.57	<chem>c1(c(cc(c1)Br)Br)N)CN[C@@H]1CC[C@H](CC1)O</chem>	2-[1-(3-(trifluoromethyl)phenyl)propan-2-ylamino]ethyl benzoate
Prestw-367		Benfluorex	23602-78-0	351.37	<chem>C(c1cc(CC(NCCOC(=O)c2cccc2)C)ccc1)(F)(F)F</chem>	N-benzyl-N-[3-(2-methylpropoxy)-2-pyrolidin-1-ylpropyl]aniline hydrochloride
Prestw-368		Bepridil hydrochloride	74764-40-2	403.01	<chem>N(CC(N1CCCC1)COCC(C)C)(Cc1cccc1)c1cccc1</chem>	4-hydroxy-2-methyl-N-(5-methyl-1,3-thiazol-2-yl)-1,1-dioxo-1lambda,6,2-benzothiazine-3-carboxamide
Prestw-369		Meloxicam	71125-38-7	351.41	<chem>S1(N(C(=C1c2c1cccc2)O)/C(Nc1ncc(s1)C)=O)C(=O)=O</chem>	(3,5-dibromo-4-hydroxyphenyl)-(2-ethyl-1-benzofuran-3-yl)methanone
Prestw-370		Benzbromarone	3562-84-3	424.09	<chem>c1(c(cc2c1cccc2)CC)C(c1cc(c(c1)Br)O)Br=O</chem>	10-(1-methylpiperidin-4-ylidene)-5H-benzo[1,2]cyclohepta[3,4-b]thiophen-4-one (E)-but-2-
Prestw-371		Ketotifen fumarate	34580-14-8	425.51	<chem>c12C1(c3c(C(c1scc2)=O)cccc3)=C1\CCN(CC1)C</chem>	3,4-dihydro-1-H-isoquinoline-2-carboximidamide sulfuric acid
Prestw-372		Debrisoquin sulfate	581-88-4	448.55	<chem>N1(C(=N)N)Cc2c(CC1)cccc2.N1(C(=N)N)Cc2c(CC1)cccc2</chem>	2-[[4-[(2,4-diaminopteridin-6-yl)methyl-methylamino]benzoyl]amino]pentanedioic acid (6aR,9R)-N-[(2S)-1-hydroxybutan-2-yl]-7-methyl-6,6a,8,9-tetrahydro-4H-indolo[4,3-fg]quinoline-9-
Prestw-373		Amethopterin (R,S)	60388-53-6	454.45	<chem>n1c(c2c(nc1N)nc(n2)CN(c1ccc(C(NC(C=O)O)CCC(=O)O)cc1)C)N</chem>	1-methyl-4-(3-methylsulfonyl)-5,6-dihydrobenzo[b][1]benzothiepin-5-yl]piperazine (Z)-but-2-
Prestw-374		Methylergometrine maleate	57432-61-8	455.52	<chem>C=1\2/[C@](N(C[C@H]([C@]1(C)C(N[C@H](CO)CC)=O)C)(Cc1c3c2cccc3[nH]c1)[H]</chem>	N,5-bis(4-chlorophenyl)-3-[[propan-2-yl]imino]-3,5-dihydrophenazin-2-amine
Prestw-375		Methiothepin maleate	19728-88-2	472.63	<chem>c12C(N3CCN(CC3)C)Cc3c(Sc1ccc(c2)SC)cccc3</chem>	2-(diethylamino)ethyl 2-(naphthalen-1-ylmethyl)-3-(oxolan-2-yl)propanoate oxalic acid
Prestw-376		Clofazimine	2030-63-9	473.41	<chem>C1=2/N(c3c1N=C1/C=C/C(=C2)/N(C)C)Nc1ccc(Cl)c(c1)cccc3)c1ccc(cc1)Cl</chem>	2-[4-(2-(4-chlorobenzoyl)amino)ethyl]phenoxyl-2-methylpropanoic acid
Prestw-377		Nafronyl oxalate	3200-06-4	473.57	<chem>C(C(Cc1c2c(ccc1)cccc2)CC1OCC1)(=O)OCCN(CC)CC</chem>	2-[4-(2-(4-chlorobenzoyl)amino)ethyl]phenoxyl-2-methylpropanoic acid
Prestw-378		Bezafibrate	41859-67-0	361.83	<chem>C(C(=O)O)(Oc1ccc(cc1)CCNC(c1ccc(cc1)Cl)=O)(C)C</chem>	chlorophenyl]piperazin-1-yl]propyl]-5-ethyl-4-(2-phenoxyethyl)-1,2,4-triazol-3-
Prestw-1152		Nefazodone hydrochloride	82752-99-6	506.48	<chem>N1(C(N(=C1)CC)CCCN1CCN(c2cc(Cl)ccc2)CC1)=O)CCOc1cccc1</chem>	4-amino-N-(1-benzylpiperidin-4-yl)-5-chloro-2-methoxybenzamide (E)-but-2-enedioic acid
Prestw-380		Clebopride maleate	84370-95-6	489.96	<chem>c1(C(NC2CCN(Cc3cccc3)CC2)=O)cc(c(c1)Cl)N)OC</chem>	

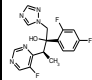
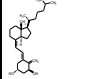
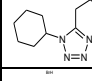
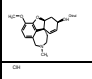
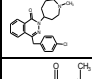
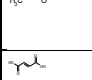
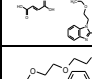
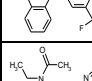
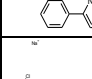
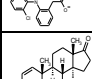
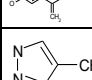
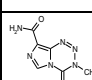
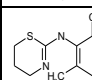
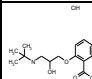
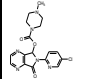
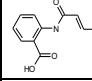
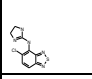
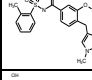
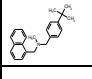
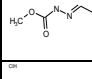
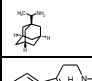
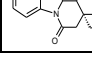

Prestw-426		Buflomedil hydrochloride	35543-24-9	343.85	<chem>c1(c(cc(cc1OC)OC)OC)C(=O)CCCN1CCCC1</chem>	4-pyrrolidin-1-yl-1-(2,4,6-trimethoxyphenyl)butan-1-one hydrochloride
Prestw-1393		Dibenzepine hydrochloride	315-80-0	331.85	<chem>N1(C(c2c(N(c3c1cccc3)C)cccc2)=O)CCN(C)C</chem>	5-[2-(dimethylamino)ethyl]-11-methylbenzo[b][1,4]benzodiazepin-6-one hydrochloride
Prestw-428		Roxatidine Acetate hydrochloride	93793-83-0	384.91	<chem>N1(Cc2cc(OCCCNC(=O)COC(=O)C)ccc2)CCCCC1</chem>	[2-oxo-2-[3-[3-(piperidin-1-ylmethyl)phenoxy]propylamino]ethyl] acetate hydrochloride
Prestw-1505		Valacyclovir hydrochloride	124832-27-5	360.80	<chem>c1\2c(non1COCCOC([C@@H](N)C(C)C)=O)C(N(C(=N2)))N=O</chem>	2-[(2-amino-6-oxo-3H-purin-9-yl)methoxy]ethyl (2S)-2-amino-3-methylbutanoate hydrochloride
Prestw-430		Cisapride	81098-60-4	465.96	<chem>c1(N(C[C@@H]2[C@@H](CN(CC2)CCCOc2cc(F)cc2)OC)=O)c(cc(c(c1)C)N)OC</chem>	4-amino-5-chloro-N-[1-[3-(4-fluorophenoxy)propyl]-3-methoxy-piperidin-4-yl]-2-methoxybenzamide
Prestw-1303		Pefloxacin	70458-92-3	333.37	<chem>C=1(\C(c2c(N(C1)CC)cc(N1CCN(CC1)C)c(c2)F)=O)/C(=O)O</chem>	1-ethyl-6-fluoro-7-(4-methylpiperazin-1-yl)-4-oxoquinoline-3-carboxylic acid
Prestw-432		Corticosterone	50-22-6	346.47	<chem>[C@]12([C@@]([C@]3([C@@]([C@@]4(C(=C/C(=O)CC4)CC3)C)([C@H](C1)O)[H])[H])(CC[C@H]2C(=O)CO)[H])C</chem>	(11beta)-11,21-dihydroxypregn-4-ene-3,20-dione
Prestw-433		Cyanocobalamin	68-19-9	1355.40	<chem>[Co+](N7C8(C1N=C(C(C1CC(=O)N)(CCC(=O)NCC(OP(=O)(O-))OC2C(OC(C2O)N4c3c(cc(c(c3)C)C)N=C4)CO)C)C(C=C5N=C(C(C5CCC(=O)N)(C)C)C=C6N=C(C(C6CCC(=O)O)O)O</chem>	
Prestw-434		Cefadroxil	50370-12-2	363.39	<chem>N1\2C([C@H]([C@]1(S(C=C2=C(O)O)C)[H])NC([C@@H](c1ccc(cc1)O)N)=O)=O</chem>	(6R,7R)-7-[(2R)-2-amino-2-(4-hydroxyphenyl)acetyl]amino-3-methyl-8-oxo-5-thia-1-azabicyclo[4.2.0]oct-2-ene-2-
Prestw-435		Cyclosporin A	59865-13-3	1202.64	<chem>N1(C([C@@H](N(C([C@@H](N(C([C@@H](N(C([C@@H](N(C(C(C(C([C@@H](N(C([C@@H]1([C@@H]([C@@H](C/C(C(C)O)[H])=O)C)=O)C)=O)C)C(C)C)=O)C)C)C)=O</chem>	
Prestw-436		Digitoxigenin	143-62-4	374.53	<chem>[C@]12([C@@]([C@]3([C@@]([C@@]4(C(=C/C(=O)CC4)CC[C@@]1([C@@]3([C@]([C@]2)1[H])(C[C@H](CC3)O)[H])C)[H])C)O</chem>	3-[[3S,5R,8R,9S,10S,13R,14S,17R]-3,14-dihydroxy-10,13-dimethyl-
Prestw-437		Digoxin	20830-75-5	780.96	<chem>[C@]12([C@@]([C@]3([C@@]([C@@]4(C(=C/C(=O)CC4)CC[C@@]1([C@@]3([C@]([C@]2)1[H])(C[C@H](CC3)O)[H])C)[H])C)O</chem>	
Prestw-438		Doxorubicin hydrochloride	25316-40-9	579.99	<chem>c12c(Cc3c(C1=O)cccc3OC)=O)c(c1c2O)C[C@]([C@@H]1O[C@@H]1O[C@H]([C@H]([C@H](C1)N)O)C(C=O)CO)O</chem>	(1S,3S)-3-Glycoloyl-3,5,12-trihydroxy-10-methoxy-6,11-dioxo-1,2,3,4,6,11-hexahydro-1-tetracyclic 3-
Prestw-439		Carbimazole	22232-54-8	186.23	<chem>N1(C(N(C=C1)C)S)C(=O)OCC</chem>	ethyl 3-methyl-2-sulfanylideneimidazole-1-carboxylate
Prestw-440		Epiandrosterone	481-29-8	290.45	<chem>[C@]12([C@@]([C@]3([C@@]([C@@]4(C(=C/C(=O)CC4)CC[C@@]1([C@@]3([C@]([C@]2)1[H])(C[C@H](CC2)O)[H])[H])C</chem>	(3S,5S,8R,9S,10S,13S,14S)-3-hydroxy-10,13-dimethyl-1,2,3,4,5,6,7,8,9,11,12,14,15,16-
Prestw-441		Estradiol-17 beta	50-28-2	272.39	<chem>[C@]12([C@@]([C@]3([C@@]([C@@]4(C(=C/C(=O)CC4)CC[C@@]1([C@@]3([C@]([C@]2)1[H])(C[C@H](C)O)[H])C</chem>	(8R,9S,13S,14S,17S)-13-methyl-6,7,8,9,11,12,14,15,16,17-decahydrocyclopenta[a]phen
Prestw-1380		Clobutinol hydrochloride	1215-83-4	292.25	<chem>C(C(CN(C)C)C)(Cc1ccc(Cl)cc1)(O)C</chem>	1-(4-chlorophenyl)-4-(dimethylamino)-2,3-dimethylbutan-2-ol hydrochloride
Prestw-443		Gabazine bromide	105538-73-6	368.23	<chem>[n+]1(nc(c2ccc(cc2)OC)ccc1N)CCCC(=O)O</chem>	4-[6-amino-3-(4-methoxyphenyl)pyridazin-1-yl]butanoic acid hydrobromide
Prestw-1156		Oxcarbazepine	28721-07-5	252.28	<chem>N1(c2c(C(Cc3c1cccc3)=O)cccc2)C(=O)N</chem>	5-oxo-6H-benzo[b][1]benzazepine-11-carboxamide
Prestw-445		Cyclobenzaprine hydrochloride	6202-23-9	311.86	<chem>C/1(\c2c(\C=C/c3c1cccc3)cccc2)=C1CCN(C)C</chem>	3-(dibenzo[1,2-a:1',2'-e][7]annulen-11-ylidene)-N,N-dimethylpropan-1-amine hydrochloride
Prestw-446		Carteolol hydrochloride	51781-21-6	328.84	<chem>N1c2c(CCC1=O)c(OCC(CNC(C)C)C)O)ccc2</chem>	5-[3-(tert-butylamino)-2-hydroxypropoxy]-3,4-dihydro-1H-quinolin-2-one hydrochloride
Prestw-447		Hydrocortisone base	50-23-7	362.47	<chem>[C@]12([C@@]([C@]3([C@@]([C@@]4(C(=C/C(=O)CC4)CC[C@@]1([C@@]3([C@]([C@]2)1[H])(C[C@H](C)O)[H])[H])C</chem>	(8S,9S,10R,11S,13S,14S,17R)-11,17-dihydroxy-17-(2-hydroxyacetyl)-10,13-dimethyl-
Prestw-448		Hydroxytacrine maleate (R,S)	118909-22-1	330.34	<chem>c12c(c3c(nc1CCCC2O)cccc3)N</chem>	9-amino-1,2,3,4-tetrahydroacridin-4-ol (Z)-but-2-enedioic acid

Prestw-1358		Vatalanib	212141-54-3	346.82	<chem>c1(nnc2c2c1cccc2)Cc1ccccc1)Nc1ccc(Cl)cc1</chem>	N-(4-chlorophenyl)-4-(pyridin-4-ylmethyl)phthalazin-1-amine
Prestw-1295		Itopride	122898-67-3	358.44	<chem>C(c1cc(c(cc1)OC)OC)(NCc1ccc(cc1)OCCN(C)C)=O</chem>	N-[[4-[2-(dimethylamino)ethoxy]phenylmethyl]-3,4-dimethoxybenzamide
Prestw-473		Cefotetan	69712-56-7	575.62	<chem>[C@@]1(C(N2[C@@]1(S(C)C(=C2)C(=O)O)CSc1n(nnn1)C)[H])=O)(NC(C1SiC(=C1(C(=O)N)C(=O)O)S1)=O)O</chem>	[carbamoyl(carboxy)methylidene]-1,3-dithietane-2-amido]-7-methoxy-3-[[1-methyl-1H-
Prestw-1254		Fentiazac	18046-21-4	329.81	<chem>n1c(c(sc1c1cccc1)CC(=O)O)c1ccc(cc1)Cl</chem>	2-[4-(4-chlorophenyl)-2-phenyl-1,3-thiazol-5-yl]acetic acid
Prestw-475		Brompheniramine maleate	980-71-2	435.32	<chem>C(CCN(C)C)(c1ccc(cc1)Br)c1ncccc1</chem>	3-(4-bromophenyl)-N,N-dimethyl-3-pyridin-2-ylpropan-1-amine (Z)-but-2-enedioic acid
Prestw-476		Primaquine diphosphate	63-45-6	455.34	<chem>c1(c2c(cc(c1)OC)ccc2)NC(CCCN)C</chem>	4-N-(6-methoxyquinolin-8-yl)pentane-1,4-diamine phosphoric acid
Prestw-477		Progesterone	57-83-0	314.47	<chem>[C@]12([C@]([C@]3([C@@]([C@@]4(\C=C/C(=O)CC4)CC3)C)C)1)[H])[H](CC[C@@H]2C(=O)C)[H]C</chem>	(8S,9S,10R,13S,14S,17S)-17-acetyl-10,13-dimethyl-1,2,6,7,8,9,11,12,14,15,16,17-
Prestw-478		Felodipine	72509-76-3	384.26	<chem>C=1(\C(\C(=N/C1/C)C)C(=O)OC)c1c(Cl)ccc1)Cl)/C(=O)OCC</chem>	5-O-ethyl 3-O-methyl 4-(2,3-dichlorophenyl)-2,6-dimethyl-1,4-dihydropyridine-3,5-dicarboxylate
Prestw-1325		Raclopride	84225-95-6	347.24	<chem>c1(c(c(cc(c1)OC)Cl)O)C(NC[C@H]1N(CCC1)CC)=O</chem>	3,5-dichloro-N-[[2-(2S)-1-ethylpyrrolidin-2-yl]methyl]-2-hydroxy-6-methoxybenzamide
Prestw-1385		Closantel	57808-65-8	663.08	<chem>c1(C(Nc2cc(c(cc2)C)C#N)c2ccc(cc2)Cl)C(=O)c(c(cc(c1)O)O</chem>	N-[5-chloro-4-[(4-chlorophenyl)-cyanomethyl]-2-methylphenyl]-2-hydroxy-3,5-diiodobenzamide
Prestw-481		Serotonin hydrochloride	153-98-0	212.68	<chem>[nH]1cc(c2c1ccc(c2)O)CCN</chem>	3-(2-aminoethyl)-1H-indol-5-ol hydrochloride
Prestw-482		Cefotiam hydrochloride	61622-34-2	598.56	<chem>N1\2C([C@]([C@]1(S(C)C(=C2)C(=O)O)CSc1n(nnn1)C)N(C)C)[H])(NC(Cc1nc(sc1)N)=O)[H])=O</chem>	(6R,7R)-7-[[2-(2-amino-1,3-thiazol-4-yl)acetyl]amino]-3-[[1-[2-(dimethylamino)ethyl]tetrazol-
Prestw-1336		Rofecoxib	162011-90-7	314.36	<chem>S(c1ccc(/C2=C/C(OC2)=O)\c2cccc2)cc1)(=O)(=O)C</chem>	3-(4-methylsulfonylphenyl)-4-phenyl-2H-furan-5-one
Prestw-484		Benperidol	2062-84-2	381.45	<chem>C1(N(c2c(N1)cccc2)C1CCN(CC1)CCCC(c1ccc(cc1)F)=O)=O</chem>	1-{1-[4-(4-fluorophenyl)-4-oxobutyl]piperidin-4-yl}-1,3-dihydro-2H-benzimidazol-2-one
Prestw-485		Cefaclor hydrate	70356-03-5	385.83	<chem>N1\2C([C@H]([C@H]1S(C)C(=C2)C(=O)O)C)NC([C@@H]1c1cccc1)N)=O=O</chem>	(6R,7R)-7-[[[(2R)-2-amino-2-phenylacetyl]amino]-3-chloro-8-oxo-5-thia-1-azabicyclo[4.2.0]oct-2-ene-2-
Prestw-486		Colistin sulfate	1264-72-8	1253.54	<chem>[H][C@]1(NC(=O)[C@H](CCN)NC(=O)[C@H](CCN)NC(=O)[C@H](CC(C)C)NC(=O)[C@H]([C@H](CC(C)C)NC(=O)[C@H](CCN)NC(=O)[C@H](CCNC(=O)N)C(=O)[C@H](CCN)NC(=O)[C@H]([C@H]([C@H](C1)N)O)C)[H])(C(=O)O)O</chem>	(7S,9S)-7-[(2R,4S,5S,6S)-4-amino-5-hydroxy-6-methyloxan-2-yl]oxy-6,9,11-trihydroxy-9-(2-hydroxyacetyl)-
Prestw-487		Daunorubicin hydrochloride	23541-50-6	563.99	<chem>c12c(C(c3c(C1=O)cccc3OC)=O)c(c1c(c2)C[C@]([C@@]1(O)[C@H]1O)[C@H]([C@H]([C@H](C1)N)O)C)[H])(C(=O)O)O</chem>	(3Z)-3-(Dibenzo[b,e]thiepin-11(6H)-ylidene)-N,N-dimethyl-1-propanamine hydrochloride
Prestw-488		Dosulepin hydrochloride	897-15-4	331.91	<chem>C1(/c2c(SCc3c1cccc3)cccc2)=C)CCN(C)C</chem>	(6R,7R)-7-[[2E)-2-(2-Amino-1,3-thiazol-4-yl)-2-[[2-carboxy-2-propanyl]oxy]imino]acetyl]ami
Prestw-489		Ceftazidime pentahydrate	78439-06-2	636.66	<chem>N1\2C([C@H]([C@]1(S(C)C(=C2)C(=O)O)=O)C[n+]1cccc1)[H])NC(\C1c1nc(sc1)N)=N/OC(C(=O)O)(C)C(=O)=O</chem>	(6R,7R)-7-[[2E)-2-(2-Amino-1,3-thiazol-4-yl)-2-[[2-carboxy-2-propanyl]oxy]imino]acetyl]ami
Prestw-490		Iobenguane sulfate	103346-16-3	373.17	<chem>C(=N)(NCc1cc(I)ccc1)N</chem>	2-(3-iodobenzyl)guanidine sulfate
Prestw-491		Metixene hydrochloride	1553-34-0	345.94	<chem>C1(c2c(Sc3c1cccc3)cccc2)CC1CN(CCC1)C</chem>	1-Methyl-3-(9H-thioxanthene-9-ylmethyl)piperidine hydrochloride
Prestw-492		Nitrofurural	59-87-0	198.14	<chem>c1([N+](=O)O)c(cc1)C=NNC(=O)N</chem>	5-nitro-2-furaldehyde semicarbazone
Prestw-493		Omeprazole	73590-58-6	345.42	<chem>c1(nc2c([nH]1)ccc(c2)OC)S(Cc1c(c(c(n1)C)OC)C)=O</chem>	6-methoxy-2-[[4-(4-methoxy-3,5-dimethylpyridin-2-yl)methanesulfanyl]-1H-1,3-benzodiazole

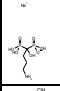
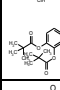
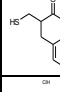
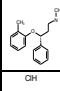
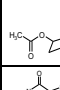
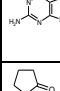
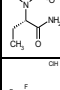
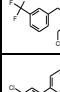
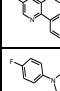
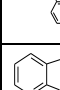
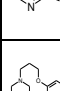
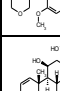
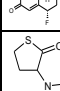
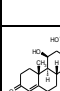
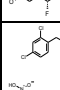
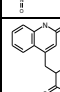
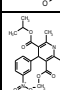
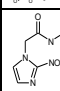
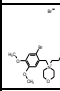
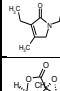
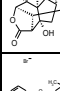
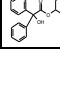

Prestw-494		Propylthiouracil	51-52-5	170.23	<chem>N1C(NC(=C/C1=O)CCC)=S</chem>	6-propyl-2-sulfanylidene-1,2,3,4-tetrahydropyrimidin-4-one
Prestw-495		Terconazole	67915-31-5	532.47	<chem>[C@@]1(c2c(cc(cc2)Cl)Cl)(Cn2ncnc2)O[C@H](CO1)COc1ccc(N2CCN(CC2)C(C)C)cc1</chem>	1-(4-((2R,4S)-2-(2,4-dichlorophenyl)-2-(1H-1,2,4-triazol-1-ylmethyl)-1,3-dioxolan-4-
Prestw-496		Tiaprofenic acid	33005-95-7	260.31	<chem>s1c(ccc1C(C)C(O)=O)C(=O)c1ccccc1</chem>	2-(5-benzoylthiophen-2-yl)propanoic acid
Prestw-497		Vancomycin hydrochloride	1404-93-9	1485.75	<chem>Clc1c5ccc(c1)C(C%10NC(=O)C(NC(=O)C3NC(=O)C(NC(=O)C(Cc2cc(c(cc2)O)c4c(c(cc3c4)O5)OC6OC(C(C6)OC7OC(C(C7)(N)C)O)C)O)C)O)NC(=O)C(NC)C(C(C)CC(=O)N)c8cc(c(cc8)O)-</chem>	
Prestw-498		Artemisinin	63968-64-9	282.34	<chem>[C@@]123[C@@]4(OC([C@H]([C@@]1(CC[C@H]([C@@]2(CC[C@]1(O4)(OO3)C)[H])[H])C)=O)[H]</chem>	(3R,5aS,6R,8aS,9R,12S,12aR)-3,6,9-trimethyloctahydro-3,12-epoxy[1,2]dioxepino[4,3-ii]isochromen-10(3H)-one
Prestw-499		Propafenone hydrochloride	34183-22-7	377.92	<chem>c1(C(=O)CCc2ccccc2)c(OCC(O)CNCCC)cccc1</chem>	1-[2-[2-hydroxy-3-(propylamino)propoxy]phenyl]-3-phenylpropan-1-one hydrochloride
Prestw-500		Ethamivan	304-84-7	223.27	<chem>C(c1cc(c(cc1)O)OC)(N(CC)CC)=O</chem>	N,N-diethyl-4-hydroxy-3-methoxybenzamide
Prestw-501		Vigabatrin hydrochloride	1391054-02-6	165.62	<chem>C(=O)(CCC(C=C)NO</chem>	4-aminohex-5-enoic acid
Prestw-502		Biperiden hydrochloride	1235-82-1	347.93	<chem>C(C1[C@]2(\C=C/[C@@](C1)(C2)[H])[H])(CCN1CCCC1)(c1ccccc1)O.Cl</chem>	1-(5-bicyclo[2.2.1]hept-2-enyl)-1-phenyl-3-piperidin-1-ylpropan-1-ol hydrochloride
Prestw-503		Cetirizine dihydrochloride	83881-52-1	461.82	<chem>N1(C(c2ccc(cc2)Cl)c2ccccc2)CCN(CC1)COC(=O)O</chem>	2-[2-[4-[(4-chlorophenyl)-phenylmethyl]piperazin-1-yl]ethoxy]acetic acid dihydrochloride
Prestw-504		Etifenin	63245-28-3	322.36	<chem>c1(NC(NC(=O)O)CC(=O)O)=O)c(cccc1CC)CC</chem>	2-[carboxymethyl-2-(2,6-diethylanilino)-2-oxoethyl]amino]acetic acid
Prestw-505		Metaproterenol sulfate, orciprenaline sulfate	5874-97-5	520.60	<chem>c1(cc(cc1)O)O)C(CNC(C)C)O.c1(cc(cc1)O)O)C(CNC(C)C)O</chem>	[2-(3,5-dihydroxyphenyl)-2-hydroxyethyl]-propan-2-ylazanium sulfate
Prestw-506		Sisomicin sulfate	53179-09-2	545.61	<chem>[C@@]H1([C@H]([C@@]H)(OC2O\C=C/CC2N)CN)(C@@]H)([C@@]H1N)N)O[C@@]H1[C@@]H([C@@]H1([C@@]H([C@@]H1(CO1)(O)C)NC)O</chem>	2-[4,6-diamino-3-[[3-amino-6-(aminomethyl)-3,4-dihydro-2H-pyran-2-yl]oxy]-2-hydroxycyclohexyl]oxy-5-
Prestw-1159		Sibutramine hydrochloride	125494-59-9	316.32	<chem>C1(C(N(C)C)CC(C)C)(c2ccc(cc2)Cl)CCC1</chem>	1-[1-(4-chlorophenyl)cyclobutyl]-N,N,3-trimethylbutan-1-amine hydrochloride
Prestw-110		Acenocoumarol	152-72-7	353.33	<chem>Cl1(=C(c2c(OC1=O)cccc2)O)C(c1ccc([N+](=O)O)cc1)CC(=O)C</chem>	4-hydroxy-3-[1-(4-nitrophenyl)-3-oxobutyl]chromen-2-one
Prestw-509		Bromperidol	10457-90-6	420.33	<chem>C1(CCN(CC1)CCCC(c1ccc(cc1)F)=O)(c1ccc(cc1)Br)O</chem>	4-[4-(4-bromophenyl)-4-hydroxypiperidin-1-yl]-1-(4-fluorophenyl)butan-1-one
Prestw-510		Cyclizine hydrochloride	303-25-3	302.85	<chem>N1(C(c2ccccc2)c2ccccc2)CCN(CC1)C</chem>	1-benzhydryl-4-methylpiperazine hydrochloride
Prestw-511		Fluoxetine hydrochloride	59333-67-4	345.80	<chem>C(c1ccc(OC(c2ccccc2)CCNC)cc1)(F)F</chem>	N-methyl-3-phenyl-3-[4-(trifluoromethyl)phenoxy]propan-1-amine hydrochloride
Prestw-512		Iohexol	66108-95-0	821.15	<chem>c1(c(c(c(c1)C(NCC(O)CO)=O))C(NCC(O)CO)=O)N(C(=O)C)C(O)CO</chem>	5-[acetyl(2,3-dihydroxypropyl)amino]-1-N,3-N-bis(2,3-dihydroxypropyl)-2,4,6-triodobenzene-1,3-
Prestw-513		Norcyclobenzaprine	303-50-4	261.37	<chem>C1(/c2c(\C=C/c3c1cccc3)cccc2)=C\CCNC</chem>	3-(5H-dibenzo[a,d][7]annulen-5-ylidene)-N-methylpropan-1-amine
Prestw-514		Pyrazinamide	98-96-4	123.12	<chem>c1(C(=O)N)ncnc1</chem>	Pyrazine-2-carboxamide
Prestw-515		Trimethadione	127-48-0	143.14	<chem>N1(C(OC(C1=O)(C)C)=O)C</chem>	3,5,5-trimethyl-1,3-oxazolidine-2,4-dione
Prestw-516		Lovastatin	75330-75-5	404.55	<chem>C=1\2/[C@]([C@@]H)(OC(=O)C)[C@@]H(CC(C)C)[C@H](\C1)(C)[C@@]H(C)[C@H]1OC(C[C@@]H)(C1)O=O)[C@H](\C=C2)C)[H]</chem>	[(1S,3R,7S,8S,8aR)-8-[2-[(2R,4R)-4-hydroxy-6-oxooxan-2-yl]ethyl]-3,7-dimethyl-1,2,3,7,8,8a-

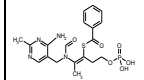
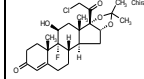
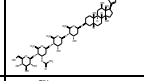
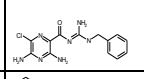
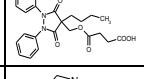
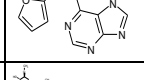
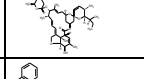
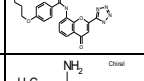
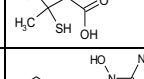
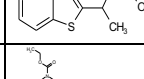
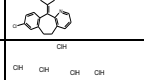
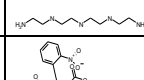
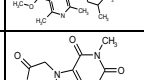
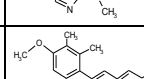
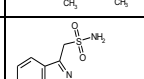
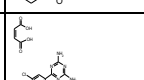
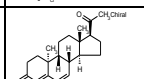
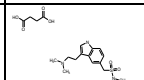
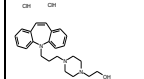
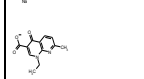
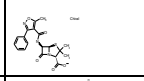
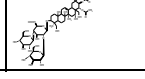

Prestw-539		Thiocolchicoside	602-41-5	563.63	<chem>C=1/2\C=C(C(C(=C/C1)SC)=O)[C@@H](NC(=O)C)C Cc1c2c(c(c(O[C@H]2[C@@H]2[C@@H]([C@H]([C@@H]([C@@H](O2)CO)O)O)c1)OC)OC</chem>	N-[1,2-dimethoxy-10-methylsulfonyl-9-oxo-3-[(2S,3R,4S,5S,6R)-3,4,5-trihydroxy-6-
Prestw-540		Clorsulon	60200-06-8	380.66	<chem>S(c1cc(S(=O)(=O)N)c(C=C(Cl)Cl)Cl)cc1N)(=O)=O)N</chem>	4-amino-6-(1,2,2-trichloroethyl)benzene-1,3-disulfonamide
Prestw-541		Ciclopirox ethanolamine	41621-49-2	268.36	<chem>N1(\C=C(C(=C1=O)/C)C1CCCC1)O</chem>	6-cyclohexyl-1-hydroxy-4-methylpyridin-2-one 2-aminoethanol
Prestw-542		Probenecid	57-66-9	285.36	<chem>S(c1ccc(C(=O)O)cc1)(N(CCC)CCC)(=O)=O</chem>	4-(dipropylsulfamoyl)benzoic acid
Prestw-543		Betahistine mesylate	54856-23-4	328.41	<chem>n1c(CCNC)cccc1</chem>	N-methyl-2-pyridin-2-ylethylamine methanesulfonic acid
Prestw-544		Tobramycin	32986-56-4	467.52	<chem>[C@H]1([C@@H]([C@H]([C@@H]([C@H](O1)CO)O)N)O)[C@@H]1[C@H]([C@H]([O[C@H]2O[C@H]([C@H]([C@H]([C@H]2N)O)CN)[C@H]([C@H]1N)N)O</chem>	(2S,3R,4S,5S,6R)-4-amino-2-[[1S,2S,3R,4S,6R)-4,6-diamino-3-[(2R,3R,5S,6R)-3-amino-6-(aminomethyl)-5-
Prestw-545		Tetramisole hydrochloride	5086-74-8	240.76	<chem>C/1\2=N/C(CN1CCS2)c1cccc1</chem>	(±)-2,3,5,6-Tetrahydro-6-phenylimidazo[2,1-b]thiazole hydrochloride
Prestw-546		Pregnenolone	145-13-1	316.49	<chem>[C@]12([C@]([C@]3([C@@]([C@@]4(/(C=C3)C)[C@H](CC4)O)C)CC1)H)H]H)CC[C@H]2C(=O)C)H]C</chem>	17-acetyl-10,13-dimethyl-2,3,4,7,8,9,11,12,14,15,16,17-dodecahydro-1H-cyclopenta[a]phenanthren-3-
Prestw-547		Molsidomine	25717-80-0	242.24	<chem>[N+]=(/[N-]O\C1C)=N/C(=O)OCC)N1CCOCC1</chem>	1-Ethoxy-N-(3-morpholino-5-oxadiazol-3-iumyl)methanimidate
Prestw-548		Chloroquine diphosphate	50-63-5	515.87	<chem>c12c(NC(CCCN(CC)C)C)ccnc1cc(cc2)Cl</chem>	N'-(7-Chloro-4-quinolinyl)-N,N-diethyl-1,4-pentanediamine diphosphate salt
Prestw-549		Trimetazidine diphosphate	13171-25-0	339.26	<chem>c1(c(c(CN2CCNCC2)ccc1OC)OC)OC</chem>	1-[(2,3,4-trimethoxyphenyl)methyl]piperazine diphosphate
Prestw-550		Parthenolide	20554-84-1	248.32	<chem>[C@@]12(O[C@@]1(CC/C=C/[C@]([C@@]1([C@@]2(O)C(C1=C)O)[H])([H])(C)C)H]</chem>	(1aR,7aS,10aS,10bS)-1a,5-dimethyl-8-methylene-2,3,6,7,7a,8,10a,10b-octahydrooxireno[9,10]cyclo-
Prestw-551		Hexetidine	141-94-6	339.61	<chem>N1(CN(C(C1)N)C)CC(C)CCCC)CC(CC)CCCC</chem>	1,3-bis(2-ethylhexyl)-5-methyl-1,3-diazinan-5-amine
Prestw-552		Selegiline hydrochloride	14611-52-0	223.75	<chem>C#C)N([C@@H](Cc1ccccc1)C)C</chem>	(2R)-N-methyl-1-phenyl-N-prop-2-ynylpropan-2-amine hydrochloride
Prestw-553		Pentamidine isethionate	140-64-7	592.69	<chem>C(c1ccc(cc1)O)CCCOc1ccc(C(=N)N)cc1)(=N)N</chem>	4-[5-(4-carbamimidoylphenoxy)pentoxy]benzenecarboximidamide 2-hydroxyethanesulfonic acid
Prestw-554		Tolazamide	1156-19-0	311.41	<chem>S(NC(NN1CCCCC1)=O)(c1ccc(cc1)C(=O)=O</chem>	1-(azepan-1-yl)-3-(4-methylphenyl)sulfonylurea
Prestw-555		Nifuroxazide	965-52-6	275.22	<chem>c1([N+](O)=O)oc(cc1)C=NINC(c1ccc(cc1)O)=O</chem>	4-hydroxy-N-[[5-nitrofuran-2-yl)methylene]benzohydrazide
Prestw-1144		Mirtazapine	61337-67-5	265.36	<chem>N12C(c3c(Cc4c1cccc4)cccc3)CN(CC2)C</chem>	(±)-2-methyl-1,2,3,4,10,14b-hexahydropyrazino[2,1-a]pyrido[2,3-cl[2]benzazepine
Prestw-557		Dirithromycin	62013-04-1	835.09	<chem>[C@H]12[C@@]([C@H](OC[C@H]([C@H]([C@H]([C@H]([C@H]([C@H]([C@@H]3[C@@]([C@H]([C@H](O3)C)N(C)C)O)[C@]([C@H]([C@@H]([C@@H]1C)N[C@](O2)(COCOC)H)C)O)C)C)O)C@H1C)C@([C@H]([C@@</chem>	N-
Prestw-558		Gliclazide	21187-98-4	323.42	<chem>S(NC(NN1CC2C(C1)CCC2)=O)(c1ccc(cc1)C(=O)=O</chem>	(hexahydrocyclopenta[c]pyrro-1(2H)-ylcarbamoyl)-4-methylbenzenesulfonamide
Prestw-559		DO 897/99	not available	490.48	<chem>N1(c2c(OC)cccc2)CCN(CC1)CCCCNC(c1cc2c(cc1)cccc2=O</chem>	N-[4-[4-(2-methoxyphenyl)piperazin-1-yl]butyl]naphthalene-2-carboxamide
Prestw-560		Prenylamine lactate	69-43-2	419.57	<chem>C(c1ccccc1)(c1ccccc1)CCNC(Cc1ccccc1)C</chem>	3,3-diphenyl-N-(1-phenylpropan-2-yl)propan-1-amine 2-hydroxypropanoic acid
Prestw-1188		Ziprasidone Hydrochloride	138982-67-9	449.41	<chem>c1(nsc2c1cccc2)N1CCN(CCC2c(cc3NC(Cc3c2)=O)Cl)C C1</chem>	5-[2-[4-(1,2-benzothiazol-3-yl)piperazin-1-yl]ethyl]-6-chloro-1,3-dihydroindol-2-one hydrate hydrochloride


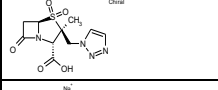
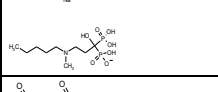
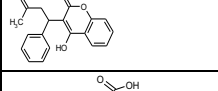
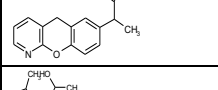

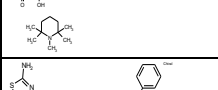
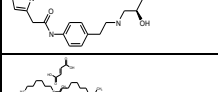
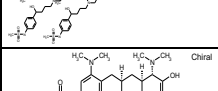
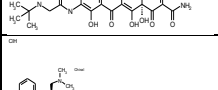
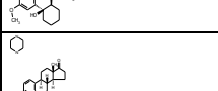
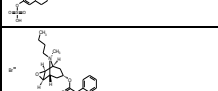
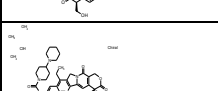
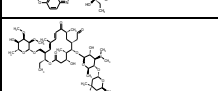
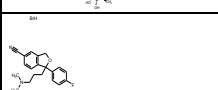
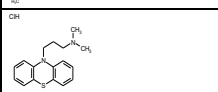
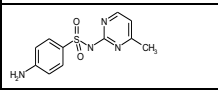
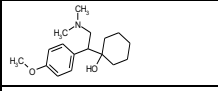
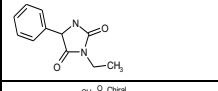
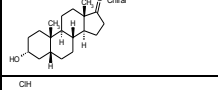
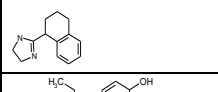
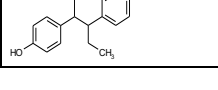

Prestw-1441		Mevastatin	73573-88-3	390.52	<chem>[C@@]12([C@H](OC(=O)[C@H](CC)C)CC=C=C1)C=C([C@@H]([C@H]2CC[C@H]1OC(C[C@@H](C1)O)=O)C)H]</chem>	[(1S,7S,8S,8aR)-8-[2-[(2R,4R)-4-hydroxy-6-oxooxan-2-yl]ethyl]-7-methyl-1,2,3,7,8,8a-
Prestw-1322		Pyridostigmine iodide	4685-03-4	308.12	<chem>C(Oc1c[n+](ccc1)C)(N)C(=O)</chem>	(1-methylpyridin-1-ium-3-yl) N,N-dimethylcarbamate iodide
Prestw-1491		Pentobarbital	76-74-4	226.28	<chem>C1(C(C(NC(N1)=O)=O)(CCC)C)CC=O</chem>	5-ethyl-5-pentan-2-yl-1,3-diazinane-2,4,6-trione
Prestw-565		Atropine sulfate monohydrate	5908-99-6	694.85	<chem>N1([C@H]2[C@@H](OC(C3CCCC3)CO)=O)C[C@H]1CC2)C.N1([C@H]2[C@@H](OC(C3CCCC3)CO)=O)C[C@H]1CC2)C</chem>	[(1R,5S)-8-methyl-8-azabicyclo[3.2.1]octan-3-yl] 3-hydroxy-2-phenylpropanoate sulfuric acid hydrate
Prestw-566		Eserine hemisulfate salt	64-47-1	648.78	<chem>[C@]12([C@@](N(c3c1cc(OC(=O)NC)cc3)C)(N(CC2)C)H]C.[C@]12([C@@](N(c3c1cc(OC(=O)NC)cc3)C)(N(CC2)C)H]C</chem>	[(3aS,8bS)-3,4,8b-trimethyl-1,2,3,3a-tetrahydropyrido[2,3-b]indol-3-ium-7-yl] N-
Prestw-1139		Itraconazole	84625-61-6	705.65	<chem>N1(C(N(N=C1)(CC)C)=O)c1ccc(N2CCN(c3ccc(OCC4OC(c5c(cc(cc5)Cl)Cl)Cn5nccn5)OC4)cc3)CC2)cc1</chem>	2-butan-2-yl-4-[4-[4-[[[2R,4S)-2-(2,4-dichlorophenyl)-2-(1,2,4-triazol-1-yl)methyl]-1,3-
Prestw-1174		Acarbose	56180-94-0	645.62	<chem>[C@H]1([C@@H]([C@H]([C@H]([C@@H]2[C@@H]([C@H]([C@H](N[C@@H]3[C@@H]([C@H]([C@@H](C(=C3)CO)O)O)[C@H](O2)C)O)O)[C@H](O1)CO)O)O)[C@H]1C[C@@H]([C@H]([C@H]([C@H]([C@@H]1CO)O)O)</chem>	
Prestw-1403		Entacapone	130929-57-6	305.29	<chem>c1([N+]([O-])=O)c(c(cc(/C=C/(C(N(CC)CC)=O)C#N)c1)O)O</chem>	(E)-2-cyano-3-(3,4-dihydroxy-5-nitrophenyl)-N,N-diethylprop-2-enamide
Prestw-1449		Nicotinamide	98-92-0	122.13	<chem>C(c1cnccc1)(=O)N</chem>	pyridine-3-carboxamide
Prestw-571		Tetracaine hydrochloride	136-47-0	300.83	<chem>C(c1ccc(NCCCC)cc1)(=O)OCCN(C)C</chem>	2-(dimethylamino)ethyl 4-(butylamino)benzoate hydrochloride
Prestw-572		Mometasone furoate	83919-23-7	521.44	<chem>[C@]12([C@@](OC(c3occc3)=O)([C@@H](C[C@]1([C@@]1([C@@]([C@@]3([C=C/C(=C3)=O)CC1)C)([C@H](C2)O)Cl)H)H)C(=O)CC)C</chem>	[(8S,9R,10S,11S,13S,14S,16R,17R)-9-chloro-17-(2-chloroacetyl)-11-hydroxy-10,13,16-trimethyl-3-oxo-5-[[4-[[6-hydroxy-2,5,7,8-tetramethyl-3,4-dihydrochromen-2-yl)methoxy]phenyl]methyl]-
Prestw-1467		Troglitazone	97322-87-7	441.55	<chem>N1C(SC(C1=O)Cc1ccc(OCC2(Oc3c(c(c(c3C)O)C)C2)C)cc1=O</chem>	yl)methoxy]phenyl]methyl]-
Prestw-574		Dacarbazine	4342-03-4	182.19	<chem>c1(c(N=NN(C)C)[nH]cn1)C(=O)N</chem>	(5E)-5-(dimethylamino)hydrazinylidene]imidazole-4-carboxamide
Prestw-1351		Tenatoprazole	113712-98-4	346.41	<chem>n1c([nH]c2c1nc(cc2)OC)S(Cc1c(c(c(cn1)C)OC)C)=O</chem>	5-methoxy-2-[4-methoxy-3,5-dimethylpyridin-2-yl)methylsulfanyl]-1H-imidazo[4,5-b]pyridine
Prestw-576		Acetopromazine maleate salt	3598-37-6	442.54	<chem>N1(c2c(Sc3c1cccc3)ccc(c2)C(=O)C)CCCN(C)C</chem>	1-[10-[3-(dimethylamino)propyl]phenothiazin-2-yl]ethanone (Z)-but-2-enedioic acid
Prestw-1271		Escitalopram oxalate	128196-01-0	414.44	<chem>[C@]1(c2c(CO1)cc(C#N)cc2)(c1ccc(cc1)F)CCCN(C)C</chem>	(1S)-1-[3-(dimethylamino)propyl]-1-(4-fluorophenyl)-3H-2-benzofuran-5-carbonitrile
Prestw-1158		Ropinirole hydrochloride	91374-20-8	296.84	<chem>N1C(Cc2c1cccc2CCN(CCC)CCC)=O</chem>	4-[2-(dipropylamino)ethyl]-1,3-dihydro-2H-indol-2-one hydrochloride
Prestw-1297		Lacidipine	103890-78-4	455.56	<chem>C=1(\C(=C(/N(C1)C)C)C(=O)OCC)c1c(/C=C/C(OC(C)C)C)C)=O)ccc1)/C(=O)OCC</chem>	Diethyl 2,6-dimethyl-4-[2-[(E)-3-[(2-methylpropan-2-yl)oxy]-3-oxoprop-1-enyl]phenyl]-1,4-dihydropyridine-3,5-
Prestw-1228		Argatroban	74863-84-6	508.64	<chem>S(c1c2NCC(Cc2ccc1)C)(N[C@H](C(N1[C@@H](C(=O)O)C[C@@H](CC1)C)=O)CCNC(=N)N)(=O)=O</chem>	(2R,4R)-1-[(2S)-5-(diaminomethylideneamino)-2-[[[3S]-3-methyl-1,2,3,4-tetrahydroquinolin-8-
Prestw-1328		Reboxetine mesylate	98769-81-4	409.51	<chem>O([C@H]([C@@]1(OCCN1)H)c1ccccc1)c1c(OCC)ccc1</chem>	(2R)-2-[(R)-(2-ethoxyphenoxy)phenylmethyl]morpholine methanesulfonic acid
Prestw-1498		Camylofine chlorhydrate	54-30-8	393.40	<chem>C(c1cccc1)NCCN(CC)CC(OCC(C)C)=O</chem>	3-methylbutyl 2-[2-(diethylamino)ethylamino]-2-phenylacetate dihydrochloride
Prestw-583		Papaverine hydrochloride	61-25-6	375.86	<chem>c12c(nccc1cc(c2)OC)OC)Cc1cc(c(cc1)OC)OC</chem>	1-[(3,4-dimethoxyphenyl)methyl]-6,7-dimethoxyisoquinoline hydrochloride
Prestw-584		Yohimbine hydrochloride	65-19-0	390.91	<chem>c12c(c3c([nH]1)cccc3)CN1[C@@]2(C[C@@]2([C@@H](C(=O)OC)[C@H](CC[C@]2(C1)H)O)H)H]</chem>	(1S,15R,18S,19R,20S)-18-hydroxy-1,3,11,12,14,15,16,17,18,19

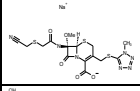
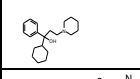
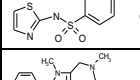
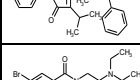
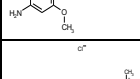
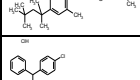
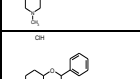
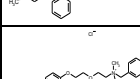
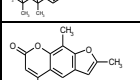
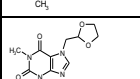
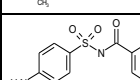
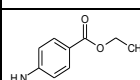
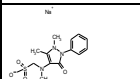
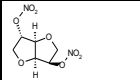
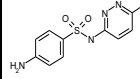
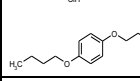
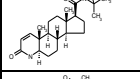
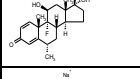
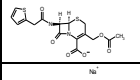
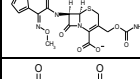
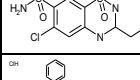
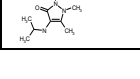

Prestw-1500		Voriconazole	137234-62-9	349.32	<chem>[C@](c1c(cc(cc1)F)F)([C@H](c1c(F)cn1)C)(Cn1ncnc1)O</chem>	(2R,3S)-2-(2,4-difluorophenyl)-3-(5-fluoropyrimidin-4-yl)-1-(1,2,4-triazol-1-yl)butan-2-ol
Prestw-1211		Alfalcidol	41294-56-8	400.65	<chem>[C@]12([C@](\C=C/C=C1/C([C@H](C[C@@H](C3)O)=O)C)CCC1)(C[C@H]2[C@@H](CCCC(C)C)[H])C</chem>	(1R,3S,5Z)-5-[(2E)-2-[(1R,3aS,7aR)-7a-Methyl-1-[(2R)-6-methylheptan-2-yl]-2,3,3a,5,6,7-hexahydro-1H-
Prestw-587		Cilostazol	73963-72-1	369.47	<chem>n1(nnnc1CCCCO)c2c2c(NC(=O)CC2)cc1)C1CCCCC1</chem>	6-[4-(1-cyclohexyltetrazol-5-yl)butoxy]-3,4-dihydro-1H-quinolin-2-one
Prestw-588		Galanthamine hydrobromide	1953-04-4	368.27	<chem>[C@]1'23c4c(O[C@H]1[C@H](\C=C2)O)c(ccc4CN(CC3)C)OC</chem>	(4aS,6R,8aS)-5,6,9,10,11,12-hexahydro-3-methoxy-11-methyl-4aH-[1]benzofuro[3a,3,2-ef][2]
Prestw-1130		Azelastine hydrochloride	79307-93-0	418.37	<chem>N1(/N=C(\c2c(C1=O)cccc2)/Cc1ccc(Cl)cc1)C1CCN(CCC1)C</chem>	4-[(4-chlorophenyl)methyl]-2-(1-methylazepan-4-yl)phthalazin-1-one hydrochloride
Prestw-1409		Etretnate	54350-48-0	354.49	<chem>c1(c(c(c(cc1)OC)C)C)C=C\C=C\C=C\C=C\C=C(=O)OCC)C)C</chem>	ethyl (2E,4E,6E,8E)-9-(4-methoxy-2,3,6-trimethylphenyl)-3,7-dimethylnona-2,4,6,8-
Prestw-1274		Emedastine	87233-61-2	534.57	<chem>c1(nc2c(n1COCC)cccc2)N1CCN(CCC1)C</chem>	1-(2-ethoxyethyl)-2-(4-methyl-1,4-diazepan-1-yl)benzimidazole
Prestw-1407		Etofenamate	30544-47-9	369.34	<chem>C(c1cc(Nc2c(C(=O)OCCOCCO)cccc2)ccc1)(F)(F)F</chem>	2-(2-hydroxyethoxy)ethyl 2-[3-(trifluoromethyl)anilino]benzoate
Prestw-1369		Zaleplon	151319-34-5	305.34	<chem>n12c(c(c1)C#N)nccc2c1cc(N(C(=O)C)CC)ccc1</chem>	N-[3-(3-cyanopyrazolo[1,5-a]pyrimidin-7-yl)phenyl]-N-ethylacetamide
Prestw-594		Diclofenac sodium	15307-79-6	318.14	<chem>N(c1c(Cl)cccc1Cl)c1c(CC([O-])=O)cccc1</chem>	2-[(2,6-Dichlorophenyl)amino]benzeneacetic acid monosodium salt
Prestw-1410		Exemestane	107868-30-4	296.41	<chem>[C@@]1'2(\C(C[C@@]3([C@@]1(CC[C@]1([C@]3)CCC1=O)[H])C)[H])[H]=C)C/C(\C=C2)=O)C</chem>	(8R,9S,10R,13S,14S)-10,13-dimethyl-6-methylidene-7,8,9,11,12,14,15,16-octahydrocyclopenta[phen
Prestw-1499		Fomepizole	7554-65-6	82.11	<chem>n1[nH]cc(c1)C</chem>	4-methyl-1H-pyrazole
Prestw-1183		Temozolomide	85622-93-1	194.15	<chem>n12c(c(nc1)C(=O)N)N=N(C2=O)C</chem>	3-methyl-4-oxoimidazo[5,1-d][1,2,3,5]tetrazine-8-carboxamide
Prestw-598		Xylazine	7361-61-7	220.34	<chem>C/1(Nc2c(ccc2C)C)=N/CCCS1</chem>	N-(2,6-dimethylphenyl)-5,6-dihydro-4H-1,3-thiazin-2-amine
Prestw-1132		Celiprolol hydrochloride	57470-78-7	415.96	<chem>C(Nc1cc(c(OCC(NC(C)C)C)O)cc1)C(=O)C(N(CC)CC)=O</chem>	3-[3-acetyl-4-[3-(tert-butylamino)-2-hydroxypropoxy]phenyl]-1,1-diethylurea hydrochloride
Prestw-1367		Zopiclone	43200-80-2	388.82	<chem>N1(C(c2c(C1=O)nccn2)OC(N1CCN(CC1)C)=O)c1ncc(cc1)Cl</chem>	[6-(5-chloropyridin-2-yl)-5-oxo-7H-pyrrolo[3,4-b]pyrazin-7-yl]-4-methylpiperazine-1-carboxylate
Prestw-1198		Tranilast	53902-12-8	327.34	<chem>c1(c(NC(\C=C/c2cc(c(cc2)OC)O)=O)cccc1)C(=O)O</chem>	2-[(E)-3-(3,4-dimethoxyphenyl)prop-2-enyl]amino]benzoic acid
Prestw-1182		Tizanidine hydrochloride	51322-75-9	290.18	<chem>c12c(c(cc1nns2)Cl)N/C1=N/CCN1</chem>	5-chloro-N-(4,5-dihydro-1H-imidazol-2-yl)-2,1,3-benzothiadiazol-4-amine hydrochloride
Prestw-1364		Zafirlukast	107753-78-6	575.69	<chem>S(NC(c1cc(c(Cc2c3c(n(c2)C)ccc(NC(OC2CCCC2)=O)c3)cc1)OC)=O)(c1c(C)cccc1)(=O)=O</chem>	cyclopentyl N-[3-[(2-methoxy-4-[(2-methylphenyl)sulfonyl]carbonyl]phenyl)methyl]-1-
Prestw-1252		Butenafine Hydrochloride	101828-21-1	353.94	<chem>c1(c2c(ccc1)cccc2)CN(Cc1ccc(C(C)C)cc1)C</chem>	1-(4-tert-butylphenyl)-N-methyl-N-(naphthalen-1-ylmethyl)methanamine
Prestw-1121		Carbadox	6804-07-5	262.23	<chem>[n+](c1(c[n+](c2c1cccc2)[O-])C=NNC(=O)OC)[O-]</chem>	Methyl (2E)-2-[(1,4-dioxido-2-quinoxaliny)methylene]hydrazinecarboxylate
Prestw-1331		Rimantadine Hydrochloride	13392-28-4	215.77	<chem>[C@]12[C@]3[C@C@](C1)C[C@](C2)(C3)[H])[H]C(N)C</chem>	1-(1-adamantyl)ethanamine hydrochloride
Prestw-607		Ebumamonine (-)	4880-88-0	294.40	<chem>n12c3c(c4c1cccc4)CCN1[C@]3([C@](CC2=O)(CCC1)C)C[H]</chem>	(4a1S,13aS)-13a-Ethyl-2,3,4a1,5,6,13a-hexahydro-1H-indolo[3,2,1-de]pyrido[3,2,1-de]-

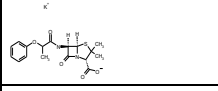
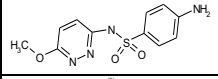
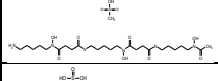
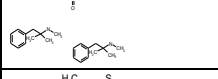
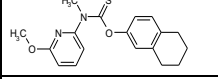
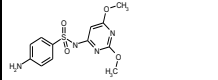
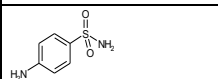
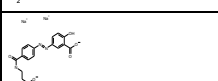
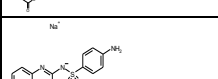
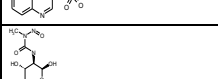
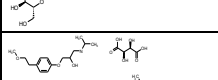
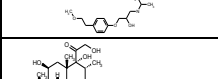
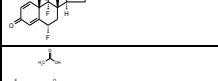
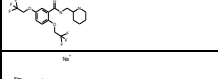
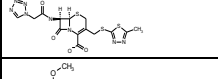
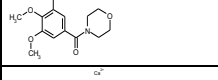
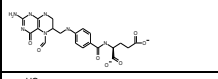
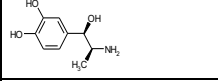
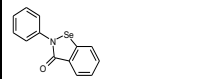
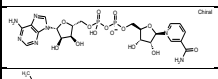

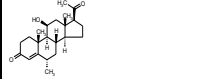
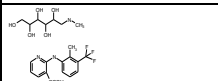
Prestw-1460		Oxibendazol	20559-55-1	249.27	<chem>c1(nc2c([nH]1)ccc(c2)OCCC)NC(=O)OC</chem>	methyl N-(6-propoxy-1H-benzimidazol-2-yl)carbamate
Prestw-1292		Ipsapirone	95847-70-4	401.49	<chem>S1(N(C(c2c1cccc2)=O)CCCCN1CCN(c2ncccc2)CC1)=O=O</chem>	1,1-dioxo-2-[(4-(4-pyrimidin-2-yl)piperazin-1-yl)butyl]-1,2-benzothiazol-3-one
Prestw-1284		Hydroxychloroquine sulfate	747-36-4	433.96	<chem>c12c(NC(CCCN(CCO)CC)CC)ccncc1cc(cc2)Cl</chem>	2-[4-[(7-chloroquinolin-4-yl)amino]pentyl]ethylamino]ethanol sulfuric acid
Prestw-1431		Loracarbef	121961-22-6	349.78	<chem>N1\2[C@H]([C@H]1CC\C(=C2\C(=O)O)C)NC([C@H]1C1CCCC1)N=O=O</chem>	(6R,7S)-7-[(2S)-2-amino-2-phenylacetamido]amino]-3-chloro-8-oxo-1-azabicyclo[4.2.0]oct-
Prestw-1501		Fenipentol	583-03-9	164.25	<chem>c1(C(O)CCCC)cccc1</chem>	1-phenylpentan-1-ol
Prestw-1503		Diosmin	520-27-4	608.56	<chem>c12C(/C=C(\Oc1cc(O)[C@H]1[C@H]([C@H]([C@@H]([C@H](O1)CO)[C@H]1[C@@H]([C@@H]([C@H]([C@@H]([C@@H](O1)C)O)O)O)O)O)O)cc2O)/c1cc(c(cc1)OC)O=O</chem>	5-hydroxy-2-(3-hydroxy-4-methoxyphenyl)-7-[(2S,3R,4S,5S,6R)-3,4,5-trihydroxy-6-
Prestw-1177		Carbidopa	28860-95-9	226.23	<chem>[C@](C(=O)O)(Cc1cc(c(cc1)O)O)(NN)C</chem>	(2S)-3-(3,4-dihydroxyphenyl)-2-hydrazinyl-2-methylpropanoic acid
Prestw-1604		(-)-Emtricitabine	143491-57-0	247.25	<chem>[C@H]1(N\2C(N=C(/C(=C2)/F)N)=O)O[C@H](SC1)CO</chem>	4-amino-5-fluoro-1-[(2R,5S)-2-(hydroxymethyl)-1,3-oxathiolan-5-yl]pyrimidin-2-one
Prestw-616		Demecarium bromide	56-94-0	716.60	<chem>C(Oc1cc([N+](C)(C)C)ccc1N)(CCCCCCCCCN(C(Oc1c c([N+](C)(C)C)ccc1)=O)C)C=O</chem>	trimethyl-[3-methyl-1]-[10-methyl-3-(trimethylazaniumyl)phenoxy]carbonylaminoldecylcarbamate
Prestw-617		Quipazine dimaleate salt	150323-78-7	445.43	<chem>n1c(N2CCNCCC2)ccc2c1cccc2</chem>	2-piperazin-1-ylquinoline (Z)-but-2-enedioic acid
Prestw-1127		Acipimox	51037-30-0	154.13	<chem>[n+]1(cc(ncc1C)C(=O)O)[O-]</chem>	5-methyl-4-oxidopyrazin-4-ium-2-carboxylic acid
Prestw-619		Diflorasone Diacetate	33564-31-7	494.54	<chem>[C@]1\12[C@@]3([C@]1[C@]4([C@@]1[C@]([C@@]1[C@]H)(C4)C)C(OC(=O)C)=O)OC(=O)C[C@]([C@@]1[C@]H)C[C@@]1/C=C/C(\C(=C2)=O)F)[H]F)C</chem>	[2-[[[6S,8S,9R,10S,11S,13S,14S,16S,17R)-17-acetyloxy-6,9-difluoro-11-hydroxy-10,13,16-
Prestw-1502		Acamprostate calcium	77337-73-6	400.49	<chem>S(CCCNC(C)=O)(=O)[O-]</chem>	3-(Acetylamino)-1-propanesulfonic acid calcium salt
Prestw-1506		Mizolastine	108612-45-9	432.50	<chem>c1(n(c2c(n1)cccc2)C)c1ccc(F)cc1N1CCC(N(C=2\NC(\C=C(N2)=O)C)CC1</chem>	2-[[1-[1-[(4-fluorophenyl)methyl]benzimidazol-2-yl]piperidin-4-yl]-methylamino]-1H-pyrimidin-6-
Prestw-1217		Amisulpride	71675-85-9	369.49	<chem>c1(S(=O)(=O)CC)cc(C(NCC2N(CCC2)CC)=O)c(cc1N)OC</chem>	4-amino-N-[(1-ethylpiperidin-2-yl)methyl]-5-ethylsulfonyl-2-methoxybenzamide
Prestw-623		Pyridoxine hydrochloride	58-56-0	205.64	<chem>c1(c(c(ncc1CO)CO)O)CO</chem>	4,5-Bis(hydroxymethyl)-2-methylpyridin-3-ol
Prestw-1469		Mercaptopurine	50-44-2	152.18	<chem>c12c(N=C/NC1=S)nc[nH]2</chem>	3,7-dihydropurine-6-thione
Prestw-1134		Cytarabine	147-94-4	243.22	<chem>N1([C@H]2[C@H]([C@@H]([C@H](O2)CO)O)O)C/N=C(C=C1)N=O</chem>	4-amino-1-[(2R,3S,4S,5R)-3,4-dihydroxy-5-(hydroxymethyl)oxolan-2-yl]piperidin-2-one
Prestw-626		Racecadotril	81110-73-8	385.49	<chem>C(C(NCC(=O)OCc1cccc1)=O)(Cc1cccc1)CSC(=O)C</chem>	[(acetylsulfanyl)methyl]-3-phenylpropanoyl]aminobenzyle acetate
Prestw-627		Folic acid	59-30-3	441.41	<chem>N=1\C(c2c(N/C1/N)ccc(n2)CNc1ccc(C(N[C@H](C(=O)O)CCC(=O)O)=O)cc1=O</chem>	(2S)-2-[4-[(2-amino-4-oxo-1H-pteridin-6-yl)methylamino]benzoyl]aminolpentanedioic acid
Prestw-1129		Benazepril hydrochloride	86541-74-4	460.96	<chem>N1(C([C@@H](N[C@H](C(=O)OCC)CCc2cccc2)CCc2c1cccc2=O)CC(=O)O</chem>	2-[(3S)-3-[[[(2S)-1-ethoxy-1-oxo-4-phenylbutan-2-yl]amino]-2-oxo-4,5-dihydro-3H-1-benzazepin-1-yl]acetic
Prestw-1178		Aniracetam	72432-10-1	219.24	<chem>N1(C(c2ccc(cc2)OC)=O)C(=O)CCC1</chem>	1-(4-methoxybenzoyl)pyrrolidin-2-one
Prestw-630		Dimethisoquin hydrochloride	2773-92-4	308.85	<chem>c1(nc(cc2c1cccc2)CCCC)OCCN(C)C</chem>	2-(3-butylisoquinolin-1-yl)oxyethyl-dimethylazanium chloride

Prestw-1210		Alendronate sodium	121268-17-5	271.08	<chem>C(P([O-])(=O)O)(P(=O)(O)O)O)CCCN</chem>	(4-amino-1-hydroxy-1-phosphonobutyl)-hydroxyphosphinate sodium
Prestw-632		Dipivefrin hydrochloride	64019-93-8	387.91	<chem>C(OC1c(OC(C(C)C)C)=O)ccc(c1)C(O)CNC)(C(C)C)C=O</chem>	[2-(2,2-dimethylpropanoyloxy)-4-[1-hydroxy-2-(methylamino)ethyl]phenyl] 2,2-dimethylpropanoate
Prestw-633		Thiorphan	76721-89-6	253.32	<chem>C(C(Cc1cccc1)CS)(NCC(=O)O)=O</chem>	2-[(2-benzyl-3-sulfanylpropanoyl)amino]acetic acid
Prestw-1463		Tomoxetine hydrochloride	82248-59-7	291.82	<chem>O(c1c(C)cccc1)[C@@H](c1cccc1)CCNC</chem>	(R)-N-Methyl-gamma-(2-methylphenoxy)-benzenepropanamine hydrochloride
Prestw-1511		Aceclidine Hydrochloride	6109-70-2	205.69	<chem>C1([C@]2(CCN(C1)CC2)[H])OC(C)=O</chem>	1-azabicyclo[2.2.2]octan-3-yl acetate hydrochloride
Prestw-1488		Penciclovir	39809-25-1	253.26	<chem>c1/2c(ncn1CCC(CO)CO)C(N/C(=N2)/N)=O</chem>	2-amino-9-[4-hydroxy-3-(hydroxymethyl)butyl]-3H-purin-6-one
Prestw-1427		Levetiracetam	102767-28-2	170.21	<chem>N1(C(=O)CCC1)[C@H](C(=O)N)CC</chem>	(2S)-2-(2-oxopyrrolidin-1-yl)butanamide
Prestw-1392		Dexfenfluramine hydrochloride	3239-45-0	267.72	<chem>C(c1cc[C@H](NCC)C)ccc1)(F)F</chem>	(2S)-N-ethyl-1-[3-(trifluoromethyl)phenyl]propan-2-amine hydrochloride
Prestw-1408		Etoricoxib	202409-33-4	358.85	<chem>S(c1ccc(c2c(nc(c2)Cl)c2cnc(cc2)C)cc1)(=O)=O)C</chem>	5-chloro-2-(6-methylpyridin-3-yl)-3-(4-methylsulfonylphenyl)pyridine
Prestw-1341		Sertindole	106516-24-9	440.95	<chem>n1(cc(c2c1ccc(c2)Cl)C1CCN(CCN2C(NCC2)=O)CC1)c1ccc(cc1)F</chem>	1-[2-[4-[5-chloro-1-(4-fluorophenyl)indol-3-yl]piperidin-1-yl]ethyl]imidazolidin-2-one
Prestw-641		Sulmazole	73384-60-8	287.34	<chem>c1(nc2c([nH]1)cccn2)c1c(cc(S(=O)C)cc1)OC</chem>	2-(2-methoxy-4-methylsulfinylphenyl)-1H-imidazo[4,5-b]pyridine
Prestw-1270		Gefitinib	184475-35-2	446.91	<chem>c12c(ncnc1cc(c2)O)CCCN1CCOCC1)OC)Nc1cc(c(cc1)F)Cl</chem>	N-(3-chloro-4-fluorophenyl)-7-methoxy-6-(3-morpholin-4-ylpropoxy)quinazolin-4-amine
Prestw-643		Flunisolide	3385-03-3	434.51	<chem>[C@@]12([C@@]3([C@]([C@]4([C@@]([C@@]5([C@]([C@H](C4)F)=C/C(=O)CC5)C)([C@H](C3)O)[H])[H])[C@H]1OC(O2)(C)C)[H])C(=O)CO</chem>	(1S,2S,4R,8S,9S,11S,12S,13R,19S)-19-fluoro-11-hydroxy-8-(2-hydroxyacetyl)-6,6,9,13-tetramethyl-5,7-
Prestw-644		N-Acetyl-DL-homocysteine Thiolactone	1195-16-0	159.21	<chem>C1(C(NC(=O)C)CCS1)=O</chem>	N-(2-oxothiolan-3-yl)acetamide
Prestw-645		Flurandrenolide	1524-88-5	436.53	<chem>[C@@]12([C@@]3([C@]([C@]4([C@@]([C@@]5([C@]([C@H](C4)F)=C/C(=O)CC5)C)([C@H](C3)O)[H])[H])[C@H]1OC(O2)(C)C)[H])C(=O)CO</chem>	6-Fluoro-11,21-dihydroxy-16,17-[(1-methylethylidene)bis(oxy)]-(6alpha,11beta,16alpha)-(Z)-1-(2,4-dichlorophenyl)-N-[(2,4-dichlorophenyl)methoxy]-2-imidazol-1-ylethanamine nitric acid
Prestw-1125		Oxiconazole Nitrate	64211-46-7	492.15	<chem>C(\c1c(cc(c1)Cl)Cl)/Cn1cnc1)=N/OCc1c(cc(c1)Cl)Cl</chem>	2-[[4-chlorobenzoyl]amino]-3-(2-oxo-1H-quinolin-4-yl)propanoic acid
Prestw-1166		Rebamipide	90098-04-7	370.80	<chem>C1(=C\C(Nc2c1cccc2)=O)/CC(NC(c1ccc(cc1)Cl)=O)C(=O)O</chem>	2-[[4-chlorobenzoyl]amino]-3-(2-oxo-1H-quinolin-4-yl)propanoic acid
Prestw-1154		Nilvadipine	75530-68-6	385.38	<chem>C=1(\C(\C(=C/N/C1/C)C#N)C(=O)OC)c1cc([N+](=[O-])=O)ccc1)/C(OC(C)C)=O</chem>	3-O-methyl 5-O-propan-2-yl 2-cyano-6-methyl-4-(3-nitrophenyl)-1,4-dihydropyridine-3,5-
Prestw-649		Etanidazole	22668-01-5	214.18	<chem>n1(ccnc1[N+](=[O-])=O)CC(=O)NCCO</chem>	N-(2-hydroxyethyl)-2-nitro-1H-imidazole-1-acetamide
Prestw-1601		Pinaverium bromide	53251-94-8	591.43	<chem>C1([C@]2[C@C@]1(CCC2CCOCC[N+])1(Cc2c(cc(c2)OC)OC)Br)CCOCC1)[H])[H])(C)C</chem>	4-[(2-bromo-4,5-dimethoxyphenyl)methyl]-4-[2-[2-(6,6-dimethyl-4-bicyclo[3.1.1]heptanyl)ethoxy-3-ethyl-4-methyl-N-(2-[4-[[4-methylcyclohexyl]carbamoyl]amino)sulfonylphenyl]ethyl)-2-yl]amino]phenyl]butane-1-ol
Prestw-651		Glimepiride	93479-97-1	490.63	<chem>N1(C(\C(=C/C1)C)CC)=O)C(=O)NCCc1ccc(S(NC(N[C@@H]2CC[C@H](CC2)C=O)(=O)=O)cc1</chem>	3-ethyl-4-methyl-N-(2-[4-[[4-methylcyclohexyl]carbamoyl]amino)sulfonylphenyl]ethyl)-2-yl]amino]phenyl]butane-1-ol
Prestw-652		Picrotoxinin	17617-45-7	292.29	<chem>[C@]123[C@]4([C@]([C5C(O[C@H]([C@]4(OC1=O)[H])[C@H]5C(=C)C)=O)(CC2O3)O)C</chem>	(1alpha,2beta,3beta,6beta,6beta,8aS*,8beta,9R*)-Hexahydro-2a-hydroxy-8b-
Prestw-653		Mepenzolate bromide	76-90-4	420.35	<chem>C(C(c1cccc1)(c1cccc1)O)(OC1C[N+](CCC1)(C)C)=O</chem>	(1,1-dimethylpiperidin-1-ium-3-yl) 2-hydroxy-2,2-diphenylacetate bromide

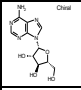
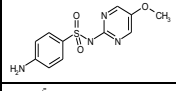
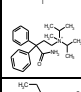
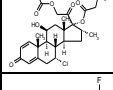
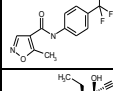
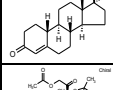
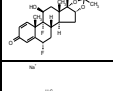
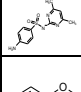
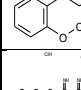
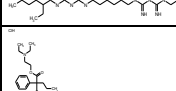
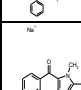
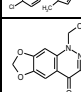
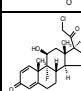
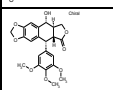
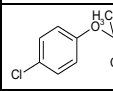
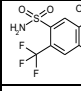
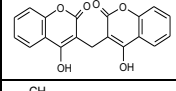
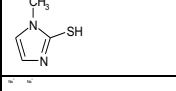
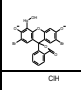
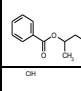
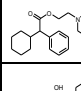
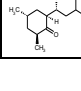

Prestw-654		Benfotiamine	22457-89-2	466.46	<chem>n1c(c(CN/C(=C(=O)C2CCCC2)/CCOP(=O)(O)O)/C(=O)nc1C)N</chem>	S-[2-[(4-amino-2-methylpyrimidin-5-yl)methyl](formyl)amino]-5-(phosphonoxy)pent-2-en-3-
Prestw-655		Halcinonide	3093-35-4	454.97	<chem>[C@@]12[C@@]3([C@]([C@]4([C@@]([C@]5(\C(=C/C(=O)CC5)CC4)C)([C@H](C3)O)F)[H])(C[C@@H]1OC(O)2)(C)C)H)C(=O)CCl</chem>	(4aS,4bR,5S,6aS,6bS,9aR,10aS,10bS)-6b-(chloroacetyl)-4b-fluoro-5-hydroxy-4a,6a,8,8-tetramethyl-
Prestw-656		Lanatoside C	17575-22-3	985.14	<chem>O1C(C(C(C(C1CO)O)O)OC2C(OC(CC2OC(=O)C)OC3C(OC(CC3O)OC4C(OC(CC4O)OC9CC8C(C5(C(C6(C(C(C5)O)C(CC6)C7=CC(=O)OC7)O)(CC8)C)C(C9)C)C)C)C</chem>	
Prestw-657		Benzamil hydrochloride	2898-76-2	356.22	<chem>c1(nc(c(nc1N)N)Cl)C(\N=C(NC1CCCC1)/N)=O</chem>	3,5-diamino-N-[(1E)-amino(benzylamino)methylidene]-6-chloropyrazine-2-carboxamide
Prestw-658		Suxibuzone	27470-51-5	438.48	<chem>N1(N(C(C1=O)(CCCC)COC(=O)CCC(O)=O)c1cccc1)c1cccc1</chem>	4-[(4-butyl-3,5-dioxo-1,2-diphenylpyrazolidin-4-yl)methoxy]-4-oxobutanoic acid
Prestw-659		6-Furfurylaminopurine	525-79-1	215.22	<chem>c12c(nc[nH]1)ncn2NCc1occc1</chem>	N-(furan-2-ylmethyl)-7H-purin-6-amine
Prestw-660		Avermectin B1a	71751-41-2	873.10	<chem>[C@@]1/2([C@@]3([C@@](OC/C3=C1C=C/[C@@H](C1(C=C[C@@]3O[C@@]4(O[C@@]([C@H](C=C4)C)([C@@]C([H])CC)[H])C[C@@H](OC1=O)C3)[H])C)O[C@@]1(O[C@@H](C1C@H(C1)OC)O[C@@]1O[C@@H)(C@@H)(C</chem>	
Prestw-1317		Pranlukast	103177-37-3	481.52	<chem>c1/(C=2/Oc3c(C(\C2=O)CCCC3NC(c2ccc(cc2)O)CCCCc2cccc2)=O)nnn[nH]1</chem>	N-[4-oxo-2-(2H-tetrazol-5-yl)chromen-8-yl]-4-(4-phenylbutoxy)benzamide
Prestw-1477		D,L-Penicillamine	52-66-4	149.21	<chem>[C@@H](C(=O)O)(C(S)C)N</chem>	2-amino-3-methyl-3-sulfanylbutanoic acid
Prestw-1365		Zileuton	111406-87-2	236.29	<chem>c1(sc2c(c1)cccc2)C(N(C(=O)N)O)C</chem>	1-[1-(1-benzothiophen-2-yl)ethyl]-1-hydroxyurea
Prestw-1432		Loratadine	79794-75-5	382.89	<chem>C1((C2C(CC2)C)CCc2c1ncccc2)=C1\CCN(C(=O)OCC)CC1</chem>	ethyl 4-(8-chloro-5,6-dihydro-11H-benzo[5,6]cyclohepta[1,2-b]pyridin-1-ylidene)-1-
Prestw-1387		Tetraethylenepentamine pentahydrochloride	4961-41-5	371.61	<chem>N(CCNCCNCCN)CCN</chem>	N'-[2-[2-(2-aminoethylamino)ethylamino]ethyl]ethane-1,2-diamine pentahydrochloride
Prestw-666		Nisoldipine	63675-72-9	388.42	<chem>C=1(\C(\C=C(/N/C1)C)\C(=O)OC)c1c([N+](=[O-])=O)cccc1)C(OCC(C)C)=O</chem>	3-O-methyl 5-O-(2-methylpropyl) 2,6-dimethyl-4-(2-nitrophenyl)-1,4-dihydropyridine-3,5-
Prestw-1507		Acefylline	652-37-9	238.20	<chem>c12c(N(C(N(C1=O)C)=O)C)ncn2CC(O)=O</chem>	2-(1,3-dimethyl-2,6-dioxapurin-7-yl)acetic acid
Prestw-1165		Acitretin	55079-83-9	326.44	<chem>c1(c(c(c(cc1)OC)C)C)C=C1C=C1C=C1C(=O)O)C)C</chem>	(2E,4E,6E,8E)-9-(4-methoxy-2,3,6-trimethylphenyl)-3,7-dimethylnona-2,4,6,8-tetraenoic acid
Prestw-1162		Zonisamide	68291-97-4	212.23	<chem>S(Cc1noc2c1cccc2)(=O)(=O)N</chem>	1,2-benzoxazol-3-ylmethanesulfonamide
Prestw-1173		Irsogladine maleate	84504-69-8	372.17	<chem>c1(nc(nc(n1)N)N)c1c(ccc(c1)Cl)Cl</chem>	6-(2,5-dichlorophenyl)-1,3,5-triazine-2,4-diamine (Z)-but-2-enedioic acid
Prestw-671		Dydrogesterone	152-62-5	312.46	<chem>[C@@]12([C@]([C@@]3([C@@]([C@]4(\C(\C3)=C/C(=O)C4)C)CC1)[H])([H])C[C@@H]2C(=O)C)[H]C</chem>	(8S,9R,10S,13S,14S,17S)-17-acetyl-10,13-dimethyl-1,2,8,9,11,12,14,15,16,17-decahydrocyclopenta[a]phen
Prestw-1346		Sumatriptan succinate	103628-48-4	413.50	<chem>S(=O)(=O)C(c1cc2c(c[nH]c2cc1)CCN(C)C)NC</chem>	1-[3-[2-(dimethylamino)ethyl]-1H-indol-5-yl]-N-methylmethanesulfonamide butanedioic acid
Prestw-1456		Opipramol dihydrochloride	909-39-7	436.43	<chem>N1(c2c(C=C/c3c1cccc3)ccc2)CCCN1CCN(CC1)CCO</chem>	4-[3-(5H-dibenzo[b,f]azepin-5-yl)propyl]-1-piperazineethanol
Prestw-1447		Nalidixic acid sodium salt	3374-05-8	254.22	<chem>C=1(\C(c2c(N/(C1)CC)nc(cc2)C)=O)C([O-])=O</chem>	1-ethyl-7-methyl-4-oxo-1,8-naphthyridine-3-carboxylate sodium
Prestw-1475		Oxacillin sodium	1173-88-2	423.43	<chem>N12[C@@H]([C@@H](C1=O)NC(c1c(nc1C)c1cccc1)=O)SC([C@@H]2C([O-])=O)C)C</chem>	(2S,5R,6R)-3,3-dimethyl-6-[(5-methyl-3-phenyl-1,2-oxazole-4-carbonyl)amino]-7-oxo-4-thia-1-
Prestw-676		Beta-Escin	11072-93-8	1131.28	<chem>C(OC1[C@@H](C2([C@H](C(C)O)/3(C4(CCC5[C@@](CO)(C(CCC5(C4C/C=C3/C2CC1(C)C)OC1O[C@@H]([C@@H](O[C@@H]2O[C@@H]([C@H]([C@@H](C@H2O)O)CO)[C@@H](C@H1O)C@@@H1O)C@@@H1O)C@@@H1O)C@@@H1O</chem>	(beta-D-Xylopyranosyl)-3(beta-D-glucopyranosyl)-4(methyl-3 acetoxabutyl)-2,8-tetrahydroxy-

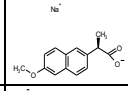
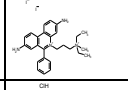
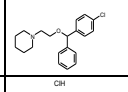
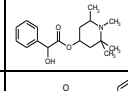
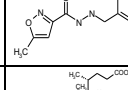
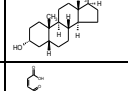
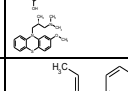
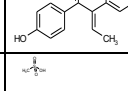
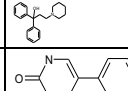
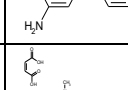
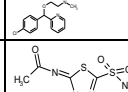
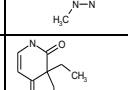
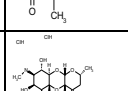
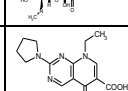
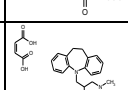
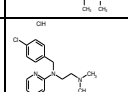
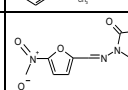
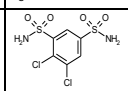
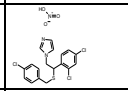
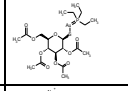
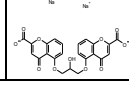

Prestw-631		Thiamine hydrochloride	67-03-8	337.27	[N+1](=CSC(=C1C)CCO)Cc2c(nc(nc2)C)N	3-[(4-Ammonio-2-methyl-5-pyrimidinyl)methyl]-5-(2-hydroxyethyl)-4-methyl-1,3-thiazol-3-ium dichloride
Prestw-1349		Tazobactam	89786-04-9	300.29	S1([C@]([C@@H]([N2[C@H]1CC2=O)C(=O)O)(Cn1nnc1)C(=O)=O	(2S,3S,5R)-3-methyl-7-oxo-3-(1H-1,2,3-triazol-1-ylmethyl)-4-thia-1-azabicyclo[3.2.0]heptane-2-
Prestw-1285		Ibandronate sodium	114084-78-5	341.22	C(P(=O)(O)O)P(=O)(O)O(CCN(CCCCC)C)O	[methyl(pentyl)amino]-1-phosphonopropyl]phosphonic acid
Prestw-1363		Warfarin	81-81-2	308.34	C/1(=C(/c2c(OC1=O)cccc2)O)C(CC(=O)C)c1cccc1	4-hydroxy-3-(3-oxo-1-phenylbutyl)chromen-2-one
Prestw-1318		Pranoprofen	52549-17-4	255.28	O1c2c(Cc3c1ccc(c3)C(C(=O)O)C)ccn2	2-(5H-chromeno[2,3-b]pyridin-7-yl)propanoic acid
Prestw-1340		Secnidazole	3366-95-8	185.18	c1(n(c(nc1)C)CC(O)C)[N+](O)=O	1-(2-methyl-5-nitroimidazol-1-yl)propan-2-ol
Prestw-683		Pempidine tartrate	546-48-5	305.37	N1(C(CCCC1(C)C)(C)C)C	(2R,3R)-2,3-dihydroxybutanedioic acid 1,2,2,6,6-pentamethylpiperidine
Prestw-1798		Mirabegron	223673-61-8	396.52	OC(c1cccc1)CNCCc1ccc(NC(Cc2csc(n2)N)=O)cc1	
Prestw-1508		Ibutilide fumarate	122647-32-9	885.25	S(Nc1ccc(cc1)C(O)CCCN(CC)CCCCC(=O)(=O)C	N-[4-[4-[ethyl(heptyl)amino]-1-hydroxybutyl]phenyl]methane sulfonamide but-2-enedioic acid
Prestw-1799		Tigecycline	220620-09-7	585.66	O=C(NC(C)(C)Nc1c(O)c2C(=O)C=3C(Cc2c(c1)N(C)C)CC1C(O)(C3O)C(=O)C(=O)C1N(C)C)C(=O)N	
Prestw-1465		Tramadol hydrochloride	27203-92-5	299.84	[C@@]1([C@@H](CN(C)C)CCCC1)(c1cc(OC)ccc1)O	(1R,2R)-2-[(dimethylamino)methyl]-1-(3-methoxyphenyl)cyclohexan-1-ol hydrochloride
Prestw-688		Estropipate	7280-37-7	436.57	S(Oc1cc2c([C@@]3([C@]([C@]4([C@@](C(CC4)=O)C3)C)H)(CC2)[H])([H])cc1)(=O)(=O)O	[(8R,9S,13S,14S)-13-Methyl-17-oxo-7,8,9,11,12,14,15,16-octahydro-6H-cyclopenta[a]phenanthren-3-
Prestw-1253		Butylscopolammonium (n-) bromide	149-64-4	440.38	[C@]12([C@@](O1)([C@]1([N+](C@]2(C[C@H](C1)OC([C@@H](c1cccc1)CO)=O)[H])(CCCC)C)[H])([H])	(17(S)- (1alpha,2beta,4beta,5alpha,7beta))-9-butyl-7-(3-hydroxy-1-oxo-2-phenylpropoxy)-9-
Prestw-1494		Irinotecan hydrochloride trihydrate	136572-09-3	677.20	N12/C(\c3c(C1)c(c1c(n3)ccc(OC(N3CCC(N4CCCC4)C3)=O)c1)CC)=C/C1=C(C2=O)/COC([C@]1(O)CC)=O	(S)-4,11-diethyl-3,4,12,14-tetrahydro-4-hydroxy-3,14-dioxo-1H-pyrano[3',4':6,7]-indolino[1,2-b]quinolin-9-yl-
Prestw-1353		Tylosin	1401-69-0	916.12	[C@H]1([C@@H]([C@H]([C@@H]([C@H](O1)C)O[C@H]1CC([C@H]([C@@H](O1)C)O)C)N(C)C)O)O[C@@H]1[C@H]([C@@H](CC(O[C@H]([C@H]([C=C(C=C[C@H]([C@H]([C@@H]1CC=O)C=O)C)O)C)O)C)O)C)O)C)O)C)O)C)O)C)O	1-[3-(dimethylamino)propyl]-1-(4-fluorophenyl)-3H-2-benzofuran-5-carbonitrile hydrobromide
Prestw-692		Citalopram Hydrobromide	59729-32-7	405.31	C1(c2c(CO1)cc(C#N)cc2)(c1ccc(cc1)F)CCCN(C)C	1-[3-(dimethylamino)propyl]-1-(4-fluorophenyl)-3H-2-benzofuran-5-carbonitrile hydrobromide
Prestw-693		Promazine hydrochloride	53-60-1	320.89	N1(c2c(Sc3c1cccc3)cccc2)CCCN(C)C	N,N-dimethyl-3-phenothiazin-10-ylpropan-1-amine hydrochloride
Prestw-694		Sulfamerazine	127-79-7	264.31	S(Nc1nc(ccn1)C)(c1ccc(N)cc1)(=O)=O	4-Amino-N-(4-methyl-2-pyrimidinyl)benzenesulfonamide
Prestw-1170		Venlafaxine	93413-69-5	277.41	C(C1(O)CCCC1)(c1ccc(cc1)OC)CN(C)C	1-[2-(dimethylamino)-1-(4-methoxyphenyl)ethyl]cyclohexan-1-ol
Prestw-696		Ethotoin	86-35-1	204.23	N1(C(NC(=O)C1)cccc1)=O)CC	3-ethyl-5-phenylimidazolidine-2,4-dione
Prestw-697		3-alpha-Hydroxy-5-beta-androstan-17-one	53-42-9	290.45	[C@]12(C3([C@]([C@]4([C@@](C(CC4)=O)(CC3)C)[H])(CC[C@@]1(C[C@@H](CC2)O)[H])([H])C	(3R,5R)-3-hydroxy-10,13-dimethyl-1,2,3,4,5,6,7,8,9,11,12,14,15,16-
Prestw-698		Tetrahydrozoline hydrochloride	522-48-5	236.75	C/1(\C2c3c(CCC2)cccc3)=N/CCN1	(RS)-2-(1,2,3,4-tetrahydronaphthalen-1-yl)-4,5-dihydro-1H-imidazole hydrochloride
Prestw-699		Hexestrol	84-16-2	270.37	C(C(c1ccc(cc1)O)CC)(c1ccc(cc1)O)CC	4-[4-(4-hydroxyphenyl)hexan-3-yl]phenol

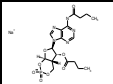
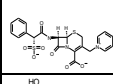
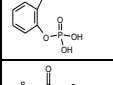
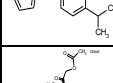
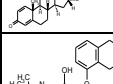
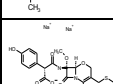
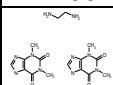
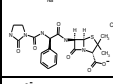
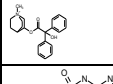
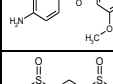
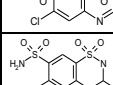
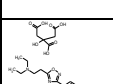
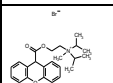
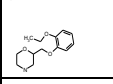
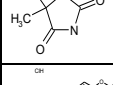
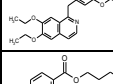
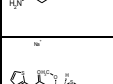
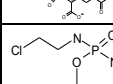
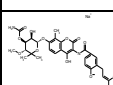
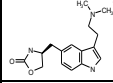


Prestw-700		Cefmetazole sodium salt	56796-39-5	493.52	<chem>[C@]1(NC(CSCC#N)=O)C(N2[C@@]1(S\C=C=C2\O)O)CSc1n(nnn1)C([H])=O)OC</chem>	(6R,7S)-7-(2-(cyanomethylthio)acetamido)-7-methoxy-3-((1-methyl-1H-tetrazol-5-ylthio)methyl)-8-oxo-
Prestw-701		Trihexyphenidyl-D,L Hydrochloride	58947-95-8	337.94	<chem>C(CCN1CCCC1)(c1ccccc1)C1CCCC1)O</chem>	1-cyclohexyl-1-phenyl-3-piperidin-1-ylpropan-1-ol hydrochloride
Prestw-702		Succinylsulfathiazole	116-43-8	355.39	<chem>c1(ccc(c1)NC(=O)CCC(O)=O)S(Nc1sccn1)(=O)=O</chem>	4-oxo-4-[4-(1,3-thiazol-2-ylsulfamoyl)anilino]butanoic acid
Prestw-703		Famprofazone	22881-35-2	377.53	<chem>C1(=C(C(N(N1C)c1ccccc1)=O)/C(C)C)/CN(Cc1ccccc1)C)C</chem>	1-methyl-5-[[methyl(1-phenylpropan-2-yl)amino]methyl]-2-phenyl-4-(propan-2-yl)-1,2-dihydro-3H-
Prestw-704		Bromopride	4093-35-0	344.25	<chem>c1(c(cc(c1)Br)N)OC(=O)NCCN(CC)CC</chem>	4-amino-5-bromo-N-[2-(diethylamino)ethyl]-2-methoxybenzamide
Prestw-705		Methyl benzethonium chloride	25155-18-4	462.12	<chem>C(c1cc(c(cc1)OCCOCC[N+](Cc1ccccc1)(C)C)C)(CC(C)C)C(C)C</chem>	(N,N-Dimethyl-N-[2-[2-[methyl-4-(1,1,3,3-tetramethylbutyl)phenoxy]ethoxy]ethyl]benzene-
Prestw-706		Chlorcyclizine hydrochloride	1620-21-9	337.30	<chem>N1(C(c2ccc(cc2)Cl)c2ccccc2)CCN(CC1)C</chem>	1-[(4-Chlorophenyl)phenylmethyl]-4-methylpiperazine
Prestw-707		Diphenylpyraline hydrochloride	132-18-3	317.86	<chem>C(OC1CCN(CC1)C)c1ccccc1)c1ccccc1</chem>	(4-Diphenylmethoxy-1-methylpiperidine) hydrochloride
Prestw-708		Benzethonium chloride	121-54-0	448.09	<chem>C(c1ccc(cc1)OCCOCC[N+](Cc1ccccc1)(C)C)(CC(C)C)C(C)C</chem>	benzyl-dimethyl-[2-[2-[4-(2,4,4-trimethylpentan-2-yl)phenoxy]ethoxy]ethyl]azanium chloride
Prestw-709		Trioxsalen	3902-71-4	228.25	<chem>c12c(C=C/C(O1)=O)C)cc1c(c2C)oc(c1)C</chem>	2,5,9-trimethylfuro[3,2-g]chromen-7-one
Prestw-1136		Doxofylline	69975-86-6	266.26	<chem>c12c(C(N(C(N1C)=O)C)=O)n(cn2)CC1OCCO1</chem>	7-(1,3-dioxolan-2-ylmethyl)-1,3-dimethylpurine-2,6-dione
Prestw-711		Sulfabenzamide	127-71-9	276.32	<chem>S(NC(=O)c1ccccc1)(c1ccc(N)cc1)(=O)=O</chem>	4-Amino-N-benzoyl-benzenesulfonamide
Prestw-712		Benzocaine	94-09-7	165.19	<chem>C(c1ccc(N)cc1)(=O)OCC</chem>	4-Aminobenzoic acid ethyl ester
Prestw-713		Dipyrone	5907-38-0	333.34	<chem>C=1(C(N(N(C1)C)C)c1ccccc1=O)N(CS([O-])(=O)=O)C</chem>	sodium [[2,3-dihydro-1,5-dimethyl-3-oxo-2-phenyl-1H-pyrazol-4-yl)methylamino]methanesulfonate
Prestw-714		Isosorbide dinitrate	87-33-2	236.14	<chem>[C@]12([C@@H](CO[C@]1([C@H](CO2)O[N+](O-)=O)[H])O[N+](O-)=O)[H]</chem>	[(3S,3aS,6R,6aS)-3-nitrooxy-2,3,3a,5,6,6a-hexahydrofuro[3,2-b]furan-6-yl] nitrate
Prestw-715		Sulfachloropyridazine	80-32-0	284.73	<chem>S(Nc1nnc(Cl)cc1)(c1ccc(N)cc1)(=O)=O</chem>	4-amino-N-(6-chloropyridazin-3-yl)benzenesulfonamide
Prestw-716		Pramoxine hydrochloride	637-58-1	329.87	<chem>N1(CCCOc2ccc(cc2)OCCCC)CCOCC1</chem>	4-[3-(4-butoxyphenoxy)propyl]morpholine hydrochloride
Prestw-717		Finasteride	98319-26-7	372.56	<chem>[C@]12([C@]([C@]3([C@@]([C@]4(C=C/C(N[C@@]4(C)C3)[H])=O)C)(CC1)[H])[H])CC[C@@H]2C(NC(C)C)C(=O)[H])C</chem>	N-(1,1-dimethylethyl)-3-oxo-(5alpha,17beta)-4-azaandrost-1-ene-17-carboxamide
Prestw-718		Fluorometholone	426-13-1	376.47	<chem>[C@]112([C@@]3([C@]([C@]4([C@@]([C@](CC4)C(=O)C)O)C[C@@]3O)C)H)C[C@@]1H/C1=C/C(C=C2)=O)C[H]F)C</chem>	(6S,8S,9R,10S,11S,13S,14S,17R)-17-acetyl-9-fluoro-11,17-dihydroxy-6,10,13-trimethyl-
Prestw-719		Cephalothin sodium salt	58-71-9	418.43	<chem>N12C([C@]([C@]1(S\C=C=C2\O)O)COC(=O)C)[H])(NC(Cc1sccc1)=O)[H])=O</chem>	7-(2-Thienylacetamido)cephalosporanic acid sodium salt
Prestw-720		Cefuroxime sodium salt	56238-63-2	446.37	<chem>N12C([C@]([C@]1(S\C=C=C2\O)O)COC(=O)N)[H])(NC(C/c1occc1)=NOC)O)[H])=O</chem>	Sodium (6R,7R)-3-(carbamoyloxymethyl)-7-[[2Z]-2-(furan-2-yl)-2-methoxyminoacet]lamino]-8-
Prestw-721		Althiazide	5588-16-9	383.90	<chem>S1(c2c(NC(N1)CSCC=C)cc(c(S(=O)(=O)N)c2)Cl)(=O)=O</chem>	(3R)-3-[(Allylsulfanyl)methyl]-6-chloro-3,4-dihydro-2H-1,2,4-benzothiadiazine-7-sulfonamide 1,1-dioxide
Prestw-722		Isopyrin hydrochloride	18342-39-7	281.79	<chem>C=1(C(N(N(C1)C)C)c1ccccc1=O)NC(C)C</chem>	1,5-dimethyl-2-phenyl-4-(propan-2-ylamino)pyrazol-3-one hydrochloride

Prestw-723		Phenethicillin potassium salt	132-93-4	402.52	<chem>N12[C@@]([C@@](C1=O)(NC(C(Oc1cccc1)C)=O)[H])(SC([C@@H]2C([O-])=O)(C)C)[H]</chem>	(2S,5R,6R)-3,3-dimethyl-7-oxo-6-(2-phenoxypropanoylamino)-4-thia-1-
Prestw-724		Sulfamethoxy pyridazine	80-35-3	280.31	<chem>S(Nc1nnc(cc1)OC)(c1ccc(N)cc1)(=O)=O</chem>	4-amino-N-(6-methoxy pyridazin-3-yl)benzenesulfonamide
Prestw-725		Deferoxamine mesylate	138-14-7	656.80	<chem>C(N(O)CCCCNC(=O)CCC(N(O)CCCCN)=O(=O)CCC(=O)NCCCCCN(C(=O)C)O</chem>	N-[5-[[4-[5-[acetyl(hydroxy)amino]pentylamino]-4-oxobutanoyl]-
Prestw-726		Mephentermine hemisulfate	1212-72-2	424.61	<chem>C(NC)(Cc1cccc1)(C)C.C(NC)(Cc1cccc1)(C)C</chem>	N,2-dimethyl-1-phenylpropan-2-amine sulfuric acid
Prestw-1140		Liranafate	88678-31-3	328.44	<chem>C(Nc1nc(OC)ccc1)C(Oc1cc2c(cc1)CCCC2)=S</chem>	O-(5,6,7,8-tetrahydronaphthalen-2-yl) N-(6-methoxy pyridin-2-yl)-N-methylcarbamothioate
Prestw-728		Sulfadimethoxine	122-11-2	310.33	<chem>S(Nc1nc(nc1)OC)OC)(c1ccc(N)cc1)(=O)=O</chem>	N1-(2,6-dimethoxy-4-pyrimidinyl)sulfanilamide
Prestw-729		Sulfanilamide	63-74-1	172.21	<chem>S(c1ccc(N)cc1)(=O)(=O)N</chem>	4-Aminobenzenesulfonamide
Prestw-730		Balsalazide Sodium	80573-04-2	401.29	<chem>c1(C([O-]=O)c(cc(N=Nc2ccc(C(=O)NCCC([O-])=O)cc2)c1)O</chem>	(3Z)-3-[[4-(2-carboxylatoethylcarbamoyl)phenyl]hydrazinylidene]-6-oxocyclohexa-1,4-diene-1-
Prestw-731		Sulfaquinoxaline sodium salt	967-80-6	322.32	<chem>S([N-]c1nc2c(nc1)ccc2)(c1ccc(N)cc1)(=O)=O</chem>	(4-aminophenyl)sulfonylquinoxalin-2-ylazanide sodium
Prestw-732		Streptozotocin	18883-66-4	265.22	<chem>[C@@H]1(NC(N(N=O)C)=O)[C@H]([C@@H]([C@H](O[C@@H]1O)CO)O)O</chem>	1-methyl-1-nitroso-3-[(2S,3R,4R,5S,6R)-2,4,5-trihydroxy-6-(hydroxymethyl)oxan-3-2,3-dihydroxybutanedioic acid 1-[4-(2-methoxyethyl)phenoxy]-3-(propan-2-ylamino)propan-2-
Prestw-733		Metoprolol(+,-) (+)-tartrate salt	56392-17-7	684.83	<chem>N(CC(COc1ccc(cc1)CCOC)O)C(C)C.N(CC(COc1ccc(cc1)CCOC)O)C(C)C</chem>	(6S,8S,9R,10S,11S,13S,14S,16R,17R)-6,9-difluoro-11,17-dihydroxy-17-(2-hydroxyacetyl)-10,13,16-N-(piperidin-2-ylmethyl)-2,5-bis(2,2,2-trifluoroethoxy)benzamide acetic acid
Prestw-734		Flumethasone	2135-17-3	410.46	<chem>[C@]112([C@@]3([C@]([C@]4([C@@]([C@]([C@@H](C4)C(=O)CO)O)[C(C@@H]3O)C)[H])[C(C@@H](C1=C/C(\C=C2)=O)F)[H])F)C</chem>	(6S,8S,9R,10S,11S,13S,14S,16R,17R)-6,9-difluoro-11,17-dihydroxy-17-(2-hydroxyacetyl)-10,13,16-N-(piperidin-2-ylmethyl)-2,5-bis(2,2,2-trifluoroethoxy)benzamide acetic acid
Prestw-735		Flecainide acetate	54143-56-5	474.40	<chem>c1(C(NCC2NCCC2)=O)c(OCC(F)F)F)cc(c1)OCC(F)F</chem>	N-(piperidin-2-ylmethyl)-2,5-bis(2,2,2-trifluoroethoxy)benzamide acetic acid
Prestw-736		Cefazolin sodium salt	27164-46-1	476.49	<chem>N12C([C@]([C@]1(SC1C=C2)C([O-])=O)CS1sc(nn1)C)[H])(NC(Nc1nnc1)=O)[H]=O</chem>	sodium (6R,7R)-3-[(5-methyl-1,3,4-thiadiazol-2-yl)sulfanyl]methyl-8-oxo-7-[2-(1H-1,2,3,4-tetrazol-1-
Prestw-1702		Trimetozine	635-41-6	281.31	<chem>COc1c(OC)cc(C(=O)N2CCOCC2)cc1OC</chem>	morpholin-4-yl-(3,4,5-trimethoxyphenyl)methanone
Prestw-738		Folinic acid calcium salt	6035-45-6	511.51	<chem>C/12=C(/N/C(=N1C=O)/N)NCCC(N2C=O)CNc1ccc(C(N[C@@H](C([O-])=O)CCC([O-])=O)cc1</chem>	(2S)-2-[[4-[(2-amino-5-formyl-4-oxo-1,6,7,8-tetrahydropteridin-6-yl)methylamino]benzoyl]amin
Prestw-739		Levonordefrin	829-74-3	183.21	<chem>c1(cc(c(cc1)O)O)[C@H]([C@@H](N)C)O</chem>	4-[(1R,2S)-2-amino-1-hydroxypropyl]benzene-1,2-diol
Prestw-740		Ebselen	60940-34-3	274.18	<chem>N1(C(c2c([Se]1)ccc2)=O)c1cccc1</chem>	2-Phenyl-1,2-benzisoselenazol-3(2H)-one
Prestw-741		Nadide	53-84-9	663.44	<chem>n1([C@H]2[C@@H]([C@@H]([C@H](O2)COP(OP(OC[C@H]2O)[C@@H]([n+3]ccc(C(=O)N)ccc3)[C@@H]([C@@H]2O)([O-])=O)O)O)O)c2c(nc1c(ncn2)N</chem>	[(2R,3S,4R,5R)-5-(6-aminopurin-9-yl)-3,4-dihydroxovoxolan-2-yl]methoxy-
Prestw-742		Sulfamethizole	144-82-1	270.33	<chem>S(Nc1sc(nn1)C)(c1ccc(N)cc1)(=O)=O</chem>	4-amino-N-(5-methyl-1,3,4-thiadiazol-2-yl)benzene-1-sulfonamide
Prestw-743		Medrysone	2668-66-8	344.50	<chem>[C@]12(\C=C/C(=O)CC1)[C@H](C[C@@]1([C@@]2([C@H](C[C@@]2([C@]1(CC[C@@H]2C(=O)C)[H])C)O)[H])C)C</chem>	(6S,8S,9S,10R,11S,13S,14S,17S)-17-acetyl-11-hydroxy-6,10,13-trimethyl-1,2,6,7,8,9,11,12,14,15,16,1
Prestw-744		Flunixin meglumine	42461-84-7	491.47	<chem>c1ccc(c(n1)Nc1c(c(ccc1)C(F)F)C)C(O)=O</chem>	(2R,3R,4R,5S)-6-(methylamino)hexane-1,2,3,4,5-pentol 2-[2-methyl-3-
Prestw-745		Spiramycin	8025-81-8	842.07	<chem>C1(C(C(C(C(O1)C)OC)1CC(C(C(O1)C)O)(O)N(C)C)O)O[C@@H]1[C@H]([C@@H]([C@H](O[C@@H](C/C=C/C/[C@@H](OC2OC(C(C2)N(C)C)C)[C@@H](C[C@@H]1CC=O)C)C=O)O)I'R)1OC</chem>	

Prestw-746		Glycopyrrolate	596-51-0	398.34	<chem>C(C(c1cccc1)(C1CCCC1O)(OC1C[N+](CC1)(C)C)=O</chem>	(1,1-dimethylpyrrolidin-1-ium-3-yl) 2-cyclopentyl-2-hydroxy-2-phenylacetate bromide
Prestw-1600		Aprepitant	170729-80-3	534.44	<chem>N/1=C/(NNC1=O)CN1[C@H]([C@@H](O)[C@H](c2cc(C(F)F)F)cc(C(F)F)c2)C)OCC1)c1ccc(cc1)F</chem>	5-[[[2R,3S]-2-[[1R)-1-[3,5-bis(trifluoromethyl)phenyl]ethoxy]-3-(4-fluorophenyl)-4-morpholinylmethyl]-1,2-
Prestw-748		Monensin sodium salt	22373-78-0	692.87	<chem>[C@]12([O][C@]([C@H]([C@H]([C@H](C(O-))=O)C)OC)C)([C@@H]([C@H](C1)O)C)[H]O[C@]([C@@]1(O)[C@]([C@@]3(O)[C@]([C@]4(O)[C@@]([C@@H]([C@C@H]4C)C)O)CO)[H])(C[C@@H]3C)[H])[H](CC</chem>	4-[2-[5-ethyl-5-[6-hydroxy-6-(hydroxymethyl)-3,5-dimethyloxan-2-yl]-3-methyl-oxolan-2-yl]oxolan-2-yl]-9-hydroxy-2,8-
Prestw-749		Isoetharine mesylate salt	7279-75-6	335.42	<chem>c1(cc(c(cc1)O)O)C(C(NC(C)C)CC)O</chem>	4-[1-hydroxy-2-(propan-2-ylamino)butyl]benzene-1,2-diol methanesulfonic acid
Prestw-750		Mevalonic-D, L acid lactone	674-26-0	130.14	<chem>C1(CC(CCO1)(O)C)=O</chem>	4-hydroxy-4-methyloxan-2-one
Prestw-751		Terazosin hydrochloride	63590-64-7	423.90	<chem>c1(nc(c2c(n1)cc(c2)OC)OC)N)N1CCN(C(C2OCC2)=O)CC1</chem>	[4-(4-amino-6,7-dimethoxyquinazolin-2-yl)piperazin-1-yl]-(oxolan-2-yl)methanone hydrochloride
Prestw-752		Phenazopyridine hydrochloride	136-40-3	249.70	<chem>n1c(c(N=N/c2ccccc2)ccc1N)N</chem>	2,6-Diamino-3-(phenylazo)pyridine
Prestw-753		Demeclocycline hydrochloride	64-73-3	501.32	<chem>[C@@]12([C=C(C3C4c([C@H]([C@]3[C]C@]1([C@@H](C=C(C(=O)N)N)O)N(C)C)[H])[H])O)c(ccc4O)Cl)=O)O)O</chem>	(4S,4aS,5aS,6S,12aS)-7-chloro-4-(dimethylamino)-3,6,10,12,12a-pentahydroxy-1,11-dioxo-
Prestw-754		Fenopropfen calcium salt dihydrate	53746-45-5	558.65	<chem>c1(cccc(c1)C(C(=O)O)-)C)Oc1cccc1.c1(cccc(c1)C(C(=O)O)-)C)Oc1cccc1</chem>	2-(3-phenoxyphenyl)propanoate calcium dihydrate
Prestw-755		Piperacillin sodium salt	59703-84-3	539.55	<chem>N12[C@@]([C@@](C1=O)NC([C@H](NC(N1C(C(N(CO1)C)C)O)O)=O)c1cccc1)=O)[H])(SC([C@@H]2C([O-])=O)(C)C)[H]</chem>	sodium (2S,5R,6R)-6-[[[(2R)-2-[[4-ethyl-2,3-dioxopiperazine-1-carbonyl]amino]-2-phenylacetyl]amino]-3,3-
Prestw-756		Diethylstilbestrol	56-53-1	268.36	<chem>C=C(/c1ccc(cc1)O)CC)(\c1ccc(cc1)O)CC</chem>	4-[(E)-4-(4-hydroxyphenyl)hex-3-en-3-yl]phenol
Prestw-757		Chlorotrianisene	569-57-3	380.88	<chem>C=C(/c1ccc(cc1)OC)Cl)(/c1ccc(cc1)OC)c1ccc(cc1)OC</chem>	1-[2-chloro-1,2-bis(4-methoxyphenyl)ethenyl]-4-methoxybenzene
Prestw-758		Ribostamycin sulfate salt	53797-35-6	552.56	<chem>[C@]1(C(O[C@]2[C@@H]([C@H]([C@H]([C@H](O2)CN)O)N)[H])([C@H]([C@H]([C@@H]1O)N)N)O)C[C@@H]1[C@@H]([C@@H]([C@H](O1)CO)O)O)[H]</chem>	(2S,3R,4S,5S,6R)-5-amino-2-(aminomethyl)-6-[[[(1S,2S,3R,4S,6R)-4,6-diamino-2-[[[(2S,3R,4R,5S)-
Prestw-759		Methacholine chloride	62-51-1	195.69	<chem>[N+](CC(OC(=O)C)C)C)C)C</chem>	2-acetyloxypropyl(trimethyl)azanium chloride
Prestw-760		Pizenzolate bromide	125-51-9	434.38	<chem>C(C(c1cccc1)(c1cccc1)O)(OC1C[N+](CCC1)(CC)C)=O</chem>	(1-ethyl-1-methylpiperidin-1-ium-3-yl) 2-hydroxy-2,2-diphenylacetate bromide
Prestw-761		Butamben	94-25-7	193.25	<chem>C(c1ccc(N)cc1)(=O)OCCCC</chem>	4-Aminobenzoic acid butyl ester
Prestw-762		Sulfapyridine	144-83-2	249.29	<chem>S(Nc1ncccc1)(c1ccc(N)cc1)(=O)=O</chem>	4-amino-N-pyridin-2-ylbenzenesulfonamide
Prestw-763		Meclofenoxate hydrochloride	3685-84-5	294.18	<chem>C(=O)(COC1ccc(Cl)cc1)OCCN(C)C</chem>	2-(dimethylamino)ethyl 2-(4-chlorophenoxy)acetate hydrochloride
Prestw-764		Furaltadone hydrochloride	3759-92-0	360.76	<chem>c1([N+](O-)=O)oc(/C=N/N2C(OC(C2)CN2CCOCC2)=O)cc1</chem>	5-(morpholin-4-ylmethyl)-3-[(E)-(5-nitrofur-2-yl)methylideneamino]-1,3-oxazolidin-2-one
Prestw-765		Ethoxyquin	91-53-2	217.31	<chem>C=1(\c2c(NC(/C1)(C)C)ccc(c2)OCC)/C</chem>	6-ethoxy-2,2,4-trimethyl-1H-quinoline
Prestw-766		Tinidazole	19387-91-8	247.27	<chem>n1(c(cnc1C)[N+](O-)=O)CCS(CC(=O)=O)=O</chem>	1-(2-ethylsulfonyl)ethyl)-2-methyl-5-nitroimidazole
Prestw-767		Guanadrel sulfate	22195-34-2	524.64	<chem>C12(OC(CO1)CNC(=N)N)CCCCC2.C12(OC(CO1)CNC(=N)N)CCCCC2</chem>	2-(1,4-dioxaspiro[4.5]decan-3-ylmethyl)guanidine sulfuric acid

Prestw-768		Vidarabine	5536-17-4	267.25	<chem>n1([C@H]2[C@H]([C@@H]([C@H](O2)CO)O)c2c(nc1)c(ncn2)N</chem>	(2R,3S,4S,5R)-2-(6-aminopurin-9-yl)-5-(hydroxymethyl)oxolane-3,4-diol
Prestw-769		Sulfameter	651-06-9	280.31	<chem>S(Nc1ncc(cn1)OC)(c1ccc(N)cc1)(=O)=O</chem>	4-amino-N-(5-methoxy-2-pyrimidinyl)benzenesulfonamide
Prestw-770		Isopropamide iodide	71-81-8	480.44	<chem>[N+](CCCC(C=O)N)(c1cccc1)c1cccc1)(C(C)C)(C(C)C).[I-]</chem>	(4-amino-4-oxo-3,3-diphenylbutyl)-methyl-di(propan-2-yl)azanium iodide
Prestw-771		Alclometasone dipropionate	66734-13-2	521.06	<chem>[C@]12C([C@@H](C[C@]1([C@]1([C@@]([C@@]1)3(C=C/C(C=C3)=O))C[C@H]1Cl)C)([C@H](C2)O)[H])[H])(H)C(COC(=O)CC(=O)OC(=O)CC)C</chem>	[2-[(7R,8S,9S,10R,11S,13S,14S,16R,17R)-7-chloro-11-hydroxy-10,13,16-trimethyl-3-
Prestw-772		Leflunomide	75706-12-6	270.21	<chem>c1(C(Nc2ccc(C(F)(F)F)cc2)=O)c(onc1)C</chem>	5-methyl-N-[4-(trifluoromethyl)phenyl]-1,2-oxazole-4-carboxamide
Prestw-773		Norgestrel(-)-D	797-63-7	312.46	<chem>[C@]12([C@]([C@]3([C@@]([C@@]4(C=C/C(=O)CC4)CC3)[H])(CC1)[H])[H])(CC[C@]2(C#C)O)[H]CC</chem>	(8R,9S,10R,13S,14S,17R)-13-ethyl-17-ethynyl-17-hydroxy-
Prestw-774		Fluocinonide	356-12-7	494.54	<chem>[C@@]12([C@@]3([C@]([C@]4([C@@]([C@@]5(C(C([C@H](C4)F)=C/C(C=C5)=O)C)([C@H](C3)O)F)[H])(C[C@@H]1OC(O2)C)C)[H])C(COC(=O)C)=O</chem>	1,2,6,7,8,9,10,11,12,14,15,16 alpha 9-Difluoro-11 beta 21-dihydroxy-16 alpha 17-(1-methylethylidenedioxy)pregna-1,4-diene-3,20-
Prestw-775		Sulfamethazine sodium salt	1981-58-4	300.32	<chem>S([N-]c1nc(cc(n1)C)C)(c1ccc(N)cc1)(=O)=O</chem>	sodium (4-aminophenyl)sulfonyl-(4,6-dimethylpyrimidin-2-yl)azanide
Prestw-776		Guaifenesin	93-14-1	198.22	<chem>O(c1c(OC)cccc1)CC(O)CO</chem>	(RS)-3-(2-methoxyphenoxy)propane-1,2-diol
Prestw-777		Alexidine dihydrochloride	22573-93-9	581.73	<chem>N(C(=N)NCC(CC)CCCC)C(=N)NCCCCCNC(NC(=N)NC(C(CC)CCCC)=N</chem>	Hexamethylene-bis[5-(2-ethylhexyl)biguanide] dihydrochloride
Prestw-778		Proadifen hydrochloride	62-68-0	389.97	<chem>C(C(=O)OCCN(CC)CC)(c1cccc1)(c1cccc1)CCC</chem>	2-(diethylamino)ethyl 2,2-diphenylpentanoate hydrochloride
Prestw-779		Zomepirac sodium salt	64092-48-4	313.72	<chem>c1(n(c(cc1)C)C([O-]=O)C)C(c1ccc(cc1)Cl)=O</chem>	5-(4-Chlorobenzoyl)-1,4-dimethyl-1H-pyrrole-2-acetate sodium
Prestw-780		Cinoxacin	28657-80-9	262.22	<chem>c12c(OCO1)cc1c(c2)C/C(=N1N1CC)/C(O)=O</chem>	1-ethyl-4-oxo-1H,4H,7H-[1,3]dioxolo[4,5-g]cinnoline-3-carboxylic acid
Prestw-781		Clobetason propionate	25122-46-7	466.98	<chem>[C@]12([C@]([C@H](C[C@]1([C@]1([C@@]([C@@]1)3(C=C/C(C=C3)=O))CC1)C)([C@H](C2)O)F)[H])[H])C(C(=O)CC)OC(=O)CC)C</chem>	[17-(2'-chloroacetyl)- 9-fluoro-11-hydroxy-10,13,16-trimethyl- 3-oxo-6,7,8,11,12,14,15,16-
Prestw-782		Podophyllotoxin	518-28-5	414.42	<chem>[C@@]12([C@@]([C@@H](c3c([C@H]1O)cc1c(c3)OCO1)c1cc(c(c1)OC)OC)OC)(C(OC2)=O)[H])[H]</chem>	(5R,5aR,8aR,9R)-5-hydroxy-9-(3,4,5-trimethoxyphenyl)-5a,6,8a,9-tetrahydro-5H-[2]benzofuro[5,6-
Prestw-783		Clofibrac acid	882-09-7	214.65	<chem>c1c(ccc(c1)OC(C)C(O)=O)Cl</chem>	2-(4-Chlorophenoxy)-2-methylpropanoic acid
Prestw-784		Bendroflumethiazide	73-48-3	421.42	<chem>S1(c2c(NC(N1)Cc1cccc1)cc(c(S(=O)(=O)N)c2)C(F)F)(=O)=O</chem>	3-benzyl-1,1-dioxo-6-(trifluoromethyl)-3,4-dihydro-2H-1,2,4-benzothiadiazine-7-sulfonamide
Prestw-785		Dicumarol	66-76-2	336.30	<chem>C1(=C(c2c(OC1=O)cccc2)O)/C/C1=C(c2c(OC1=O)cccc2)O</chem>	4-hydroxy-3-[(4-hydroxy-2-oxochromen-3-yl)methyl]chromen-2-one
Prestw-786		Methimazole	60-56-0	114.17	<chem>c1(n(ccn1)C)S</chem>	1-methyl-3H-imidazole-2-thione
Prestw-787		Merbromin	129-16-8	750.66	<chem>C12(c3c(c(c(c3)Br)[O-])[Hg]O)Oc3c1cc(c(c3)[O-])Br)OC(c1c2cccc1)=O</chem>	(2',7'-dibromo-3',6'-dioxido-3-oxospiro[2-benzofuran-1,9'-xanthene]-4'-yl)mercury hydrate disodium
Prestw-788		Hexylcaine hydrochloride	532-76-3	297.83	<chem>C(OC(CNC1CCCCC1)C(=O)c1cccc1</chem>	1-(cyclohexylamino)propan-2-yl benzoate hydrochloride
Prestw-789		Drofenine hydrochloride	548-66-3	353.94	<chem>C(C(c1cccc1)C1CCCC1)(=O)OCCN(CC)CC</chem>	2-(diethylamino)ethyl 2-cyclohexyl-2-phenylacetate hydrochloride
Prestw-790		Cycloheximide	66-81-9	281.35	<chem>[C@]1(C([C@H](C[C@@H](C1)C)C)=O)([C@@H](CC1CC(NC(=O)C1)=O)O)[H]</chem>	4-[(2R)-2-[(1S,3S,5S)-3,5-dimethyl-2-oxocyclohexyl]-2-hydroxyethyl]piperidine-2,6-dione


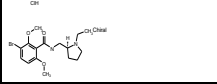
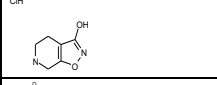
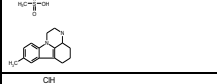
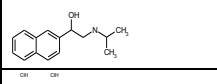
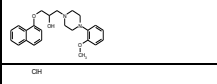
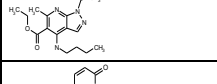
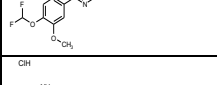
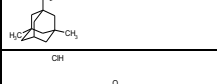
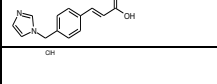
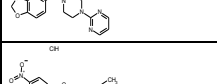
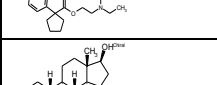
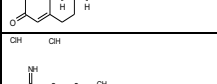
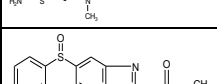
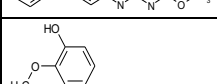
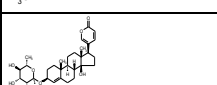
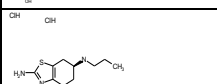
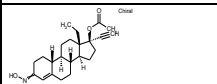
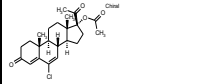
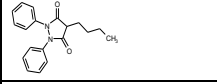
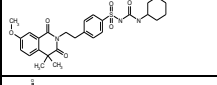
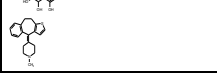

Prestw-791		(R)-Naproxen sodium salt	23979-41-1	252.25	<chem>c1(cc2c(cc(cc2)OC)cc1)[C@H](C([O-])=O)C</chem>	(2R)-2-(6-methoxynaphthalen-2-yl)propanoate sodium
Prestw-792		Propidium iodide	25535-16-4	668.41	<chem>[n+](c2c(c3c(c1c1ccccc1)cc(cc3)N)ccc(c2)N)CCC[N+](CC)(CC)C</chem>	3-(3,8-diamino-6-phenylphenanthridin-5-ium-5-yl)propyl-diethyl-methylazanium diiodide
Prestw-793		Cloperastine hydrochloride	14984-68-0	366.33	<chem>N1(CCOC(c2ccc(cc2)Cl)c2cccc2)CCCC1</chem>	1-[2-[(4-chlorophenyl)-phenylmethoxy]ethyl]piperidine hydrochloride
Prestw-794		Eucatropine hydrochloride	536-93-6	327.85	<chem>N1(C(CC(OC(C(c2ccccc2)O)=O)CC1)C)(C)C</chem>	(1,2,2,6-tetramethylpiperidin-4-yl) 2-hydroxy-2-phenylacetate hydrochloride
Prestw-795		Isocarboxazid	59-63-2	231.26	<chem>c1(noc(c1)C)C(=O)NNCc1ccccc1</chem>	N'-benzyl-5-methyl-1,2-oxazole-3-carbohydrazide
Prestw-796		Lithocholic acid	434-13-9	376.58	<chem>[C@@]12([H])[C@@]([C@@]3([H])[C@]([C@@]([C@@]([C@@]1(CCC(=O)O)C)(CC3)[H])(C)CC1)([H])CC[C@@]1([H])[C@@]2(CC[C@H](C1)O)C</chem>	(4R)-4-[(3R,5R,8R,9S,10S,13R,14S,17R)-3-hydroxy-10,13-dimethyl-(2R)-3-(2-methoxyphenothiazin-10-yl)-N,N,2-trimethylpropan-1-amine (Z)-but-2-enedioic acid
Prestw-797		Methotrimeprazine maleate salt	7104-38-3	444.55	<chem>N1(c2c(Sc3c1cccc3)ccc(c2)OC)C[C@H](CN(C)C)C</chem>	(2R)-3-(2-methoxyphenothiazin-10-yl)-N,N,2-trimethylpropan-1-amine (Z)-but-2-enedioic acid
Prestw-798		Dienestrol	84-17-3	266.34	<chem>C(\C(\c1ccc(cc1)O)=C)/c1ccc(cc1)O)=C/C</chem>	4-[(2E,4E)-4-(4-hydroxyphenyl)hexa-2,4-dien-3-yl]phenol
Prestw-799		Pridinol methanesulfonate salt	6856-31-1	391.53	<chem>C(CCN1CCCC1)(c1ccccc1)(c1ccccc1)O</chem>	1,1-diphenyl-3-piperidin-1-ylpropan-1-ol methanesulfonic acid
Prestw-800		Amrinone	60719-84-8	187.20	<chem>C=1(C(N(C=C(/C1)c1ccccc1)=O)/N</chem>	3-amino-5-pyridin-4-yl-1H-pyridin-2-one
Prestw-801		Carbinoxamine maleate salt	3505-38-2	406.87	<chem>C(c1ccc(cc1)Cl)(c1ncccc1)OCCN(C)C</chem>	2-[(4-chlorophenyl)pyridin-2-ylmethoxy]-N,N-dimethylethanamine but-2-enedioic acid
Prestw-802		Methazolamide	554-57-4	236.27	<chem>C=1(/SC(N(N1)C)=NC(=O)C)S(=O)(=O)N</chem>	N-(3-methyl-5-sulfamoyl-1,3,4-thiadiazol-2-ylidene)acetamide
Prestw-803		Pyrithydione	77-04-3	167.21	<chem>C1(C(N(C=C/C1)O)=O)(CC)CC</chem>	3,3-diethyl-1H-pyridine-2,4-dione
Prestw-804		Spectinomycin dihydrochloride	21736-83-4	405.28	<chem>[C@@]12([C@]([O][C@]3([C@](O1)([C@H]([C@H]([C@]([C@@]([C@@]1(CCC(=O)O)C)(CC3)N)C)N)C)O)[C@@]([C@@]2(C=O)C)H)O</chem>	(1R,3S,5R,8R,10R,11S,12S,13R,14S)-8,12,14-trihydroxy-5-methyl-11,13-bis(methylamino)-2,4,9-
Prestw-805		Piromidic acid	19562-30-2	288.31	<chem>c1(ncc2c(n1)N/C=C(/C2=O)/C(O)=O)CC)N1CCCC1</chem>	8-ethyl-5-oxo-2-pyrrolidin-1-ylpyrido[2,3-d]pyrimidine-6-carboxylic acid
Prestw-806		Trimipramine maleate salt	521-78-8	410.52	<chem>N1(c2c(CCc3c1cccc3)cccc2)CC(CN(C)C)C</chem>	3-(5,6-dihydrobenzo[b][1]benzazepin-11-yl)-N,N,2-trimethylpropan-1-amine (Z)-
Prestw-807		Chloropyramine hydrochloride	6170-42-9	326.27	<chem>N(c1ncccc1)(Cc1ccc(Cl)cc1)CCN(C)C</chem>	N'-[(4-chlorophenyl)methyl]-N,N-dimethyl-N'-pyridin-2-ylethane-1,2-diamine hydrochloride
Prestw-808		Furazolidone	67-45-8	225.16	<chem>c1([N+]([O-])=O)oc(C=NN2C(OCC2)=O)cc1</chem>	3-[(E)-(5-nitrofuran-2-yl)methylideneamino]-1,3-oxazolidin-2-one
Prestw-809		Dichlorphenamide	120-97-8	305.16	<chem>c1(S(=O)(=O)N)c(cc(S(=O)(=O)N)c1)Cl</chem>	4,5-dichlorobenzene-1,3-disulfonamide
Prestw-810		Sulconazole nitrate	61318-91-0	460.77	<chem>c1(c(cc(c1)Cl)Cl)C(S(Cc1ccc(Cl)cc1)Cn1cncc1</chem>	1-[2-[(4-chlorophenyl)methylsulfanyl]-2-(2,4-dichlorophenyl)ethyl]imidazol
Prestw-1233		Auranofin	34031-32-8	678.49	<chem>[C@H]1([C@H]([C@]([C@]([C@]([O][C@]1S[Au]=P(CC)(CC)CC)COC(=O)C)OC(=O)C)OC(=O)C)OC(=O)C</chem>	3,4,5-triacetyloxy-6-(acetyloxymethyl)oxane-2-thiolate gold(1+) triethylphosphane
Prestw-812		Cromolyn disodium salt	15826-37-6	512.34	<chem>C/1(c2c(O/C(=C1)/C([O-])=O)cccc2OCC(COC1c2C(C=C/Oc2ccc1)C([O-])=O)O)=O</chem>	5-[3-(2-carboxylato-4-oxochromen-5-yl)oxy-2-hydroxypropoxy]-4-oxochromene-2-carboxylate


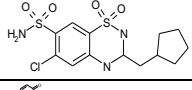
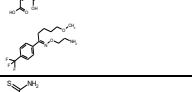
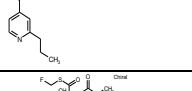
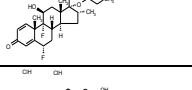
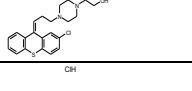
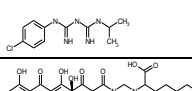
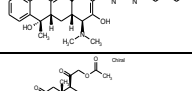
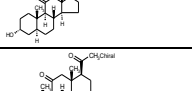
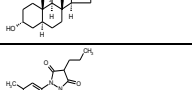
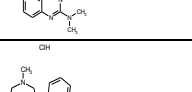
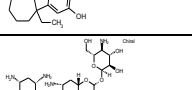
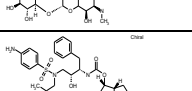
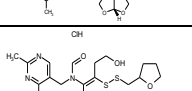
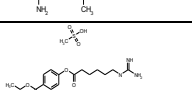
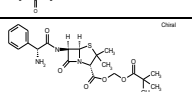
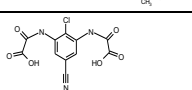
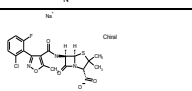
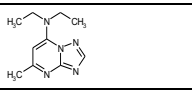

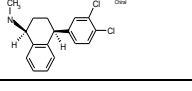

Prestw-813		Bucladesine sodium salt	16980-89-5	491.38	<chem>n1([C@H]2O[C@@]3(OP(OC[C@]3([C@H]2OC(=O)CCC)[H])([O-])=O)[H])c2c(nc1)c(NC(=O)CCC)n2</chem>	[(4aR,6R,7R,7aR)-6-[6-(butanoylamino)purin-9-yl]-2-oxido-2-oxo-4a,6,7,7a-tetrahydro-4H-furo[3,2-(6R,7R)-3-[(4-carbamoylpyridin-1-ium-1-yl)methyl]-8-oxo-7-[(2R)-2-phenyl]-2-
Prestw-814		Cefsulodin sodium salt	52152-93-9	554.54	<chem>N12C([C@]([C@]1(SC=C=C2[C([O-])=O)C[n+]1ccc(C(=O)N)cc1)[H])NC([C@H](S([O-])(X=O)c1cccc1)=O)[H])=O</chem>	2-(Phosphonoxy)benzoic acid
Prestw-815		Fosfosal	6064-83-1	218.10	<chem>P(Oc1c(C(=O)O)cccc1)(=O)(O)O</chem>	2-[4-(thiophene-2-carbonyl)phenyl]propanoic acid
Prestw-816		Suprofen	40828-46-4	260.31	<chem>c1(ccc(cc1)C(C)C(O)=O)C(c1sccc1)=O</chem>	2-[4-(thiophene-2-carbonyl)phenyl]propanoic acid
Prestw-1509		Deflazacort	14484-47-0	441.53	<chem>[C@]1/2([C@]3([C@]([C@]4([C@]([C@]5(C=C/C(C=C5)=O)CC4)C)[C@H](C3O)[H])[H])C[C@]1(O/C(N=2)/C)[H])[H])C(COC(=O)C)=O</chem>	(11beta,16beta)-21-(acetyloxy)-11-hydroxy-2'-methyl-5'H-pregna-1,4-dieno[17,16-d]oxazole-3,20-
Prestw-818		Nadolol	42200-33-9	309.41	<chem>c12[C@@H]([C@@H](Cc1cccc2OCC(CNC(C)C)C)O)O</chem>	(2R,3S)-5-[3-(tert-butylamino)-2-hydroxypropoxy]-1,2,3,4-tetrahydronaphthalene-2,3-diol
Prestw-819		Moxalactam disodium salt	64953-12-4	564.44	<chem>[C@]1(C(N2[C@@]1(OC(C=C2[C([O-])=O)CS1n(nnn1)C)[H])=O)NC([C@H](C([O-])=O)c1cccc1O)=O)OC</chem>	Disodium (6R,7R)-7-[[carboxylato(4-hydroxyphenyl)acetyl]amino]-7-methoxy-3-[(1-methyl-1H-
Prestw-820		Aminophylline	317-34-0	420.43	<chem>N1(c2c(C(N(C1=O)C)=O)[nH]cn2).N1(c2c(C(N(C1=O)C)=O)[nH]cn2)C</chem>	1,3-dimethyl-7H-purine-2,6-dione ethane-1,2-diamine
Prestw-821		Azlocillin sodium salt	37091-65-9	483.48	<chem>N12[C@@]([C@]([C1=O)NC([C@H](NC(N1C(NCC1)=O)=O)c1cccc1)=O)[H])S(C([C@H]2C([O-])=O)(C)C)[H]</chem>	(2S,5R,6R)-3,3-dimethyl-7-oxo-6-[[2R)-2-[[2-oxo-1-imidazolidinyl)carbonyl]amino]-2-phenylacetyl]amino]-4-thia-
Prestw-822		Clidinium bromide	3485-62-9	432.36	<chem>C(C(c1cccc1)(c1cccc1)O)OC1C[N+]2(CCC1CC2)C=O</chem>	(1-methyl-1-azoniabicyclo[2.2.2]octan-3-yl) 2-hydroxy-2,2-diphenylacetate bromide
Prestw-823		Sulfamonomethoxine	1220-83-3	280.31	<chem>S(Nc1ncnc(c1)OC)(c1ccc(N)cc1)(=O)=O</chem>	4-amino-N-(6-methoxy-pyrimidin-4-yl)benzenesulfonamide
Prestw-824		Benzthiazide	91-33-8	431.94	<chem>S1(c2c(N=C(N1)C)SCCc1cccc1)cc(c(S(=O)(=O)N)c2)Cl(=O)=O</chem>	3-(benzylsulfanylmethyl)-6-chloro-1,1-dioxo-4H-1lambda,6,2,4-benzothiazine-7-
Prestw-825		Trichlormethiazide	133-67-5	380.66	<chem>S1(NC(Nc2c1cc(S(=O)(=O)N)c(c2)Cl)C(Cl)Cl(=O)=O</chem>	6-chloro-3-(dichloromethyl)-1,1-dioxo-3,4-dihydro-2H-1lambda,6,2,4-benzothiazine-7-
Prestw-826		Oxalamine citrate salt	1949-20-8	437.45	<chem>n1c(noc1CCN(CC)CC)c1cccc1</chem>	N,N-diethyl-2-(3-phenyl-1,2,4-oxadiazol-5-yl)ethanamine 2-hydroxypropane-1,2,3-tricarboxylic acid
Prestw-827		Propantheline bromide	50-34-0	448.40	<chem>C1(c2c(Oc3c1cccc3)cccc2)C(=O)OCC[N+](C(C)C)(C(C)C)C</chem>	methyl-di(propan-2-yl)-[2-(9H-xanthene-9-carbonyloxy)ethyl]azanium bromide
Prestw-1361		Viloxazine hydrochloride	35604-67-2	273.76	<chem>N1CC(OCC1)COc1c(OCC)cccc1</chem>	2-[(2-ethoxyphenoxy)methyl]morpholine hydrochloride
Prestw-829		Dimethadione	695-53-4	129.12	<chem>N1C(OC(C1=O)(C)C)=O</chem>	5,5-Dimethyl-2,4-oxazolidinedione
Prestw-830		Ethaverine hydrochloride	985-13-7	431.96	<chem>c12c(nccc1cc(c2)OCC)OCC)Cc1cc(c(cc1)OCC)OCC</chem>	1-[(3,4-diethoxyphenyl)methyl]-6,7-diethoxyisoquinoline hydrochloride
Prestw-831		Butacaine	149-16-6	306.45	<chem>C(c1ccc(N)cc1)(=O)OCCCN(CCCC)CCCC</chem>	3-(Dibutylamino)-1-propanol 4-aminobenzoate
Prestw-832		Cefoxitin sodium salt	33564-30-6	449.44	<chem>[C@]1(C(N2[C@@]1(SC=C=C2[C([O-])=O)COC(=O)N)[H])=O)NC(Cc1sccc1)=O)OC</chem>	(6R,7S)-3-(carbamoyloxymethyl)-7-methoxy-8-oxo-7-[(2-thiophen-2-ylacetyl]amino]-5-thia-1-
Prestw-833		Ifosfamide	3778-73-2	261.09	<chem>P1(N(CCC)CCCC1)(=O)NCCCl</chem>	N,3-bis(2-chloroethyl)-2-oxo-1,3,2lambda5-oxazaphosphinan-2-amine
Prestw-834		Novobiocin sodium salt	1476-53-5	634.62	<chem>C1(=C(c2c(OC1=O)c(c(O[C@H]1[C@@H]([C@@H]([C@H](C(O1)C)C)OC)OC(=O)N)O)cc2)C)O)NC(c1cc(c([O-])cc1)C)C=C(C)C)=O</chem>	sodium 7-(4-carbamoyloxy-3-hydroxy-5-methoxy-6,6-dimethylxan-2-yl)oxy-3-[[4-hydroxy-3-(3-methylbut-2-
Prestw-1800		Zolmitriptan	139264-17-8	287.36	<chem>O=C1NC(Cc2ccc3[nH]cc(CCN(C)C)c3c2)CO1</chem>	


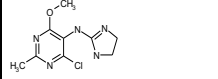
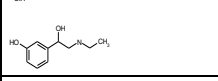
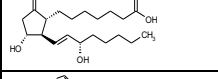
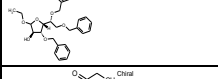
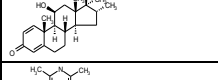
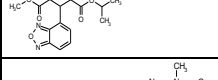
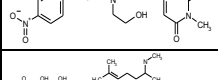
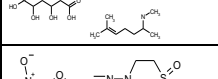
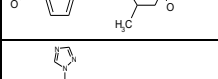
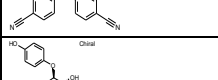
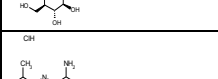
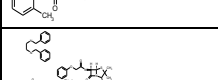
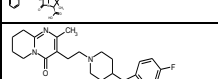
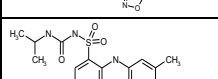
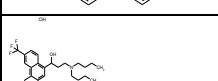
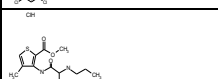
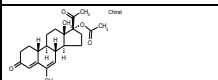
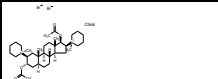
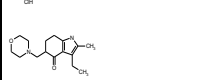
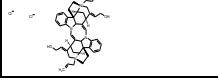

Prestw-858		Doxazosin mesylate	77883-43-3	547.59	<chem>c1(nc2c(c(n1)cc(c2)OC)OC)N)N1CCN(C(C2OC3c(OC2)cccc3)=O)CC1</chem>	[4-(4-amino-6,7-dimethoxyquinazolin-2-yl)piperazin-1-yl]-[2,3-dihydro-1,4-benzodioxin-3-(E,3R,5S)-7-[3-(4-fluorophenyl)-1-propan-2-ylindol-2-yl]-3,5-dihydroxyhept-6-enoate
Prestw-859		Fluvastatin sodium salt	93957-55-2	433.46	<chem>c1(n(c2c(c1c1ccc(cc1)F)cccc2)C(C)C)C=C/[C@@H](C[C@@H](C(C([O-])=O)O)O</chem>	(5S)-5-methylimidazolidine-2,4-dione
Prestw-860		Methylhydantoin-5-(L)	40856-73-3	114.10	<chem>N1C(N[C@H](C1=O)C)=O</chem>	(5S)-5-methylimidazolidine-2,4-dione
Prestw-861		Gabapentin	60142-96-3	171.24	<chem>C1(CCCCC1)(CC(O)=O)CN</chem>	2-[1-(aminomethyl)cyclohexyl]acetic acid
Prestw-862		Raloxifene hydrochloride	82640-04-8	510.06	<chem>c1(c(sc2c1ccc(c2)O)c1ccc(cc1)O)C(c1ccc(cc1)O)CCN1CCCC1=O</chem>	[6-hydroxy-2-(4-hydroxyphenyl)-1-benzothiophen-3-yl]-[4-(2-piperidin-1-
Prestw-1801		Ciclesonide	126544-47-6	540.70	<chem>OC1CC2(C)C(C3C1C1(C=CC(=C1CC3)=O)C)CC1C2(OC(C2CCCC2)O1)C(COC(C1C)C)=O</chem>	
Prestw-864		Methylhydantoin-5-(D)	55147-68-7	114.10	<chem>N1C(N[C@H](C1=O)C)=O</chem>	(5R)-5-methylimidazolidine-2,4-dione
Prestw-865		Simvastatin	79902-63-9	418.58	<chem>C=1\2/[C@]([C@@H](OC(C(CC)C)C)=O)C[C@H](\C1)C)([C@@](C[C@]1(OC(C[C@@H](C1)O)=O)[H])([C@H](\C=C2)C)[H])[H]</chem>	[(1S,3R,7S,8S,8aR)-8-[2-[(2R,4R)-4-hydroxy-6-oxooxan-2-yl]ethyl]-3,7-dimethyl-1,2,3,7,8,8a-
Prestw-866		Azacytidine-5	320-67-2	244.21	<chem>[N@@]1(C2[C@H]([C@H]([C@H](O2)CO)O)C)/N=C(\N=C1)/N=O</chem>	4-Amino-1-beta-D-ribofuranosyl-1,3,5-triazin-2(1H)-one
Prestw-867		Paromomycin sulfate	1263-89-4	713.72	<chem>[C@H]1([C@](OC2[C@@H]([C@H]([C@H]([C@H](O2)CO)O)N)([C@H]([C@H]([C@H]([C@H](O)N)N)[H])O[C@@]1([C@@H]([C@H](O[C@]2([C@@H]([C@H]([C@H]([C@H]([C@H](O2)CN)O)N)[H])C@H(O1)CO)H)</chem>	
Prestw-868		Acetaminophen	103-90-2	151.17	<chem>C(Nc1ccc(cc1)O)(=O)C</chem>	N-(4-Hydroxyphenyl)acetamide
Prestw-869		Phthalylsulfathiazole	85-73-4	403.44	<chem>c1cccc(c1C(O)=O)C(Nc1ccc(cc1)S(Nc1ncc1)(=O)=O)=O</chem>	2-[[[4-[(1,3-thiazol-2-ylamino)sulfonyl]phenyl]amino]carbonyl]benzoic acid
Prestw-870		Luteolin	491-70-3	286.24	<chem>c12c(\C=C/[O]c1cc(cc2O)O)c1cc(c(cc1)O)O)=O</chem>	2-(3,4-dihydroxyphenyl)-5,7-dihydroxychromen-4-one
Prestw-871		Iopamidol	60166-93-0	777.09	<chem>c1(c(c(c(c1)NC(=O)C[C@@](O)(C)[H])C(NC(CO)CO)=O)C)NC(CO)CO)=O</chem>	1-N,3-N-bis(1,3-dihydroxypropan-2-yl)-5-[[[2S]-2-hydroxypropanoyl]amino]-2,4,6-triodobenzene-1,3,1-N,3-N-bis(2,3-dihydroxypropyl)-2,4,6-triodo-5-[[[2-methoxyacetyl]amino]-3-N-methylbenzene-1,3-
Prestw-872		Iopromide	73334-07-3	791.12	<chem>c1(c(c(c(c1)C(NCC(O)CO)=O)C)NC(=O)COC)C)N(CC(O)CO)C)=O</chem>	1-N,3-N-bis(1,3-dihydroxypropyl)-2,4,6-triodo-5-[[[2-methoxyacetyl]amino]-3-N-methylbenzene-1,3-
Prestw-873		Theophylline monohydrate	5967-84-0	198.18	<chem>N1(c2c(C(N1=O)C)=O)[nH]cn2)C</chem>	1,3-dimethyl-7H-purine-2,6-dione hydrate
Prestw-874		Theobromine	83-67-0	180.17	<chem>c12c(C(NC(N1C)=O)=O)n(cn2)C</chem>	3,7-dimethylpurine-2,6-dione
Prestw-875		Reserpine	50-55-5	608.69	<chem>c12[nH]c3c(c1CCN1[C@@]2(C[C@@]2[C@@H]([C@H]([C@H](OC(c4cc(c(c4)OC)OC)OC)=O)C[C@@]2(C1)H])OC)C(=O)OC)[H])ccc(c3)OC</chem>	methyl (1R,15S,17R,18R,19S,20S)-6,18-dimethoxy-17-(3,4,5-trimethoxybenzoyloxy)-N-(4-cyano-3-(trifluoromethyl)phenyl)-3-[[4-fluorophenyl)sulfonyl]-2-hydroxy-2-
Prestw-1239		Bicalutamide	90357-06-5	430.38	<chem>S(CC(C(Nc1cc(C(F)F)C(C#N)cc1)=O)O)C)(c1ccc(cc1)F)=O</chem>	(-)-(S)-3-Hydroxy-2-phenylpropionic acid (1R,2R,4S,7S,9S)-9-methyl-3-oxa-9-
Prestw-877		Scopolamine hydrochloride	55-16-3	339.82	<chem>[C@@H]12[C@@H](O1)[C@H]1N([C@@H]2[C@H](C1)OC([C@H](c1cccc1)CO)=O)C</chem>	1-N,3-N-bis(2,3-dihydroxypropyl)-5-[[[2-hydroxyacetyl]-2-hydroxyethyl]amino]-2,4,6-
Prestw-878		Ioversol	87771-40-2	807.12	<chem>c1(c(c(c(c1)C(NCC(O)CO)=O)C)NC(=O)CO)=O)N(C(=O)CO)CCO</chem>	2-[[[4-(3-methoxypropoxy)-3-methylpyridin-2-yl]methylsulfonyl]benzimidazol-1-ide sodium
Prestw-1495		Rabepazole Sodium salt	117976-89-3	382.44	<chem>c1(nc2c([nH]1)cccc2)S(Cc1c(c(c1)O)CCCCOC)C=O</chem>	

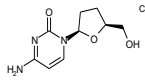
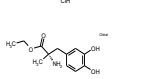
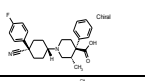
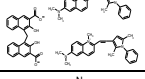
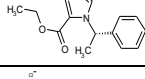
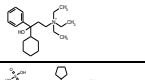
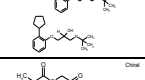
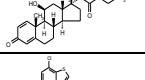
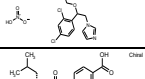
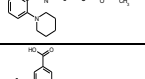
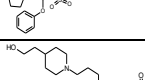
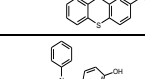
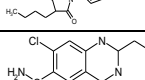
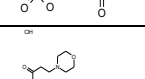
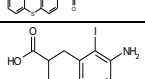
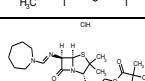
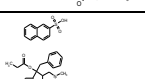
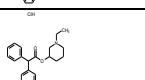
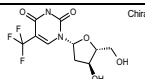
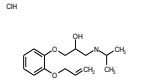
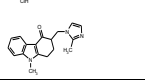

Prestw-880		Carbachol	51-83-2	182.65	<chem>C(=O)N(OCC[N+](C)(C)C)</chem>	2-carbamoyloxyethyl(trimethyl)azanium chloride
Prestw-881		Niacin	59-67-6	123.11	<chem>C1=CC=CC=C1C(=O)O</chem>	pyridine-3-carboxylic acid
Prestw-882		Bemegride	64-65-3	155.20	<chem>N1C(=O)CC(CC1=O)(CC)C</chem>	4-Ethyl-4-methyl-2,6-dioxo-piperidine
Prestw-883		Digoxigenin	1672-46-4	390.52	<chem>[C@]12([C@@]1([C@H]1C3=C1C(OC3)=O)CC1)([C@@H]1[C@@]2([C@@]3([C@]1(C)C)C(C)C)O)C(=O)O</chem>	3-[[3S,5R,8R,9S,10S,12R,13S,14S,17R]-3,12,14-trihydroxy-10,13-dimethyl-
Prestw-884		Meglumine	6284-40-8	195.22	<chem>[C@H]1([C@@H]([C@@H]1O)CNC)O([C@H]1O)CO</chem>	1-Deoxy-1-(methylamino)-D-glucitol
Prestw-1510		Dolasetron mesilate	115956-13-3	438.50	<chem>c1(C(O[C@H]2C[C@@]3(N4[C@](C2)C[C@@](C(C4)=O)C3)H)[H])=O)c[nH]c2c1cccc2</chem>	(2 alpha,6 alpha,8 alpha,9a beta)-octahydro-3-oxo-2,6-methano-2H-quinolin-8-yl-1H-indole-3-carboxylate
Prestw-886		Clioquinol	130-26-7	305.50	<chem>c12c(c(cc1ccn2)Cl)I)O</chem>	5-chloro-7-iodoquinolin-8-ol
Prestw-887		Oxybenzone	131-57-7	228.25	<chem>c1(C(=O)c2cccc2)c(cc1c)OC)O</chem>	(2-hydroxy-4-methoxyphenyl)-phenylmethanone
Prestw-888		Promethazine hydrochloride	58-33-3	320.89	<chem>N1(c2c(Sc3c1cccc3)cccc2)CC(N(C)C)C</chem>	N,N-dimethyl-1-phenothiazin-10-ylpropan-2-amine hydrochloride
Prestw-1167		Diacerein	13739-02-1	368.30	<chem>c12C(c3c(C1cc(C(=O)O)cc2OC(=O)C)=O)cccc3OC(=O)C)=O</chem>	4,5-diacetyloxy-9,10-dioxoanthracene-2-carboxylic acid
Prestw-1137		Esmolol hydrochloride	81161-17-3	331.84	<chem>C(=O)(CCc1ccc(OCC(CNC(C)C)O)cc1)OC</chem>	methyl 3-[4-[2-hydroxy-3-(propan-2-ylamino)propoxy]phenyl]propanoate hydrochloride
Prestw-1486		Cortisol acetate	50-03-3	404.51	<chem>[C@]12([C@@]1(C(COC(=O)C)=O)CC[C@]1([C@]1([C@@]2([C@@]3(C=C(C(=O)CC3)CC1)C)[C@H](C2)O)[H])[H])O)C</chem>	[[8S,9S,10R,11S,13S,14S,17R]-11,17-dihydroxy-10,13-dimethyl-3-oxo-
Prestw-1416		Flubendazol	31430-15-6	313.29	<chem>c1(nc2c([nH]1)ccc(C1ccc(cc1)F)=O)c2)NC(=O)OC</chem>	Methyl N-[6-(4-fluorobenzoyl)-1H-benzimidazol-2-yl]carbamate
Prestw-893		Felbinac	5728-52-9	212.25	<chem>C(=O)(Cc1ccc(c2cccc2)cc1)O</chem>	2-(4-phenylphenyl)acetic acid
Prestw-894		Butylparaben	94-26-8	194.23	<chem>C1=CC=C(C=C1)OC(=O)CCCC</chem>	butyl 4-hydroxybenzoate
Prestw-895		Aminohippuric acid	61-78-9	194.19	<chem>C(NCC(=O)O)(c1ccc(N)cc1)=O</chem>	2-[(4-aminobenzoyl)amino]acetic acid
Prestw-896		N-Acetyl-L-leucine	1188-21-2	173.21	<chem>[C@@](C(=O)O)(NC(=O)C)(CC(C)C)[H]</chem>	(2S)-2-acetamido-4-methylpentanoic acid
Prestw-897		Pipemidic acid	51940-44-4	303.32	<chem>C=1(C(c2c(nc(nc2)N2CCNCC2)N(C1)CC)=O)/C(=O)O</chem>	8-Ethyl-5,8-dihydro-5-oxo-2-(1-piperazinyl)pyrido[2,3-d]pyrimidine-6-carboxylic acid
Prestw-898		Dioxybenzone	131-53-3	244.25	<chem>C1=CC=C(C=C1)OC)O)(c1c(O)cccc1)=O</chem>	(2-hydroxy-4-methoxyphenyl)-(2-hydroxyphenyl)methanone
Prestw-899		Adrenosterone	382-45-6	300.40	<chem>[C@]12([C@@]1([C@@]3([C@@]1([C@@]4(C=C(C(=O)CC4)CC3)C)(C1)=O)[H])[H])(CC2=O)[H])C</chem>	(8S,9S,10R,13S,14S)-10,13-dimethyl-1,2,6,7,8,9,12,14,15,16-decahydrocyclopenta[a]phen
Prestw-900		Methylatropine nitrate	52-88-0	366.42	<chem>[N@@+][C@@H]2C[C@@H]1(OC(C3CCCC3)CO)=O)CC1CC2)C)C</chem>	[(1R,5S)-8,8-dimethyl-8-azoniabicyclo[3.2.1]octan-3-yl] 3-hydroxy-2-phenylpropanoate nitrate
Prestw-901		Hymecromone	90-33-5	176.17	<chem>c12OC/C=C(c1ccc(c2)O)/C=O</chem>	7-hydroxy-4-methylchromen-2-one

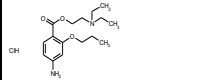
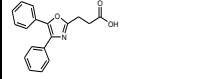

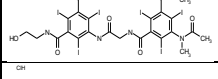
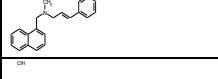

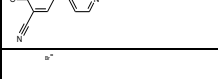
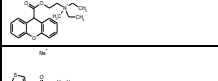
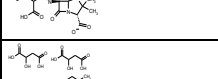
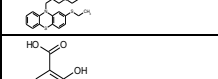
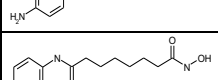
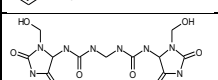
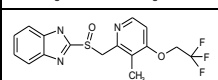
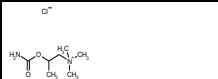
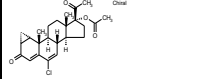
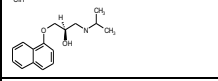
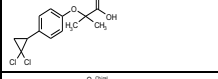
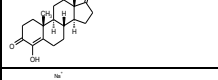
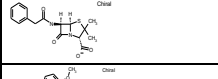
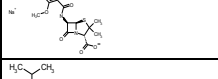
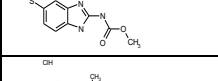
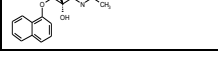

Prestw-925		Thonzonium bromide	553-08-2	591.73	<chem>c1(CN(CC[N+](CC)(C)C)c2ncccc2)ccc(cc1)OC</chem>	hexadecyl-2-[(4-methoxyphenyl)methylpyrimidin-2-ylamino]ethyl]-dimethylazanium bromide
Prestw-926		Idazoxan hydrochloride	79944-56-2	240.69	<chem>C1(Oc2c(OC1)cccc2)C1=NCCN1</chem>	(±)-2-[1,4-Benzodioxan-2-yl]-2-imidazoline hydrochloride
Prestw-927		Quinapril hydrochloride	82586-55-8	474.99	<chem>N1(C(C@@H)(N[C@H](C(=O)OCC)CCc2cccc2)C(=O)[C@@H](Cc2c(C1)cccc2)C(=O)O</chem>	(3S)-2-[(2S)-2-[(2S)-1-ethoxy-1-oxo-4-phenylbutan-2-yl]amino]propanoic acid, 3,4-dihydro-1H-isoquinoline-3-
Prestw-928		Nilutamide	63612-50-0	317.23	<chem>N1(C(NC(C1=O)(C)C)=O)c1cc(c([N+](O-)=O)cc1)C(F)(F)F</chem>	5,5-dimethyl-3-[4-nitro-3-(trifluoromethyl)phenyl]imidazolidine-2,4-dione
Prestw-929		Ketorolac tromethamine	74103-07-4	376.41	<chem>n12c(C(C(=O)O)CC1)ccc2C(=O)c1cccc1</chem>	5-benzoyl-2,3-dihydro-1H-pyrrolidine-1-carboxylic acid, 2-amino-2-(hydroxymethyl)propane-1,3-
Prestw-930		Protriptyline hydrochloride	1225-55-4	299.85	<chem>C1(c2c(C=C/c3c1cccc3)cccc2)CCCN1</chem>	3-(11H-dibenzo[1,2-a:1',2'-e][7]annulen-1-yl)-N-methylpropan-1-amine hydrochloride
Prestw-931		Propofol	2078-54-8	178.28	<chem>c1(c(C(C)C)cccc1C(C)C)O</chem>	2,6-di(isopropyl)phenol
Prestw-932		S(-)-Eticlopride hydrochloride	97612-24-3	377.31	<chem>c1(c(c(cc1OC)Cl)CC)O)C(NC[C@H]1N(CCC1)CC)=O</chem>	S(-)-3-Chloro-5-ethyl-N-[(1-ethyl-2-pyrrolidinyl)methyl]-6-hydroxy-2-methoxybenzamide
Prestw-933		Primidone	125-33-7	218.26	<chem>C1(C(NCNC1=O)=O)(c1cccc1)CC</chem>	5-ethyl-5-phenyl-1,3-diazinane-4,6-dione
Prestw-934		Flucytosine	2022-85-7	129.09	<chem>N1=C(C(=C/NC1=O)F)/N</chem>	6-amino-5-fluoro-1H-pyrimidin-2-one
Prestw-935		(-)-MK 801 hydrogen maleate	77086-19-2	337.38	<chem>[C@@]12(N[C@H](c3c1cccc3)Cc1c2cccc1)C</chem>	(5S,10R)-(-)-5-Methyl-10,11-dihydro-5H-dibenzo-[a,d]-cyclo-hepten-5,10-imine hydrogen maleate
Prestw-936		Bephenium hydroxynaphthoate	3818-50-6	443.55	<chem>[N+](Cc1cccc1)(CCOc1cccc1)(C)C</chem>	benzyl-dimethyl-(2-phenoxyethyl)azanium 3-carboxynaphthalen-2-olate
Prestw-937		Dehydroisoandrosterone 3-acetate	853-23-6	330.47	<chem>[C@@]12(C(=C)C[C@@]3([C@@]1(CC[C@]1([C@]3(CCC1=O)[H])C)[H])[H])C[C@@H](OC(=O)C)CC2)C</chem>	3-beta-Acetoxy-5-androsten-17-one
Prestw-938		Benserazide hydrochloride	14919-77-8	293.71	<chem>c1(c(c(cc1O)CN)C(N)C(=O)O)O</chem>	2-amino-3-hydroxy-N-[(2,3,4-trihydroxyphenyl)methyl]propanehydrazide hydrochloride
Prestw-939		Iodipamide	606-17-7	1139.77	<chem>c1(c(c(c(cc1I))NC(=O)CCCC(Nc1c(c(c(cc1I))C(=O)O))=O))C(=O)O</chem>	3-[[6-(3-carboxy-2,4,6-triiodoanilino)-6-oxohexanoyl]amino]-2,4,6-triiodobenzoic acid
Prestw-1213		Allopurinol	315-30-0	136.11	<chem>c12c(N=C/NC1=O)[nH]nc2</chem>	1,2-dihydropyrazolo[3,4-d]pyrimidin-4-one
Prestw-941		Pentetic acid	67-43-6	393.35	<chem>N(CCN(CCN(CC(O)=O)CC(O)=O)CC(=O)O)(CC(O)=O)C(C(O)=O)</chem>	2-[bis[2-[bis(carboxymethyl)amino]ethyl]amino]acetic acid
Prestw-942		Bretylium tosylate	61-75-6	414.36	<chem>c1(C[N+](CC)(C)C(Br)cccc1</chem>	(2-bromophenyl)methyl-ethyl-dimethylazanium 4-methylbenzenesulfonate
Prestw-943		Pralidoxime chloride	51-15-0	172.62	<chem>[n+]1(c(C=N)O)cccc1)C</chem>	[(E)-(1-methylpyridin-2-ylidene)methyl]-oxoazanium chloride
Prestw-944		Phenoxybenzamine hydrochloride	63-92-3	340.30	<chem>N(Cc1cccc1)(C(COc1cccc1)C)CCCl</chem>	N-(2-chloroethyl)-N-(1-methyl-2-phenoxyethyl)-benzenemethanamine hydrochloride
Prestw-945		Salmeterol	89365-50-4	415.58	<chem>c1(cc(ccc1O)C(O)CNCCCCCOCCCCc1cccc1)CO</chem>	2-(hydroxymethyl)-4-[1-hydroxy-2-[6-(4-phenylbutoxy)hexylamino]ethyl]phenol
Prestw-946		Altretamine	645-05-6	210.28	<chem>n1c(nc(nc1N(C)C)N(C)C)N(C)C</chem>	2-N,2-N,4-N,4-N,6-N,6-N-hexamethyl-1,3,5-triazine-2,4,6-triamine

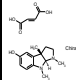
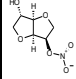
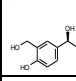
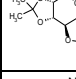
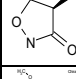
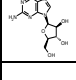
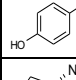
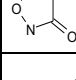
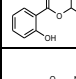
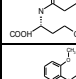
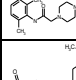
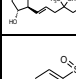
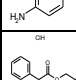

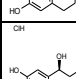
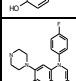
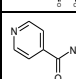
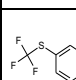
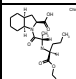
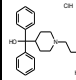
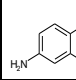

Prestw-1602		Indatraline hydrochloride	86939-10-8	328.67	[C@@H]1(c2c([C@@H](C1)NC)cccc2)c1cc(c(cc1)Cl)Cl	(1R,3S)-3-(3,4-dichlorophenyl)-N-methyl-2,3-dihydro-1H-inden-1-amine hydrochloride
Prestw-971		Remoxipride Hydrochloride	73220-03-8	407.74	c1(C(NC[C@]2(N(CCC2)C)[H])=O)c(c(ccc1OC)Br)OC	3-bromo-N-[(2S)-1-ethylpyrrolidin-2-yl]methyl]-2,6-dimethoxybenzamide hydrochloride
Prestw-972		THIP Hydrochloride	85118-33-8	176.60	c12c(noc1CNCC2)O	4,5,6,7-tetrahydro-[1,2]oxazol[5,4-c]pyridin-3-one hydrochloride
Prestw-973		Pirlindole mesylate	60762-57-4	322.43	n12c3c(c4c1ccc(c4)C)CCCC3NCC2	2,3,3a,4,5,6-Hexahydro-8-methyl-1H-pyrazino[3,2,1-j,k]carbazole
Prestw-974		Pronethalol hydrochloride	51-02-5	265.79	c1(cc2c(cc1)cccc2)C(CNC(C)C)O	a{[(1-Methylethylamino)methyl]-2-naphthalene-methanol hydrochloride
Prestw-975		Naftopidil dihydrochloride	57149-08-3	465.42	N1(c2c(OC)cccc2)CCN(CC(CO2c3c(ccc2)cccc3)O)CC1	1-[4-(2-methoxyphenyl)piperazin-1-yl]-3-naphthalen-1-ylxypropan-2-ol
Prestw-976		Tracazolate hydrochloride	41094-88-6	340.86	c12c(nc(c1NCCCC)C(=O)OCC)Cn(nc2)CC	ethyl 4-(butylamino)-1-ethyl-6-methylpyrazolo[3,4-b]pyridine-5-carboxylate hydrochloride
Prestw-977		Zardaverine	101975-10-4	268.22	N=1NC(\C=C/C1/c1cc(c(OC(F)F)cc1)OC)=O	3-[4-(difluoromethoxy)-3-methoxyphenyl]-1H-pyridazin-6-one
Prestw-978		Memantine Hydrochloride	41100-52-1	215.77	C12(CC3(CC(C1)CC(C2)C3)C)N	1-Amino-3,5-dimethyladamantane hydrochloride
Prestw-979		Ozagrel hydrochloride	78712-43-3	264.71	n1cn(cc1)Cc1ccc(\C=C(O)O)cc1	(E)-3-[4-(imidazol-1-ylmethyl)phenyl]prop-2-enoic acid hydrochloride
Prestw-980		Piribedil hydrochloride	78213-63-5	334.81	c1(N2CCN(Cc3cc4c(OCO4)cc3)CC2)ncccn1	2-[4-(1,3-benzodioxol-5-ylmethyl)piperazin-1-yl]pyrimidine hydrochloride
Prestw-981		Nitrocaramphen hydrochloride	98636-73-8	370.88	[N+](c1ccc(C2(C(=O)OCCN(CC)CC)CCCC2)cc1)[O-]=O	2-(diethylamino)ethyl 1-(4-nitrophenyl)cyclopentane-1-carboxylate hydrochloride
Prestw-982		Nandrolone	434-22-0	274.41	[C@]12([C@@]([C@]3([C@@]([C@@]4(\C=C/C(=O)CC4)CC3)[H])(C1)[H])([H])(C[C@H]2O)[H])C	(8R,9S,10R,13S,14S,17S)-17-hydroxy-13-methyl-2,6,7,8,9,10,11,12,14,15,16,17-dodecahydro-1H-
Prestw-983		Dimaprit dihydrochloride	23256-33-9	234.19	C(=N)(SCCCN(C)C)N	3-(dimethylamino)propyl carbamimidothioate dihydrochloride
Prestw-1459		Oxendazol	53716-50-0	315.35	c1(nc2cc(S(=O)c3ccccc3)ccc2[nH]1)NC(=O)OC	methyl N-[6-(benzenesulfinyl)-1H-benzimidazol-2-yl]carbamate
Prestw-1268		Guaiacol	90-05-1	124.14	c1(c(OC)cccc1)O	2-methoxyphenol
Prestw-986		Proscillaridin A	466-06-8	530.66	[C@]12([C@@]([C@H](/C3=C/OC(/C=C3)=O)CC1)(C[C@]1([C@@]3([C=C([C@H](O[C@]4([C@H](C[C@H](C[C@H](C[C@H](O4)C)O)O)[H])CC3)CC[C@@]21[H])C)H)C)O	5-[14-hydroxy-10,13-dimethyl-3-[(2R,3R,4R,5R,6S)-3,4,5-trihydroxy-6-methyloxan-2-yl]oxy-
Prestw-1316		Pramipexole dihydrochloride	104632-25-9	284.25	n1c(sc2c1CC[C@@H](C2)NCCC)N	(6S)-6-N-propyl-4,5,6,7-tetrahydro-1,3-benzothiazole-2,6-diamine dihydrochloride
Prestw-1452		Norgestimate	35189-28-7	369.51	[C@]12([C@@]([C#C](OC(=O)C)CC[C@]1([C@]1([C@@]([C@@]3(\C=C/C(=NO)CC3)CC1)[H])(CC2)[H])(H)H)CC	[(3E,8R,9S,10R,13S,14S,17R)-13-ethyl-17-ethynyl-3-hydroxyimino-1,2,6,7,8,9,10,11,12,14,15,16,17-dodecahydro-1H-
Prestw-1374		Chlormadinone acetate	302-22-7	404.94	C/1=2\([C@@]([C@]3([C@@]([C=C1/Cl])([C@]1([C@@]([C@@]([C@]1)OC(=O)C)C(=O)C)CC3)C)[H])(H)H)CCC(C2)=O)C	[(8R,9S,10R,13S,14S,17R)-17-acetyl-6-chloro-10,13-dimethyl-3-oxo-2,8,9,11,12,14,15,16-
Prestw-1310		Phenylbutazone	50-33-9	308.38	N1(N(C(C(C1=O)CCCC)=O)c1cccc1)c1cccc1	4-butyl-1,2-diphenylpyrazolidine-3,5-dione
Prestw-991		Gliquidone	33342-05-1	527.64	N1(C(C(c2c(C1=O)cc(cc2)OC)(C)C)=O)CCc1ccc(S(NC(NC2CCCC2)=O)(=O)O)cc1	1-cyclohexyl-3-[4-[2-(7-methoxy-4,4-dimethyl-1,3-dioxoisquinolin-2-yl)ethyl]phenyl]sulfonyleurea
Prestw-992		Pizotifen malate	5189-11-7	429.54	C1(/c2c(scc2)CCc2c1cccc2)=C1/CCN(CC1)C	4-(4,5-dihydrobenzo[1,2]cyclohepta[3,4-b]thiophen-10-ylidene)-1-methylpiperidine 2-

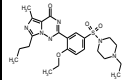
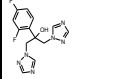
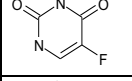
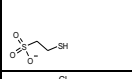
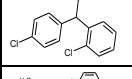
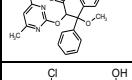
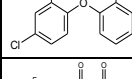
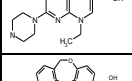
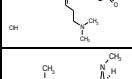
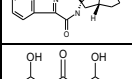
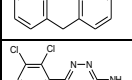
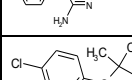
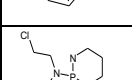
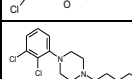
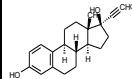
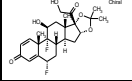
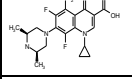
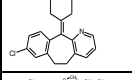
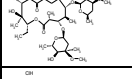
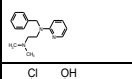
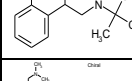
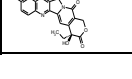

Prestw-993		Ribavirin	36791-04-5	244.21	n1([C@H]2[C@@H]([C@@H]([C@H](O2)CO)O)nc(nc1)C(=O)N	1-[(2R,3R,4S,5R)-3,4-dihydroxy-5-(hydroxymethyl)oxolan-2-yl]-1,2,4-triazole-3-carboxamide
Prestw-994		Cyclophentiazide	742-20-1	379.89	S1(c2c(NC(N1)CC1CCCC1)cc(c(S(=O)(=O)N)c2)Cl)(=O)=O	6-chloro-3-(cyclopentylmethyl)-1,1-dioxo-3,4-dihydro-2H-1lambda6,2,4-benzothiadiazine-7-
Prestw-995		Fluvoxamine maleate	61718-82-9	434.42	C(c1ccc(C(=N)OCCN)CCCCOC)cc1(F)(F)F	2-[(E)-5-methoxy-1-[4-(trifluoromethyl)phenyl]pentylidene]amino]oxyethanamine (Z)-but-2-enedioic acid
Prestw-1321		Prothionamide	14222-60-7	180.27	C(c1cc(ncc1)CCC)(=S)N	2-propylpyridine-4-carbothioamide
Prestw-997		Fluticasone propionate	80474-14-2	500.58	[C@]112([C@@]3([C@]([C@]4([C@@]([C@]([C@@H]([C4)C)(C(SCF)=O)OC(=O)CC)(C[C@@H]3O)C)[H])(C[C@@H]([C1=C/C(C=C2)=O)F][H])F)C	[(6S,8S,9R,10S,11S,13S,14S,16R,17R)-6,9-difluoro-17-(fluoromethylsulfanylcarbonyl)-11-hydroxy-10,13,16-
Prestw-998		Zuclopenthixol dihydrochloride	633-59-0	473.90	C1(c2c(Cc3c1cccc3)ccc(c2)Cl)=C/CCN1CCN(CC1)CCO	2-[4-[(3Z)-3-(2-chlorothioxanthen-9-ylidene)propyl]piperazin-1-yl]ethanol dihydrochloride
Prestw-999		Proguanil hydrochloride	637-32-1	290.20	C(NC(=N)NC(C)C)(Nc1ccc(Cl)cc1)=N	(1E)-1-[amino-(4-chloroanilino)methylidene]-2-propan-2-ylguanidine hydrochloride
Prestw-1000		Lymecycline	992-21-2	602.65	[C@@]12(C(=C3/C(C4c([C@]([C@]3(C[C@]1([C@@H]([C=C(C12=O)C(NCNC(C(=O)O)CCCCN)=O)O)N(C)C)[H])[H])(O)C)ccc4O)=O)O	(+)-N-(5-amino-5-carboxypentylaminomethyl)-4-dimethylamino-1,4,4a,5,5a,6,11,12a-
Prestw-1001		Alfadolone acetate	23930-37-2	390.52	[C@]12([C@]([C@]3([C@@]([C@@]4([C@@]([C@]([C@@H]([C4)O)[H])C(C1=O)[H])[H])CC[C@@H]2(COC(=O)C)=O)[H])C	[(3R,5S,8S,9S,10S,13S,14S,17S)-3-hydroxy-10,13-dimethyl-11-oxo-
Prestw-1002		Alfaxalone	23930-19-0	332.49	[C@]12([C@]([C@]3([C@@]([C@@]4([C@@]([C@]([C@@H]([C4)O)[H])C(C1=O)[H])[H])CC[C@@H]2(C=O)C)[H])C	(3R,5S,8S,9S,10S,13S,14S,17S)-17-acetyl-3-hydroxy-10,13-dimethyl-1,2,3,4,5,6,7,8,9,12,14,15,1-
Prestw-1003		Azapropazone	13539-59-8	300.36	N12N(C(C1=O)CCC)=O)c1c(N=C2N(C)C)ccc(c1)C	5-(dimethylamino)-9-methyl-2-propylpyrazolo[1,2-a][1,2,4]benzotriazine-1,3-dione
Prestw-1004		Meptazinol hydrochloride	59263-76-2	269.82	C1(c2cc(O)ccc2)(CN(C)CCCC1)CC	3-(3-ethyl-1-methylazepan-3-yl)phenol hydrochloride
Prestw-1005		Apramycin	37321-09-8	539.59	C12O[C@H](O[C@]3([C@@H]([C@H]([C@@H]([C@@H]([C@@H]3N)N)O)O)[H])C[C@@H]([C@@]1(O[C@H]([C@H]2)NC)O)[C@@]1([C@@H]([C@H]([C@@H]([C@@H]([C@@H](O1)CO)N)O)O)[H])[H])N	(2R,3R,4R,5S,6R)-5-amino-2-[[[(1R,2R,3R,4R,6R,8R)-8-amino-9-[(1R,2S,3R,4R,6R)-4,6-diamino-2,3-dihydroxy-
Prestw-1802		Darunavir	635728-49-3	547.68	O=S(N(CC(C)C)CC(O)C(NC(=O)OC1COC2OCCC12)Cc1cccc1)(c1ccc(N)cc1)=O	
Prestw-1007		Fursultiamine Hydrochloride	2105-43-3	435.01	n1c(c(CN(C=C(SSCC2OCCC2)/CCO)C)C=O)cn(c1)C	N-(4-Amino-2-methylpyrimidin-5-ylmethyl)-N-[4-hydroxy-1-methyl-2-[(tetrahydrofurfuryl)dithio]-1-ethyl 4-[6-(diaminomethylideneamino)hexanoyloxy]benzoate methanesulfonic acid
Prestw-1008		Gabexate mesilate	56974-61-9	417.48	C(=N)(NCCCCC(Oc1ccc(C(=O)OCC)cc1)=O)N	2,2-(diaminomethylideneamino)hexanoyloxy]benzoate methanesulfonic acid
Prestw-1009		Pivampicillin	33817-20-8	463.56	N12[C@@]([C@@]([C1=O)NC([C@@H](c1cccc1)N)=O)[H])(SC([C@@H]2C(OCOC(C(C)C)C)=O)O)(C)C)[H]	dimethylpropanoilyloxymethyl (2S,5R,6R)-6-[(2R)-2-amino-2-phenylacetyl]amino]-3,3-
Prestw-1746		Lodoxamide	53882-12-5	311.64	c1(c(c(NC(C(=O)O)=O)cc(C#N)c1)Cl)NC(C(=O)O)=O	2-[2-chloro-5-cyano-3-(oxaloamino)anilino]-2-oxoacetic acid
Prestw-1011		Flucloxacillin sodium	1847-24-1	475.86	N12[C@@]([C@@]([C1=O)NC(c1c(noc1)C)c1(C)cccc1)C(=O)[H])(SC(C2C(O)=O)(C)C)[H]	(2S,5R,6R)-6-[[3-(2-chloro-6-fluorophenyl)-5-methyl-1,2-oxazole-4-carbonyl]amino]-3,3-dimethyl-7-oxo-4-thia-1-
Prestw-1012		Trapidil	15421-84-8	205.26	n12c(ncn1)nc(cc2N(CC)CC)C	N,N-diethyl-5-methyl-[1,2,4]triazolo[1,5-a]pyrimidin-7-amine
Prestw-1013		Deptopine citrate	2169-75-7	525.60	C1(c2c(CCC3c1cccc3)cccc2)OC1C[C@@H]2N([C@H](C1)CC2)C	3-(6,11-dihydro-5H-dibenzo[1,2-a:1',2'-e][7]annulen-11-yloxy)-8-methyl-8-
Prestw-1014		Sertraline	79617-96-2	306.24	c12[C@]([c3cc(c(cc3)Cl)Cl)CC[C@@]([c1cccc2)(NC)[H])[H]	(1S,4S)-4-(3,4-dichlorophenyl)-N-methyl-1,2,3,4-tetrahydronaphthalen-1-amine

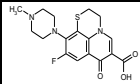
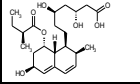
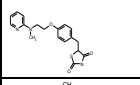
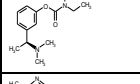
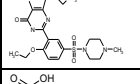
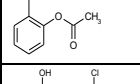
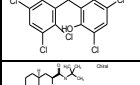
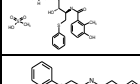
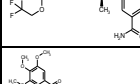
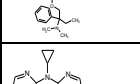
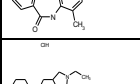
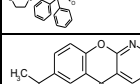
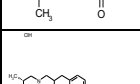
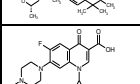
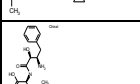
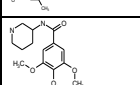
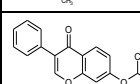
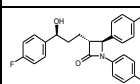
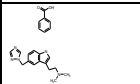
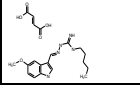
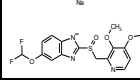

Prestw-1015		Ethamsylate	2624-44-4	263.31	<chem>S(c1cc(ccc1O)O)(=O)=O</chem>	2,5-dihydroxybenzenesulfonic acid N-ethylethanamine
Prestw-1016		Moxonidine	75438-57-2	241.68	<chem>c1c(nc(nc1OC)C)Cl)N/C1=N/CCN1</chem>	4-chloro-N-(4,5-dihydro-1H-imidazol-2-yl)-6-methoxy-2-methylpyrimidin-5-amine
Prestw-1017		Etilefrine hydrochloride	534-87-2	217.70	<chem>c1(cc(O)ccc1)C(O)CNCC</chem>	2-Ethylamino-1-(3-hydroxyphenyl)ethanol monohydrochloride
Prestw-1018		Alprostadil	745-65-3	354.49	<chem>C1(C[C@H]([C@H](C=C[C@H](O)CCCC)[C@H]1C)CCCC(=O)O)O=O</chem>	7-[(1R,2R,3R)-3-hydroxy-2-[(E,3S)-3-hydroxyoct-1-enyl]-5-oxocyclopentyl]heptanoic acid
Prestw-1019		Tribenoside	10310-32-4	478.59	<chem>[C@@H]1([C@](OC([C@@H]1O)OCC)([C@H](OCc1ccc(O)COc1)COc1cccc1)[H])OCC1CCCC1</chem>	(3R,4R,5R)-5-[1,2-bis(phenylmethoxy)ethyl]-2-ethoxy-4-phenylmethoxyoxolan-3-ol
Prestw-1020		Rimexolone	49697-38-3	370.54	<chem>[C@]12([C@]([C@]3([C@@]([C@@]4(C=C/C(C=C4)=O)CC3)C)[C@H](C1O)[H])[H]C[C@H]([C@@]2(C=O)CC)C)[H]C</chem>	(8S,9S,10R,11S,13S,14S,16R,17S)-11-hydroxy-10,13,16,17-tetramethyl-17-propanoyl-
Prestw-1021		Isradipine	75695-93-1	371.40	<chem>C=1(/C/C=C(N1C1C)/C(=O)OC)c1c2c(non2)ccc1)C(OC)C(=O)</chem>	3-O-methyl 5-O-propan-2-yl 4-(2,1,3-benzoxadiazol-4-yl)-2,6-dimethyl-1,4-dihydropyridine-3,5-
Prestw-1774		Nifekalant	130636-43-0	405.46	<chem>C1(N(/C=C(C1N1C)=O)/NCCN(CCCc1ccc([N+](O-)=O)cc1)CCO)C=O</chem>	6-[2-[2-hydroxyethyl]-3-(4-nitrophenyl)propyl]amino]ethylamino]-1,3-dimethylpyrimidine-2,4-dione
Prestw-1023		Isometheptene mucate	7492-31-1	492.66	<chem>C=C(CCC(NC)C)(C)/C.C=C(CCC(NC)C)(C)/C</chem>	(2S,3R,4S,5R)-2,3,4,5-tetrahydroxyhexanedioic acid N,6-dimethylhept-5-en-2-amine
Prestw-1024		Nifurtimox	23256-30-6	287.30	<chem>S1(CC(N(N=Cc2oc([N+](O-)=O)cc2)CC1)C(=O)=O</chem>	(E)-N-(3-methyl-1,1-dioxo-1,4-thiazinan-4-yl)-1-(5-nitrofuran-2-yl)methanimine
Prestw-1025		Letrozole	112809-51-5	285.31	<chem>n1(ncnc1)C(c1ccc(C#N)cc1)c1ccc(C#N)cc1</chem>	4-[(4-cyanophenyl)-(1,2,4-triazol-1-yl)methyl]benzotrile
Prestw-1026		Arbutin	497-76-7	272.26	<chem>[C@@H]1([C@@H]([C@H]([C@H]([C@H](O1)CO)O)O)O)c1ccc(cc1)O</chem>	(2R,3S,4S,5R,6S)-2-(hydroxymethyl)-6-(4-hydroxyphenoxy)oxane-3,4,5-triol
Prestw-1027		Tocainide hydrochloride	71395-14-7	228.72	<chem>N(C(=O)C(N)C)c1c(cccc1)C</chem>	2-amino-N-(2,6-dimethylphenyl)propanamide hydrochloride
Prestw-1028		Benzathine benzylpenicillin	5928-84-7	941.14	<chem>N12[C@@]([C@@](C1=O)(NC=O)COc1cccc1)[H])(SC(C2C(=O)O)C)C[H].N12[C@@]([C@@](C1=O)(NC=O)COc1cccc1)[H])(SC(C2C(=O)O)C)C[H]</chem>	3,3-dimethyl-7-oxo-6-[(2-phenylacetyl)amino]-4-thia-1-azabicyclo[3.2.0]heptane-2-carboxylic acid N,N'-
Prestw-1029		Risperidone	106266-06-2	410.50	<chem>C=1(\C(N2(C=N/C1/C)CCCC2)=O)/CCN1CCC(c2noc3c2cc(c3)F)CC1</chem>	3-[2-[4-(6-fluoro-1,2-benzisoxazol-3-yl)piperidino]ethyl]-6,7,8,9-tetrahydro-2-methylpyridol[1,2-
Prestw-1030		Torsemide	56211-40-6	348.43	<chem>S(NC(NC(C)C)=O)(c1c(Nc2cc(ccc2)ccnc1)(=O)=O</chem>	1-[4-(3-methylanilino)pyridin-3-yl]sulfonyl-3-propan-2-ylurea
Prestw-1031		Halofantrine hydrochloride	36167-63-2	536.90	<chem>c12c3c(cc(c1ccc(C(F)(F)F)c2)C(CCN(CCCC)CCCC)O)c(c(c3)Cl)Cl</chem>	3-(dibutylamino)-1-[1,3-dichloro-6-(trifluoromethyl)phenanthren-9-yl]propan-1-ol
Prestw-1032		Articaine hydrochloride	23964-57-0	320.84	<chem>c1(c(NC(=O)N(CCC)C)c(cs1)C)C(=O)OC</chem>	methyl 4-methyl-3-[2-(propylamino)propanoylamino]thiophene-2-carboxylate hydrochloride
Prestw-1033		Nomegestrol acetate	58652-20-3	370.49	<chem>[C@]12([C@@]([C@]3([C@@]([C@@]4(C=C[C@H]([N+]5(C)CCCC5)[C@H](C[C@@]4(C3)C)OC(=O)C)CC1)[H])[H])(OC(=O)C)C(=O)C</chem>	[(8S,9S,10R,13S,14S,17R)-17-acetyl-6,13-dimethyl-3-oxo-1,2,8,9,10,11,12,14,15,16-decahydrocyclopenta[α]phen
Prestw-1034		Pancuronium bromide	15500-66-0	732.69	<chem>[C@]12([C@@]([C@]3([C@@]([C@@]4(C=C[C@H]([N+]5(C)CCCC5)[C@H](C[C@@]4(C3)C)OC(=O)C)CC1)[H])[H])([C@]([C@@]([C@@]2OC(=O)C)[N+]1(C)CCCC1)[H])C</chem>	[(2S,3S,5S,8R,9S,10S,13S,14S,16S,17R)-17-acetyloxy-10,13-dimethyl-2,16-bis(1-methylpiperidin-1-ium-1-yl)-
Prestw-1035		Molindone hydrochloride	15622-65-8	312.84	<chem>c12c([nH]c(c1CC)C)CC(C2=O)CN1CCOCC1</chem>	3-ethyl-2-methyl-5-(morpholin-4-ylmethyl)-1,5,6,7-tetrahydroindol-4-one hydrochloride
Prestw-1036		Alcuronium chloride	15180-03-7	737.82	<chem>[C@@]123C4N(C=C5/C6[C@@]17([C@]8([N@+](C/C([C@@]5(C8)[H])=C)CO)(CC7)CC=C)[H])c5c(N6(C=C4[C@@]4(C(C(N@@+)([C@]1(C4)[H])(CC2)CC=C)C)C)O)[H])cccc5c1c3cccc1</chem>	4,4'-Didemethyl-4,4'-di-propenyltoxiferin-1-dichloride

Prestw-1037		Zalcitabine	7481-89-2	211.22	<chem>N1(C(N=C(C=C1)/N)=O)[C@@H]1O[C@@H](CC1)CO</chem>	4-amino-1-[(2R,5S)-5-(hydroxymethyl)oxolan-2-yl]pyrimidin-2-one
Prestw-1038		Methyldopate hydrochloride	2508-79-4	275.73	<chem>c1(C[C@](C(OCC)=O)(C)N)cc(c(cc1)O)O</chem>	ethyl (2S)-2-amino-3-(3,4-dihydroxyphenyl)-2-methylpropanoate hydrochloride
Prestw-1039		Levocabastine hydrochloride	79547-78-7	456.99	<chem>[C@]1([C@H](CN([C@]2(CC[C@](C#N)(c3ccc(cc3)F)CC2)[H])CC1)C)(C=O)O)c1cccc1</chem>	(3S,4R)-1-[4-cyano-4-(4-fluorophenyl)cyclohexyl]-3-methyl-4-phenylpiperidine-4-carboxylic acid hydrochloride
Prestw-1040		Pyrvinium pamoate	3546-41-6	1151.43	<chem>n1(c(cc(c1)C)=Cc1ccc2cc(ccc2[n+](1)C)N(C)C)C)c1cccc1.n1(c(cc(c1)C)=Cc1ccc2cc(ccc2[n+](1)C)N(C)C)C)c1cccc1</chem>	2-[(E)-2-(2,5-dimethyl-1-phenylpyrrol-3-yl)ethenyl]-N,N,1-trimethylquinolin-1-ium-6-amine 3-carboxy-1-[(3-ethyl 3-(1-phenylethyl)imidazole-4-carboxylate
Prestw-1041		Etomidate	33125-97-2	244.30	<chem>c1(n(cnc1)[C@H](c1cccc1)C)C(=O)OCC</chem>	ethyl 3-(1-phenylethyl)imidazole-4-carboxylate
Prestw-1042		Tridihexethyl chloride	4310-35-4	353.98	<chem>C(CC[N+](CC)(CC)CC)(c1cccc1)(C1CCCC1)O</chem>	(3-cyclohexyl-3-hydroxy-3-phenylpropyl)-triethylazanium chloride
Prestw-1043		Penbutolol sulfate	38363-32-5	680.95	<chem>c1(c(OCC(CNC(C)C)C)O)[H])cccc1)C1CCCC1.c1(c(OCC(CNC(C)C)C)O)[H])cccc1)C1CCCC1</chem>	(2S)-1-(tert-butylamino)-3-(2-cyclopentylphenoxy)propan-2-ol sulfuric acid
Prestw-1044		Prednicarbate	73771-04-7	488.58	<chem>[C@]12([C@](C(COC(=O)CC)=O)(OC(=O)OCC)CC[C@]1([C@]1([C@]([C@]13(C=C(C(C=C3)=O)CC1)C)(C@H)(C2)O)[H])H)H)C</chem>	[2-[(8S,9S,10R,11S,13S,14S,17R)-17-ethoxycarbonyloxy-11-hydroxy-10,13-dimethyl-3-oxo-1-[2-[(7-chlorobenzo[b]thien-3-yl)methoxy]-2-(2,4-dichlorophenyl)ethyl]-1H-imidazole-(RS) nitrate
Prestw-1045		Sertaconazole nitrate	99592-39-9	500.79	<chem>s1c2c(c(c1)COC(c1cc(cc1)Cl)Cl)Cn1cncc1)cccc2Cl</chem>	1-[2-[(7-chlorobenzo[b]thien-3-yl)methoxy]-2-(2,4-dichlorophenyl)ethyl]-1H-imidazole-(RS) nitrate
Prestw-1046		Repaglinide	135062-02-1	452.60	<chem>c1(C(=O)O)c(cc(CC(N[C@H](c2c(N3CCCC3)cccc2)CC(C)C)=O)cc1)OCC</chem>	2-ethoxy-4-[2-[(1S)-3-methyl-1-(2-piperidin-1-ylphenyl)butylamino]-2-oxoethyl]benzoic acid
Prestw-1047		Piretanide	55837-27-9	362.41	<chem>c1(S(=O)(=O)N)c(c(cc(c1)C(=O)O)N1CCCC1)Oc1cccc1</chem>	4-phenoxy-3-pyrrolidin-1-yl-5-sulfamoylbenzoic acid
Prestw-1048		Piperacetazine	3819-00-9	410.58	<chem>N1(c2c(Sc3c1cccc3)ccc(c2)C(=O)C)CCCN1CCC(CC1)C=O</chem>	1-[10-[3-[4-(2-hydroxyethyl)piperidin-1-yl]propyl]phenothiazin-2-yl]ethanone
Prestw-1049		Oxyphenbutazone	129-20-4	324.38	<chem>N1(N(C(C(C1=O)CCCC)=O)c1cccc1)c1ccc(cc1)O</chem>	4-butyl-1-(4-hydroxyphenyl)-2-phenylpyrazolidine-3,5-dione
Prestw-1050		Quinethazone	73-49-4	289.74	<chem>S(c1cc2C(NC(Nc2cc1Cl)CC)=O)(=O)=O)N</chem>	7-chloro-2-ethyl-4-oxo-2,3-dihydro-1H-quinazoline-6-sulfonamide
Prestw-1051		Moricizine hydrochloride	31883-05-3	463.99	<chem>N1(c2c(Sc3c1cccc3)ccc(c2)NC(=O)OCC)C(CCN1CCOC)C1=O</chem>	ethyl N-[10-(3-morpholin-4-ylpropanoyl)phenothiazin-2-yl]carbamate hydrochloride
Prestw-1052		Iopanoic acid	96-83-3	570.94	<chem>c1c(c(c(c1)CC(CC)C(O)=O))N)I</chem>	2-[(3-amino-2,4,6-triodophenyl)methyl]butanoic acid
Prestw-1053		Pivmecillinam hydrochloride	32887-03-9	476.04	<chem>N12[C@@]([C@@](C1=O)(N=C1N1CCCCC1)[H])(SC([C@@H]2)C(OCOC(C)C)C)C(=O)=O)C)C)H</chem>	(2,2-Dimethyl-1-oxo-propoxy)methylester 6-[[[hexahydro-1H-azepin-1-yl)methylene]amino]-3,3-[4-(dimethylamino)-3-methyl-1,2-diphenylbutan-2-yl]propanoate naphthalene-2-sulfonic acid
Prestw-1054		Levopropoxyphene napsylate	5714-90-9	547.72	<chem>C(C(CN(C)C)C)OC(=O)CC)(Cc1cccc1)c1cccc1</chem>	(4-(dimethylamino)-3-methyl-1,2-diphenylbutan-2-yl]propanoate naphthalene-2-sulfonic acid
Prestw-1055		Piperidolate hydrochloride	129-77-1	359.90	<chem>C(C(c1cccc1)c1cccc1)(OC1CN(CCC1)CC)=O</chem>	N-Ethyl-3-piperidyl diphenylacetate hydrochloride
Prestw-1056		Trifluridine	70-00-8	296.20	<chem>N1(C(NC(C=C1)C(F)(F)F)=O)O[C@@H]1O[C@@H]([C@H](C1)O)CO</chem>	1-[(2R,4S,5R)-4-hydroxy-5-(hydroxymethyl)oxolan-2-yl]-5-(trifluoromethyl)pyrimidine-2,4-dione
Prestw-1057		Oxprenolol hydrochloride	6452-73-9	301.82	<chem>O(c1c(OCC=C)cccc1)CC(CNC(C)C)O</chem>	1-(propan-2-ylamino)-3-(2-prop-2-enoxyphenoxy)propan-2-ol hydrochloride
Prestw-1058		Ondansetron Hydrochloride	103639-04-9	329.83	<chem>c12c(n(c3c1cccc3)C)CC(C2=O)Cn1c(ncc1)C</chem>	1,2,3,9-Tetrahydro-9-methyl-3-[(2-methyl-1H-imidazol-1-yl)methyl]-4H-carbazol-4-one hydrochloride

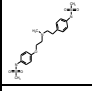
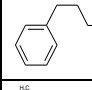
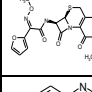
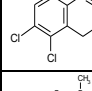
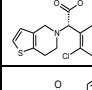
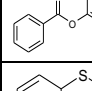
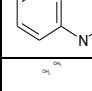
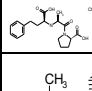
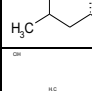
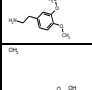
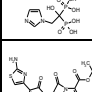
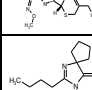
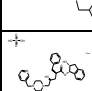
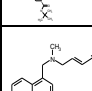
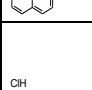
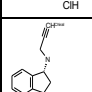
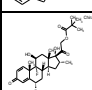
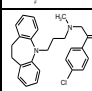
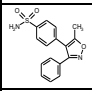
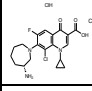
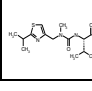

Prestw-1059		Propoxycaine hydrochloride	550-83-4	330.86	<chem>c1(cc(cc1)N)OCCC(=O)OCCN(CC)CC</chem>	2-(diethylamino)ethyl 4-amino-2-propoxybenzoate hydrochloride
Prestw-1060		Oxaprozin	21256-18-8	293.33	<chem>c1(cc(cc1)CCC(=O)O)c1ccccc1)c1ccccc1</chem>	3-(4,5-diphenyl-1,3-oxazol-2-yl)propanoic acid
Prestw-1061		Phensuximide	86-34-0	189.22	<chem>N1(C(C(C(=O)c1ccccc1)=O)C</chem>	1-methyl-3-phenylpyrrolidine-2,5-dione
Prestw-1062		Ioxaglic acid	59017-64-0	1268.89	<chem>c1(c(c(c(c1)C(NCC(Nc1c(c(c(c1)C(=O)O)))C(=O)NC(CO)I)=O)I)C(=O)NC)N(C(=O)C)C</chem>	3-[[2-[[3-[acetyl(methyl)amino]-2,4,6-triido-5-(methylcarbamoyl)benzoyl]amino]acetyl]amino]propanoic acid
Prestw-1063		Naftifine hydrochloride	65473-14-5	323.87	<chem>c1(c2c(ccc1)cccc2)CN(C=C/c1ccccc1)C</chem>	(E)-N-methyl-N-(naphthalen-1-ylmethyl)-3-phenylprop-2-en-1-amine hydrochloride
Prestw-1064		Meprylcaine hydrochloride	956-03-6	271.79	<chem>C(OCC(NCCC)(C)C(=O)c1ccccc1</chem>	[2-methyl-2-(propylamino)propyl] benzoate hydrochloride
Prestw-1065		Milrinone	78415-72-2	211.23	<chem>C1(=C\C=C(/NC1=O)C)c1ccccc1)C#N</chem>	6-methyl-2-oxo-5-pyridin-4-yl-1H-pyridine-3-carbonitrile
Prestw-1066		Methantheline bromide	53-46-3	420.35	<chem>C1(c2c(Oc3c1cccc3)cccc2)C(=O)OCC[N+](CC)(CC)C</chem>	diethyl-methyl-[2-(9H-xanthene-9-carboxyloxy)ethyl]azanium bromide
Prestw-1067		Ticarcillin sodium	74682-62-5	406.41	<chem>N12[C@@]([C@@](C1=O)NC(C(C([O-])=O)c1ccsc1)=O)[H])(SC([C@@H]2C([O-])=O)(C)C)[H]</chem>	(2S,5R,6R)-6-[2-carboxylato-2-(3-thienyl)acetamido]-3,3-dimethyl-7-oxo-4-thia-1-azabicyclo[3.2.0]heptane-2-
Prestw-1068		Thiethylperazine dimalate	52239-63-1	667.80	<chem>N1(c2c(Sc3c1cccc3)ccc(c2)SCC)CCCN1CCN(CC1)C</chem>	2-ethylsulfanyl-10-[3-(4-methylpiperazin-1-yl)propyl]phenothiazine 2-hydroxybutanedioic acid
Prestw-1069		Mesalamine	89-57-6	153.14	<chem>c1(C(=O)O)c(ccc1)N)O</chem>	5-amino-2-hydroxybenzoic acid
Prestw-1362		Vorinostat	149647-78-9	264.33	<chem>C(Nc1ccccc1)(=O)CCCCCCC(=O)NO</chem>	N'-hydroxy-N-phenyloctanediamide
Prestw-1071		Imidurea	39236-46-9	388.30	<chem>N1(C(NC(C1NC(NCNC1N(C(NC1=O)=O)CO)=O)=O)=O)=O)CO</chem>	1-[3-(hydroxymethyl)-2,5-dioxoimidazolidin-4-yl]-3-[[[3-(hydroxymethyl)-2,5-dioxoimidazolidin-4-2-[[3-methyl-4-(2,2,2-trifluoroethoxy)pyridin-2-yl]methylsulfanyl]-1H-benzimidazole
Prestw-1072		Lansoprazole	103577-45-3	369.37	<chem>c1(nc2c([nH]1)cccc2)S(Cc1c(c(OCC(F)F)F)ccn1)C=O</chem>	2-[[[3-methyl-4-(2,2,2-trifluoroethoxy)pyridin-2-yl]methylsulfanyl]-1H-benzimidazole
Prestw-1073		Bethanechol chloride	590-63-6	196.68	<chem>C(OC(C[N+](C)(C)C)C(=O)N</chem>	2-carbamoyloxypropyl(trimethyl) azanium chloride
Prestw-1074		Cyproterone acetate	427-51-0	416.95	<chem>[C@@]12(C(C(=C(C[C@@]3([C@@]1(CC[C@@]1([C@@]([C@]([C@]13[H])(OC(=O)C)C(=O)C)[H])([H])C)I)=C/C(C1C2C1)=O)C</chem>	(1R,3aS,3bR,7aR,8aS,8bS,8cS,10aS)-1-Acetyl-5-chloro-8b,10a-dimethyl-7-oxo-1,2,3,3a,3b,7,7a,8,8a,8b,8c,
Prestw-1075		(R)-Propranolol hydrochloride	13071-11-9	295.81	<chem>c12c(OCC(CNC(C)C)(O)[H])cccc1cccc2</chem>	(2R)-1-naphthalen-1-yloxy-3-(propan-2-ylamino)propan-2-ol hydrochloride
Prestw-1076		Ciprofibrate	52214-84-3	289.16	<chem>C1(C(C1)c1ccc(OC(C(=O)O)(C)C)cc1)(Cl)Cl</chem>	2-[4-(2,2-dichlorocyclopropyl)phenoxy]-2-methylpropanoic acid
Prestw-1420		Formestane	566-48-3	302.42	<chem>[C@@]12(C(C(=C(C(C1)=O)O)/CC[C@@]1([C@@]2(CC[C@@]2([C@@]1(CCC2=O)[H])C)[H])C</chem>	(8R,9S,10R,13S,14S)-4-hydroxy-10,13-dimethyl-2,6,7,8,9,11,12,14,15,16-decahydro-1H-
Prestw-1078		Benzylpenicillin sodium	69-57-8	356.38	<chem>N12[C@@]([C@@](C1=O)NC(=O)Cc1ccccc1)[H])(SC([C@@H]2C([O-])=O)(C)C)[H]</chem>	(2S,5R,6R)-3,3-dimethyl-7-oxo-6-[(2-phenylacetyl)amino]-4-thia-1-azabicyclo[3.2.0]heptane-2-
Prestw-1803		Methicillin sodium	7246-14-2	402.40	<chem>OC1C(n2cnc3c(OC)nc(nc23)N)OC(CO)C1O</chem>	
Prestw-1080		Methiazole	108579-67-5	265.34	<chem>c1(nc2c([nH]1)ccc(c2)SC(C)C)NC(=O)OC</chem>	methyl N-(6-propan-2-ylsulfanyl-1H-benzimidazol-2-yl)carbamate
Prestw-1081		(S)-propranolol hydrochloride	4199-10-4	295.81	<chem>c12c(OCC(CNC(C)C)(O)[H])cccc1cccc2</chem>	(2S)-1-naphthalen-1-yloxy-3-(propan-2-ylamino)propan-2-ol hydrochloride

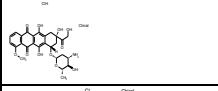
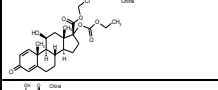
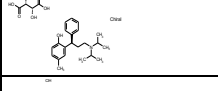

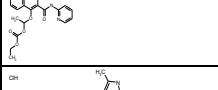
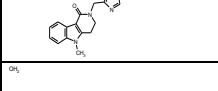
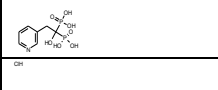
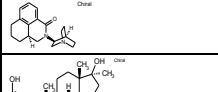
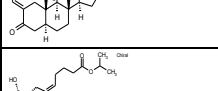
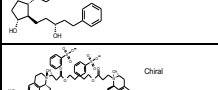
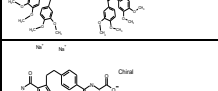
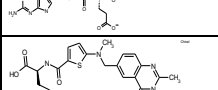
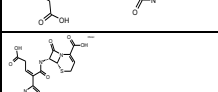
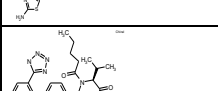
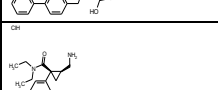
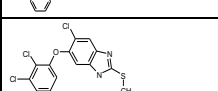
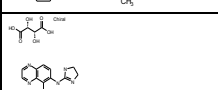
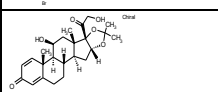
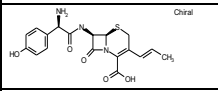

Prestw-1082		(-)-Eseroline fumarate salt	104015-29-4	334.38	[C@]12([C@](N(c3c1cc(cc3)O)C)(N(CC2)C)[H])C	(3aR,8bS)-3,4,8b-trimethyl-2,3a-dihydro-1H-pyrrolo[2,3-b]indol-7-ol (E)-but-2-enedioic acid
Prestw-1294		Isosorbide mononitrate	16051-77-7	191.14	[N+](O[C@H]1[C@@]2([C@](OC1)([C@H](CO2)O)[H])H)([O-])=O	[(3S,3aR,6R,6aS)-3-hydroxy-2,3,3a,5,6,6a-hexahydrofuro[3,2-b]furan-6-yl] nitrate
Prestw-1516		Levalbuterol hydrochloride	50293-90-8	275.78	c1(ccccc1O)[C@H](CNC(C)C)CO	4-[(1R)-2-(tert-butylamino)-1-hydroxyethyl]-2-(hydroxymethyl)phenol hydrochloride
Prestw-1493		Topiramate	97240-79-4	339.37	[C@@]12([C@H]([C@H]3[C@H](OC(O3)C)C)CO1)OC(O2)(C)C)C(=O)N	[(3aS,5aR,8aR,8bS)-2,2,7,7-tetramethyl-5,5a,8a,8b-tetrahydro[1,3]dioxolo[4,5-a:5',3'-d]pyran-3a-yl]methyl
Prestw-1086		D-cycloserine	68-41-7	102.09	C1([C@](CON1)(N)[H])=O	(4R)-4-Amino-1,2-oxazolidin-3-one
Prestw-1804		Nelarabine	121032-29-9	297.27	CCOc1c(c(OC)ccc1)C(NC1C2N(C(C([O-])=O)C)C)S2)C1=O.[Na+]	
Prestw-1088		(+,-)-Synephrine	94-07-5	167.21	c1(ccc(cc1)O)C(O)CNC	4-[1-hydroxy-2-(methylamino)ethyl]phenol
Prestw-1089		(S)-(-)-Cycloserine	339-72-0	102.09	C1([C@@](CON1)(N)[H])=O	(4S)-4-Amino-1,2-oxazolidin-3-one
Prestw-1090		Homosalate	118-56-9	262.35	C(c1c(O)cccc1)OC1CC(CC(C1)C)C(=O)O	(3,3,5-trimethylcyclohexyl) 2-hydroxybenzoate
Prestw-1091		Spaglumic acid	4910-46-7	304.26	[C@H](CCC(O)=O)(NC(=O)C[C@H](NC(=O)C)C(O)=O)C(O)=O	2-[(2-acetamido-3-carboxypropanoyl)amino]pentanedioic acid
Prestw-1092		Ranolazine	95635-55-5	427.55	c1(NC(CN2CCN(CC(CO3c3c(OC)cccc3)OC2)=O)c(ccccc1)C	N-(2,6-dimethylphenyl)-2-[4-[2-hydroxy-3-(2-methoxyphenoxy)propyl]piperazin-1-yl]acetamide
Prestw-1443		Misoprostol	59122-46-2	382.55	C1(C[C@H]([C@@H]([C@H]1CCCCC(=O)OC)C=C)CC(O)(CCCC)O)=O	hydroxy-2-[(E)-4-hydroxy-4-methyloct-1-enyl]-5-oxocyclopentylheptanoate
Prestw-1094		Sulfadoxine	2447-57-6	310.33	S(Nc1c(c(ncn1)OC)OC)(c1ccc(N)cc1)(=O)=O	Amino-4 N-(dimethoxy-5,6-pyrimidinyl-4)benzenesulfonamide
Prestw-1095		Cyclopentolate hydrochloride	5870-29-1	327.85	C(C(=O)OCCN(C)C)C1(O)CCCC1)c1cccc1	2-(dimethylamino)ethyl 2-(1-hydroxycyclopentyl)-2-phenylacetate hydrochloride
Prestw-1096		Estriol	50-27-1	288.39	[C@]12([C@]([C@]3([C@@]([C@]4(C3)cc(cc4)O)(CC1)[H])H)C[C@H]([C@@]2O)O)[H]C	(8R,9S,13S,14S,16R,17R)-13-methyl-6,7,8,9,11,12,14,15,16,17-decahydrocyclopenta[a]phen
Prestw-1097		(-)-Isoproterenol hydrochloride	5984-95-2	247.72	c1c(c(ccc1[C@H](CNC(C)C)O)O	4-[(1R)-1-hydroxy-2-(propan-2-ylamino)ethyl]benzene-1,2-diol hydrochloride
Prestw-1339		Sarafloxacin	98105-99-8	385.37	C=1(C(c2c(N(C1)ccc(cc2)F)cc(c(c2)F)N1CCNCC1)=O)C(=O)O	6-fluoro-1-(4-fluorophenyl)-4-oxo-7-piperazin-1-ylquinoline-3-carboxylic acid
Prestw-1099		Nialamide	51-12-7	298.35	C(=O)(c1ccncc1)NNCCC(NC1CCCC1)=O	N-benzyl-3-[2-(pyridine-4-carbonyl)hydrazinyl]propanamide
Prestw-1195		Toltrazuril	69004-03-1	425.39	N1(C(N(C(NC1=O)O)O)O)c1cc(c(Oc2ccc(SC(F)(F)F)cc2)cc1)C	1-Methyl-3-(3-methyl-4-[4-(trifluoromethyl)sulfanyl]phenoxy)phenyl)-1,3,5-triazinane-2,4,6-trione
Prestw-1101		Perindopril	82834-16-0	368.48	N1([C@H]([C@]2([C@@]1(CCCC2)[H])C(=O)O)C([C@@](N[C@](C(=O)OCC)(CCC)[H])(C)[H])=O	(2S,3aS,7aS)-1-[(2S)-2-[(2S)-1-ethoxy-1-oxopentan-2-yl]amino]propanoyl]-octahydro-1H-indole-2-
Prestw-1102		Fexofenadine hydrochloride	153439-40-8	538.13	C(C1CCN(CC1)CCCC(c1ccc(C(=O)O)(C)cc1)O)(c1cccc1)O	2-[4-[1-hydroxy-4-[4-[hydroxy(diphenyl)methyl]piperidin-1-yl]butyl]phenyl]-2-methylpropanoic acid
Prestw-1202		4-aminosalicylic acid	65-49-6	153.14	c1(c(cc(cc1)N)O)C(=O)O	4-amino-2-hydroxy-benzoic acid

Prestw-1356		Vardenafil	224785-90-4	488.61	<chem>n12c(C/N=C(N1)/c1cc(S(N3CCN(CC3)CC)(=O)=O)ccc1OCC)=O)c(nc2CCC)C</chem>	2-[2-ethoxy-5-(4-ethylpiperazin-1-yl)sulfonylphenyl]-5-methyl-7-propyl-1H-imidazo[5,1-
Prestw-1417		Fluconazole	86386-73-4	306.28	<chem>C(c1c(cc(cc1)F)F)(Cn1ncnc1)(Cn1ncnc1)O</chem>	2-(2,4-difluorophenyl)-1,3-bis(1,2,4-triazol-1-yl)propan-2-ol
Prestw-1203		5-fluorouracil	51-21-8	130.08	<chem>N1C(\C=C/NC1=O)F=O</chem>	5-fluoro-1H-pyrimidine-2,4-dione
Prestw-1487		Mesna	19767-45-4	164.18	<chem>S([O-])(CCS)=O=O</chem>	2-sulfanylethanesulfonate sodium
Prestw-1444		Mitotane	53-19-0	320.05	<chem>C(c1c(Cl)cccc1)(C(Cl)Cl)c1ccc(cc1)Cl</chem>	1-chloro-2-[2,2-dichloro-1-(4-chlorophenyl)ethyl]benzene
Prestw-1497		Ambrisentan	177036-94-1	378.43	<chem>C(C(c1cccc1)(c1cccc1)OC)(C(=O)O)c1nc(cc(n1)C)C</chem>	2-(4,6-dimethylpyrimidin-2-yl)oxy-3-methoxy-3,3-diphenylpropanoic acid
Prestw-1479		Triclosan	3380-34-5	289.55	<chem>O(c1c(cc(cc1)Cl)Cl)c1c(cc(cc1)Cl)O</chem>	5-chloro-2-(2,4-dichlorophenoxy)phenol
Prestw-1401		Enoxacin	84294-96-2	320.33	<chem>C=1(/C(c2c(nc(c2)F)N2CCNCC2)N(\C1)CC=O)C(=O)O</chem>	1-ethyl-6-fluoro-4-oxo-7-(piperazin-1-yl)-1,4-dihydro-1,8-naphthyridine-3-carboxylic acid
Prestw-1307		Olopatadine hydrochloride	140462-76-6	373.88	<chem>C/1(\c2c(OCc3c1cccc3)ccc(c2)CC(=O)O)=C1CCN(C)C</chem>	2-[(1Z)-1-[3-(dimethylamino)propylidene]-6H-benzo[c][1]benzoxepin-2-yl]acetic acid
Prestw-1187		Granisetron	109889-09-0	312.42	<chem>c1(nn(c2c1cccc2)C(N[C@]1(C[C@]2)N([C@](C1)C)CC2)[H])C([H])[H])=O</chem>	1-methyl-N-[(1S,5R)-9-methyl-9-azabicyclo[3.3.1]nonan-3-yl]indazole-3-carboxamide
Prestw-1224		Anthralin	1143-38-0	226.23	<chem>C1(c2c(Cc3c1c(O)ccc3)cccc2O)=O</chem>	1,8-dihydroxy-10H-anthracen-9-one
Prestw-1492		Lamotrigine	84057-84-1	256.10	<chem>c1(c(nc(nn1)N)N)c1c(c(Cl)ccc1)Cl</chem>	6-(2,3-dichlorophenyl)-1,2,4-triazine-3,5-diamine
Prestw-1383		Clofibrate	637-07-0	242.70	<chem>C(C(=O)OCC)(Oc1ccc(Cl)cc1)(C)C</chem>	ethyl 2-(4-chlorophenoxy)-2-methylpropanoate
Prestw-1481		Cyclophosphamide	50-18-0	261.09	<chem>P1(NCCCO1)(N(CCC)CC)C=O</chem>	N,N-bis(2-chloroethyl)-2-oxo-1,3,2lambda 5-oxazaphosphinan-2-amine
Prestw-1229		Aripiprazole	129722-12-9	448.40	<chem>N1c2cc(ccc2CCC1=O)OCCCN1CCN(c2c(c(Cl)ccc2)Cl)CC1</chem>	dichlorophenyl)piperazin-1-yl]butoxy]-3,4-dihydro-1H-
Prestw-1405		Ethinylestradiol	57-63-6	296.41	<chem>[C@]12([C@@]1([C@]3([C@@]4(c4c(CC3)cc(cc4)O)(CC1)[H])[H])CC[C@]2(C#C)O)[H])C</chem>	(8R,9S,13S,14S,17R)-17-ethynyl-13-methyl-7,8,9,11,12,14,15,16-octahydro-6H-
Prestw-1419		Fluocinonone acetonide	67-73-2	452.50	<chem>[C@@]12([C@@]3([C@]4([C@@]5([C@@]6([C@]([C@@]7(C4)F)=C/C(\C=C5)=O)C)([C@]([C3]O)F)[H])([C]C[C@]1OC(O2)(C)C)[H])C(=O)CO</chem>	(1S,2S,4R,8S,9S,11S,12R,13S,19S)-12,19-difluoro-11-hydroxy-8-(2-hydroxyacetyl)-6,6,9,13-tetramethyl-5,7-5-amino-1-cyclopropyl-7-
Prestw-1343		Sparfloxacin	110871-86-8	392.41	<chem>c12c(N(\C=C/(\C1=O)C(=O)O)C1CC1)c(c(c2N)F)N1C[C@]H([N[C@]H](C1)C)C)F</chem>	[(3R,5S)-3,5-dimethylpiperazin-1-yl]-6,8-difluoro-4-oxo-1,4,8-chloro-11-piperidin-4-ylidene-5,6-dihydrobenzo[1,2]cyclohepta[2,4-b]pyridine
Prestw-1390		Desloratadine	100643-71-8	310.83	<chem>C\1(/c2c(cc(cc2)Cl)CCc2c1cccc2)=C\1/CCNCC1</chem>	
Prestw-1378		Clarithromycin	81103-11-9	747.97	<chem>[C@]12([C@@]1([C@]3([C@@]4([C@@]5([C@@]6([C@]([C@@]7(C4)F)=C/C(\C=C5)=O)C)([C@]([C3]O)F)[H])([C]C[C@]1OC(O2)(C)C)[H])C(=O)CO</chem>	
Prestw-1199		Tripelennamine hydrochloride	154-69-8	291.83	<chem>N(c1cccc1)(Cc1cccc1)CCN(C)C</chem>	N'-benzyl-N,N-dimethyl-N'-pyridin-2-ylethane-1,2-diamine hydrochloride
Prestw-1352		Tulobuterol	41570-61-0	227.74	<chem>c1(c(Cl)cccc1)C(CNC(C)C)C)O</chem>	2-(tert-butylamino)-1-(2-chlorophenyl)ethanol
Prestw-1196		Topotecan	123948-87-8	421.46	<chem>N12C(\c3c(C1)cc1c(c(cc1n3)O)CN(C)C)=C/C/1=C(\C2=O)COC([C@]1(O)C)=O</chem>	(S)-10-[[dimethylamino)methyl]-4-ethyl-4,9-dihydroxy-1H-pyrano[3',4':6,7]indolizino[1,2-

Prestw-1338		Rufloxacin	101363-10-4	363.41	<chem>C=1(\C(c2c3N(\C1)CCSc3c(c2)F)N1CCN(CC1)C)=O)/C(=O)O</chem>	9-Fluoro-10-(4-methylpiperazin-1-yl)-7-oxo-2,3-dihydro-7H-[1,4]thiazino[2,3,4-ij]quinoline (3R,5R)-7-[[1S,2S,6S,8S,8aR)-6-hydroxy-2-methyl-8-[(2S)-2-methylbutanoyloxy]-5-[[4-[2-[methyl(pyridin-2-yl)amino]ethoxy]phenyl]methyl]-1,3-thiazolidine-2,4-dione hydrochloride
Prestw-1319		Pravastatin	81093-37-0	424.54	<chem>C=1\2/[C@]([C@@H](OC(=O)[C@H](CC)C)C[C@H](\C1)O)([C@@H](CC[C@H](C[C@H](CC(=O)O)O)O)[C@H](\C=C2)C)[H]</chem>	5-[[4-[2-[methyl(pyridin-2-yl)amino]ethoxy]phenyl]methyl]-1,3-thiazolidine-2,4-dione hydrochloride
Prestw-1337		Rosiglitazone Hydrochloride	122320-73-4	393.90	<chem>N1C(SC(C1=O)C)C1ccc(cc1)OCCN(c1ncccc1)C=O</chem>	5-[[4-[2-[methyl(pyridin-2-yl)amino]ethoxy]phenyl]methyl]-1,3-thiazolidine-2,4-dione hydrochloride
Prestw-1334		Rivastigmine	123441-03-2	250.34	<chem>C(Oc1cc([C@@H](N(C)C)C)ccc1)(N(CC)C)=O</chem>	[3-[(1S)-1-(dimethylamino)ethyl]phenyl]N-ethyl-N-methylcarbamate
Prestw-1342		Sildenafil	139755-83-2	474.59	<chem>c1/2c(n(nc1CCC)C)C(N/C(=N2)/c1cc(S(N2CCN(CC2)C)(=O)=O)ccc1OCC)=O</chem>	5-[2-ethoxy-5-(4-methylpiperazin-1-yl)sulfonylphenyl]-1-methyl-3-propyl-4H-pyrazolo[4,3-
Prestw-1207		Acetylsalicylic acid	50-78-2	180.16	<chem>c1(C(=O)O)c(OC(=O)C)cccc1</chem>	2-acetoxybenzoic acid
Prestw-1472		Hexachlorophene	70-30-4	406.91	<chem>c1(Cc2c(c(cc2O)Cl)Cl)c(c(cc1O)Cl)Cl)Cl</chem>	3,4,6-trichloro-2-[(2,3,5-trichloro-6-hydroxyphenyl)methyl]phenol
Prestw-1764		Nelfinavir mesylate	159989-65-8	663.90	<chem>N1([C@H](C(NC(C)C)C)=O)C[C@]2([C@@](C1)(CCCC2)[H])[H]C[C@H]([C@@H](NC(c1c(c(O)ccc1)C)=O)C)Sc1cccc1)O</chem>	(3S,4aS,8aS)-N-tert-butyl-2-[[2R,3R)-2-hydroxy-3-[(3-hydroxy-2-methylbenzoyl)amino]-4-(1-(3-hydroxypropyl)-5-[[2R)-2-[2-(2,2,2-trifluoroethoxy)phenoxy]ethylamino]propyl]-2,3-
Prestw-1749		Silodosin	160970-54-7	495.55	<chem>c1(c2c(cc1)C[C@H](NCCOc1c(OCC(F)F)F)cccc1)C(CN2CCCO)C(=O)N</chem>	1-(3-hydroxypropyl)-5-[[2R)-2-[2-(2,2,2-trifluoroethoxy)phenoxy]ethylamino]propyl]-2,3-
Prestw-1777		Trimebutine	39133-31-8	387.48	<chem>c1(c(cc(C(OCC(N(C)C)(c2cccc2)CC)=O)cc1OC)OC)OC</chem>	[2-(dimethylamino)-2-phenylbutyl] 3,4,5-trimethoxybenzoate
Prestw-1739		Nevirapine	129618-40-2	266.31	<chem>N1(c2c(C(Nc3c1nccc3C)=O)cccn2)C1CC1</chem>	11-cyclopropyl-4-methyl-5H-dipyrido[2,3-e:2',3'-f][1,4]diazepin-6-one
Prestw-1707		Doxapram hydrochloride	7081-53-0	414.98	<chem>C1(C(C(CN1CC)CCN1CCOCC1)(c1cccc1)c1cccc1)=O</chem>	1-ethyl-4-(2-morpholin-4-ylethyl)-3,3-diphenylpyrrolidin-2-one
Prestw-1718		Amlexanox	68302-57-8	298.30	<chem>c12c(nc(c1)C(=O)O)N)O)c1c(C2=O)ccc(cc1)C(C)C</chem>	2-amino-5-oxo-7-propan-2-ylchromeno[2,3-b]pyridine-3-carboxylic acid
Prestw-1719		Amorolfine hydrochloride	78613-38-4	353.98	<chem>N1(C[C@H](O[C@H](C1)C)C)CC(Cc1ccc(C(C)C)C)cc1)C</chem>	(2R,6S)-2,6-dimethyl-4-[2-methyl-3-[4-(2-methylbutan-2-yl)phenyl]propyl]morpholine
Prestw-1786		Enrofloxacin	93106-60-6	359.40	<chem>C=1/(C(c2c(N(C1)C1CC1)cc(N1CCN(CC1)CC)c2F)=O)C(=O)O</chem>	1-Cyclopropyl-7-(4-ethyl-1-piperazinyl)-6-fluoro-1,4-dihydro-4-oxo-3-quinolonecarboxylic acid
Prestw-1784		Ubenimex	58970-76-6	308.38	<chem>C([C@H]([C@@H](Cc1cccc1)N)O)(N[C@H](C(=O)O)C(C)C)=O</chem>	(2S)-2-[[2S,3R)-3-amino-2-hydroxy-4-phenylbutanoyl]amino]-4-methylpentanoic acid
Prestw-1778		Troxipide	99777-81-8	294.35	<chem>C(c1cc(c(c1)OC)OC)OC)(NC1CNCCC1)=O</chem>	3,4,5-trimethoxy-N-piperidin-3-ylbenzamide
Prestw-1773		Ipriflavone	35212-22-7	280.33	<chem>C=1(\C(c2c(O/C1)cc(OC(C)C)cc2)=O)/c1cccc1</chem>	3-phenyl-7-propan-2-yloxychromen-4-one
Prestw-1762		Ezetimibe	163222-33-1	409.44	<chem>N1(C([C@@H]([C@H]1c1ccc(cc1)O)CC[C@@H](c1ccc(cc1)F)O)=O)c1ccc(cc1)F</chem>	(3R,4S)-1-(4-fluorophenyl)-3-[[3S)-3-(4-fluorophenyl)-3-hydroxypropyl]-4-(4-hydroxyphenyl)azetidin-2-one
Prestw-1761		Rizatriptan benzoate	145202-66-0	391.48	<chem>n1cnn(c1)Cc1cc2c(c[nH]c2c1)CCN(C)C</chem>	N,N-dimethyl-2-[5-(1,2,4-triazol-1-ylmethyl)-1H-indol-3-yl]ethanamine benzoic acid
Prestw-1760		Tegaserod maleate	189188-57-6	417.47	<chem>c1(c2c([nH]c1)ccc(c2)OC)C=N\N(=N)NCCCC</chem>	1-[[[(Z)-(5-methoxyindol-3-ylidene)methyl]amino]-2-pentylguanidine (Z)-but-2-enedioic acid
Prestw-1758		Pantoprazole sodium	138786-67-1	405.36	<chem>c1([n-jc2c(n1)cc(OC(F)F)cc2)S(C1c1c(ccn1)OC)OC)=O</chem>	5-(difluoromethoxy)-2-[(3,4-dimethoxy-pyridin-2-yl)methylsulfinyl]benzimidazol-1-ide sodium

Prestw-1753		Tegafur	17902-23-7	200.17	<chem>N1(C(NC(C(=C1)F)=O)=O)C1OCCC1</chem>	5-fluoro-1-(oxolan-2-yl)pyrimidine-2,4-dione
Prestw-1732		Tolcapone	134308-13-7	273.25	<chem>c1([N+](=[O-])=O)c(c(cc(c1)C)C1ccc(cc1)C)=O)O</chem>	(3,4-dihydroxy-5-nitrophenyl)-(4-methylphenyl)methanone
Prestw-1716		Altrenogest	850-52-2	310.44	<chem>C/1\2=C\3/C(=C(C(=O)CC3)/CC[C@]1([C@]1([C@](\C=C2)([C@](CC1)(O)CC=C)C)[H])[H]</chem>	(8S,13S,14S,17R)-17-hydroxy-13-methyl-17-prop-2-enyl-1,2,6,7,8,14,15,16-octahydrocyclopenta[a]phen
Prestw-1711		Felbamate	25451-15-4	238.25	<chem>C(OCC(COC(=O)N)c1cccc1)(=O)N</chem>	(3-carbamoyloxy-2-phenylpropyl) carbamate
Prestw-1709		Estramustine	2998-57-4	440.41	<chem>[C@]12([C@]([C@]3([C@@]([C@]4(c4cc(OC(N(CCC)CC)C)O)cc4)CC3)(CC1)[H])[H])(CC[C@]([H]2)O)[H]C</chem>	(17 beta)-17-Hydroxyestra-1(10),2,4-trien-3-yl bis(2-chloroethyl)carbamate
Prestw-1708		(R)-Duloxetine hydrochloride	116539-60-7	333.88	<chem>c1(sccc1)[C@H](O)c1c2c(ccc1)cccc2)CCNC</chem>	(3R)-N-methyl-3-naphthalen-1-yloxy-3-thiophen-2-ylpropan-1-amine
Prestw-1706		Donepezil hydrochloride	120011-70-3	415.96	<chem>c12C(C(Cc1cc(c2)OC)OC)CC1CCN(Cc2cccc2)CC1)=O</chem>	(RS)-2-[(1-benzyl-4-piperidyl)methyl]-5,6-dimethoxy-2,3-dihydroinden-1-one
Prestw-1703		1,8-Dihydroxyanthraquinone	117-10-2	240.22	<chem>C1(c2c(C(c3c1c(O)ccc3)=O)cccc2O)=O</chem>	1,8-dihydroxy-9,10-dihydroanthracene-9,10-dione
Prestw-1733		Nitazoxanide	55981-09-4	307.29	<chem>c1(sc(NC(c2c(OC(=O)C)cccc2)=O)nc1)[N+](=[O-])=O</chem>	[2-[(5-nitro-1,3-thiazol-2-yl)carbamoyl]phenyl] acetate
Prestw-1748		Nateglinide	105816-04-4	317.43	<chem>C(N[C@@H](C(=O)O)Cc1cccc1)([C@H]1CC[C@@H](CC1)C(C)C)=O</chem>	(2R)-3-phenyl-2-[(4-propan-2-ylcyclohexanecarbonyl)amino]propanoic acid
Prestw-1721		Avobenzene	70356-09-1	310.40	<chem>C(C(c1ccc(C(C)C)cc1)=O)C(c1ccc(cc1)OC)=O</chem>	1-(4-Methoxyphenyl)-3-(4-tert-butylphenyl)propane-1,3-dione
Prestw-1715		Algestone acetophenide	24356-94-3	448.61	<chem>[C@]12([C@@]3([C@]([C@]4([C@]([C@]5(\C(=C/C(=O)CC5)CC4)C)CC3)[H])[H])(C[C@H]1O(C(=O)C)C)C)C(=O)C</chem>	(4aR,4bS,6aS,6bS,8R,9aR,10aS,10bR)-6b-Acetyl-4a,6a,8-trimethyl-8-phenyl-3,4,4a,4b,5,6,6a,6b,9a,10,11
Prestw-1763		Actarit	18699-02-0	193.20	<chem>C(Nc1ccc(CC(=O)O)cc1)(=O)C</chem>	2-(4-acetamidophenyl)acetic acid
Prestw-1710		Ethoxzolamide	452-35-7	258.32	<chem>c1(S(=O)(=O)N)nc2c(s1)cc(cc2)OCC</chem>	6-ethoxy-1,3-benzothiazole-2-sulfonamide
Prestw-1722		Azatidine maleate	3978-86-7	522.56	<chem>C1(\c2ncccc2CCc2c1cccc2)=C/1\CCN(CC1)C</chem>	11-(1-methylpiperidin-4-ylidene)-5,6-dihydrobenzo[1,2]cyclohepta[3,4-b]pyridine (Z)-but-2-
Prestw-1717		Aminacrine	90-45-9	194.24	<chem>c1(c2c(nc3c1cccc3)cccc2)N</chem>	acridin-9-amine
Prestw-1792		Pidotimod	121808-62-6	244.27	<chem>N1(C([C@]2(NC(=O)CC2)[H])=O)[C@](C(=O)O)(CSC1)[H]</chem>	(4R)-3-[(2S)-5-oxopyrrolidine-2-carbonyl]-1,3-thiazolidine-4-carboxylic acid
Prestw-1766		Benidipine hydrochloride	91599-74-5	542.04	<chem>C=1([C@@H](\C=C(/N/C1)C)C)C(=O)OC)c1cc([N+](=[O-])=O)ccc1)C(O[C@H]1CN(Cc2cccc2)CCC1)=O</chem>	5-O-[(3R)-1-benzylpiperidin-3-yl] 3-O-methyl (4R)-2,6-dimethyl-4-(3-nitrophenyl)-1,4-dihydropyridine-3,5-
Prestw-1770		Perospirone	150915-41-6	426.59	<chem>N1(C([C@@]2([C@](C1=O)(CCCC2)[H])[H])=O)CCCCN1CCN(c2nsc3c2cccc3)CC1</chem>	(3aR,7aS)-2-[4-(1,2-benzothiazol-3-yl)piperazin-1-yl]butyl]-3a,4,5,6,7,7a-hexahydroisindole-1,3-(6R)-7-[(2R)-2-(4-hydroxyphenyl)-2-[(6-methyl-4-oxo-1H-pyridine-3-carbonyl)amino]acetyl]amino]
Prestw-1726		Cefpiramide	70797-11-4	612.65	<chem>N1/2[C@H]([C@]1(SC/C=C2/C(=O)O)/CSc1n(nnn1)C)[H]NC([C@H](NC(c1c(cc(nc1)C)O)=O)c1ccc(cc1)O)=O)=O</chem>	hydroxyphenyl)-2-[(6-methyl-4-oxo-1H-pyridine-3-carbonyl)amino]acetyl]amino]
Prestw-1713		Fenoldopam	67227-56-9	305.76	<chem>c12c(c(c(c1)O)O)C)CCNCC2c1ccc(cc1)O</chem>	9-chloro-5-(4-hydroxyphenyl)-2,3,4,5-tetrahydro-1H-3-benzazepine-7,8-diol
Prestw-1714		Adapalene	106685-40-9	412.53	<chem>[C@@]12(c3cc(c4cc5c(cc(C(=O)O)cc5)cc4)ccc3OC)C[C@@]3(C[C@@]([C1]C[C@@]([C2]C3)[H])[H])[H]</chem>	6-[3-(1-adamantyl)-4-methoxyphenyl]naphthalene-2-carboxylic acid
Prestw-1705		Diatrizoic acid dihydrate	50978-11-5	649.95	<chem>c1(c(c(c(c1)N)C(=O)C)N)C(=O)C)C(=O)O</chem>	3,5-diacetamido-2,4,6-triiodobenzoic acid dihydrate

Prestw-1743		Dofetilide	115256-11-6	441.57	<chem>S(Nc1ccc(cc1)OCCN(CCC1ccc(NS(=O)(=O)C)cc1)C)(=O)(=O)C</chem>	N-[4-[2-[2-[4-(methanesulfonamido)phenoxy]ethyl]methylamino]ethyl]phenyl]me
Prestw-1776		Phenprobamate	673-31-4	179.22	<chem>C(=O)N(O)CCc1ccccc1</chem>	3-phenylpropyl carbamate
Prestw-1730		Cefuroxime axetil	64544-07-6	510.48	<chem>N1\2C([C@H]([C@H]1SC1C(=C2\C(OC(=O)C)C)=O)\COC(=O)N)NC(1C1occc1)=N/O)C(=O)O</chem>	1-acetyloxyethyl (6R,7R)-3-(carbamoyloxymethyl)-7-[[2Z]-2-(furan-2-yl)-2-methoxyiminoacetyl]amino]-8-
Prestw-1720		Anagrelide	68475-42-3	256.09	<chem>C1=2/NC(CN1Cc1c(N2)ccc(c1Cl)Cl)=O</chem>	6,7-dichloro-5,10-dihydro-3H-imidazo[2,1-b]quinazolin-2-one
Prestw-1701		Clopidogrel	113665-84-2	321.83	<chem>N1([C@@H](c2c(Cl)cccc2)C(=O)OC)Cc2c(scc2)CC1</chem>	methyl (2S)-2-(2-chlorophenyl)-2-(6,7-dihydro-4H-thieno[3,2-c]pyridin-5-yl)acetate
Prestw-1723		Benzoxiquine	86-75-9	249.27	<chem>C(Oc1c2ncccc2ccc1)(=O)c1ccccc1</chem>	8-quinolyl benzoate
Prestw-1785		Phenothiazine	92-84-2	199.28	<chem>N1c2c(Sc3c1cccc3)cccc2</chem>	10H-phenothiazine
Prestw-1769		Enalaprilat dihydrate	84680-54-6	384.43	<chem>N1(C([C@@H](N[C@H](C(=O)O)CCc2ccccc2)C)=O)[C@H](C(=O)O)CCC1</chem>	(2S)-1-[(2S)-2-[[[(1S)-1-carboxy-3-phenylpropyl]amino]propanoyl]pyrrolidine-2-carboxylic acid
Prestw-1791		Pregabalin	148553-50-8	159.23	<chem>C(=O)C[C@H](CC(C)C)CN(O)</chem>	(3S)-3-(aminomethyl)-5-methylhexanoic acid
Prestw-1787		Homoveratrylamine	120-20-7	217.70	<chem>c1(c(ccc1)CCN)OC)OC</chem>	[2-(3,4-Dimethoxyphenyl)ethyl]amine hydrochloride
Prestw-1731		Zoledronic acid hydrate	165800-06-6	290.11	<chem>C(P(=O)(O)O)(P(=O)(O)O)(Cn1cncc1)O</chem>	(1-hydroxy-2-imidazol-1-yl-1-phosphonoethyl)phosphonic acid hydrate
Prestw-1727		Cefpodoxime proxetil	87239-81-4	557.61	<chem>N1\2C([C@H]([C@]1(SC/C(=C2\C(OC(=O)OC(C)C)C)=O)\COC([H]NC(/C(/c1nc(scn1)N)=NOC)=O)O)O</chem>	1-propan-2-yloxy-carbonyloxyethyl (6R,7R)-7-[[4-[2-(2H-tetrazol-5-yl)phenyl]phenyl]methyl]-1,3-diazaspiro[4.4]non-1-en-4-one
Prestw-1736		Irbesartan	138402-11-6	428.54	<chem>N1(C(C2(N=C1\CCCC)CCCC2)=O)Cc1ccc(c2c(c3nn[nH]3)cccc2)cc1</chem>	2-butyl-3-[[4-[2-(2H-tetrazol-5-yl)phenyl]phenyl]methyl]-1,3-diazaspiro[4.4]non-1-en-4-one
Prestw-1737		Indinavir sulfate	157810-81-6	711.88	<chem>[C@@H]1(N[C(C@H](C[C@H](C(N[C@H]2C3C(C[C@H]2O)cccc3)=O)Cc2ccccc2)O)CCN(C1)Cc1cnccc1)C(NC(C)C)=O</chem>	(2S)-1-[(2S,4R)-4-benzyl-2-hydroxy-5-[[[(1S,2R)-2-hydroxy-2,3-dihydro-1H-inden-1-yl]amino]-5-oxopentyl]-N-
Prestw-1750		Terbinafine	91161-71-6	291.44	<chem>C(#CC(C)C)C=C/CN(Cc1c2c(ccc1)cccc2)C</chem>	(E)-N,6,6-trimethyl-N-(naphthalen-1-ylmethyl)hept-2-en-4-yn-1-amine
Prestw-1700		Histamine dihydrochloride	56-92-8	184.07	<chem>n1c(c[nH]c1)CCN</chem>	2-(1H-imidazol-5-yl)ethanamine dihydrochloride
Prestw-1734		Rasagiline	136236-51-6	171.24	<chem>C(#C)CN[C@H]1c2c(CC1)cccc2</chem>	(1R)-N-prop-2-ynyl-2,3-dihydro-1H-inden-1-amine
Prestw-1712		Flumethasone pivalate	2002-29-1	494.58	<chem>[C@]112([C@@]3([C@]4([C@@]([C@]([C@@H](C4)C)(COC(C(C)C)C)=O)O)O)C[C@H]3O)C)[H](C[C@@H]1/C1=C/C(C=C2)=O)F)[H]F)C</chem>	[2-[[[6S,8S,9R,10S,11S,13S,14S,16R,17R]-6,9-difluoro-11,17-dihydroxy-10,13,16-1-(4-chlorophenyl)-2-[3-(5,6-dihydrobenzo[b][1]benzazepin-11-yl)propyl]methylamino]ethanone
Prestw-1756		Lofepramine	23047-25-8	418.97	<chem>N1(c2c(Cc3c1cccc3)cccc2)CCCN(CC(c1ccc(cc1)Cl)=O)C</chem>	1-(4-chlorophenyl)-2-[3-(5,6-dihydrobenzo[b][1]benzazepin-11-yl)propyl]methylamino]ethanone
Prestw-1759		Valdecoxib	181695-72-7	314.37	<chem>S(c1ccc(c2c(noc2C)c2cccc2)cc1)(=O)=O)N</chem>	4-(5-methyl-3-phenyl-1,2-oxazol-4-yl)benzenesulfonamide
Prestw-1740		Besifloxacin hydrochloride	141388-76-3	430.31	<chem>N1(c2c(C(\C=C1)C(=O)O)O)cc(c(c2Cl)N1C[C@H](N)CCCC1)F)C1CC1</chem>	7-[(3R)-3-aminoazepan-1-yl]-8-chloro-1-cyclopropyl-6-fluoro-4-oxoquinoline-3-carboxylic acid hydrochloride
Prestw-1782		Ritonavir	155213-67-5	720.96	<chem>n1c(scc1CN(C(N[C@H](C(N[C@H](C[C@H](C[C@@H]([C@@H](NC(=O)OCc1scnc1)Cc1ccccc1)O)Cc1ccccc1)=O)C(C)C)=O)C(C)C</chem>	1,3-thiazol-5-ylmethyl N-[[2S,3S,5S]-3-hydroxy-5-[[[2S]-3-methyl-2-[[methyl-[(2-propan-2-yl-1,3-thiazol-4-

Prestw-1752		Epirubicin hydrochloride	56390-09-1	579.99	<chem>c12c(Cc3c(C1=O)cccc3OC=O)c(c1c(c2O)C[C@](C[C@@]1(O)[C@H]1O[C@H]([C@@H]([C@H](C1)N)O)C)[H])(C(=O)CO)O</chem>	(7S,9S)-7-[(2R,4S,5R,6S)-4-amino-5-hydroxy-6-methyloxan-2-yl]oxy-6,9,11-trihydroxy-9-(2-hydroxyacetyl)-
Prestw-1741		Loteprednol etabonate	82034-46-6	466.96	<chem>[C@]12([C@](C(OCC)=O)(OC(=O)OCC)CC[C@]1([C@]1([C@@]([C@@]3(C=C/C(C=C3)=O)CC1)C)([C@H](C2)O)[H])[H])C</chem>	chloromethyl (8S,9S,10R,11S,13S,14S,17R)-17-ethoxycarbonyloxy-11-hydroxy-10,13-dimethyl-3-oxo-
Prestw-1744		Tolterodine tartrate	209747-05-7	475.59	<chem>c1([C@H](CCN(C(C)C)C(C)C)c2cccc2)c(ccc(c1)C)O</chem>	2-[(1R)-3-[di(propan-2-yl)amino]-1-phenylpropyl]-4-methylphenol (2R,3R)-2,3-dihydroxybutanedioic acid
Prestw-1775		Lomerizine hydrochloride	101477-54-7	505.01	<chem>c1(c(c(CN2CCN(C(c3ccc(cc3)F)c3ccc(cc3)F)CC2)ccc1O)C)OC</chem>	1-[bis(4-fluorophenyl)methyl]-4-[(2,3,4-trimethoxyphenyl)methyl]piperazine hydrochloride
Prestw-1772		Ampiroxicam	99464-64-9	447.47	<chem>S1(N(C=C(c1c2c1cccc2)/OC(OC(=O)OCC)C)/C(Nc1cccc1)=O)C(=O)=O</chem>	ethyl 1-[[2-methyl-1,1-dioxo-3-(pyridin-2-ylcarbamoyl)-1lambda6,2-benzothiazin-4-yl]oxy]ethyl carbonate
Prestw-1781		Alosetron hydrochloride	122852-69-1	330.82	<chem>c12c(n(c3c1cccc3)C)CCN(C2=O)Cc1nc[nH]c1C</chem>	5-methyl-2-[(5-methyl-1H-imidazol-4-yl)methyl]-3,4-dihydropyrido[4,3-b]indol-1-one hydrochloride
Prestw-1738		Risedronic acid monohydrate	105462-24-6	301.13	<chem>C(P(=O)(O)O)(P(=O)(O)O)(Cc1cnccc1)O</chem>	(1-hydroxy-1-phosphono-2-pyridin-3-ylethyl)phosphonic acid
Prestw-1783		Palonosetron hydrochloride	135729-62-3	332.88	<chem>N1(C(c2c3[C@@](C1)CCCc3ccc2[H])=O)[C@@H]1CN2CC[C@@]1(CC2)[H]</chem>	(3aS)-2-[(3S)-1-azabicyclo[2.2.2]octan-3-yl]-3a,4,5,6-tetrahydro-3H-benzofdelisoquinolin-1-one
Prestw-1780		Oxymetholone	434-07-1	332.49	<chem>[C@]12([C@]3([C@]([C@]4([C@]([C@](CC4)O)C)(CC3)C)[H])[C[C@]1(CC/C/C2=C/O)=O)[H])[H])[H]C</chem>	(2Z,5S,8R,9S,10S,13S,14S,17S)-17-hydroxy-2-(hydroxymethylidene)-10,13,17-trimethylpropan-2-yl (Z)-7-
Prestw-1765		Latanoprost	145773-22-4	432.61	<chem>[C@H]1([C@H]([C@H](C[C@H]1O)O)C)C=C/CCCC(=O)OC(C)C[C@H](CCc1cccc1)O</chem>	[(1R,2R,3R,5S)-3,5-dihydroxy-2-[(3R)-3-hydroxy-5-phenylpentyl]cyclopentyl]hep-
Prestw-1745		Cisatracurium besylate	64228-79-1	1243.51	<chem>[N@@+](1([C@H]([C@]2(c(c(c2)OC)OC)CC1)Cc1cc(c(c1)OC)OC)(CC(=O)O)CCCCOC(C)[N@@+](1([C@H]([C@]2(c(c(c2)OC)OC)CC1)Cc1cc(c(c1)OC)OC)C(=O)O)C</chem>	
Prestw-1794		Pemetrexed disodium	357166-30-4	471.38	<chem>c12/N=C(NC(c1c[nH]2)CCc1ccc(CN[C@H](C([O-])=O)CCC([O-])=O)cc1)=O)/N</chem>	(2S)-2-[[4-[2-(2-amino-4-oxo-1,7-dihydropyrrolo[2,3-d]pyrimidin-5-yl)ethyl]benzoyl]amino]penta-
Prestw-1793		Raltitrexed	112887-68-0	458.50	<chem>C1(c2c(N=C(N1)C)ccc(c2)CN(c1sc(N[C@H](C(=O)O)CCC(=O)O)=O)cc1)C=O</chem>	(2S)-2-[[5-methyl-[2-methyl-4-oxo-1H-quinazolin-6-yl)methyl]amino]thiophene-2-carbonyl]amino]pentanedioic
Prestw-1729		Ceftibuten	97519-39-6	410.43	<chem>N12C([C@H]([C@H]1SC)C=C2)C(=O)O)NC(C1)C1nc(s c1)N=C/CC(=O)O)=O</chem>	(6R,7R)-7-[(2Z)-2-(2-amino-1,3-thiazol-4-yl)-4-carboxybut-2-enamido]-8-oxo-5-thia-1-azabicyclo[4.2.0]oct-2-ene-2-
Prestw-1735		Valsartan	137862-53-4	435.53	<chem>N([C@H](C(=O)O)C(C)C)(C(=O)CCCC)Cc1ccc(c2c(c3nn n[nH]3)cccc2)cc1</chem>	(2S)-3-methyl-2-[(4-[2-(2H-1,2,3,4-tetrazol-5-yl)phenyl]phenyl)methyl]pentanamido]butanoic acid
Prestw-1788		Milnacipran hydrochloride	101152-94-7	282.82	<chem>[C@]1([C@H](C1)CN)(C(N(CC)CC)=O)c1cccc1</chem>	(1R,2S)-2-(aminomethyl)-N,N-diethyl-1-phenylcyclopropane-1-carboxamide hydrochloride
Prestw-1768		Triclabendazole	68786-66-3	359.66	<chem>n1c([nH]c2c1cc(c2)Oc1c(c(Cl)ccc1)Cl)Cl)SC</chem>	6-chloro-5-(2,3-dichlorophenoxy)-2-methylsulfanyl-1H-benzimidazole
Prestw-1751		Brimonidine L-Tartrate	70359-46-5	442.23	<chem>c1(c2nccnc2ccc1N)C1=NCCN1Br</chem>	5-Bromo-N-(4,5-dihydro-1H-imidazol-2-yl)-6-quinoxalinamine 2,3-dihydroxysuccinate
Prestw-1704		Desonide	638-94-8	416.52	<chem>[C@@]12([C@@]3([C@]([C@]4([C@]([C@@]5(C=C/C(C=C5)=O)CC4)C)([C@H](C3)O)[H])[H])[C@]1(O)C(O2)C(C)[H])[H])C(=O)CO</chem>	(1S,2S,4R,8S,9S,11S,12S,13R)-11-hydroxy-8-(2-hydroxyacetyl)-6,6,9,13-tetramethyl-5,7-
Prestw-1728		Cefprozil	121123-17-9	389.43	<chem>N12C([C@H]([C@H]1SC)C=C2)C(=O)O)C=C)NC(C[C@@H](c1ccc(cc1)O)N)=O</chem>	(6R,7R)-7-[(2R)-2-amino-2-(4-hydroxyphenyl)acetamido]-8-oxo-3-(prop-1-en-1-yl)-5-thia-1-azabicyclo[4.2.0]oct-2-ene-

Sophie Rivara



EPFL Engineer in Life Sciences and Technologies, PhD student in Biotechnology & Bioengineering

05.11.1992, Swiss

Avenue de la Gare 20
CH-1022 Chavannes-près-Renens
Switzerland
+41(0)79 612 42 28
sophie.rivara@protonmail.ch

PROFESSIONAL EXPERIENCES

PhD in Biotechnology & Bioengineering (Laboratory of Prof. Andrea Ablasser) <ul style="list-style-type: none">➤ Research projects on my PhD thesis and other cGAS-STING related topics➤ Teaching for EPFL students (laboratory practical course for bachelor students, advanced immunology course for master students)➤ Participation to conferences and seminars	01/2018 – 12/2022	Ecole Polytechnique Fédérale de Lausanne (EPFL), Switzerland
Scientific assistant at the Institute of Innate Immunity (Laboratory of Prof. Eicke Latz) <ul style="list-style-type: none">➤ Pursuing the master thesis project on the NLRP3 inflammasome	08/2017 – 09/2017	University of Bonn, Germany
Scientific intern at TES Pharma S.r.l. (Prof. Roberto Pellicciari) <ul style="list-style-type: none">➤ Studying the distribution of ACMSD inhibitors in mice (collaboration with the laboratory of Prof. Auwerx, EPFL)	01/2015 – 03/2015	TES Pharma, Perugia, Italy
Scientific intern at the EPFL Laboratory of Integrative Systems Physiology (Prof. Johan Auwerx) <ul style="list-style-type: none">➤ Characterization of the effects of new ACMSD inhibitors on metabolism	09/2014 – 01/2015	EPFL, Switzerland

EDUCATION

PhD in the EPFL laboratory of Innate immunity Supervision: Prof. Andrea Ablasser <ul style="list-style-type: none">➤ Thesis title: <i>Tracking spatiotemporal localisation and interactions of the innate immune sensor STING</i>➤ PhD classes for 15 ECTS (scientific topics + soft skills)	01/2018 – planned 10/02/2023	EPFL, Switzerland
Master thesis at the Institute of Innate Immunity <ul style="list-style-type: none">➤ Thesis title: <i>Deciphering the mechanism of activation of the NLRP3 inflammasome in human macrophages in response to Clostridium difficile toxin B</i> <p style="text-align: right;">Grade: 6.00/6.00</p>	02/2017 – 08/2017	University of Bonn, Germany
Master of Science MSc in Life Sciences and Technologies Final grade: 5.87/6.00	08/2015 – 08/2017	EPFL, Switzerland
Bachelor of Science BSc in Life Sciences and Technologies Final grade: 5.66/6.00	09/2011 – 07/2014	EPFL, Switzerland
Maturité gymnasiale (high school), majors in ancient Greek and German Final grade: 6.0/6.0	08/2007 – 06/2011	Collège de Saussure, Geneva, Switzerland

OTHER EXPERIENCES OR WORKSHOPS

<p>Ma thèse en 180 secondes: PhD students' competition grouping all possible PhD fields aiming at presenting in French your thesis in exactly 3 minutes to a general audience</p> <ul style="list-style-type: none"> ➤ Several workshops about sci-comm and oral presentation ➤ EPFL selection round passed; EPFL final (including English-speaking students): 1st jury prize and public prize; Swiss final: 1st jury prize; international final (Montréal): 2nd jury prize <p>https://www.youtube.com/watch?v=iZE55CDq-Vs</p>	<p>01/2022 – 10/2022</p>	<p>EPFL and University of Geneva, Switzerland;</p> <p>University of Montreal, Canada</p>
<p>SciFilmIt Hackathon Lausanne:</p> <ul style="list-style-type: none"> ➤ Creation of a short sci-comm movie in 3 days: <i>Dr. StrangeSymbiosis</i>, https://www.youtube.com/watch?v=3vAwE9XdSU8 	<p>20/02/2020 – 22/02/2020</p>	<p>University of Lausanne Switzerland</p>
<p>EMBO Practical Course: High-throughput protein production and crystallization</p>	<p>10/06/2019 – 19/06/2019</p>	<p>Harwell Campus, Oxfordshire, UK</p>
<p>International Day for Women and Girls in Science: Presenting my research to 7-13 years old children in their schools</p>	<p>11/02/2019 – 12/02/2019</p>	<p>Geneva, Switzerland</p>
<p>Storytelling & Storyboarding Science:</p> <ul style="list-style-type: none"> ➤ Workshop on scientific movies and science communication for Life Sciences' PhD students across Switzerland ➤ Organized by the Swiss Academy of Sciences (SCNAT) under the supervision of scientist and filmmaker Dr. Samer Angelone 	<p>02/08/2018 – 05/08/2018</p>	<p>Locarno Film Festival, Switzerland</p>
<p>iGEM: international Genetically Engineered Machine competition</p> <ul style="list-style-type: none"> ➤ Conception and implementation of a synthetic biology project with the EPFL team: <i>Taxi.Coli: smart drug delivery</i> ➤ Selection for the Final World Championship at MIT; project underlined in <i>Popular Science</i>: The 9 Coolest Student Biology Projects At The 2013 iGEM Competition 	<p>06/2013 – 11/2013</p>	<p>EPFL, Switzerland; MIT, Boston, USA</p>

DISTINCTIONS AND PUBLICATIONS

<p>19/10/2022</p>	<p>Research article, co-first author: Liu Y, Xu P, Rivara S, et al. <i>Clathrin-associated AP-1 controls termination of STING signalling</i>. <i>Nature</i>. 2022;610(7933):761-767. doi:10.1038/s41586-022-05354-0</p>
<p>06/10/2022</p>	<p>Ma thèse en 180 secondes, international final in Montréal, 2nd jury prize</p>
<p>19/05/2022</p>	<p>Ma thèse en 180 secondes, Swiss final, 1st jury prize</p>
<p>24/03/2022</p>	<p>Ma thèse en 180 secondes, EPFL final, 1st jury prize and public prize</p>
<p>29/09/2020</p>	<p>Insights article, first author: Rivara S, Ablasser A. <i>COPA silences STING</i>. <i>J Exp Med</i>. 2020;217(11):e20201517. doi:10.1084/jem.20201517</p>
<p>10/2017</p>	<p>Award for the best grade point average of the Life Sciences Master's degree and certificate of excellence for the results obtained during the degree</p>
<p>2015 – 2017</p>	<p>EPFL Excellence Fellowship</p>
<p>10/2014</p>	<p>Certificate of excellence for the results obtained during the Bachelor's degree</p>
<p>06/2011</p>	<p>High school excellence prizes (global results, French, mathematics and ancient Greek)</p>

SKILLS

LANGUAGES

- French:** native speaker
- English:** excellent understanding and expression
- German:** excellent understanding and very good expression
- Italian:** good understanding and expression
- Russian:** basics

INTERPERSONAL AND TRANSVERSAL SKILLS

- Team spirit:** capacity to listen, diplomacy, easy contact, good ability to initiate conversations, eager to help, collaborative attitude, empathy, positivity
- Communication:** ease to talk in public, eagerness and pleasure to transmit and explain, well-structured presentations, ability to simplify, analytical mind, adaptability to the target audience
- Stress resistance:** perseverance, good problem-solving abilities, motivation, efficiency, focus
- Critical mind:** rapidity and flexibility in learning, good analysis abilities, reflexion, curiosity, creativity

TECHNICAL SKILLS

- Molecular biology techniques, cell culture, microscopy** (fluorescence and confocal)
- Data analysis, image processing and programming:** KNIME, Fiji, OMERO, GraphPad Prism, notions in R, Matlab, Python and C/C++
- Design and drawing:** Inkscape, Affinity Design, Affinity Publisher, Adobe Illustrator
- Microsoft Office and Open Office**

EXTRA-CURRICULAR EDUCATION AND ACTIVITIES

Theater

- Writing poetry and short stories** (awarded 4 prizes from EPFL literature association PLUME)
- Treble recorder and musical notation** (Certificates obtained with honors at the Popular Music Conservatory of Geneva in 2011)
- Singing in **choirs** (member of the University Choir executive committee from 2018 to 2022)
- Skiing, hiking, sailing, basketball (U16 Swiss Champion in 2008)
- Backpack travels by train (Trans-Siberian railway—Russia, Mongolia and China, 05-07/2015; Northern Europe—Germany, Denmark, Sweden and Norway, 08/2016)